Olfactory and thermoregulatory capacities in small terrestrial mammals : a turbinal bone approach

Quentin Martinez

THÈSE POUR OBTENIR LE GRADE DE DOCTEUR
DE L'UNIVERSITÉ DE MONTPELLIER

En biologie des populations et écologie

École doctorale GAIA

Institut des Sciences de l'Evolution de Montpellier
ISEM – UMR554

Olfactory and thermoregulatory capacities in small terrestrial mammals: a turbinal bone approach

Présentée par Quentin Martinez
Le 29 Avril 2021

Sous la direction de Pierre-Henri Fabre

Devant le jury composé de :

Anthony Herrel, Directeur de recherche, CNRS, Paris, France	Rapporteur
Sharlene Santana, Associate Professor, Burke Museum, Seattle, USA	Rapporteur
Marcelo Sanchez-Villagra, Professor, University of Zurich, Switzerland	Examinateur
Francesco Bonadonna, Directeur de recherche, CEFE, Montpellier, France	Examinateur
Irina Ruf, Associate Professor, Senckenberg Institute, Frankfurt, Germany	Invité
Pierre-Henri Fabre, Maître de conférences, ISEM, Montpellier, France	Directeur de thèse

UNIVERSITÉ DE MONTPELLIER

Message in a bottle for passionate students

To all students who do not view themselves in a highly competitive system, be assured that if you are motivated you will always find your place in science.

After a technical degree in conservation biology, I was not up to the standard university level. Despite some OK grades, I was ranked last of my first year of master. Therefore, I did not qualify for the 2nd year of the master's degree. At that time, it was a big deal but I found another master. Despite the difficulty to find a PhD position in France, I was accepted in two positions, thanks to my motivation and hard work.

Finally, I still get some hope that one day, the French government will stop cutting research budgets and understand that education and research are key to get us out of the current health, environmental, and social crises.

Corrected version of the PhD manuscript from the 29/07/2021.

Illustration of the subterranean rodent *Cryptomys mechowi* created from turbinals and skull surfaces generated in the following studies, with the original draw of Martina Nacházelová and the background picture of Raymond Mendez. Illustration: Quentin Martinez.

SUMMARY

Part I - Turbinal bones

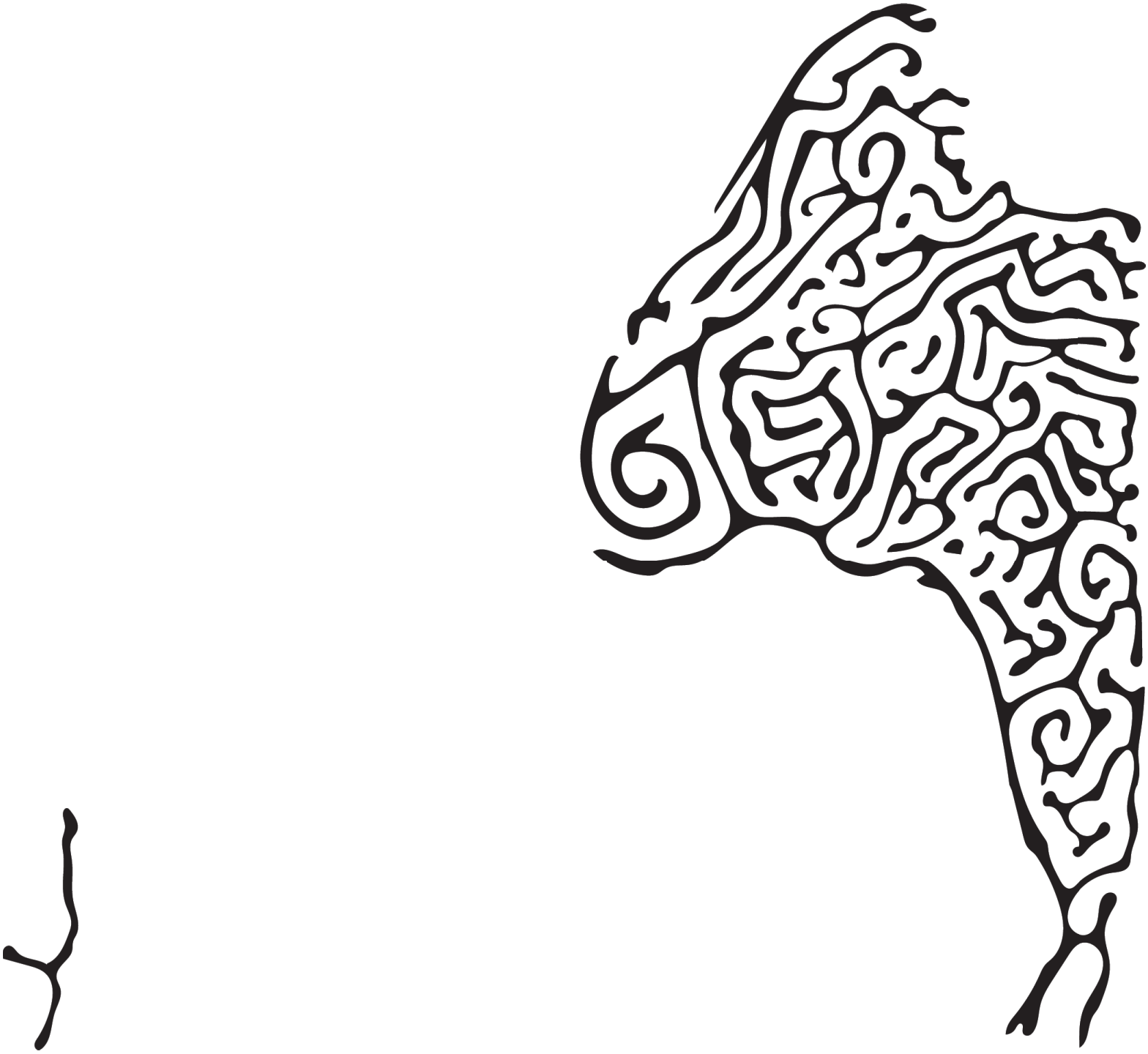

Maxillo-turbinals: *Mus musculus domesticus* (left) and *Castor canadensis* (right).

1. Turbinal bones

Turbinals (= turbinates) are bony structures involved in olfaction, heat, and moisture conservation, as well as protection of the respiratory tract (e.g. Negus 1958). First works on turbinals probably refers to human medicine where turbinals were named conchae (e.g. Bourgery & Jacob 1831). During the last decades, turbinals were largely understudied in comparison to other parts of the skull (Rowe *et al.* 2005). Indeed, turbinals are thin perforated and scrolled bony or cartilaginous plates (Fig. 1). Therefore, they are fragile and difficult to extract from the skull. Past anatomists spent a lot of time to access these structures using tedious protocols such as saw band, fancy transparency projector, cardboard models, and different types of casts (Watson 1913, Dawes 1952, Negus 1958, Folkow *et al.* 1988, Morgan & Monticello 1990). In this context, we may recognize the astonishing works of Simon Paulli and Sir Victor Negus (Paulli 1900 a, b, c, Negus 1958) that became landmarks for the field.

Invented in the 80's, high-resolution X-ray micro-computed tomography (micro–computed tomography, micro-CT, μCT) was first extremely expensive and dedicated to exceptional projects. Then, the improvements and popularization of this tool resulted in a significant cost reduction. Micro-CT completely revolutionized the sensory ecology field and especially for turbinals. Moreover, in a context where biodiversity drastically decreased, museum specimens became rare and highly valuable material. Therefore, micro-CT that is non-destructive, enables acquiring data from rare specimens such as holotypes or specimens from extinct or endangered species. It is also possible to perform micro-CT on alive animals (anesthetized) and even during movements (cineradiography). One of the first work on turbinals that used micro-CT was probably Ruben *et al.* (1996) who investigated respiratory turbinals in birds, crocodilians, and theropods. Since, the number of publications related to turbinals has exponentially increased.

However, the nasal cavity (and therefore turbinals) is probably still the least studied region of the mammalian skull despite its large volume occupancy (Rowe *et al.* 2005). Van Valkenburg and her team widely developed quantitative analyses based on turbinal data, acquired by micro-CT (e.g. Van Valkenburg *et al.* 2004, 2011, 2014a, Green *et al.* 2012). One of the biggest challenges is now the required time to process the data and in particular the segmentation (= isolation of an area of interest). In mammals, segmentation ranges from half a day to several days to properly extract all turbinals from one side (e.g. left side in the following studies). This process is longer in the case of noisy micro-CT images, fossils (Fig. 2), or for the species with highly complex turbinals (e.g. amphibious species). In the next few years, deep learning technology may considerably reduce this segmentation time. To date, some freeware already does exceptional interpolation jobs in structures such as endocasts (e.g. Biomedisa, Losel *et al.* 2020), but will need some customized protocols for structures such as turbinals.

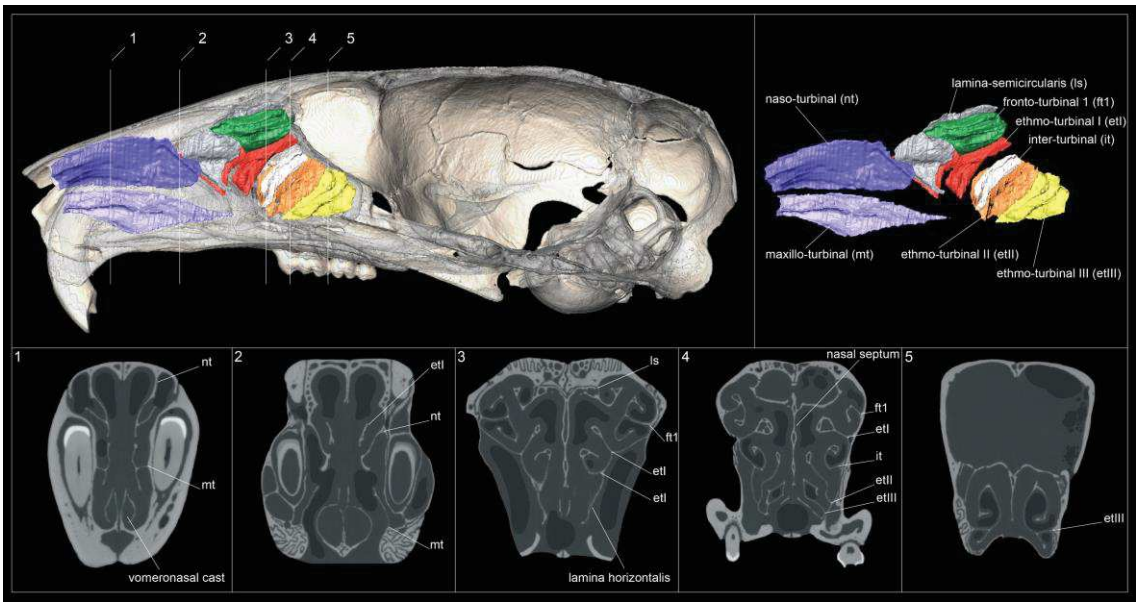

Figure 1: (Up) Sagittal views of the skull of *Mus musculus domesticus* with 3D representations of turbinals. Colors follow turbinal homology. (Down) Five coronal sections along the nasal cavity. Figure extracted from Martinez *et al.* in prep. (c).

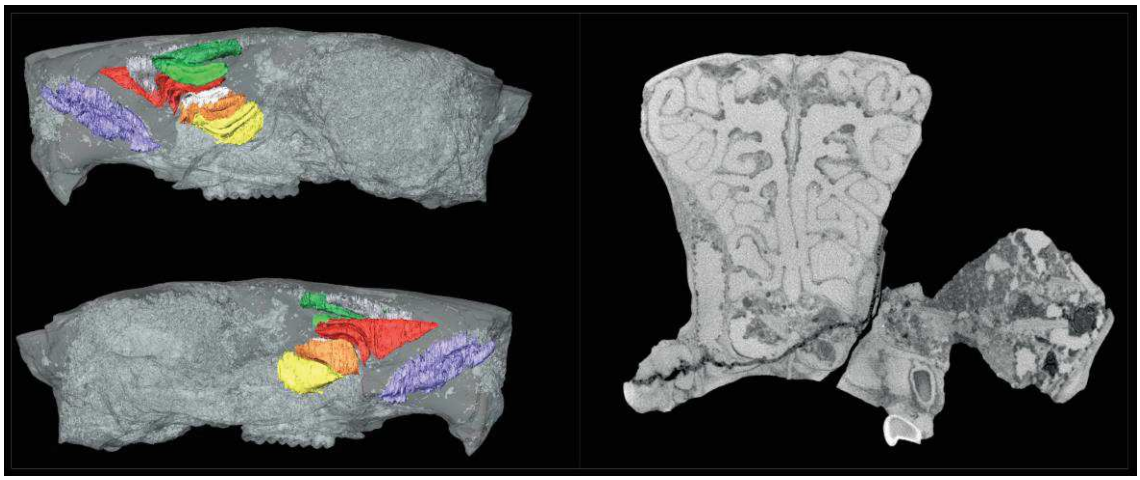

Figure 2: Exceptional turbinal preservation in fossils. (Left) Sagittal views of the skull of *Paradelomys sp.* (Theridomyidae, UM-ACQ-6619 Quercy France) with superimposed 3D representations of turbinals. The segmentation of respiratory turbinals is still ongoing. (B) Coronal section of the nasal cavity showing the olfactory turbinals. This rodent probably occurred between the Eocene and the Oligocene (≃ 33.9 to 28.4 mya). Figure extracted from Martinez *et al.* in prep. (c).

The number of studies related to mammalian turbinals are high and keep growing. However, studies remain rare in other tetrapods (e.g. birds or lizards) where most of their turbinals are cartilaginous and therefore not visible with micro-CT. Recent development of staining methods (e.g. iodine or acid) provide further avenues in this field by enabling the contrast enhancement of soft tissue and therefore make them visible in micro-CT (Pauwels *et al.* 2013, Gignac *et al.* 2016).

2. Turbinals in amniotes

Turbinals are present in most amniotes with the exception of turtles and some fully aquatic mammals (Negus 1958, Parsons 1971, Hillenius 1994). However, these structures largely differ between groups in their relative size, complexity, location, and epithelial cover (Negus 1958, Parsons 1971, Hillenius 1994, Owerkowicz *et al.* 2015). A common dichotomy is made between respiratory and olfactory turbinals (e.g. Negus 1958, Parsons 1971). The first involved heat and moisture conservation whereas the latter involved olfaction (Fig. 3). Turbinals are mostly cartilaginous in sauropsids (e.g. lizards and birds) whereas they are mostly ossified in synapsids (e.g. extant mammals, Hillenius 1994).

In lizards and snakes (= extant lepidosaurs) turbinals are generally represented by a simplified lamella mostly covered by sensory epithelium (= olfactory turbinal) and therefore involved in smell (Parsons 1971). Again, some reductions are known in aquatic and arboreal forms (Parson 1971). Three turbinals are present in crocodilians that are mostly covered by sensory epithelium (Hillenius 1994). Apparently, turtles are the only amniote to lack turbinals even at a very early embryonic stage (Parsons 1971). In general, turbinals are more developed in endotherms and therefore have a huge morphological disparity related to their phylogenetic relationships, skull morphology, and ecology (Bang 1961, 1964, 1965, 1968, Parsons 1971, Hillenius 1994, Van Valkenburg *et al.* 2004, 2011, 2014a, Green *et al.* 2012, Ruf 2014, 2020, Martinez *et al.* 2018, 2020, in prep. b). Birds generally possess two respiratory and one olfactory turbinals. The olfactory turbinal that is located in the posterior part varies from highly complex in kiwi to highly reduced in pigeons (Parsons *et al.* 1971).

In mammals, turbinals generally occupied a large portion of the nasal cavity (Parsons 1971, Hillenius 1994, Van Valkenburg *et al.* 2004, 2011, 2014a, Martinez *et al.* in prep. b, c, Fig. 1, 2, 3). Mammalian turbinals are usually discriminated in two distinct functional parts: the anterior respiratory turbinals and the posterior olfactory turbinals (Fig. 3). However, some turbinals (e.g. ethmo-tubinal I (etI) or naso-turbinal (nt), Fig. 1) may have a dual function. The number of respiratory turbinals in terrestrial mammals varies from 1 in the naked mole rat (*Heterocephalus glaber*) to 3 or 4 in some other rodent species (Martinez *et al.* in prep. a, b, Fig. 4). The number of olfactory turbinals in terrestrial mammals varies from 1 or 2 in humans to about thirty in some perissodactyls or anteaters (Paulli 1900 b, Hautier *et al.* 2019, pers. obs.). Fully

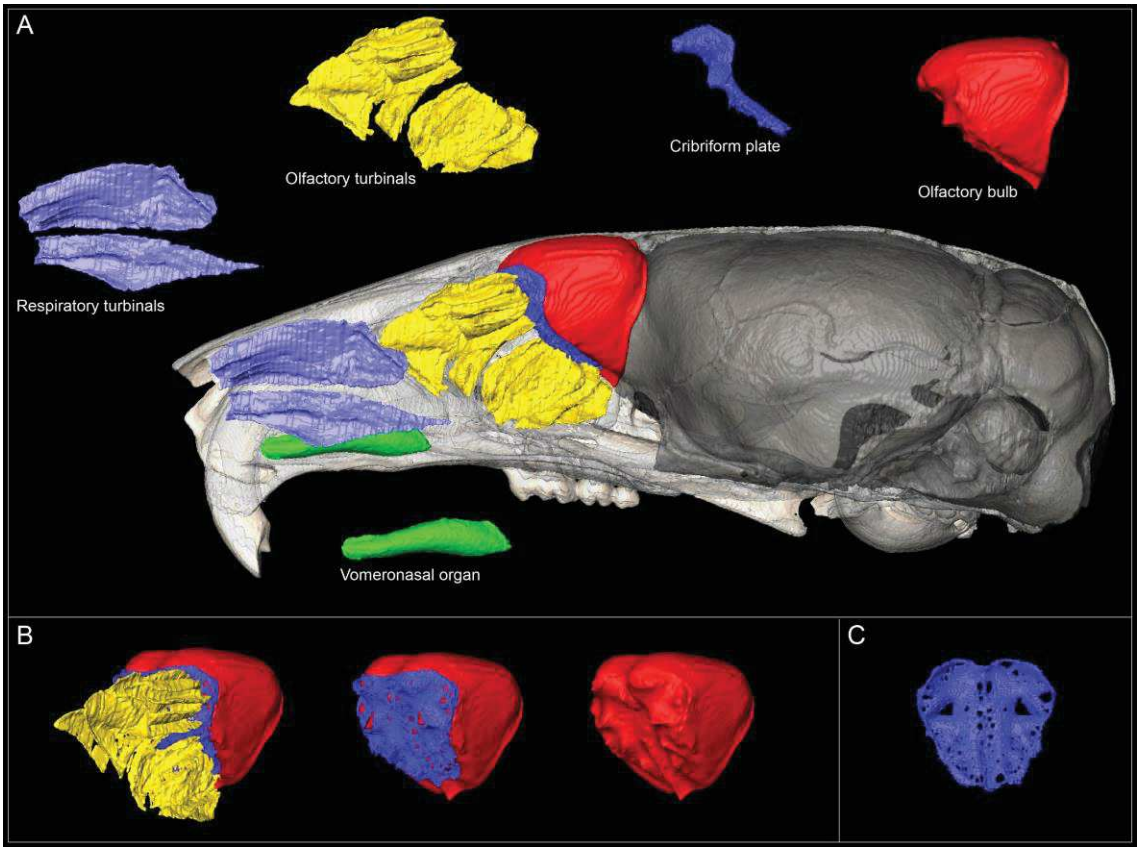

Figure 3: Sagittal views of the skull of *Mus musculus domesticus* with 3D representations of organs and structures related to olfaction and heat and moisture conservation. (A) Sagittal view of respiratory turbinals (cyan), olfactory turbinals (yellow), cribriform plate (dark blue), olfactory bulb (red), and vomeronasal organ (green). (B) View of the connection between olfactory turbinals, cribriform plate, and olfactory bulb. (C) Posterior view of cribriform plate illustrating the foramina of the olfactory nerves. Illustration: Quentin Martinez.

aquatic mammals may lack turbinals (Parsons 1971), but further investigations on these organisms are still awaited. In addition to the relative number of turbinals, their relative size and complexity highly vary between mammalian species (Parsons 1971, Hillenius 1994, Van Valkenburg *et al.* 2004, 2011, 2014a, Green *et al.* 2012, Ruf 2014, 2020, Martinez *et al.* 2018, 2020, in prep. a, b, c). As a result, and in the light of the lack of developmental studies, there are difficulties to determine clear homology hypotheses in the turbinal of extant amniotes. This work is even more complicated in fossils and to date the origin of turbinals is not fully elucidated (Parsons 1971). Maxillo-turbinal (one of the respiratory turbinals) might be one of the only turbinals for which the homology hypothesis was clearly identified in the amniote clade (Parsons 1971).

In synapsids, bony scars are interpreted as potential respiratory turbinals in the upper Permian therapsid *Glanosuchus* (~ 260 Mya, Hillenius 1992, 1994). Respiratory ridges are also found in subsequent mesozoic therocephalians and cynodonts (= theriodonts, Hillenius 1994). Olfactory turbinal ridges are described in some cynodonts, *Diademodon* and *Thrinaxodon* (Watson 1913, Brink 1956, Parsons 1971, Hillenius 1994) whereas hadrosaur dinosaurs may have large olfactory turbinals (Parsons 1971). Evidence of respiratory and olfactory turbinals in the nasal cavity of non-mammaliaform cynodonts suggested that in the upper Triassic, turbinals may have been already similar to those in extant mammals (Ruf *et al.* 2014).

Since turbinals are mostly cartilaginous in sauropsids, fossil evidence is still unclear and highly debated. Concerning respiratory turbinals, paleontologists extrapolate on the shape and the cross section of the nasal cavity of sauropsids (Ruben *et al.* 1996, Ruben & Jones 2000). For example, late cretaceous ornithurine *Hesperornis* (~ 80 Mya) presents a nasal cavity similar to the one of extant birds (Witmer 1997). Therefore, Hillenius & Ruben (2004) hypothesized that this genus may have similar respiratory turbinals than extant birds. Based on the absence of respiratory turbinals in theropod dinosaurs (e.g. *Archaeopteryx*), Ruben & Jones (2000) hypothesized that early birds may have been ectotherms. Also, some scars found in *Tyrannosaurus* (~ 75 Mya) may be interpreted as potential olfactory turbinals (Ruben *et al.* 1996).

Synapsids and sauropsids probably diverged in the Carboniferous (~ 319–310 Mya, Reisz & Muller 2004, Van Tuinen & Hadly 2004) whereas recent studies suggested that mammals evolved from the late Triassic (Bi *et al.* 2014). Therefore, giving an age to the origins of turbinals is not possible and we do not know if it originates from a single event or from a convergence between synapsids and sauropsids (Gauthier *et al.* 1988).

3. Turbinals in mammals

Among extant tetrapods, mammals have on average, the largest turbinals relative to their skull length (e.g. Negus 1958, Parson 1971). Despite some studies in primates, Carnivora, bats, lagomorphs as well as rodents, the homology of turbinals remains unclear in several species of mammals with a lack of studies in some orders (Hillenius 1994). The difficulty of turbinal homology is mainly associated with olfactory turbinals (= fronto- and ethmo-turbinals, Fig. 1) where increasing in turbinal complexity may increase the number of small and potentially independent lamellae. Even in rodents, the homology in olfactory turbinals is sometimes unclear, with some fronto-turbinal numbers ranging from 0 to 3 (Martinez *et al.* in prep. c, Fig. 4). In the light of variation in shape, location and number of these fronto-turbinals, some proper developmental studies must be done before providing some homological hypotheses that could be used into a phylogenetic framework. Similarly, it is difficult to distinguish between inter-turbinals and the potential lamellae of the olfactory-turbinals (Rowe *et al.* 2005). It is especially true for species with complex olfactory turbinal bones such as armadillos, elephants or tapirs (e.g.

Paulli 1900 b, Hautier *et al.* 2019, pers. obs.). In some cases, examinations of young individuals are enough because turbinals are often less complex in younger stages. However, in most cases precise developmental studies are necessary. To date, developmental studies remain rare and limited to some families (e.g. Ruf 2004, 2020 Smith *et al.* 2016, 2020 a, Smith & Rossie 2008, Wagner & Ruf 2020). Therefore, more developmental studies will be necessary in the near future to further test hypotheses of turbinal homologies.

During the development of mammals, turbinals emerge from the nasal capsule (Hillenius 1994, Rowe *et al.* 2005). At early developmental stages, turbinals have three centers of chondrification: the pars anterior, the pars intermedia (= lateralis), and the pars posterior (Reinbach 1952 b, Van Valkenburg *et al.* 2014 b, Smith & Rossie 2008, Maier and Ruf 2014, Ruf 2020). Anteriorly, turbinals are generally separated in the nasal cavity from left to right by the nasal septum. This structure that arises early in the ontogeny (from neural crest cells), remains mostly cartilaginous (Rowe *et al.* 2005, Ruf 2020). The posterior part, that will be ossified in adult stages is name mesethmoid (Rowe *et al.* 2005). Turbinals from the left and right side are symmetric and apart from some rare exceptions (Martinez *et al.* in prep. a, c), intra-individual variation (left to right) is rare (Rowe *et al.* 2005, Martinez *et al.* 2018, 2020, in prep. a, c).

Turbinal bones are generally discriminated in two categories, the (1) heat and moisture conservation on the one hand, and the (2) olfaction on the other hand (e.g. Negus 1958, Parsons 1971, Hillenius 1992). These categories often fit with an antero-posterior discrimination with turbinals that are functionally named as respiratory and olfactory turbinals (Fig. 3). These bony structures exponentially increase the surface area of the nasal cavity covered by epithelium (Rowe *et al.* 2005). However, epithelial composition worn by turbinals varies between species. Therefore, extensive histological studies in rats and mice (e.g. Le Gros Clark 1951, Ressler *et al.* 1993, Harkema & Morgan 1996, Harkema *et al.* 2006, Barrios *et al.* 2014, Herbert *et al.* 2018) and in some non-model species (e.g. Negus 1958, Maier 1980, Smith *et al.* 2004, 2012, Smith & Rossie 2008, Eiting *et al.* 2014 a, Yee *et al.* 2016, Martinez *et al.* 2020) allow us to detail the distinct functions of turbinals.

In the two following parts, we will discuss anatomy of the turbinals from the anterior portion where the nares are located (= respiratory turbinals) to the posterior part that reaches the limit between the cribriform plate and the olfactory bulb (= olfactory turbinals, Fig. 3). In the respiratory turbinals we will discuss several structures that are named (1) margino- and atrio-, (2) maxillo-, and (3) naso-turbinals. In the olfactory turbinals we will discuss (1) lamina semicircularis, (2) fronto-, (3) ethmo-, and (4) inter-turbinals.

a. Respiratory turbinals

Respiratory turbinals are involved in heat and moisture conservation. During inhalation, the air is warmed up to body temperature with the contact of the vascularised anterior part of the respiratory turbinals. Simultaneously, the air in contact with nasal mucus is moistened. During subsequent exhalation, this warmed air is cooled down by the anterior portion of the respiratory turbinals that were previously cooled down by inspired air. This process condensates water from the nasal cavity and therefore conserves on average 66% of the humidity of the exhaled air (Fig. 6, Negus 1958, Walker & Wells 1961, Jackson & Schmidt-Nielsen 1964, Schmidt-Nielsen *et al.* 1970, Collins *et al.* 1971, Hillenius 1992, Ruben *et al.* 1996, Hillenius & Ruben 2004).

Respiratory turbinals are mostly covered to transitional and respiratory epithelium. By simplification, and in opposition to olfactory epithelium, several authors merged transitional and respiratory epithelium and only refer to the latter to describe the epithelium that lines respiratory turbinals. Respiratory epithelium is composed of six cell types: ciliated columnar, nonciliated columnar, mucous, brush, cuboidal, and basal cells. The variation in the composition of these cell types will change the properties of the respiratory epithelium in production of mucus, capacity to retain macro- and microscopic elements as well as enzyme activities (Herbert *et al.* 2018). The lamina propria (= most ventral part of the epithelium) of the respiratory epithelium is highly vascularized and contains many mucous glands. The transitional epithelium is a thin layer composed of cuboidal or low columnar cells that vary in their degree of ciliation.

Finally, respiratory turbinals are involved in the protection of the lower respiratory tract and of the posterior neuroepithelium. Indeed, respiratory turbinals filter, absorb, and dispose of both macro- and microscopic elements but also volatile elements causing injuries (e.g. Morgan & Monticello 1990, Harkema *et al.* 2006). These processes are performed thanks to the ciliated morphology of the respiratory epithelium but also by its absorption and regeneration properties.

We will discuss respiratory turbinals following: (1) margino- and atrio-, (2) maxillo-, and (3) naso-turbinals.

i. Margino- and atrio-turbinals

In mammals the most anterior portion of the nasal cavity houses a cartilaginous structure named the outer nasal cartilage (Maier 2020, Ruf 2020). This structure makes up the junction between the external nares and the nasal bones. Therefore, species with elongated rhinariums or trunks (e.g. shrews or macroscelides) bears a long outer nasal cartilage (Maier 2020).

Anteriorly, the two first turbinals are fully cartilaginous at the adult stage and respectively named margino- and atrio-turbinals. In rodents, these turbinals are formed by the pars anterior (Ruf 2020). Due to their cartilaginous composition, these two turbinals are difficult to identify without precise histology. Therefore, in mammals, the mentions of margino- and atrio-turbinals are rare (e.g. De Beer 1929, Reinbach 1952 a, b, Maier 1980, 2000, 2020, Ruf 2004, 2014, 2020,

Rossie & Smith 2007, Macrini 2012, 2014, Maier & Ruf 2014), especially in group like rodents (e.g. Fawcett 1917, Parsons 1971, Ruf 2004, 2020). Because they are directly in contact with the exterior environment, margino- and atrio-turbinals are composed of lightly keratinized and squamous epithelium that may protect the posterior epithelium (Ruf 2014, 2020, Herbert *et al.* 2018). Margino- and atrio-turbinals are extremely complicated to discriminate and some authors refer to the first or the latter without clear homology, or even wrongly (see result section in Ruf 2020). Rare studies with very precise histology are able to differentiate between margino-, atrio-, and maxillo-turbinals by an incisura (e.g. Reinbach 1952 a, b, in armadillo and Ruf 2004, 2020 in rodents). Maier (2000) identified a lack of atrio-turbinals in cercopithecoids and therefore a gap between margino- and maxillo-turbinals. In addition to their role in heat and moisture conservation, margino- and atrio-turbinals may also play a role in the shape of the nostril. Finally some link with facial muscles may imply a role in airflow direction into upper and lower components and even in the sniffing process (Hofer 1980, Gobbel 2000, Maier & Ruf 2014). Due to the difficulty to identify these two cartilaginous turbinals even with dice-ct scans, these turbinals remain widely understudied.

ii. Maxillo-turbinals

Maxillo-turbinals start at the end of the atrio-turbinals when both atrio- and margino-turbinals are present (Maier 2000, Ruf 2020). Maxillo-turbinals originate from the pars anterior and are generally fully ossified with the exception of the tip of the turbinal that remains cartilaginous in some species (Ruf 2020). Maxillo-turbinals are thought to be the largest respiratory turbinal, however there is a significant variation at the mammalian scale (Martinez *et al.* in prep. a, b, c, Fig. 7).

iii. Naso-turbinals

Naso-turbinals are located dorsally to the maxillo-turbinals and also originate from the pars anterior. In rodents, it is a distinct turbinal with no connection to other turbinals. In some mammals, the naso-turbinal is connected to the lamina semicircularis and therefore reaches the posterior part of the olfactory recess. In this case, some authors (mostly old literature) do not discriminate between the naso-turbinals and the lamina semicircularis (e.g. Le Gros Clark 1951 with the rabbit). The medio-posterior part of the naso-turbinal is often covered by olfactory epithelium, inducing a dual function in respiratory and olfactory processes. However, the epithelial cover of the naso-turbinals greatly varies between species (Smith *et al.* 2004, 2012, Smith & Rossie 2008, Yee *et al.* 2016, Herbert *et al.* 2018).

Finally, naso-turbinals have a key function in directing the anterior airflow to the posterior olfactory recess and the olfactory turbinals. At least in placentals, the passage of the air through the naso-turbinal results in a decreasing airflow velocity in the olfactory recess that may

increase absorption and therefore the correct detection of volatile odorant molecules (e.g. Craven *et al.* 2010).

b. Olfactory turbinals

Olfactory turbinals are responsible for olfaction in supporting olfactory epithelium and neurons (Ressler *et al.* 1993, 1994, Harkema *et al.* 2006, Barrios *et al.* 2014, Herbert *et al.* 2018). Olfactory turbinals chondrified and ossified antero-posteriorly and are generally fully ossified in adult stages (Van Valkenburg *et al.* 2014 b, Ruf 2020). It is well known that the relative size and complexity of olfactory turbinals significantly vary between species. Developmentally, extreme reduction is attributed to the merging of embryonic structures whereas extreme development may result from repetitive mesenchymal growth (Van Valkenburg *et al.* 2014 b).

Olfactory turbinals are almost completely covered by olfactory epithelium. The olfactory epithelium is pseudostratified and composed of olfactory neurons, supporting cells, and basal cells (Herbert *et al.* 2018). At the dorsal surface of the olfactory epithelium, the olfactory vesicles of the olfactory neurons participate in increasing the surface area for the reception of odorant molecules. Olfactory neurons are ventrally extended by an axon that joins other axons and nerve fascicles. These nerve fascicles traverse the perforated cribriform plate to join glomeruli from the olfactory bulb (Fig. 5). The olfactory neurons are constantly regenerated with an estimated turnover rate of 30 days in the laboratory rat (Graziadei & Graziadei 1978). The lamina propria (= most ventral part of the epithelium) of the olfactory epithelium includes Bowman's glands (= submucosal glands) which participates in moistening the olfactory epithelium and secrete a solvent between volatile odorant molecules and olfactory receptors. Some parts of the nasal roof, the nasal septum and the lateral wall of the olfactory recess, are also covered by olfactory epithelium (Rowe *et al.* 2005, Herbert *et al.* 2018, Ruf 2020).

We will discuss olfactory turbinals following: (1) lamina semicircularis, (2) fronto-, (3) ethmo-, and (4) inter-turbinals (Fig. 1).

i. Lamina semicircularis

Because the lamina semicircularis is mostly covered by olfactory epithelium, it is often considered functionally as an olfactory turbinal (e.g. Martinez *et al.* 2018, 2020). However, it is not a turbinal but a part of the anterior paries nasi (pars anterior, Ruf 2014, 2020). Here, we also consider the ventral projection named the uncinate process. The presence of this process and its size significantly varies between species without any particular phylogenetic or ecological pattern identified so far (Macrini 2012, 2014, Ruf 2014, 2020, Martinez *et al.* in prep. c).

ii. Fronto-turbinals

Fronto-turbinals are defined as turbinals located in the frontal recess and therefore do not meet the lamina transversalis (Rowe *et al.* 2005, Ruf 2020). The fronto-turbinals originate from the pars intermedia (Van Valkenburg 2014 b, Ruf 2020) and are the first turbinals to ossify in *Tupaia* (Scandentia, Ruf 2020 citing Spatz 1964). Fronto-turbinals can be attached to the lamina horizontalis (Ruf 2020) and are also described as turbinals that do not develop medially and remain far from the nasal septum (Rowe *et al.* 2005 citing Allen 1882).

iii. Ethmo-turbinals

Ethmo-turbinals originate from the pars posterior and therefore from the ethmoid bone (Van Valkenburg 2014 b, Ruf 2020). The ethmoid bone comprises several sub-structures: the ethmo-turbinals, the nasal septum, the cribriform plate, and the crista galli (Fig. 1, 3, Ruf 2020). Ethmo-turbinals attached to the lamina horizontalis or on the sidewall of the olfactory recess (Ruf 2020). These turbinals are often connected posteriorly to the cribriform plate and therefore to the olfactory bulb via olfactory nerves (Fig. 5, Herbert *et al.* 2018, Ruf 2020). Ethmo-turbinals are generally more developed than fronto-turbinals and therefore considered as the structures that are most involved into olfactory processes.

Among ethmo-turbinals, the ethmo-turbinal I (etI) received much more attention than the others. Indeed, by its anterior projection and its division in two distinct pars (the pars anterior and posterior, Fig. 1), it is easy to identify the etI in divergent species (Ruf *et al.* 2020, Hautier *et al.* 2019, pers. obs., turbinals in red in the Fig. 4). The etI is generally the largest ethmo-turbinal and the first ethmo-turbinal that appears in ontogeny (Rowe *et al.* 2005). EtI is the olfactory turbinal that reaches the most anterior part of the nasal cavity. In rodents, etI anteriorly originates just before, at the limit or with a small overlap to the respiratory turbinals (Martinez *et al.* in prep. c). In other orders such as Eulipotyphla (e.g. shrews and moles), Afrosoricida (e.g. tenrecs), and scandentia (e.g. the treeshrew *Ptilocercus lowii*), the pars anterior of the etI originates in the anterior part of the respiratory turbinals and highly overlaps them (Ruf *et al.* 2015, Martinez *et al.* 2020). In these species and similarly to the naso-turbinal of some species, the etI may have a dual function as a respiratory and olfactory turbinal. Indeed, a part of the pars anterior is covered of respiratory epithelium and the rest is covered by olfactory epithelium (Martinez *et al.* 2020). Using histology and micro-CT-scan images, Martinez *et al.* (2020) identified in most Eulipotyphla and Afrosoricida investigated, a small incisura that may be used to precisely estimate the antero-posterior functional subdivision.

iv. Inter-turbinals

Inter-turbinals are olfactory turbinals that can develop between both fronto- and ethmo-turbinals. In rodents, lagomorphs, and Carnivora, inter-turbinals develop later than fronto- and ethmo-turbinals (Ruf 2014, 2020, Wagner & Ruf 2019). Apparently inter-turbinals never extend as far medially as the fronto- and ethmo-turbinals (Ruf 2020) but some exceptions may occur (Macrini 2012, Martinez *et al.* in prep. c). In mammals, the number of inter-turbinals varies greatly between species (Paulli 1900, a, b, c, Ruf 2014, Martinez *et al.* 2018, 2020, in prep. c) and their homology is unclear in some order with highly complex olfactory turbinals (e.g. cingulata or proboscidea, Paulli 1900, a, b, c, Hautier *et al.* 2019, pers. obs.).

However, one particular inter-turbinal located between ethmo-turbinal I (etI) and II (etII) received more attention and may be homologous in mammals. In the common fronto- ethmo-turbinals terminology, this inter-turbinal is name “inter-turbinal” (it) in rodents, lagomorphs and primates (e.g. Ruf 2014, 2020, Ruf *et al.* 2015, Martinez *et al.* 2018, Fig. 1). However, the presence of additional inter-turbinals before this homologous inter-turbinal, complicates the anatomical nomenclature (e.g. Wagner & Ruf 2019, 2020). These additional inter-turbinals are probably the most variable turbinals in the mammalian clade and do not seem to follow a particular pattern. For example, in rodents, intra-individual (left to right), intra- and inter-specific variations were observed in these additional inter-turbinals (Martinez *et al.* 2018, in prep. c).

Finally, we must notice that in some rodents, new turbinals have been identified between naso- and maxillo-turbinals and may be also considered as inter-turbinals (Martinez *et al.* 2020, Martinez *et al.* in prep. c, Fig. 4).

c. Other terminologies

As usual in anatomy, the finding of clear homology hypotheses is complexified by heterogeneous terminologies that keep continuing to be used (Rowe *et al.* 2005) and even to evolve (e.g. with "rostroturbinal" in Macrini 2014). To this problem, we must add the difficulty of identifying certain published errors (see results and discussion in Ito *et al.* 2019, Ruf 2020). Most variations in employed terminology occured for the olfactory turbinals. In the past, comparative studies of turbinal bones do not have access to precise developmental studies preventing them to identify proper homology (e.g. Le Gros Clark 1951 who named in the rabbit, the lamina semicircularis, “naso-turbinal”). Therefore, several authors refer to ethmo-turbinals without naming them accurately (e.g. Voit 1909). Others used the endo- and ecto-turbinal terminology mixed with reference to the ethmo-tubinal bone (e.g. Paulli 1900 a, b, c, Negus 1958). As an example, Negus (1958) named in *Boselaphus tragocamelus* (Artiodactyla) the pars anterior of the ethmo-turbinal I (etI) “second ethmo-turbinal”. Further, he named in *Tupaia* (tree shrew) the pars posterior of the ethmo-turbinal I (etI) “second endo-turbinal” (Negus 1958).

Progressively, two terminologies emerged, which have been confronted to one another: (1) the fronto-, ethmo-turbinal terminology and (2) the endo-, ecto-turbinal one (see also discussion of the terminology in Macrini 2012, Maier & Ruf 2014). The fronto-, ethmo-turbinal terminology is mostly based on homology determined by developmental studies, which is the most widespread approach in comparative and systematic studies. The endo-, ecto-turbinal terminology is based on the observation of adult specimens and by the order of appearance of the turbinals. It presents the advantage to be easy to understand and to illustrate, but has rather poor significance in evolutionary biology. This last terminology makes the comparison and discussion about particular turbinals between species difficult. In most cases, ecto-turbinals correspond to the turbinals found in the frontal recess (fronto- and inter-turbinals) whereas endo-turbinals correspond to the rest of olfactory turbinals (lamina semicircularis and ethmo-turbinals) with the exception for some authors of the inter-turbinal located between ethmo-turbinal I (etI) and II (etII, Macrini 2012, but see Paulli 1900, a, b, c). We can also notice that some authors mixed both terminologies (e.g. Rossie 2006) or duplicate their captions to be didactic (Macrini 2014).

Here (see above), and in the following articles we used the fronto-, ethmo-turbinal terminology which is meaningful from an evolutionary perspective (Fig. 1). We mostly studied groups where some development studies exist and who do not have weird or rather complex olfactory turbinals that would require extensive embryological studies to disentangle a proper terminology. Furthermore, our results will be easily comparable to recent studies (Martinez *et al.* 2018, 2020, Lundeen & Kirk 2019, Wagner & Ruf 2019, 2020, Ruf 2020, Smith *et al.* 2020 a, b), which employed the fronto-, ethmo-turbinal terminology adapted from Paulli (1900, a, b, c). However, all these studies do not refer to mammals with complex olfactory turbinals and with a large number of inter- and ethmo-turbinals. Homology of olfactory turbinals is not elucidated in species with highly complex olfactory turbinals such as Carnivora, perissodactyls or anteaters (e.g. Paulli 1900 b, Van Valkenburg *et al.* 2014 a, Hautier *et al.* 2019). Therefore, we must admit that for these species, it may be hazardous to accurately name olfactory turbinals with the fronto-, ethmo-turbinal terminology. However, to date, no recent study investigated the question.

d. Selective pressures affecting turbinals

It was widely hypothesized that the number and the shape of turbinal bones are conserved across orders while their relative size and complexity are more labile, with variation related to species ecology (e.g. Van Valkenburg *et al.* 2011, 2014 a, b, Green *et al.* 2012, Macrini 2012, Ruf 2014, 2020, Yee *et al.* 2016, Curtis & Simmons 2017, Martinez *et al.* 2018, 2020, Lundeen & Kirk 2019, Wagner & Ruf 2019). However, few studies have tackled the question using proper statistics, geometric morphometrics, evolutionary models or developmental approaches.

At a higher taxonomic scale, turbinals are thought to carry a phylogenetic signal and several studies identified in turbinal bones potential characters linked to phylogenetic relationships (Paulli 1900 a, b, c, Negus 1958). However, in some cases, characters were later found to be wrong. As an example, Gardiner (1982) described synapomorphies related to turbinal morphologies that were later refuted (see examples in Gauthier *et al.* 1988). In mammalian orders or families, the gross turbinal anatomy generally does not significantly vary. For example, Ruf (2020) identified a rodent grundplan for olfactory turbinals that comprises two fronto-turbinals, three ethmo-turbinals, and one inter-turbinal between ethmo-turbinal I and II (see also dog grundplan in Wagner & Ruf 2019). Maier (2000) also suggested that the marginoturbinal is "typical" of therian mammals. However, as usual, exceptions exist. In rodents, some species need histological investigation to be properly used in quantitative analysis. This is for example the case of the naked mole rat (*Heterocephalus glaber*), some porcupines (e.g. *Hystrix*), or some anomaluromorpha (Martinez *et al.* in prep. a, c, Fig. 4). Other studies attempted to score some characters in turbinal bones from adult mammals (e.g. Voss & Jansa 2003, Macrini 2012, Ruf 2014, 2020, Lundeen & Kirk 2019). However, at least in rodents the story is more complicated than expected. Indeed, potential characters previously identified as phylogenetically informative, were proven to be wrong or present numerous exceptions with an exhaustive taxon sampling (Martinez *et al.* in prep. c; Fig. 4). Considering mammals, the shape, complexity and relative size of maxillo-turbinals greatly varies with phylogenetic relationships (Rowe *et al.* 2005, Martinez *et al.* 2020, in prep. a, b, Fig. 7). For example, in Carnivora, Van Valkenburg *et al.* (2014 a) demonstrated that the complexity of maxillo-turbinal differs between caniforms and feliforms with apparent similar ecologies (e.g. terrestrial).

Developmental constraints are also hypothesized to impact turbinal evolution (e.g. Rowe *et al.* 2005). Indeed, turbinals and other structures or organs may be in conflict for space in the nasal cavity. This hypothesis was widely discussed for eyes and some good evidence may have been found in Carnivora (Van Valkenburg *et al.* 2014 b, Ruf 2020). Rodents have ever growing incisors with roots occupying an important part of the nasal cavity. Therefore, it is likely that the variation of shape and orientation of their incisors constrained the shape and development of turbinals (Martinez *et al.* in prep c, Fig. 4). The geometric organization of the masticatory apparatus that starts earlier in the development than the ossification of the ethmoid complex, supports this hypothesis (e.g. Rowe *et al.* 2005). However, an example found in the naked mole rat (*Heterocephalus glaber*) may contradict this hypothesis. Indeed, we identified in the naked mole rat, the loss of the maxillo-turbinal resulting in the presence of a partially empty nasal cavity (Martinez *et al.* in prep. a). The absence of replacement of this empty space by other structures leads us to assume that there is not a strong conflict for space between different structures in the nasal cavity. An alternative hypothesis is that the loss of this structure is ongoing (as suggested by the intra-individual and intra-specific variations) and that there is a delay between the loss and

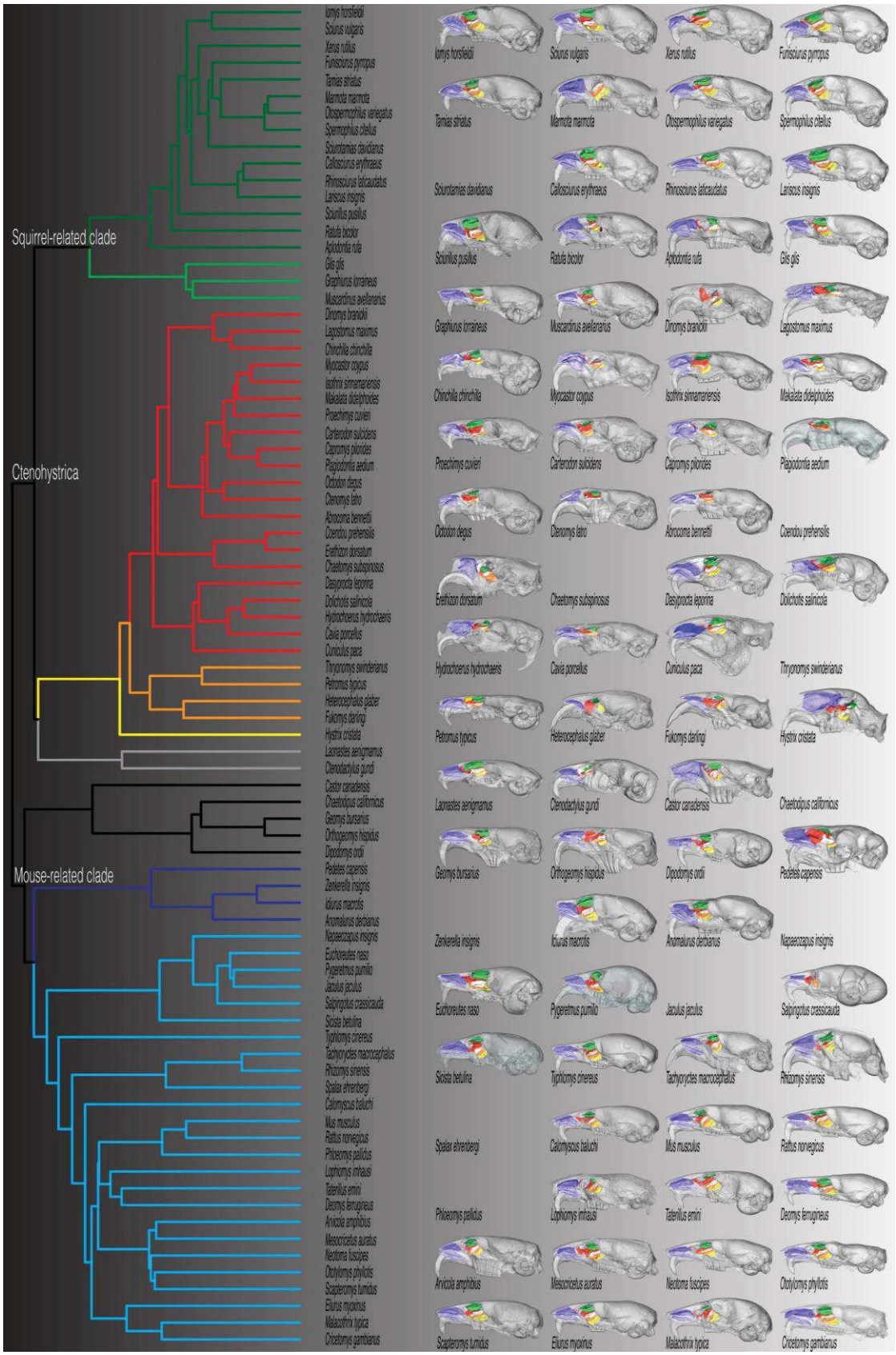

Figure 4: Evolution of turbinals along the rodent phylogeny. Sagittal views of skulls with superimposed 3D representations of turbinals. Ongoing view of the 80 planned species. Colors represent the hypothesised turbinal homologies. Some alternative hypotheses will be presented in the final version. Figure extracted from Martinez *et al.* in prep. (c).

the replacement of these structures. However, this question needs to be addressed using co-variations and / or landmark-based geometric morphometric approaches that remain extremely rare in the field (e.g. Martinez & Fabre 2017 master thesis, Curtis *et al.* 2020). Finally, the loss of the maxillo-turbinal in the naked mole rat (*Heterocephalus glaber*) also suggests that in mammals, maxillo-turbinals may be energetically costly to maintain. Indeed, it is expected that structures or functions that are not costly to maintain may be conserved even if they are no longer under strong selective pressures (Jeffery 2005, Lahti *et al.* 2009, Charles *et al.* 2013).

We previously introduced that turbinal bones may vary with phylogenetic relationships and developmental constraints. However, they cannot explain all the differences observed along the mammalian diversity. Indeed, it is now well known that the relative surface area and complexity of turbinals greatly varies with species ecology. In the following two sections, we will discuss the evolution of olfaction and heat and moisture conservation in the light of species ecology. However, our following discussion will be non-exhaustive. Indeed, species ecology have different meanings (e.g. habitat, diet, sociality) and both olfaction and, heat and moisture conservation may be tackled by different approaches (e.g. morphology, histology, genomics) and anatomical proxies (e.g. turbinals, olfactory bulb, vomeronasal organ).

↑ Back to summary ↑

Part II - Olfaction

Picture of *Mus mattheyi* with superimposed skull and turbinals. Illustration: Quentin Martinez.

1. From a human perspective

From a human perspective, smell has something mysterious that through invisible particles evokes a remembrance of past things (Dugan 2011). As often with unexplained phenomena, mystic interpretations and representations flourished and evolved with societies and cultures. First references of use of products for perfumery may be attributed to ancient Egypt (Dugan 2011). In Europe, it mostly developed in ancient Rome then later in France during the eighteen century with the birth of modern perfume industries (Dugan 2011). In the Greek myths the women of Lemnos were rejected by their husbands because Aphrodite had caused the women to omit a foul odor. This example reflects how most humans perceive the scent of smell: a non-essential scent that gives them comfort in their daily life. However, anosmia, or the loss of the sense of smell is a psychological trauma where people suffer from depression, eating disorders, or sexual problems (e.g. Toller 1999, Boesveldt *et al.* 2017). For example, olfaction plays a key role in the fact that most humans enjoy eating. Indeed, olfaction is responsible for most of what people popularly called taste. However, in medical term, taste is only the discrimination between salt, sweet, sour, bitter, and umami. From a medical perspective, the mix between odors and taste are called flavors. Because the senses of smell and taste have similar receptors, the alteration of the sense of smell will directly affect the sense of taste (e.g. Rouby *et al.* 2002, Labbe *et al.* 2008). Despite the recent media coverage for this trouble linked to the COVID-19, anosmia has various origins such as injuries, viruses, genetic, or neuronal disorders (e.g. Toller 1999, Boesveldt *et al.* 2017). Despite our anthropocentric vision in our industrial world, the scent of smell may have been of major importance in the evolution of the hominid lineage. Indeed, humans discriminate at least 1 trillion olfactory stimuli that is more than the number of colors (several millions) or tones (half a million, Bushdid *et al.* 2014). Also, olfactory receptor genes (ORs) form the largest multigene family in the human genome (Niimura & Nei 2003).

To date, olfaction is a highly dynamic field. In 2004, Linda B. Buck and Richard Axel received the nobel prize in physiology or medicine for their work on olfactory receptors (Buck & Axel 1991). Indeed, they participated in the discovery, the estimation, and the description of the olfactory receptor gene superfamily (ORs). For example, they revealed the specialization of the different olfactory receptors that can only detect a limited number of odorant molecules. They also discovered the connection to the olfactory neurons to specific glomeruli from the olfactory bulb that will later process the information in other parts of the brain, allowing for example the association between the odor and a past experience. Therefore, they significantly contributed to clarify our understanding of odor recognition.

Studies on olfactory neurons participated to change long term dogma indicating that neurons are not replaceable in adult vertebrates (Graziadei & DeHan 1973, Graziadei & Graziadei 1978). Indeed, olfactory neurons are naturally replaced during vertebrate adult life but also after injury (Graziadei & Graziadei 1978). Since these seminal discoveries, other studies

demonstrated that these neuronal replacements may have been underestimated through different parts of the nervous system. As an example, neuronal replacement was highlighted in the high vocal center (HVC) of songbirds, a region associated with song learning (Alvarez-Buylla *et al.* 1988, Scharff *et al.* 2000). In shrews, neuronal number and neocortex width varied with seasons (Ray *et al.* 2020). The reasons for neuronal replacement are not well understood (Nottebohm 2002) but may be advantageous in the case of olfactory epithelium that is widely exposed to injuries (e.g. Harkema *et al.* 2006, Herbert *et al.* 2018). Indeed, it was demonstrated that the nasal cavity and its olfactory pathway was a reservoir but also an entry to the central nervous system for several viruses and pathogens (e.g. Harberts *et al.* 2011). Olfactory ensheathing cells (OECs) are the main target for viruses in the nasal cavity and potentially for COVID-19 (Butowt & Bilinska 2020, Yazdanpanah *et al.* 2020). However, OECs are essential in olfactory neuron neurogenesis in guiding olfactory axons but also in dead cell clearance (e.g. Lankford *et al.* 2008, Harberts *et al.* 2011). In this context, goblet cells (= mucous glands) may play a key role in protection, enzyme activity, and potential immune response (e.g. Harkema *et al.* 2006, Birchenough *et al.* 2015, Herbert *et al.* 2018).

To date, innovations related to olfaction for human applications are numerous and can't be exhaustively listed herein. For example, research and development links to odors are found in evolution, conservation biology, engineering, agro-industry, pest-control, marketing, and public safety (e.g. Stoddart 1980, Hayden & Teeling 2014, Nielsen *et al.* 2016).

2. Olfaction in mammals

a. Olfactory organs

Paleontological discoveries indicated that early cynodonts may have had low olfactory capacities (Rowe *et al.* 2011). In comparison to the basal cynodonts (~260 Mya), *Morganucodon* (~220-200 Mya), has a significant higher encephalization quotient (+ 50%) partially due to the enlargement of the olfactory bulb (Rowe *et al.* 2011). These observations approximately correspond to the expansion of some ethmo-turbinals (Ruf *et al.* 2014). Therefore, it is hypothesized that somewhere between 260 and 220 Mya, cynodonts and mammaliaforms started to significantly rely on olfactory cues. Later, a second pulse of encephalization and increase of the olfactory bulb occurred in *Hadrocodium* (~195 Mya, Rowe *et al.* 2011). A third expansion is described with the development of several olfactory turbinals hypothesized to develop in concomitance to the large mammalian repertoire of olfactory receptor genes (Parsons 1971, Niimura 2009, Rowe *et al.* 2011). Extant mammals largely relied on olfaction and centuries of naturalist observations have highlighted a countless number of examples ranging from the detection of a prey scent track, to mating courtship, or defensive behavior (Stoddart 1980, Evans

2003). Some examples also demonstrated that in an odorant world, mammal olfaction might be tricked or impacted by plants and animals (e.g. Miller *et al.* 2015).

Prior to giving an overview of mammalian olfaction, we need to define what olfactory capacities are (= capabilities). Olfactory performances are mostly discriminated in two major components: (1) the sensitivity (= sensibility, threshold of perception) that is the ability to detect odors at low concentration or at long distance and (2) the discrimination that is the ability to distinguish between two similar odors (e.g. Van Valkenburg *et al.* 2011, 2014 b). Some authors discussed a third component: (3) the acuity (also known as "resolution", Rowe *et al.* 2005) that is sometimes defined as the range of odors that can be detected (e.g. Van Valkenburg *et al.* 2011, 2014 b). However, olfactory acuity is sometime inconsistently employed in reference to olfactory discrimination, sensitivity and of the overall olfactory capacities (e.g. Eayrs & Moulton 1960, Moulton *et al.* 1960, Jones *et al.* 2001, Fletcher & Wilson 2002).

Historically, olfaction was mostly discriminated between two systems: (1) the main olfactory system (including olfactory turbinals) covered by bowman's glands and connected to the main olfactory bulb and (2) the vomeronasal organ (= Jacobson's organ or accessory olfactory organ), without bowman's glands and connected to the accessory olfactory bulb (e.g. Negus 1958, Parsons 1971). These two systems were hypothesized to participate in the detection of distinct components: volatile odorant molecules for the main olfactory system and non-volatile pheromones for the vomeronasal organ. To date, we know that the distinction of the odorant components is more complex and varied between species. Indeed, it was demonstrated that there exists some bridges between these two olfactory apparatuses. In addition, we currently know that the olfactory system is subdivided in more than two systems (Fig. 5).

As discussed in the first section, the olfactory turbinals are considered as the main olfactory system (with some part of the nasal cavity including roof, floor, and sidewalls). Olfactory neurons from these parts project posteriorly via olfactory nerves through the cribriform plate and join the glomeruli from the main olfactory bulb (Fig. 5). Comparative work demonstrated a relation between the relative size of turbinals and species ecology such as diet (e.g. earthworm consumption, scavengers) or lifestyle (e.g. amphibious, terrestrial, e.g. Van Valkenburg *et al.* 2004, 2011, 2014a, Green *et al.* 2012, Martinez *et al.* 2018, 2020). Based on other studies Van Valkenburg *et al.* (2011, citing Laska *et al.* 2005 and Kowalewsky *et al.* 2006) hypothesized that the relative surface area of turbinals may not be correlated to olfactory capacity nor sensitivity. Therefore, they hypothesized that it may characterize the diversity of odorants that can be perceived (herein defined as acuity). However, Martinez *et al.* (2018) demonstrated that highly specialised worm-eating rodents have significantly higher relative surface area and complexity of olfactory turbinals as compared to their close omnivorous and carnivorous relatives. This gave new insights suggesting that the relative size of olfactory turbinals may be linked to olfactory

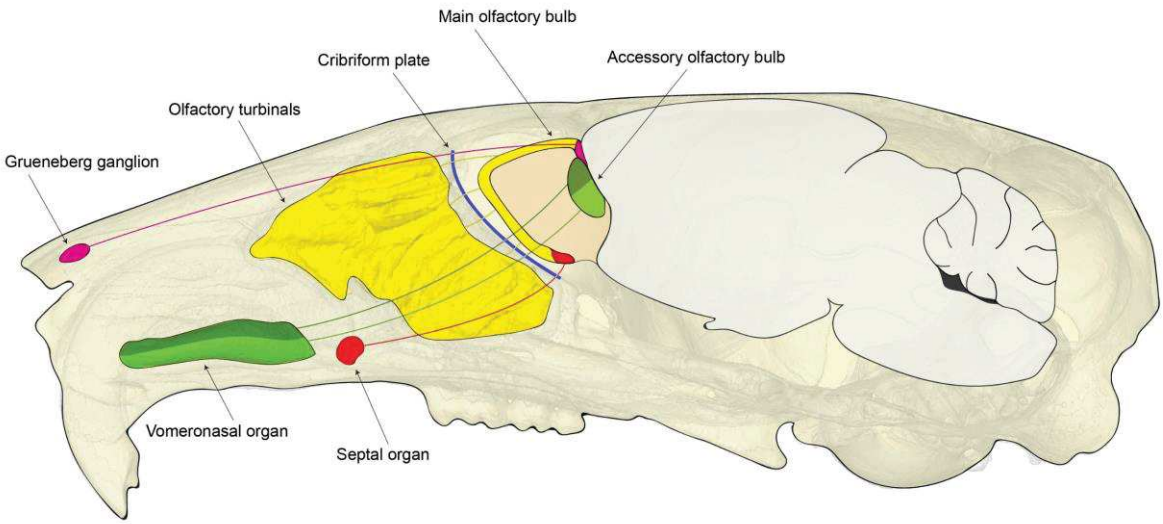

Figure 5: The olfactory system. Grueneberg ganglion (pink), olfactory turbinals (yellow), cribriform plate (dark blue), vomeronasal organ (green), septal organ (red), and their respective nerves connected to the main or the accessory olfactory bulb. Illustration: Quentin Martinez based on Kaluza *et al.* 2004, Storan & Key 2006, Roppolo *et al.* 2006, Ekberg *et al.* 2011, Salazar & Sanchez-Quinteiro 2011.

sensitivity. However, the very small number of studies linking olfactory performance and the relative size of olfactory organs leaves many open questions. Therefore, it might be possible that olfactory proxies based on bony structures inform us on potential olfactory capacities but not on its components namely: sensitivity, acuity, and discrimination. It is likely that it might be essentially impacted by the nature of the olfactory receptors. New evidence will probably emerge from medical studies. Indeed, pathologies of the scent of smell are numerous and include the reduction or the loss of the scent of smell (hyposmia, microsmia, or anosmia), the increase of olfactory sensitivity (hyperosmia), the inability to correctly associated a smell to its nature (parosmia), or even smelling odors that are not actually there (phantosmia). Therefore, by cross-checking the information of these pathologies in relation to neuronal pathways, causes, and organ differences, it will likely be possible to fine tune our knowledge on these olfactory components of the olfactory capacities.

Another well studied organ related to olfaction is the vomeronasal organ. In mammals, the vomeronasal organ is a tubular organ that may be included in a bony or cartilaginous cast in the rostrum (Fig. 5). The vomeronasal organ is mainly composed of olfactory receptors and blood vessels (Evans 2003). Olfactory receptors from the vomeronasal organ morphologically differ from those of the main olfactory epithelium (Stoddart 1980, Villamayor *et al.* 2018). Its highly

vascularized system participates in a pumping mechanism that fills and empties the cavity with air during an active process (Allison 1953). The vomeronasal organ is present or absent in several species without a clearly identified pattern (Evans 2003). Species without a vomeronasal organ in the adult stage generally have it early in the development, such as humans (Evans 2003). The vomeronasal organ is associated with the spectacular flehmen response (= flehmane, flehman) well known in Perissodactyla and Carnivora and that consists of curling back the lips to exposed nasopalatine opening (= ductus, canal). This mechanism may facilitate the inhalation of volatile and nonvolatile molecules through the vomeronasal organ and may be seen as a sniffing process in relation to the vomeronasal organ (Evans 2003). Not all mammals present the main flehmen response with the curling back of the lips and there is a large diversity of active processes related to this response such as mouth opening, direct contact of the nares, lapping, and tongue protrusion. The vomeronasal organ allows the detection of pheromones (= intraspecific level) and kairomones (= interspecific level). It has been demonstrated to have an active role in mating preferences, conspecific recognition as well as aggressivity induction (Evans 2003, Chamero *et al.* 2012). Therefore, it plays an important role in sexual and social behaviors. Extensive studies in house mice suggested that the discrimination of major urinary proteins (MUPs) by the vomeronasal organ may be responsible for assortative mating and therefore involves in speciation (e.g. Smadja & Ganeme 2002, Smadja & Butlin 2009, Hurst *et al.* 2017). Despite some histological and descriptive works (e.g. Cooper & Bhatnagar 1976, Bhatnagar *et al.* 1996, Salazar & Sanchez-Quinteiro 2009, 2011, Villamayor *et al.* 2018), a proper quantification of the vomeronasal organ is rare in a comparative context (Yohe *et al.* 2018).

The Grueneberg ganglion (GG, = septal organ of Grueneberg (SOG), Storan & Key 2006, ≃ terminal endings of the nervus terminalis, Stoddart 1980) is an olfactory subsystem that was "recently" described in comparison to other organs (Grueneberg 1973). This is the smallest of all olfactory organs with for example in mice, a sized range from 300 to 500 cells. It is located anteriorly in the nasal cavity where margino- and atrio-turbinals develop (Fig. 5). In coronal view, the Grueneberg ganglion is located on the dorsal part of the nasal septum with the junction of the wall of the nasal cavity. The Grueneberg ganglion is a cluster of neurons that project posteriorly via olfactory nerves to a specific area of the main olfactory bulb (Fig. 5, Fleischer *et al.* 2006, Roppolo *et al.* 2006, Salazar & Sanchez-Quinteiro 2009). Therefore, some authors have considered this organ to be part of the main olfactory system (Storan & Key 2006) but since it also expresses vomeronasal cell types, the question remains open (Fleischer *et al.* 2006). This organ presents a particular morphology for an olfactory organ because the cilia are not visible in the exterior environment and are included in cells that have a permeable envelope (Brechbuhl *et al.* 2008). The Grueneberg ganglion seems to have a specific role in the detection of the poorly known alarm pheromones (APs, Brechbuhl *et al.* 2008). These pheromones signal conspecific, injury, distress, or the presence of predators (Brechbuhl *et al.* 2008). Outside the seminal work of

Grueneberg (1973), very few studies attempt to investigate this organ in other species (Tachibana 1990, Brechbuhl *et al.* 2014).

The septal organ is a very small organ located on the ventral part of the nasal septum and posteriorly to the vomeronasal organ (Fig. 5). In the mouse, the septal organ is located ventrally to the anterior part of the pars anterior of the etmo-turbinal I (etI). This organ has a ciliated epithelium with olfactory receptors that project posteriorly to a specific area of the main olfactory bulb (Fig. 5, Ma *et al.* 2003). The septal organ expresses olfactory receptor genes of the main olfactory system and not from the vomeronasal organ (Kaluza *et al.* 2004, Tian & Ma 2004). However, the septal organ is probably the least studied olfactory organ and to date, it is attributed to general odor detection, inducing food detection and social interactions (Ma 2007).

The olfactory bulb is a key organ that encodes information that converges from all olfactory organs through olfactory nerves. It is now well known that the olfactory bulb is partitioned in specific areas dedicated to olfactory nerves from different olfactory organs (Fig. 5, Salazar & Sanchez-Quinteiro 2009). This is the case for the main olfactory bulb which is subdivided into specific areas that host olfactory nerves from the Grueneberg ganglion, septal organ, and olfactory turbinals (Fig. 5). The accessory olfactory bulb (AOB) is an area that encodes information from the vomeronasal organ, distinct from the main olfactory process (Fig. 5, Larriva-Sahd 2008). The accessory olfactory bulb is probably mostly present in species with a well-developed vomeronasal organ (Salazar & Sanchez-Quinteiro 2009, Yohe & Davalos 2018). However, some details about the identification and the presence of the accessory olfactory bulb (even in humans) remain controversial (Larriva-Sahd 2008, Salazar & Sanchez-Quinteiro 2009). Despite some rare exceptions, the brain region and therefore the olfactory bulb is probably the most studied and understood organ related to olfaction.

b. Chemosensory receptors and genes

The discovery of a superfamily of olfactory receptor genes (ORs, Buck & Axel 1991) was quickly followed by the identification of the vomeronasal receptor gene family (VRs, Dulac & Axel 1995). Later, the raw data of the human genome were simultaneously published by a private company and a public research consortium (Venter *et al.* 2001, International Human Genome Sequencing Consortium 2001). In 2004, a more accurate human genome was available (International Human Genome Sequencing Consortium 2004). To date, the number and the quality of mammalian genomes have increased exponentially, with more than 400 genomes currently available (e.g. Allio *et al.* 2020 bioRxiv). These resources provide an extraordinary possibility to study the evolution of olfaction.

Chemosensory receptors and therefore genes that coded for these are clustered in four different classes: (1) the olfactory receptors (ORs), (2) the vomeronasal receptors (VNRs), (3) the trace amine associated receptors (TAARs), and (4) the membrane-spanning 4A receptors

(MS4As). Olfactory receptors are mostly expressed in the main olfactory epithelium (= olfactory turbinals, septum nasal, sidewalls, roof, and floor of the nasal cavity). They represent the largest olfactory surface within the nasal cavity and for example, as compared to the vomeronasal neuroepithelium. This observation matches with the fact that ORs are the most represented chemosensory receptors in mammals. A gross estimation in 32 mammals gave 1259 ORs genes in mammals (Hayden & Teeling 2014). However, ORs gene composition and number highly vary across mammalian phylogeny (Niimura & Nei 2007, Hayden *et al.* 2010) and species ecology (e.g. Kishida *et al.* 2007, 2015, Hayden *et al.* 2010, Hayden & Teeling 2014, Hughes *et al.* 2018, Yohe *et al.* 2021 bioRxiv, Courcelle *et al.* in prep.). This is for example the case for diet (e.g. Hayden & Teeling 2014, Hughes *et al.* 2018, Yohe *et al.* 2021 bioRxiv) or lifestyle (e.g. Stathopoulos *et al.* 2014, Courcelle *et al.* in prep.). An astonishing number of studies demonstrated that amphibious or aquatic mammals have a larger number of pseudogene and / or a different ORs genes composition than terrestrial species (Freitag *et al.* 1998, Kishida *et al.* 2007, 2015, Niimura 2009, Zhou *et al.* 2013, Springer & Gatesy 2017, Hughes *et al.* 2018, Beichman *et al.* 2019). ORs genes are classified in two major classes (Class I, II) and are supposed to detect general odors such as environmental conditions and food. Class I is composed of four families of ORs genes specialised in water-soluble odorants (Mezler *et al.* 2001, Zhang & Firestein 2002, Hayden *et al.* 2010). Class II is composed of 9 to 15 families specialised in volatile odorants (Mezler *et al.* 2001, Zhang & Firestein 2002, Hayden *et al.* 2010). As with the turbinal terminology, ORs classification and terminology also differ between authors and the phylogenetic scale of the study (Hayden & Teeling 2014).

Vomeronasal receptors (VNRs) are subdivided in three subfamilies: vomeronasal type-1 receptors (V1Rs), vomeronasal type-2 receptors (V2Rs), and formyl peptide receptors (FPRs). They are mostly expressed in the vomeronasal organ and marginally in the main olfactory epithelium. As previously discussed, VRs are supposed to mostly involve social interactions. The role of the FPRs remains more ambiguous and could be involved in the detection of contaminated compounds such as spoiled food or unhealthy conspecifics (Riviere *et al.* 2009).

Trace amine associated receptors (TAARs) are expressed in the main olfactory epithelium and in the Grueneberg ganglion. They are thought to be involved in social interactions, aversion, and fear detection (Dewan *et al.* 2013, Hayden & Teeling 2014). Five TAARs sub-families are known (I to V) and in mice sixteen genes were identified. However, they remain poorly studied in other mammals (Hashiguchi & Nishida 2007).

As ORs, Membrane-spanning 4A receptors (MS4As) are also expressed in the main olfactory epithelium. However, they may be marginally expressed and are poorly known. One of their particularities is that they projected posteriorly in an area named the “necklace” (= necklace glomeruli) located at the interface between the main olfactory bulb and the accessory olfactory bulb (Juilfs *et al.* 1997, Shinoda *et al.* 1989, Greer *et al.* 2016, Poncelet & Shimeld 2020).

Despite this apparent distinction of chemosensory receptors, several gene expression and performance studies demonstrated that the clustering is less strict than previously thought. Therefore, some pheromone-based receptors (e.g. VRs) are known to be expressed in the main olfactory epithelium (e.g. turbinals). Some environmental based receptors (e.g. ORs) are expressed in the accessory olfactory epithelium (e.g. vomeronasal organ, Mandiyan *et al.* 2005, Yoon *et al.* 2005, Kelliher 2007, Wang *et al.* 2007, Salazar & Sanchez-Quinteiro 2009). However, we do not know if these systems work independently (Kelliher 2007).

Here we gave an overview of the olfactory organs including olfactory turbinals. However, turbinals also play other important functions such as heat and moisture conservation.

↑ Back to summary ↑

Part III - Heat and water conservation

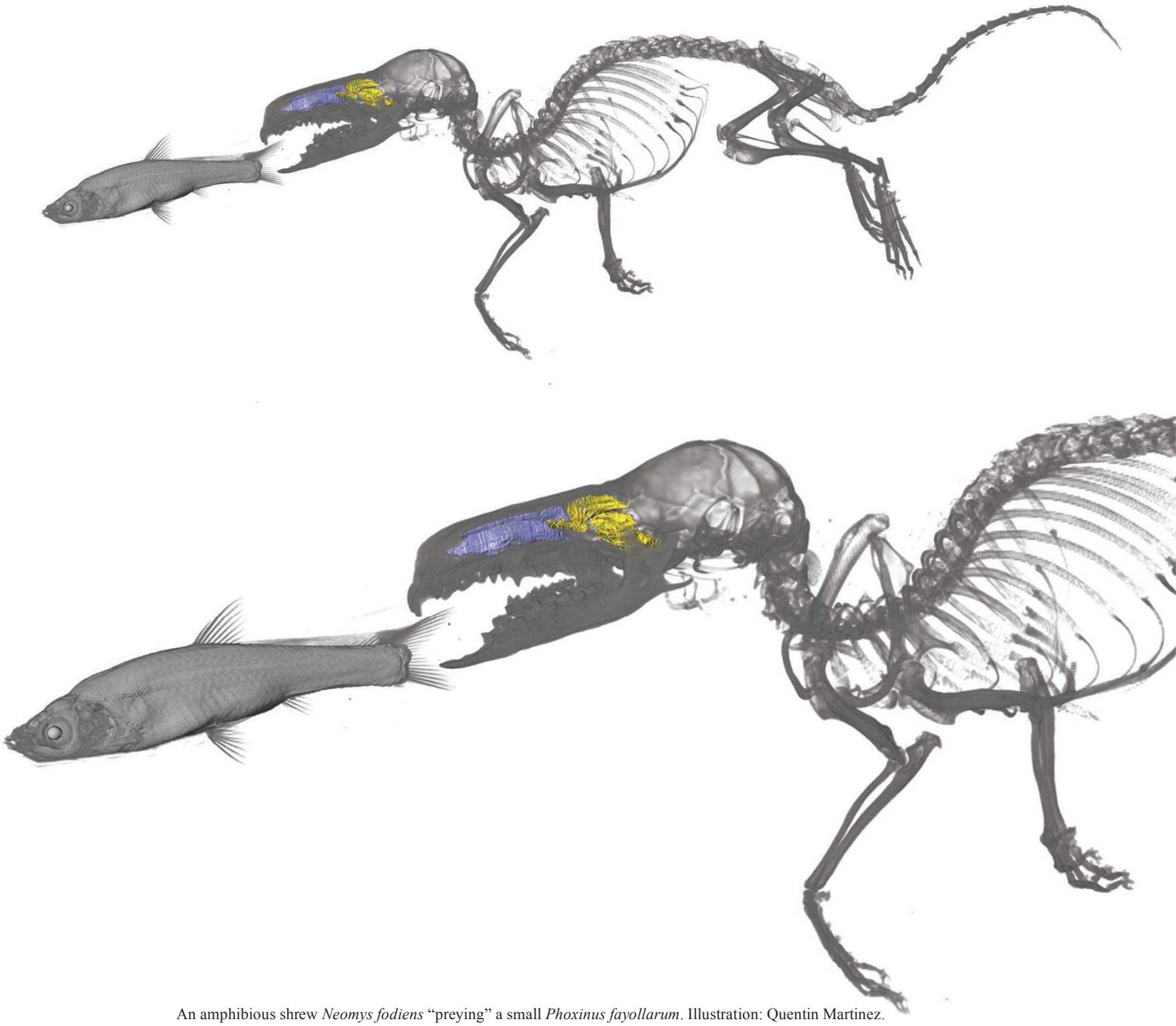

An amphibious shrew *Neomys fodiens* “preying” a small *Phoxinus fayollarum*. Illustration: Quentin Martinez.

Physiological studies related to heat and moisture conservation capacities were legion during the 20th century but have been rarely linked to respiratory turbinals. As an example, experiments tested and demonstrated physiological performance in many animals (e.g. Martin 1903, Schmidt-Nielsen 1965, Collins *et al.* 1971, Whittow 1971). As with olfactory turbinals, the field underwent a renewal with the development of micro-CT (Ruben *et al.* 1996). However, since the last decade, the number of studies linking respiratory turbinals to both heat and moisture conservation capacities has drastically decreased. This phenomenon might be partially explained by the retirement or the death of some eminent researchers in the field (e.g. Knut Schmidt-Nielsen 1915 – 2007 see in Weibel 2007) and the lack of interest for this "non-fashion field".

Respiratory turbinals (= naso- and maxillo-turbinals) are covered with an epithelium that is highly vascularized and made up of several mucus glands. These participate in the warming and humidifying the nasal cavity. In most cases, the inspired air is warmed up and humidified. During the expiration, the air that came from the respiratory tract is at body temperature and fully saturated with water. The temperature of this expired air will decrease in the contact to the anterior part of the respiratory turbinals that were previously cooled down by the inspired air (e.g. Negus 1958, Jackson & Schmidt-Nielsen 1964, Collins *et al.* 1971). This heat reduction will condensate water from the nasal cavity and allow the expiration of drier air (Fig. 6). Therefore, respiratory turbinals play a key role in heat and moisture conservation. This back and forth exchange system is a widespread physiological system often referred as a "countercurrent heat exchange" system (Fig. 6, e.g. Jackson & Schmidt-Nielsen 1964). In rabbits and in some rodent species, it was properly demonstrated that during inhalation, the maxillo-turbinal participated in increasing temperature through the nasal cavity and reach the body temperature (Jackson & Schmidt-Nielsen 1964, Schmidt-Nielsen 1969, Schmidt-Nielsen *et al.* 1970, Caputa 1979). However, in vertebrates, heat and water saving during exhalation, widely varies between species (Schmidt-Nielsen *et al.* 1981).

Kangaroo rats (*Dipodomys spectabilis*) live in hot environments where water resources are limited. This species mostly relies on food for its water needs (Jackson & Schmidt-Nielsen 1964). In the absence of intense activity, sweating evaporation is relatively low, therefore the most important source of water loss is breathing. Several studies demonstrated that this species has more efficient heat and moisture conservation capacities than other species of rodents (e.g. *Rattus norvegicus*). For example, they are able to recover between 54% and 75% of the exhaled water (Schmidt-Nielsen *et al.* 1970, 1981, Collins *et al.* 1971). Surprisingly, they are also able to exhale air 14°C below their body temperature and even below the exterior temperature (Jackson & Schmidt-Nielsen 1964, Schmidt-Nielsen 1969). In a similar environment, experimentations were performed on highly dehydrated camels with presumed drier nasal cavity. They demonstrated that the water saving process works similarly compared to normal conditions (Schmidt-Nielsen *et al.* 1981).

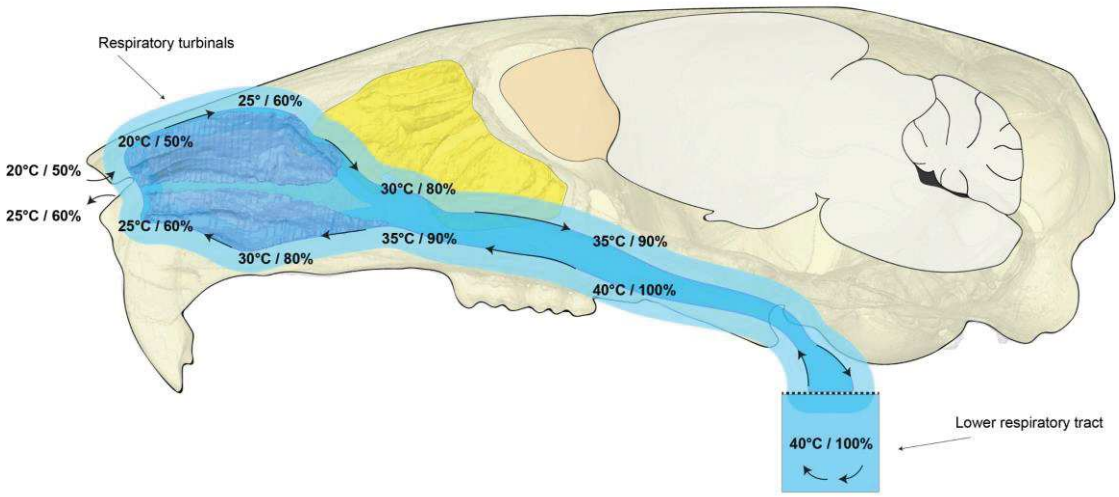

Figure 6: Principle of heat and moisture conservation along the respiratory tract. Heat transfers are the result of convection, whereas water transfers are driven by evaporation and condensation. In this example, performances of the respiratory tract allow to save 15°C and 40% of humidity at expiration. Illustration: Quentin Martinez based on Walker & Wells 1961, Jackson & Schmidt-Nielsen 1964, Collins *et al.* 1971.

However, in hot environments, variations were observed in the efficiency of respiratory turbinals between day and night. Indeed, camels recovered 70% of the water loss during night exhalation whereas this recovery fell to 25% during the day. Similar variations were observed for heat cooling efficiency. These variations may be explained by the variation in blood pressure intensity and airflow current (Langman *et al.* 1978, Schmidt-Nielsen *et al.* 1981).

Unexpectedly, cold deserts such as in arctic regions have generally drier air than hot deserts (e.g. Langman 1985). Experimental studies on reindeer demonstrated that this species exhaled relatively cold and dry air. Therefore, it was estimated that this species was required to drink only 73 ml of water per day (resting at -5 °C, Langman 1985). However, if this species had been exhaling saturated and warm air (as humans do) it would require to drink 17 times more (1.24l, Langman 1985). Langman (1985) also estimated that during expiration, this species recovered 75% of heat that was previously added to the inspired air. Therefore, this species, that experiences drastic climatic conditions, presents some adaptation to save energy. In a similar context, due to the high thermal inertia of water, mammals lose heat quicker in water than in air of the same temperature (Molnar 1946, Smith & Hanna 1975). Therefore, amphibious and aquatic mammals may be adapted to limit heat loss with for example an efficient heat exchanger (e.g. large respiratory turbinals, Van Valkenburg *et al.* 2011, Martinez *et al.* 2020).

To date, the correlation between the relative size of respiratory turbinals and the capacity of heat and moisture conservations was not properly tested. However, preliminary investigation supported this correlation (Martinez *et al.* in prep. b, Fig. 7). For example, the reindeer (*Rangifer tarandus*) has the largest relative surface area of maxillo-turbinals (Maxillo RSA) of any investigated mammals (Martinez *et al.* in prep. a, b, Fig. 7). This arctic species is known to have efficient heat and moisture conservation capacities (Langman 1985). Similarly, Pinnipedia that are known to have extremely complex and well developed maxillo-turbinals (Van Valkenburg *et al.* 2011, Mason *et al.* 2020, Martinez *et al.* in prep. b) have a high efficiency in their moisture conservation capacities that may be an adaptation to a salty environment (Lester & Costa 2006). Humans (*Homo sapiens*) that are known to expire fully saturated air at a temperature close to the body temperature (Walker & Wells 1961, Schmidt-Nielsen 1969) have a medium-size Maxillo RSA as compared to other mammalian orders (Martinez *et al.* in prep. a, b). Finally, the naked mole rat (*Heterocephalus glaber*) has among the highest evaporative water loss recorded in mammals (Collins *et al.* 1971, Buffenstein & Jarvis 1985, Buffenstein & Yahav 1991) and also the lowest thermoregulatory capacities among terrestrial mammals (Martin 1903). This species presents a unique pattern of the reduction of maxillo-turbinals (Martinez *et al.* in prep. a, b).

Lastly, a positive correlation was found between metabolic rate and the residuals of respiratory turbinal surface area to body mass (based on 10 species, Owerkowics *et al.* 2015). However, using the relative surface area of maxillo-turbinals (Maxillo RSA), preliminary investigations across mammalian orders (424 individuals from 310 species, Martinez *et al.* in prep. b, Fig. 7) seem to not recover this pattern. This is especially true for species known to have poor temperature regulation, low body temperature and / or low rates of metabolism such as some marsupials, monotremes, Xenarthra and anteaters (Martin 1903, Wislocki 1933, Enger 1957, McNab 1966).

Despite their additional protective role against abrasive and toxic external elements (e.g. Morgan & Monticello 1990, Harkema *et al.* 2006), respiratory turbinals are also assumed to participate in cooling brain temperature via the carotid rete (Baker & Hayward 1968, Langman *et al.* 1978, Schmidt-Nielsen *et al.* 1981). As with olfaction, the heat and moisture conservation capacities are multifactorial processes and other factors than turbinals have to be considered. This is for example the case of the efficiency of oxygen extraction (Schmidt-Nielsen 1969), body surface evaporation (Burch & Winsor 1944), efficient renal mechanism for water conservation (Schmidt-Nielsen & Haines 1964), lung structure (e.g. alveoli and exchange surface, Lester & Costa 2006), or the fur and keratinous cover of the skin.

Finally, despite the title of this PhD thesis and the published papers, we mostly focused our research and our discussion on the olfactory aspect of turbinals. Ongoing and future work will more precisely explore these questions (Martinez *et al.* in prep. a, b).

↑ Back to summary ↑

Part IV - Discussion and perspectives

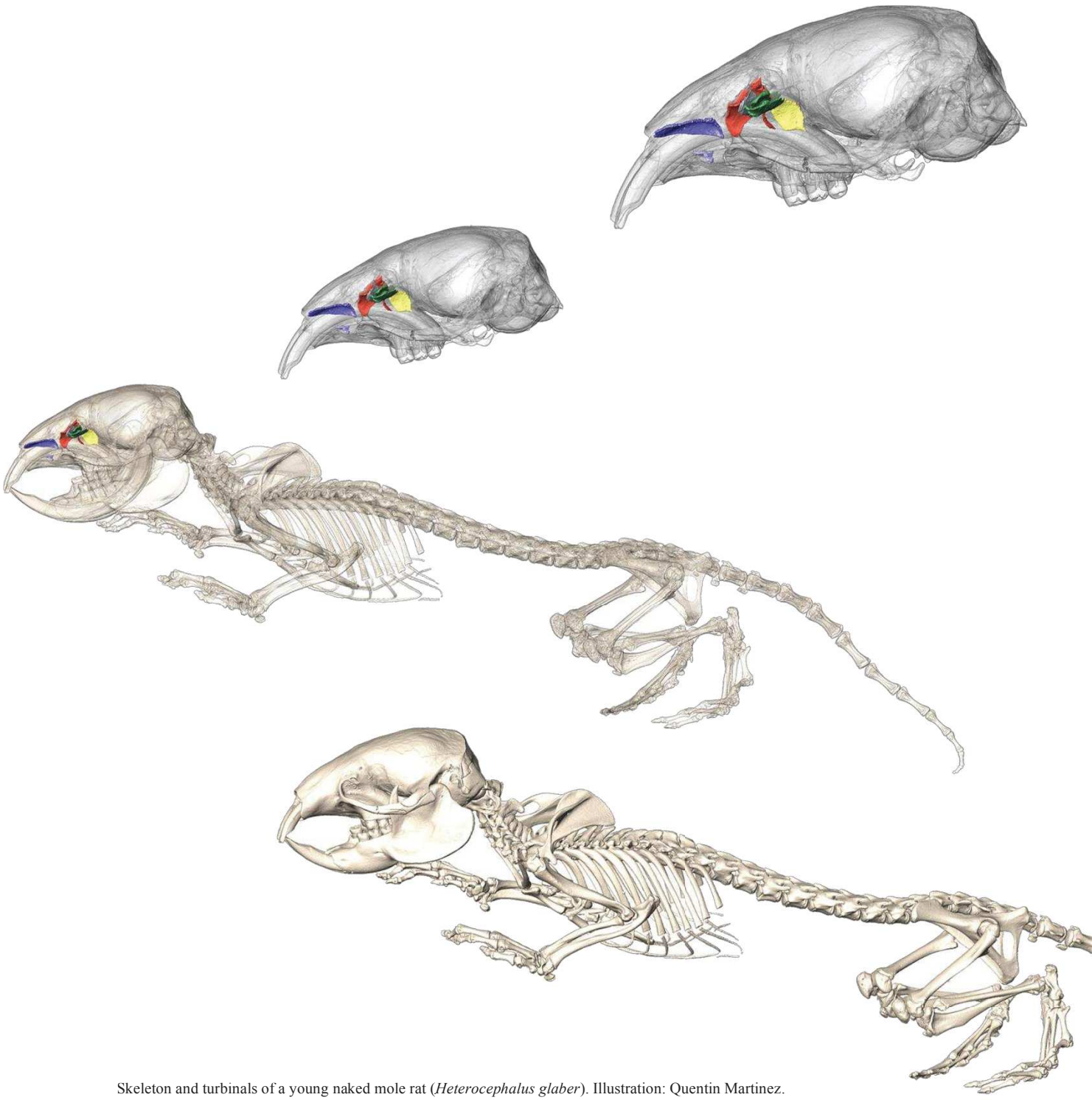

Skeleton and turbinals of a young naked mole rat (*Heterocephalus glaber*). Illustration: Quentin Martinez.

1. Refining quantification

Since the very beginning of comparative studies on turbinals, authors have described turbinal complexity with their own words (e.g. Paulli 1900, a, b, c, Negus 1958, Parsons 1971, Schreider & Raabe 1981, Hillenius 1992). To date, the increasing of turbinal complexity is described as the development of infolding and small lamellae called epiturbinals and resulting from repetitive mesenchymal growth (e.g. Van Valkenburg *et al.* 2014 b, Ruf 2020). From a statistical perspective, turbinal complexity is often described as the degree of details in a predefined area (e.g. Martinez *et al.* 2018). This definition is often considered close to the fractal dimension (or fractal pattern), an index of complexity (e.g. Craven *et al.* 2007, Martinez *et al.* 2018, Wagner & Ruf 2019). Turbinal complexity is rarely quantified and always in 2D. Recent methodological advances allow to study the 3D complexity directly on segmented surfaces (Martinez *et al.* 2018, method developed by Renaud Lebrun and implemented in MorphoDig freeware, www.morphomuseum.com/morphodig, Lebrun 2018). In rodents, results do not significantly change between 2D and 3D methodologies (Martinez *et al.* 2018). However, in some species, turbinal complexity differs antero-posteriorly, and therefore may be problematic for 2D complexity quantification. Therefore, we recommend the use of 3D complexity that is also more convenient and less sensitive (Martinez *et al.* 2018, pers. obs.). In rodents, Martinez *et al.* (2018) demonstrated that there is a significant correlation between complexity and surface area. However, at least for olfactory turbinals, the significance and the R are low. Nevertheless, the use of one proxy or another in statistical analyses provides similar results. These results support the functional significance of most turbinal studies that only used the surface area proxy. However, similar work has to be made for all other mammalian clade where strong differences exist. In Monotrema, the surface area of the maxillo-turbinal of the platypus (*Ornithorhynchus anatinus*) and echidnas (*Tachyglossus aculeatus*) only differs by a factor of 4 (that is not huge for mammals) but their morphology is remarkably different (Martinez *et al.* in prep. a b, Fig. 7). The platypus has a very complex maxillo-turbinal with several small lamellae originating from the main three branches, being similar to some Carnivora and aquatic/amphibious species (e.g. Van Valkenburg *et al.* 2011, Martinez *et al.* 2020, in prep. b). In contrast, the echidna has no additional lamellae to the main three branches but an unusual thickening that is proportionally thicker than pachyostosis turbinals found in giant and amphibious sloths (Amson *et al.* 2018). In these examples, complexity tests (e.g. fractal dimension) and work on airflow dynamics may significantly improve our knowledge of how turbinal complexity improves performances. Indeed, we do not know how turbinal complexity changes the airflow dynamics and the odorant deposition. It is known that increasing turbinal surface area will consistently increase the surface area of epithelium and potentially olfactory performance. Based on fluid dynamic principles, Martinez *et al.* (2018) hypothesized that the increase in turbinal complexity may increase the

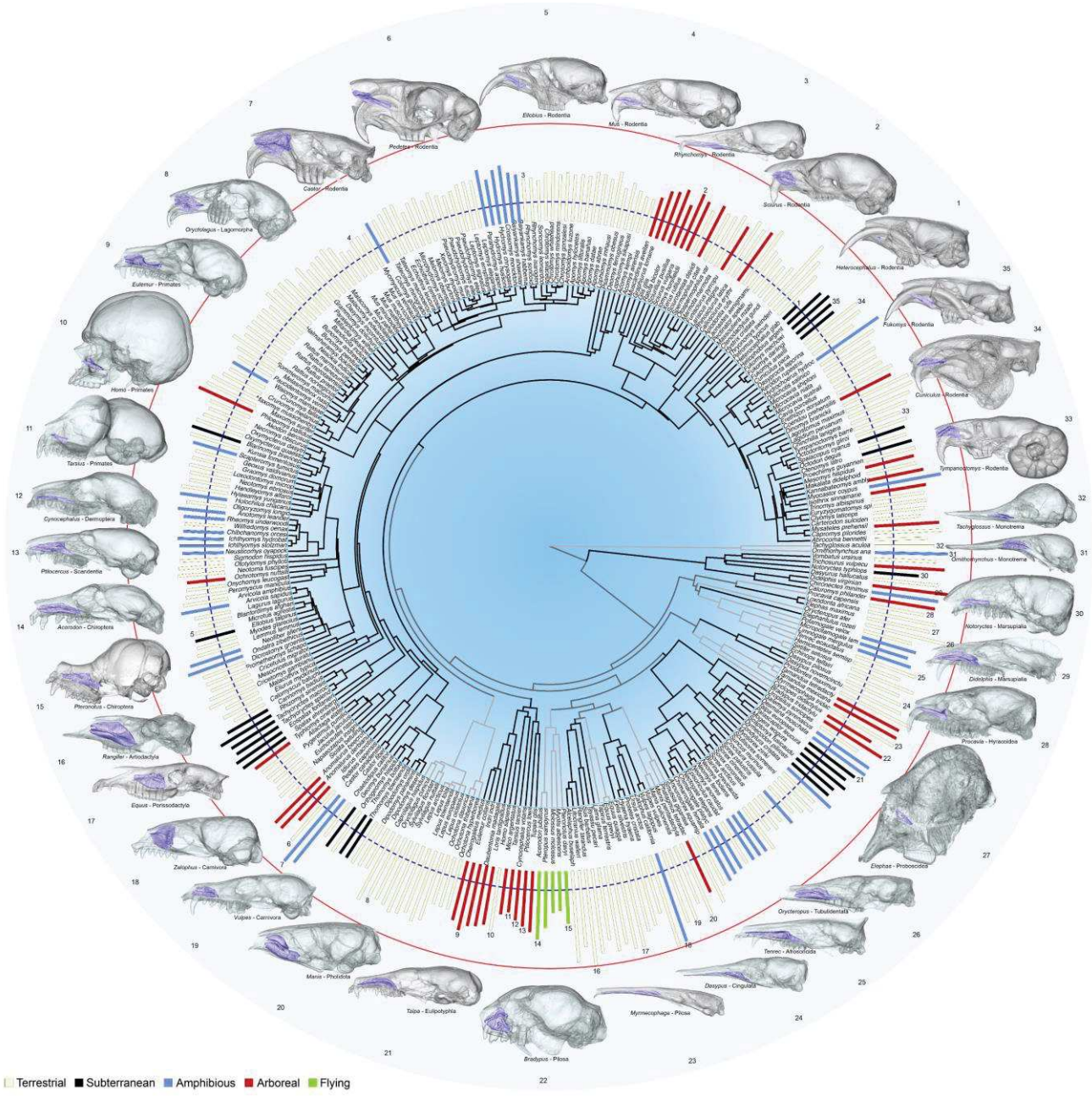

Figure 7: Evolution of maxillo-turbinal at the mammalian scale. Phylogeny of the sampled species with barplots of the relative surface area of maxillo-turbinals (log). Blue and red circles respectively represent the minimum and the maximum logged values from the naked mole rat (*Heterocephalus glaber*) and the reindeer (*Rangifer tarandus*). Barplot legend colors: beige = terrestrial, red = arboreal, blue = amphibious, black = subterranean, and yellow = flying species. Figure based on 424 individuals and 310 species and extracted from Martinez *et al.* in prep. (b).

proportion of air in contact with epithelium. Therefore, the increasing in turbinal complexity may facilitate an increase in air temperature and the absorption of odorant molecules to olfactory receptors.

As previously introduced, the epithelia (e.g. respiratory and olfactory epithelium) do not only line turbinals but the complete nasal cavity that includes turbinals, nasal roof, floor, recess, sidewalls, and laminae (Rowe *et al.* 2005, Herbert *et al.* 2018, Ruf 2020). Therefore, to estimate the intrinsic olfactory, and heat and moisture conservation capacities, we need to precisely estimate the extent of epithelial cover. However, this presents some problems. First, the exact composition and localization of the epithelium is only known in a few species, which is a major methodological limitation while using a micro-CT-scan bony inference. Unlike turbinals or laminae, the nasal roof, floor, and some parts of the sidewalls do not present a clear bony delimitation that matches with their epithelium. Therefore, which bone and how thick a bone structure must be segmented? Even using a mean value based on the mean epithelial thickness covering the nasal cavity, it is likely that there will be significant variation between segmentation sessions and users. Using additional histological data, Martinez *et al.* (2020) refined the antero-posterior discrimination of the ethmo-turbinal I (etI) in rodents, Afrosoricida, and Eulipotyphla. However, the inclusion or the exclusion of the anterior part of the pars anterior of the etI, does not significantly affect quantitative results and conclusions (Martinez *et al.* 2020, pers. obs.). Similar observations were made with naso-turbinals and the uncinate process of the lamina semicircularis (Martinez *et al.* 2018, 2020, pers. obs.). Consequently, we believed that the most important in comparative studies is to be consistent. Indeed, in the light of our current knowledge and since some olfactory organs are complicate to quantify, it is very delicate to estimate the true intrinsic size of all structures related to one particular function (e.g. olfaction).

Concerning mammalian brains, the limits of the different anatomical parts are well known and rarely debated. Therefore, analyses using brain endocast volumes or encephalization quotients (EQ) issued from different studies, may be performed with a good degree of confidence. However, for turbinals where delimitations are still debated and with an important heterogeneity in the quality of scans, we do not recommend to employ turbinal datasets issued from different segmentation sources. Indeed, as other small bony structures, turbinal bones are sensitive to the resolution, the quality of the acquired images, and to the segmentation. Our experience and our control tests in small terrestrial mammals demonstrated that differences are marginal for scans of the skull acquired with a good resolution (pers. obs.). However, for large mammals presenting highly complex olfactory turbinals (e.g. artiodactyls) the scan of the skull is not enough and required a proper scan of their ethmoidal area. For more complex structures such as the cribriform plate and despite the use of different proxies (e.g. the number and the surfaces of holes, the complete surface area, and the surface area from a single view), our personal experience demonstrated that there is an extremely high sensitivity to the resolution, the quality of the

acquired images (e.g. contrast, blur or noise) and the segmentation (Hautier *et al.* 2019, pers. obs.). Indeed, the cribriform plate is a very thin bony structure with sutures only visible in high resolution. In addition to the main large foramina, the cribriform plate is composed of several very small foramina that are only visible with very well acquired images (Fig. 3).

The last aspect of an accurate estimation of the turbinal surface area is the condition of the scanned specimens. Cleaned skulls using dermestid beetles have generally well preserved turbinals (Voss & Jansa 2003) but this is not the case for other methods of preparation (e.g. maceration, boiling). In museums, a significant portion of the skull manually cleaned presents damaged respiratory turbinals. Therefore, it is sometimes challenging to find proper specimens with undamaged turbinals and for some rare species these may not exist. The identification of partially damaged respiratory turbinals may be very delicate in some species or between orders (Martinez *et al.* in prep. a, b, c, pers. obs.) and therefore, some prior studies used or kept specimens with broken turbinals (e.g. Pang 2017). Also, macroscopic inspection did not always prevent the selection of undamaged specimens. Olfactory turbinals may also be damaged due to trapping methods or brain extraction. In some individuals, agglomerates of dry epithelium may be difficult to discriminate from bony turbinals. The use of fluid preserved heads or full body specimens generally avoids bad surprises, however it will decrease scan quality and resolution.

Lastly, the high number of papers related to turbinals, largely demonstrates the scientific value of this bony structure. However, we must notice that turbinal bones are still employed for DNA extraction, sometimes in rare and historical specimens (Martinez *et al.* 2018).

2. Integration

Olfaction is a complicated function relying on multifactorial processes, under many different selective pressures. For example, a single odorant molecule can be detected by a specialized receptor or multiple receptors operating independently or in combination. However, a single olfactory receptor could also bind several odorant molecules. In addition, odorant molecules with different structures may be perceived as a single odor and different odorant molecules with a similar structure may be perceived as different odors (reviewed in Niimura 2012, Hayden & Teeling 2014, Yohe & Brand 2018). Therefore, without a clear understanding of the covariation between olfactory organs, it is difficult to confidently discuss the intrinsic olfactory capacities of a species. Concerning mammalian brains, extensive tests were implemented using different brain areas and different anatomical layers (e.g. encephalization, neurons) mainly including the olfactory bulbs both for model and non-model species (e.g. Ribeiro *et al.* 2014, McGann 2017). Relative brain volume and other brain proxies, may not always correlate with the actual performance in comparison to more accurate proxies such as neuronal activity or the absolute neuron number (e.g. Herculano-Houzel *et al.* 2014, Oliveira-pinto *et al.* 2014).

Based on alternative non-brain proxies, researchers have discussed patterns related to olfaction (e.g. Martinez *et al.* 2020). However, few studies have properly tested co-variation between different organs or proxies related to olfaction. One of the first works investigating co-variation in olfactory-related organs was probably Bhatnagar & Kallen (1974). Using forty species of bats, they found interesting correlations between the number of perforations of the cribriform plate and its surface area, between the diameter of the olfactory bulb and the cerebral hemisphere, and finally between the volume of the olfactory bulb and the surface area of the cribriform plate. Investigating sixteen mammal species, Pihlstrom *et al.* (2005) found a relation between the surface area of the cribriform plate (estimated by linear measurements) and the surface area of olfactory epithelium of the nasal cavity (therefore, including olfactory turbinals). Based on eight species, they also found a relation between olfactory sensitivity to butyric acid and the estimated surface area of the cribriform plate. However, this relation turned out to be non-significative while considering the relative surface area of the cribriform plate. Because the cribriform plate is linked to the olfactory bulb (being part of the brain endocast), the olfactory sensitivity may be linked to the absolute size of the cribriform plate and the olfactory bulb. Despite the quality of this paper and the fact it became a landmark for the field, we believe that similar work must be done with the current technologies and estimations (see also Bird *et al.* 2018). Indeed, the estimation of the cover of olfactory epithelium methodologically differs among studies and it is unclear what is considered as the ethmoid bone. Moreover, since the class of odorant molecules is highly diverse it may not be sufficient to isolate which component of the olfactory performance is related to morphological variation (e.g. sensitivity vs discrimination). For example, faunivorous mammal predators (e.g. Carnivora, Eulipotyphla, and sanguivorous bats) may be highly sensitive to carboxylic acids whereas frugivorous species (e.g. squirrel monkey) are highly sensitive to acetate and 1,8-cineole (Laska *et al.* 2000).

In 2014, Garrett & Steiper pushed the boundaries of the field in studying genetic and morphology (Garrett & Steiper 2014). They found a positive correlation of the absolute size of the cribriform plate (there, named ethmoid bone) and the total number of functional OR genes. This correlation turned out non-significant while correcting the cribriform plate for size. They did not find a correlation between the functional V1R genes and both the relative and the absolute length of the vomeronasal groove (from the vomeronasal organ). However, they decided to present the positive correlation between the proportion of functional V1R genes (= functional genes / all genes) and the relative length of the vomeronasal groove. In spite of the novelty of this integrative study, several methodological and conceptual problems can be pointed out. First, quantitative data of morphological proxies originated from several different studies with divergent methodological protocols. Then, the study made the inference that linear measurements of the cribriform plate positively correlated with the total surface area of the main olfactory epithelium (therefore based on Pihlstrom *et al.* 2005). Finally, and this is our major concern, they

decided to present (1) the positive correlation between the functional OR genes and the cribriform plate proxy and (2) the positive correlation between the proportion of functional V1R genes (= functional genes / all genes) and the vomeronasal organ proxy. Since, there is no correlation between the absolute number of functional V1R genes and the morphological proxy (Garrett & Steiper 2014 supplementary data), the proportion of the functional V1R genes does not provide any information about potential functions and performance. Therefore, the reader needs to carefully read the supplementary data to avoid misinterpretations. Using available data on the olfactory receptor genes (ORs, from Hayden *et al.* 2010, Matsui *et al.* 2010, Hughes *et al.* 2013, Montague *et al.* 2014, Niimura *et al.* 2014), Bird *et al.* (2018) demonstrated in 26 mammalian species a correlation between the relative surface area of the cribriform plate and the functional ORs genes. In Carnivora the surface area of the cribriform plate but also the estimated cross section of their foramina correlated with the surface area of the olfactory turbinals (Bird *et al.* 2014). Therefore, based on the mammalian correlation between the cribriform plate and the functional olfactory receptor genes (ORs), we may hypothesise that turbinals may correlate with ORs. However, this must be further tested. Indeed, a correlation was found in myrmecophagous mammals between the cribriform plate and olfactory turbinals, but also between the cribriform plate and the respiratory turbinals where no apparent functional hypothesis exists (Hautier *et al.* 2019). Interestingly, they found similar correlations with the olfactory bulb, the olfactory turbinals, and the cribriform plate (Hautier *et al.* 2019). Comparing four phyllostomid species, Yohe *et al.* (2018) described a reduction or loss of the vomeronasal organ. These observations not always matched the pseudogenization of a gene that generally encodes for vomeronasal neuronal transduction (TRPC2). Similarly, they described the covariation between the vomeronasal organ and olfactory turbinals without finding a clear pattern.

Despite some limits, we believe that all these studies significantly contribute to this very complicated field by studying covariation. In addition, we may notice that some organs were never quantified in a comparative and inter-specific approach such as Grueneberg or septal organs and our understanding of the mechanisms is limited. Also, in this section we do not discuss organs related to the heat and moisture conservation capacities. However, it is clear that similar integrative studies may improve our understanding of these functional processes.

Two of our ongoing projects try to refine current functional hypotheses in studying covariation in olfactory-related organs. First, in collaboration with Nelly Pirot from “Réseau d’Histologie Expérimentale de Montpellier”, we are currently working on the mapping of the nasal cavity of non-model rodents and on the quantification (= semi-quantification) of the olfactory receptors in the olfactory epithelium (Martinez *et al.* d, Fig. 8). To do so, we worked on fluorescent immunostaining that detects olfactory neurons and their axons (= goat anti olfactory marker protein, OMP, Wako, cat#019-22291, 1:8000). Contrary to classical histology and staining (e.g. HES, hematoxylin, eosin, and safran) where we differentiate epithelia from the

morphology and the composition of their cells, immunohistochemistry reveals the expression and provides actual proof of function (e.g. for olfactory neurons in this case). In order to increase the repeatability of the protocol and the accuracy of our results, our goal was to adapt the immunostaining protocol on an automated staining instrument (VENTANA Discovery Ultra, Ventana Medical Systems). We succeeded in the development of the OMP protocol and its adaptation on an automated system in inbreed and wild mice (Fig. 8). We are currently working to adapt it to non-model rodent species with different conditions of tissue fixation. Using this methodology, we will be able to map the nasal cavity of several rodent species across the phylogeny and include in addition, species with contrasted ecological lifestyles. This work may improve our understanding of the variation in mammalian orders and help us to refine quantitative approaches based turbinal proxies. In addition, we should be able to study the neuronal density of homologous areas in order to test the potential correlation with turbinal or epithelial surface area.

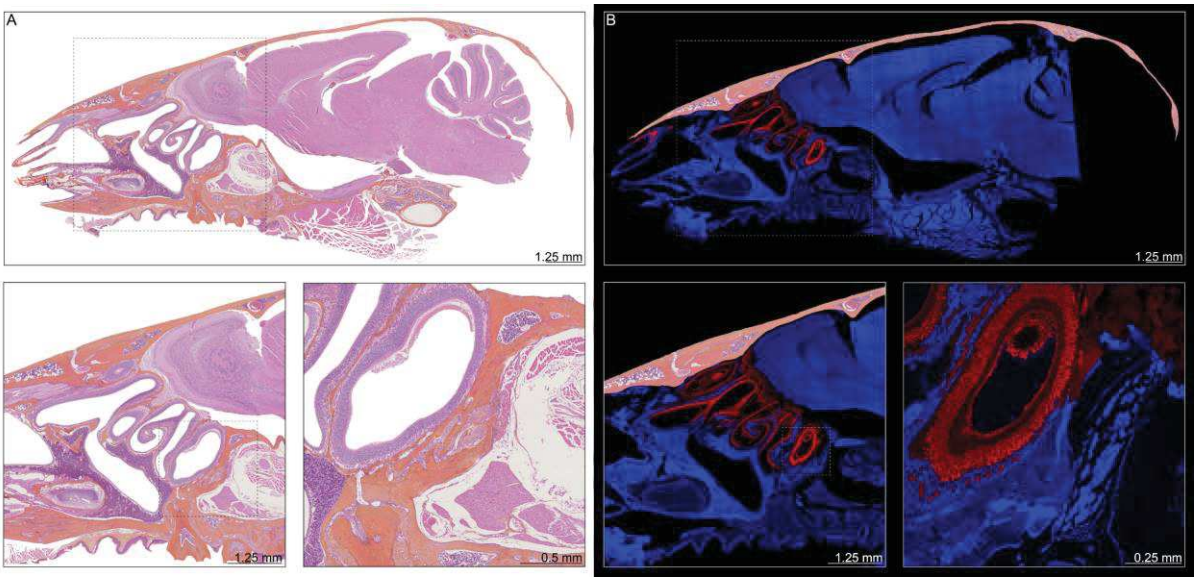

Figure 8: Sagittal sections of the head of *Mus musculus domesticus* (inbred strain named "wild type" WLA) with a zoom on the ethmo-turbinal III. (A) Haematoxilin-Eosin-Saffron (HES) staining. (B) Superimposition of two fluorescent spectra (cy5 in red and DAPI in blue) from the combination of two antibodies (= multiplex staining, OMP x PCK): the olfactory marker protein (OMP, goat anti OMP Wako, cat#019-22291, 1:8000) and the Pan-Cytokeratin (PanCK). Therefore, olfactory receptors are marked in red and cell nuclei in blue. Figure extracted from Martinez *et al.* in prep. (d).

In collaboration with Marie-Ka Tilak and Rémi Allio, we are currently working on the transcriptomics of olfactory turbinals in two non-model species (Martinez *et al.* e, Fig. 9). Indeed, Martinez *et al.* (2020) demonstrated that the amphibious *Myocastor coypus* has highly reduced olfactory turbinals (= relative surface area and the number of olfactory turbinals) in comparison to one of its close terrestrial relative, the *Proechimys* genus. Therefore, we sampled olfactory turbinals in *Myocastor coypus* and *Proechimys cuvieri* and we succeeded to obtain good quality transcriptomes. These data will allow us to test for potential differential expression of coding genes in the olfactory turbinals. We will test whether these results match the relative surface area of the olfactory turbinals. In addition, we plan to correlate these results with quantitative data extracted from other olfactory-related organs such as the vomeronasal organ, cribriform plate, and olfactory bulb (Fig. 9).

3. Proofs of concepts and performances

It is common to read in popular press or even in research articles that a particular species has an x time higher scent of smell than another one. For example, in Brooker & Wong (2020): “sharks have an olfactory sense hundreds of times better than ours”. However, such affirmations are extremely imprecise and complicated to demonstrate. Do the authors refer to the relative size of an olfactory organ or to accurate olfactory performances in sensitivity or discrimination?

The major paradigm of olfaction that persists since more than a century, contrasts macrosmatic and microsmatic organisms (e.g. Turner 1890, Parsons 1971, Stoddart 1980). The first having good olfactory capacities and the latter, poor ones. Following these misleading terms, researchers inconsistently described vertebrates as macrosmatic, and for example contrasted microsmatic birds to the macrosmatic mammals (e.g. Stoddart 1980). One of the most popular examples is probably the comparison between the “very good” sense of smell of the dog and the “very bad” one of humans. This common affirmation probably originated to the quantification of the olfactory epithelium that lines the nasal cavity (e.g. Negus 1958, Harkema & Morgan 1996). To date, this statement is admitted as a fact and by extension several authors extrapolated it affirming for example that Carnivora and mammals have a good sense of smell (e.g. Parsons 1971, Hillenius 1994). However, the question is still highly debated and, in the absence of exhaustive and integrative studies, it remains open (e.g. McGann 2017). As an example, it is true that the relative size of olfactory organs (olfactory turbinals, vomeronasal organs, and olfactory bulbs) significantly differs between dogs and humans (e.g. Negus 1958, Adams & Wiekamp 1984). Moreover, dogs have twice the number of functional olfactory receptor genes compared to humans (Niimura *et al.* 2017). On the other hand, some olfactory capacities may be linked to the absolute number of neurons and for example, humans have better discriminatory and sensitivity capacities than dogs for particular odorant molecules (Herculano-Houzel *et al.* 2014, Oliveira-pinto *et al.* 2014, McGann 2017). Experimental studies in dogs and humans suggested that the

apparently poor human olfaction may be partially due to the current absence of behavioral demands. Indeed, humans are able to follow a scent-track as dogs and significantly improved with training (Porter *et al.* 2007). Similarly, olfactory performance tests in squirrel monkeys demonstrated that this "microsmatic" species has "good" capacities for sensitivity and discrimination, sometimes better than "macrosmatic" dogs or rats (e.g. Laska & Hudson 1995, Laska & Freyer 1997, Laska *et al.* 2000). Another good example of these "shortcuts", is the apparent lack of olfactory organs in odontocetes (= toothed whales) that are often considered as anosmic mammals (Turner 1890, Parsons 1971). However, due to the difficulty of studying odontocetes, these affirmations are based on the gross anatomy and precise anatomical and developmental investigations may tell a different story (Klima 1995, 1999, Mead & Fordyce 2009, Berta *et al.* 2014). In addition, it was recently demonstrated that bottlenose dolphins (*Tursiops truncatus*) may be able to detect and even discriminate olfactory composants, suggesting that they may rely on olfaction for their diet (Kremers *et al.* 2016, Bouchard *et al.* 2017). In a similar environment, recent discoveries demonstrated that some amphibious shrews and desmans (= Eulipotyphla) are able to detect odorant molecules underwater using bubbling behavior (Catania 2006, Catania *et al.* 2008, Ivlev *et al.* 2013). This behavior may be underestimated in amphibious mammals.

Therefore, are these macrosmatic and microsmatic 19th-century terms (Turner 1890) still valid concepts? Probably not (see also Laska *et al.* 2000, Smith *et al.* 2004, McGann 2017). Indeed, it is not too hazardous to realise some comparisons and even extrapolations to potential olfactory capacities between similar organs in relatively closely related taxa (e.g. family, order). However, is it relevant for highly divergent species, with different ecology, and selective pressures (e.g. shark vs human)? Also, precise terminology (e.g. olfactory performance component or class of odorant molecules) may be used to avoid strong hypothetical interpretations.

In an era where the cost for scanning specimens and acquiring genomic data constantly decreased, the number of available data exponentially increase. The explosion of data in biology and in science in general faced the big challenge of how to handle and analyze them (e.g. Marx 2013). However, it provides us a unique opportunity to unravel the last mysteries of vertebrate rostrum evolution with unprecedented integrative studies. In 2014, Van Valkenburg *et al.* (2014 b) mentioned that "it is an especially exciting time to study the nose". Seven years later, I smell this is still the case.

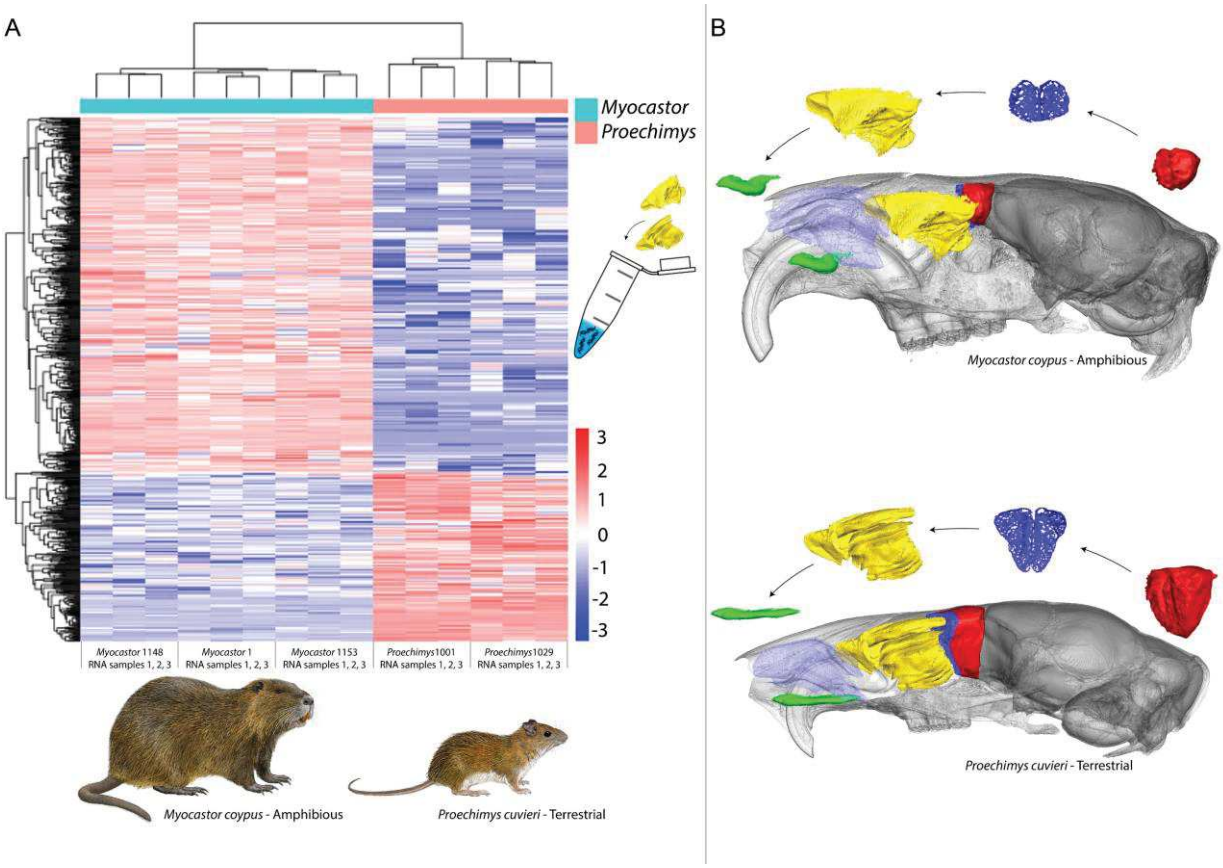

Figure 9: Ongoing investigation of the covariation between the gene expression (= transcriptomic) of olfactory turbinals and different anatomical proxies related to olfaction. These investigations compare the amphibious *Myocastor coypus* and the terrestrial *Proechimys cuvieri*. (A) Heatmap (= cluster analysis) of the gene expression of olfactory turbinals respectively in three and two *Myocastor coypus* and *Proechimys cuvieri*. Each line represents a gene and each column a RNA sample. Colors from red to blue indicate the degree of gene expression level from high to low. (B) Sagittal views of the skull of *Myocastor coypus* and *Proechimys cuvieri* with 3D representations of organs and structures related to olfaction: vomeronasal organ (green), olfactory turbinals (yellow), cribriform plate (dark blue), and olfactory bulb (red). These preliminary results demonstrated that there is a differential pattern in gene expression of olfactory turbinals between two closely related rodents with different ecological lifestyles. In these species, Martinez *et al.* (2020) demonstrated a differential pattern between the relative surface area of olfactory turbinals.

↑ Back to summary ↑

References

Adams, D. R., & Wiekamp, M. D. (1984). The canine vomeronasal organ. *Journal of anatomy*, *138*(Pt 4), 771.

Allen, H. (1882). On a revision of the ethmoid bone in the Mammalia, with special reference to the description of this bone and of the sense of smelling in the Cheiroptera. Bull. Mus. comp. 2001. Harv., 10: 135-171.

Allio, R., Tilak, M. K., Scornavacca, C., Avenant, N. L., Corre, E., Nabholz, B., & Delsuc, F. (2020). High-quality carnivore genomes from roadkill samples enable species delimitation in aardwolf and bat-eared fox. *bioRxiv*.

Allison, A. C. (1953). The morphology of the olfactory system in the vertebrates. *Biological Reviews*, *28*(2), 195-244.

Alvarez-Buylla, A., Theelen, M., & Nottebohm, F. (1988). Birth of projection neurons in the higher vocal center of the canary forebrain before, during, and after song learning. *Proceedings of the National Academy of Sciences*, *85*(22), 8722-8726.

Amson, E., Billet, G., & de Muizon, C. (2018). Evolutionary adaptation to aquatic lifestyle in extinct sloths can lead to systemic alteration of bone structure. *Proceedings of the Royal Society B: Biological Sciences*, *285*(1878), 20180270.

Baker, M. A., & Hayward, J. N. (1968). The influence of the nasal mucosa and the carotid rete upon hypothalamic temperature in sheep. *The Journal of Physiology*, *198*(3), 561-579.

Bang, B. G. (1961). The surface pattern of the nasal mucosa and its relation to mucous flow–a study of chicken and herring gull nasal mucosae. *Journal of Morphology*, *109*(1), 57-71.

Bang, B. G. (1964). The nasal organs of the Black and Turkey Vultures; a comparative study of the cathartid species *Coragyps atratus* atratus and Cathartes aura septentrionalis (with notes on Cathartes aura falklandica, *Pseudogyps bengalensis*, and *Neophron percnopterus*). *Journal of Morphology*, *115*, 153.

Bang, B. G. (1965). Anatomical adaptations for olfaction in the snow petrel. *Nature*, *205*(4970), 513-515.

Bang, B. G. (1968). Olfaction in Rallidae (Gruiformes), a morphological study of thirteen species. *Journal of Zoology*, *156*(1), 97-107.

Barrios, A. W., Núñez, G., Sánchez Quinteiro, P., & Salazar, I. (2014). Anatomy, histochemistry, and immunohistochemistry of the olfactory subsystems in mice. *Frontiers in neuroanatomy*, *8*, 63.

Beichman, A. C., Koepfli, K. P., Li, G., Murphy, W., Dobrynin, P., Kliver, S., ... & Wayne, R. K. (2019). Aquatic adaptation and depleted diversity: a deep dive into the genomes of the sea otter and giant otter. *Molecular biology and evolution*, *36*(12), 2631-2655.

Berta, A., Ekdale, E. G., & Cranford, T. W. (2014). Review of the cetacean nose: form, function, and evolution. *The Anatomical Record*, *297*(11), 2205-2215.

Bhatnagar, K. P., & Kallen, F. C. (1974). Cribriform plate of ethmoid, olfactory bulb and olfactory acuity in forty species of bats. *Journal of Morphology*, *142*(1), 71-89.

Bhatnagar, K. P., Wible, J. R., & Karim, K. B. (1996). Development of the vomeronasal organ in *Rousettus leschenaulti* (Megachiroptera, Pteropodidae). *Journal of anatomy*, *188*(Pt 1), 129.

Bi, S., Wang, Y., Guan, J., Sheng, X., & Meng, J. (2014). Three new Jurassic euharamiyidan species reinforce early divergence of mammals. *Nature*, *514*(7524), 579-584.

Birchenough, G. M., Johansson, M. E., Gustafsson, J. K., Bergström, J. H., & Hansson, G. C. (2015). New developments in goblet cell mucus secretion and function. *Mucosal immunology*, *8*(4), 712-719.

Bird, D. J., Amirkhanian, A., Pang, B., & Van Valkenburgh, B. (2014). Quantifying the cribriform plate: influences of allometry, function, and phylogeny in Carnivora. *The Anatomical Record*, *297*(11), 2080-2092.

Bird, D. J., Murphy, W. J., Fox-Rosales, L., Hamid, I., Eagle, R. A., & Van Valkenburgh, B. (2018). Olfaction written in bone: cribriform plate size parallels olfactory receptor gene repertoires in Mammalia. *Proceedings of the Royal Society B: Biological Sciences*, *285*(1874), 20180100.

Boesveldt, S., Postma, E. M., Boak, D., Welge-Luessen, A., Schöpf, V., Mainland, J. D., ... & Duffy, V. B. (2017). Anosmia—a clinical review. *Chemical senses*, *42*(7), 513-523.

Bouchard, B., Lisney, T. J., Campagna, S., & Célérier, A. (2017). Do bottlenose dolphins display behavioural response to fish taste?. *Applied Animal Behaviour Science*, *194*, 120-126.

Bourgery, J. M., & Jacob, N. H. (1831). Traité complet de l'anatomie de l'homme: comprenant la médecine opératoire, avec planches lithographiées d'après nature. Delaunay Paris -54

Brechbühl, J., Klaey, M., & Broillet, M. C. (2008). Grueneberg ganglion cells mediate alarm pheromone detection in mice. *Science*, *321*(5892), 1092-1095.

Brechbühl, J., Klaey, M., Moine, F., Bovay, E., Hurni, N., Nenniger-Tosato, M., & Broillet, M. C. (2014). Morphological and physiological species-dependent characteristics of the rodent Grueneberg ganglion. *Frontiers in neuroanatomy*, *8*, 87.

Brink, A. S. (1956). Speculations on some advanced mammalian characteristics in the higher mammal-like reptiles. Palaeontol. Africana 4:77-95.

Brooker, R. M., & Wong, B. B. (2020). Non-visual camouflage. *Current Biology*, *30*(21), R1290-R1292.

Buck, L., & Axel, R. (1991). A novel multigene family may encode odorant receptors: a molecular basis for odor recognition. *Cell*, *65*(1), 175-187.

Buffenstein, R., & Jarvis, J. U. (1985). Thermoregulation and metabolism in the smallest African gerbil, *Gerbillus pusillus*. *Journal of Zoology*, *205*(1), 107-121.

Buffenstein, R., & Yahav, S. (1991). Is the naked mole-rat *Hererocephalus glaber* an endothermic yet poikilothermic mammal?. *Journal of Thermal Biology*, *16*(4), 227-232.

Burch, G. E., & Winsor, T. (1944). Rate of insensible perspiration (diffusion of water) locally through living and through dead human skin. *Archives of Internal Medicine*, *74*(6), 437-444.

Bushdid, C., Magnasco, M. O., Vosshall, L. B., & Keller, A. (2014). Humans can discriminate more than 1 trillion olfactory stimuli. *Science*, *343*(6177), 1370-1372.

Butowt, R., & Bilinska, K. (2020). SARS-CoV-2: olfaction, brain infection, and the urgent need for clinical samples allowing earlier virus detection. *ACS chemical neuroscience*, *11*(9), 1200-1203.

Caputa, M. (1979). Temperature gradients in the nasal cavity of the rabbit. *Journal of Thermal Biology*, *4*(4), 283-286.

Chamero, P., Leinders-Zufall, T., & Zufall, F. (2012). From genes to social communication: molecular sensing by the vomeronasal organ. *Trends in neurosciences*, *35*(10), 597-606.

Catania, K. C. (2006). Underwater 'sniffing' by semi-aquatic mammals. *Nature*, *444*(7122), 1024-1025.

Catania, K. C., Hare, J. F., & Campbell, K. L. (2008). Water shrews detect movement, shape, and smell to find prey underwater. *Proceedings of the National Academy of Sciences*, *105*(2), 571-576.

Charles, C., Solé, F., Rodrigues, H. G., & Viriot, L. (2013). Under pressure? Dental adaptations to termitophagy and vermivory among mammals. *Evolution*, *67*(6), 1792-1804.

Collins, J. C., Pilkington, T. C., & Schmidt-Nielsen, K. (1971). A model of respiratory heat transfer in a small mammal. *Biophysical journal*, *11*(11), 886-914.

Cooper, J. G., & Bhatnagar, K. P. (1976). Comparative anatomy of the vomeronasal organ complex in bats. *Journal of anatomy*, *122*(Pt 3), 571.

Craven, B. A., Neuberger, T., Paterson, E. G., Webb, A. G., Josephson, E. M., Morrison, E. E., & Settles, G. S. (2007). Reconstruction and morphometric analysis of the nasal airway of the dog (*Canis familiaris*) and implications regarding olfactory airflow. *The Anatomical Record: Advances in Integrative Anatomy and Evolutionary Biology*, *290*(11), 1325-1340.

Craven, B. A., Paterson, E. G., & Settles, G. S. (2010). The fluid dynamics of canine olfaction: unique nasal airflow patterns as an explanation of macrosmia. *Journal of the Royal Society Interface*, *7*(47), 933-943.

Curtis, A. A., & Simmons, N. B. (2017). Unique turbinal morphology in horseshoe bats (Chiroptera: Rhinolophidae). *The Anatomical Record*, *300*(2), 309-325.

Curtis, A. A., Smith, T. D., Bhatnagar, K. P., Brown, A. M., & Simmons, N. B. (2020). Maxilloturbinal aids in nasophonation in horseshoe bats (Chiroptera: Rhinolophidae). *The Anatomical Record*, *303*(1), 110-128.

Dawes, J. D. K. (1952). The course of the nasal airstreams. *The Journal of Laryngology & Otology*, *66*(12), 583-593.

De Beer, G. R. (1929). IX. The development of the skull of the shrew. *Philosophical Transactions of the Royal Society of London. Series B, Containing Papers of a Biological Character*, *217*(440-449), 411-480.

Dewan, A., Pacifico, R., Zhan, R., Rinberg, D., & Bozza, T. (2013). Non-redundant coding of aversive odours in the main olfactory pathway. *Nature*, *497*(7450), 486-489.

Dugan, H. (2011). *The ephemeral history of perfume: Scent and sense in early modern England*. JHU Press.

Dulac, C., & Axel, R. (1995). A novel family of genes encoding putative pheromone receptors in mammals. *Cell*, *83*(2), 195-206.

Eayrs, J. T., & Moulton, D. G. (1960). Studies in olfactory acuity. I: Measurement of olfactory thresholds in the rat. *Quarterly Journal of Experimental Psychology*, *12*(2), 90-98.

Eiting, T. P., Smith, T. D., Perot, J. B., & Dumont, E. R. (2014). The role of the olfactory recess in olfactory airflow. *Journal of Experimental Biology, 217(10)*, 1799-1803.

Ekberg, J. A., Amaya, D., Chehrehasa, F., Lineburg, K., Claxton, C., Windus, L. C., ... & St John, J. A. (2011). OMP-ZsGreen fluorescent protein transgenic mice for visualisation of olfactory sensory neurons in vivo and in vitro. *Journal of neuroscience methods*, *196*(1), 88-98.

Enger, P. S. (1957). Heat regulation and metabolism in some tropical mammals and birds. *Acta Physiologica Scandinavica*, *40*(2-3), 161-166.

Evans, C. (2003). Vomeronasal chemoreception in vertebrates. *A Study of the Second Nose*. Imperial College Press.

Fawcett, E. (1917). The primordial cranium of microtus amphibius (water-rat), as determined by sections and a model of the 25mm stage. With comparative remarks. *Journal of anatomy*, *51*(Pt 4), 309-359.

Fleischer, J., Schwarzenbacher, K., Besser, S., Hass, N., & Breer, H. (2006). Olfactory receptors and signalling elements in the Grueneberg ganglion. *Journal of neurochemistry*, *98*(2), 543-554.

Fletcher, M. L., & Wilson, D. A. (2002). Experience modifies olfactory acuity: acetylcholine-dependent learning decreases behavioral generalization between similar odorants. *Journal of Neuroscience*, *22*(2), RC201-RC201.

Folkow, L. P., Blix, A. S., & Eide, T. J. (1988). Anatomical and functional aspects of the nasal mucosal and ophthalmic retia of phocid seals. *Journal of Zoology*, *216*(3), 417-436.

Freitag, J., Ludwig, G., Andreini, I., Rössler, P., & Breer, H. (1998). Olfactory receptors in aquatic and terrestrial vertebrates. *Journal of Comparative Physiology A*, *183*(5), 635-650.

Gardiner, B. G. (1982). Tetrapod classification. *Zoological Journal of the Linnean Society*, *74*(3), 207-232.

Garrett, E. C., & Steiper, M. E. (2014). Strong links between genomic and anatomical diversity in both mammalian olfactory chemosensory systems. *Proceedings of the Royal Society B: Biological Sciences*, *281*(1783), 20132828.

Gauthier, J., Kluge, A. G., & Rowe, T. (1988). Amniote phylogeny and the importance of fossils. *Cladistics*, *4*(2), 105-209.

Gignac, P. M., Kley, N. J., Clarke, J. A., Colbert, M. W., Morhardt, A. C., Cerio, D., ... & Echols, M. S. (2016). Diffusible iodine-based contrast-enhanced computed tomography (diceCT): an emerging tool for rapid, high-resolution, 3-D imaging of metazoan soft tissues. *Journal of anatomy*, *228*(6), 889-909.

Göbbel, L. (2000). The external nasal cartilages in Chiroptera: significance for intraordinal relationships. *Journal of Mammalian Evolution*, *7*(3), 167-201.

Graziadei, P. P. C., & DeHan, R. S. (1973). Neuronal regeneration in frog olfactory system. *The Journal of Cell Biology*, *59*(2), 525.

Graziadei, P. P. C., & Graziadei, G. M. (1978). Continuous nerve cell renewal in the olfactory system. In *Development of sensory systems* (pp. 55-83). Springer, Berlin, Heidelberg.

Green, P. A., Van Valkenburgh, B., Pang, B., Bird, D., Rowe, T., & Curtis, A. (2012). Respiratory and olfactory turbinal size in canid and arctoid carnivorans. *Journal of Anatomy*, *221*(6), 609-621.

Greer, P. L., Bear, D. M., Lassance, J. M., Bloom, M. L., Tsukahara, T., Pashkovski, S. L., ... & Datta, S. R. (2016). A family of non-GPCR chemosensors defines an alternative logic for mammalian olfaction. *Cell*, *165*(7), 1734-1748.

Grüneberg, H. (1973). A ganglion probably belonging to the N. terminalis system in the nasal mucosa of the mouse. *Zeitschrift für Anatomie und Entwicklungsgeschichte*, *140*(1), 39-52.

Harberts, E., Yao, K., Wohler, J. E., Maric, D., Ohayon, J., Henkin, R., & Jacobson, S. (2011). Human herpesvirus-6 entry into the central nervous system through the olfactory pathway. *Proceedings of the National Academy of Sciences*, *108*(33), 13734-13739.

Harkema, J. R., & Morgan, K. T. (1996). Normal morphology of the nasal passages in laboratory rodents. In *Respiratory System* (pp. 3-17). Springer, Berlin, Heidelberg.

Harkema, J. R., Carey, S. A., & Wagner, J. G. (2006). The nose revisited: a brief review of the comparative structure, function, and toxicologic pathology of the nasal epithelium. *Toxicologic pathology*, *34*(3), 252-269.

Hashiguchi, Y., & Nishida, M. (2007). Evolution of trace amine–associated receptor (TAAR) gene family in vertebrates: lineage-specific expansions and degradations of a second class of vertebrate chemosensory receptors expressed in the olfactory epithelium. *Molecular biology and evolution*, *24*(9), 2099-2107.

Hautier, L., Garland, K., Ferreira-Cardoso, S., Wright, M., Martinez, Q., Fabre, P. H., ... & Delsuc, F. (2019). Sniffing out covariation patterns in the olfactory system of myrmecophagous mammals. *Journal of morphology* (Vol. 280, pp. S133-S133).

Hayden, S., Bekaert, M., Crider, T. A., Mariani, S., Murphy, W. J., & Teeling, E. C. (2010). Ecological adaptation determines functional mammalian olfactory subgenomes. *Genome research*, *20*(1), 1-9.

Hayden, S., & Teeling, E. C. (2014). The molecular biology of vertebrate olfaction. *The Anatomical Record*, *297*(11), 2216-2226.

Herbert, R. A., Janardhan, K. S., Pandiri, A. R., Cesta, M. F., & Miller, R. A. (2018). Nose, larynx, and trachea. *Boorman's Pathology of the Rat* (pp. 391-435). Academic Press.

Herculano-Houzel, S., Avelino-de-Souza, K., Neves, K., Porfírio, J., Messeder, D., Mattos Feijó, L., ... & Manger, P. R. (2014). The elephant brain in numbers. *Frontiers in neuroanatomy*, *8*, 46.

Hillenius, W. J. (1992). The evolution of nasal turbinates and mammalian endothermy. *Paleobiology*, *18*(1), 17-29.

Hillenius, W. J. (1994). Turbinates in therapsids: evidence for Late Permian origins of mammalian endothermy. *Evolution*, *48*(2), 207-229.

Hillenius, W. J., & Ruben, J. A. (2004). The evolution of endothermy in terrestrial vertebrates: Who? When? Why?. *Physiological and Biochemical Zoology*, *77*(6), 1019-1042. b

Hofer, H. O. (1980). The external anatomy of the oro-nasal region of primates. *Zeitschrift für Morphologie und Anthropologie*, 233-249.

Hughes, G. M., Gang, L., Murphy, W. J., Higgins, D. G., & Teeling, E. C. (2013). Using Illumina next generation sequencing technologies to sequence multigene families in de novo species. *Molecular ecology resources*, *13*(3), 510-521.

Hughes, G. M., Boston, E. S., Finarelli, J. A., Murphy, W. J., Higgins, D. G., & Teeling, E. C. (2018). The birth and death of olfactory receptor gene families in mammalian niche adaptation. *Molecular biology and evolution*, *35*(6), 1390-1406.

Hurst, J. L., Beynon, R. J., Armstrong, S. D., Davidson, A. J., Roberts, S. A., Gómez-Baena, G., ... & Ganem, G. (2017). Molecular heterogeneity in major urinary proteins of *Mus musculus* subspecies: potential candidates involved in speciation. *Scientific reports*, *7*(1), 1-17.

International Human Genome Sequencing Consortium. (2001). Initial sequencing and analysis of the human genome. *Nature*, *409*(6822), 860-921.

International Human Genome Sequencing Consortium. (2004). Finishing the euchromatic sequence of the human genome. *Nature*, *431*(7011), 931.

Ito, K., Nojiri, T., & Koyabu, D. (2019). On the development of the nasal capsule and turbinate homology in Laurasiatherians, with special reference to bats. *Journal of morphology* (Vol. 280, pp. S10-S10).

Ivlev, Y. F., Rutovskaya, M. V., & Luchkina, O. S. (2013). The use of olfaction by the Russian desman (*Desmana moschata* L.) during underwater swimming. *Doklady Biological Sciences* (Vol. 452, No. 1, p. 280). Springer Nature BV.

Jackson, D. C., & Schmidt-Nielsen, K. (1964). Countercurrent heat exchange in the respiratory passages. *Proceedings of the National Academy of Sciences of the United States of America*, *51*(6), 1192.

Jeffery, W. R. (2005). Adaptive evolution of eye degeneration in the Mexican blind cavefish. *Journal of Heredity*, *96*(3), 185-196.

Jones, J. B., Wathes, C. M., Persaud, K. C., White, R. P., & Jones, R. B. (2001). Acute and chronic exposure to ammonia and olfactory acuity for n-butanol in the pig. *Applied Animal Behaviour Science*, *71*(1), 13-28.

Juilfs, D. M., Fülle, H. J., Zhao, A. Z., Houslay, M. D., Garbers, D. L., & Beavo, J. A. (1997). A subset of olfactory neurons that selectively express cGMP-stimulated phosphodiesterase (PDE2) and guanylyl cyclase-D define a unique olfactory signal transduction pathway. *Proceedings of the National Academy of Sciences*, *94*(7), 3388-3395.

Kaluza, J. F., Gussing, F., Bohm, S., Breer, H., & Strotmann, J. (2004). Olfactory receptors in the mouse septal organ. *Journal of neuroscience research*, *76*(4), 442-452.

Kelliher, K. R. (2007). The combined role of the main olfactory and vomeronasal systems in social communication in mammals. *Hormones and behavior*, *52*(5), 561-570.

Kishida, T., Kubota, S., Shirayama, Y., & Fukami, H. (2007). The olfactory receptor gene repertoires in secondary-adapted marine vertebrates: evidence for reduction of the functional proportions in cetaceans. *Biology letters*, *3*(4), 428-430.

Kishida, T., Thewissen, J. G. M., Hayakawa, T., Imai, H., & Agata, K. (2015). Aquatic adaptation and the evolution of smell and taste in whales. *Zoological letters*, *1*(1), 1-10.

Klima, M. (1995). Cetacean phylogeny and systematics based on the morphogenesis of the nasal skull. *Aquatic mammals*, *21*, 79-79.

Klima, M. (1999). *Development of the cetacean nasal skull* (Vol. 149). Springer Science & Business Media.

Kowalewsky, S., Dambach, M., Mauck, B., & Dehnhardt, G. (2006). High olfactory sensitivity for dimethyl sulphide in harbour seals. *Biology letters*, *2*(1), 106-109.

Kremers, D., Célérier, A., Schaal, B., Campagna, S., Trabalon, M., Böye, M., ... & Lemasson, A. (2016). Sensory perception in cetaceans: Part II—Promising experimental approaches to study chemoreception in dolphins. *Frontiers in Ecology and Evolution*, *4*, 50.

Labbe, D., Gilbert, F., & Martin, N. (2008). Impact of olfaction on taste, trigeminal, and texture perceptions. *Chemosensory Perception*, *1*(4), 217-226.

Lahti, D. C., Johnson, N. A., Ajie, B. C., Otto, S. P., Hendry, A. P., Blumstein, D. T., ... & Foster, S. A. (2009). Relaxed selection in the wild. *Trends in ecology & evolution*, *24*(9), 487-496.

Langman, V. A., Schmidt-Nielsen, G. M. K., Schroter, R. C., & Maloiy, G. M. O. (1978). Respiratory water and heat loss in camels subjected to dehydration. *Journal of Physiology, 278*, 35.

Langman, V. A. (1985). Nasal heat exchange in a northern ungulate, the reindeer (*Rangifer tarandus*). *Respiration physiology*, *59*(3), 279-287.

Lankford, K. L., Sasaki, M., Radtke, C., & Kocsis, J. D. (2008). Olfactory ensheathing cells exhibit unique migratory, phagocytic, and myelinating properties in the X-irradiated spinal cord not shared by Schwann cells. *Glia*, *56*(15), 1664-1678.

Larriva-Sahd, J. (2008). The accessory olfactory bulb in the adult rat: a cytological study of its cell types, neuropil, neuronal modules, and interactions with the main olfactory system. *Journal of Comparative Neurology*, *510*(3), 309-350.

Laska, M., & Hudson, R. (1995). Ability of female squirrel monkeys (*Saimiri sciureus*) to discriminate between conspecific urine odours. *Ethology*, *99*(1-2), 39-52.

Laska, M., & Freyer, D. (1997). Olfactory discrimination ability for aliphatic esters in squirrel monkeys and humans. *Chemical senses*, *22*(4), 457-465.

Laska, M., Seibt, A., & Weber, A. (2000). 'Microsmatic' primates revisited: olfactory sensitivity in the squirrel monkey. *Chemical senses*, *25*(1), 47-53.

Laska, M., Genzel, D., & Wieser, A. (2005). The number of functional olfactory receptor genes and the relative size of olfactory brain structures are poor predictors of olfactory discrimination performance with enantiomers. *Chemical senses*, *30*(2), 171-175.

Lauruschkus, G. (1942). *Über Riechfeldgrösse und Riechfeldkoeffizient bei einigen Hunderassen und der Katze* (Doctoral dissertation, Verlag nicht ermittelbar) 77:473-497.

Le Gros Clark, W. (1951). The projection of the olfactory epithelium on the olfactory bulb in the rabbit. *Journal of neurology, neurosurgery, and psychiatry*, *14*(1), 1.

Lebrun, R. (2018). MorphoDig, an open-source 3D freeware dedicated to biology. In *IPC5 The 5th International Palaeontological Congress*.

Lester, C. W., & Costa, D. P. (2006). Water conservation in fasting northern elephant seals (*Mirounga angustirostris*). *Journal of Experimental Biology*, *209*(21), 4283-4294.

Lösel, P. D., van de Kamp, T., Jayme, A., Ershov, A., Faragó, T., Pichler, O., ... & Heethoff, M. (2020). Introducing Biomedisa as an open-source online platform for biomedical image segmentation. *Nature communications*, *11*(1), 1-14.

Lundeen, I. K., & Kirk, E. C. (2019). Internal nasal morphology of the Eocene primate *Rooneyia viejaensis* and extant Euarchonta: Using μCT scan data to understand and infer patterns of nasal fossa evolution in primates. *Journal of human evolution*, *132*, 137-173.

Ma, M., Grosmaitre, X., Iwema, C. L., Baker, H., Greer, C. A., & Shepherd, G. M. (2003). Olfactory signal transduction in the mouse septal organ. *Journal of Neuroscience*, *23*(1), 317-324.

Ma, M. (2007). Encoding olfactory signals via multiple chemosensory systems. *Critical reviews in biochemistry and molecular biology*, *42*(6), 463-480.

Macrini, T. E. (2012). Comparative morphology of the internal nasal skeleton of adult marsupials based on x-ray computed tomography. *Bulletin of the American Museum of Natural History*, *2012*(365), 1-91.

Macrini, T. E. (2014). Development of the ethmoid in *Caluromys philander* (Didelphidae, Marsupialia) with a discussion on the homology of the turbinal elements in marsupials. *The Anatomical Record*, *297*(11), 2007-2017.

Maier, W. (1980). Nasal structures in Old and New World primates. In *Evolutionary biology of the New World monkeys and continental drift* (pp. 219-241). Springer, Boston, MA.

Maier, W. (2000). Ontogeny of the nasal capsule in cercopithecoids: a contribution to the comparative and evolutionary morphology of catarrhines. *Old world monkeys*.

Maier, W., & Ruf, I. (2014). Morphology of the nasal capsule of Primates—With special reference to Daubentonia and Homo. *The Anatomical Record*, *297*(11), 1985-2006.

Maier, W. (2020). A neglected part of the mammalian skull: The outer nasal cartilages as progressive remnants of the chondrocranium. *Vertebrate Zoology*, *70*(3), 367-382.

Mandiyan, V. S., Coats, J. K., & Shah, N. M. (2005). Deficits in sexual and aggressive behaviors in Cnga2 mutant mice. *Nature neuroscience*, *8*(12), 1660-1662.

Martin, C. J. (1903). Thermal adjustment and respiratory exchange in monotremes and marsupials.—A study in the development of homæothermism. *Philosophical Transactions of the Royal Society of London. Series B, Containing Papers of a Biological Character*, *195*(207-213), 1-37.

Martinez, Q., & Fabre, P. H. (2017). Convergent evolution and adaptations of fossorial lifestyle: a study of rodents turbinates. *Master thesis.*

Martinez, Q., Lebrun, R., Achmadi, A. S., Esselstyn, J. A., Evans, A. R., Heaney, L. R., ... & Fabre, P. H. (2018). Convergent evolution of an extreme dietary specialisation, the olfactory system of worm-eating rodents. *Scientific reports*, *8*(1), 1-13.

Martinez, Q., Clavel, J., Esselstyn, J. A., Achmadi, A. S., Grohé, C., Pirot, N., & Fabre, P. H. (2020). Convergent evolution of olfactory and thermoregulatory capacities in small amphibious mammals. *Proceedings of the National Academy of Sciences*, *117*(16), 8958-8965.

Martinez, Q., Sumbera, R., Wright, M., Braude, S., Broyon, M., Cox, P., Delsuc, F., Ferreira-Cardoso, S., Hautier, L., Hildebrandt, T., Holtze, S., Lovy, M., Okrouhlík, J., Pirot, N., Ruf, I., & Fabre, P. H. (a). Mammalian maxillo turbinal evolution highlighted unique loss and reduction related to poikilothermy

Martinez, Q., [...] & Fabre, P. H. (b). The evolution of maxillo turbinal bones in mammals.

Martinez, Q., [...] & Fabre, P. H. (c). The evolution of turbinal bones in rodents.

Martinez, Q., [...] & Fabre, P. H. (d). Mapping nasal cavity with immunohistochemistry along rodent phylogeny.

Martinez, Q., [...] & Fabre, P. H. (e). Transcriptomic, histology and 3D μCT-scan demonstrated the reduction of olfactory capacities in an amphibious rodent.

Marx, V. (2013). The big challenges of big data. *Nature*, *498*(7453), 255-260.

Mason, M. J., Wenger, L. M., Hammer, O., & Blix, A. S. (2020). Structure and function of respiratory turbinates in phocid seals. *Polar Biology*, *43*(2), 157-173.

Matsui, A., Go, Y., & Niimura, Y. (2010). Degeneration of olfactory receptor gene repertories in primates: no direct link to full trichromatic vision. *Molecular biology and evolution*, *27*(5), 1192-1200.

McGann, J. P. (2017). Poor human olfaction is a 19th-century myth. *Science*, *356*(6338).

McNab, B. K. (1966). The metabolism of fossorial rodents: a study of convergence. *Ecology*, *47*(5), 712-733.

Mead, J. G., & Fordyce, R. E. (2009). The therian skull: a lexicon with emphasis on the odontocetes. *Smithsonian contributions to zoology*.

Mezler, M., Fleischer, J., & Breer, H. (2001). Characteristic features and ligand specificity of the two olfactory receptor classes from *Xenopus laevis*. *Journal of Experimental Biology*, *204*(17), 2987-2997.

Miller, A. K., Maritz, B., McKay, S., Glaudas, X., & Alexander, G. J. (2015). An ambusher's arsenal: chemical crypsis in the puff adder (*Bitis arietans*). *Proceedings of the Royal Society B: Biological Sciences*, *282*(1821), 20152182.

Molnar, G. W. (1946). Survival of hypothermia by men immersed in the ocean. *Journal of the American Medical Association*, *131*(13), 1046-1050.

Montague, M. J., Li, G., Gandolfi, B., Khan, R., Aken, B. L., Searle, S. M., ... & Warren, W. C. (2014). Comparative analysis of the domestic cat genome reveals genetic signatures underlying feline biology and domestication. *Proceedings of the National Academy of Sciences*, *111*(48), 17230-17235.

Morgan, K. T., & Monticello, T. M. (1990). Airflow, gas deposition, and lesion distribution in the nasal passages. *Environmental health perspectives*, *85*, 209-218.

Moulton, D. G., Ashton, E. H., & Eayrs, J. T. (1960). Studies in olfactory acuity. 4. Relative detectability of n-aliphatic acids by the dog. *Animal Behaviour*, *8*(3-4), 117-128.

Negus, V. (1958). The Comparative Anatomy and Physiology of the Nose and Paranasal Sinuses. E. & S. Livingstone, London, pp. 103-129.

Nielsen, T. P., Jackson, G., & Bull, C. M. (2016). A nose for lizards; can a detection dog locate the endangered pygmy bluetongue lizard (*Tiliqua adelaidensis*)?. *Transactions of the Royal Society of South Australia*, *140*(2), 234-243.

Niimura, Y., & Nei, M. (2003). Evolution of olfactory receptor genes in the human genome. *Proceedings of the National Academy of Sciences*, *100*(21), 12235-12240.

Niimura, Y., & Nei, M. (2007). Extensive gains and losses of olfactory receptor genes in mammalian evolution. *PloS one*, *2*(8), e708.

Niimura, Y. (2009). On the origin and evolution of vertebrate olfactory receptor genes: comparative genome analysis among 23 chordate species. *Genome biology and evolution*, *1*, 34-44.

Niimura, Y. (2012). Olfactory receptor multigene family in vertebrates: from the viewpoint of evolutionary genomics. *Current genomics*, *13*(2), 103-114.

Niimura, Y., Matsui, A., & Touhara, K. (2014). Extreme expansion of the olfactory receptor gene repertoire in African elephants and evolutionary dynamics of orthologous gene groups in 13 placental mammals. *Genome research*, *24*(9), 1485-1496.

Nottebohm, F. (2002). Neuronal replacement in adult brain. *Brain research bulletin*, *57*(6), 737-749.

Oliveira-Pinto, A. V., Santos, R. M., Coutinho, R. A., Oliveira, L. M., Santos, G. B., Alho, A. T., ... & Lent, R. (2014). Sexual dimorphism in the human olfactory bulb: females have more neurons and glial cells than males. *PloS one*, *9*(11), e111733.

Owerkowicz, T., Musinsky, C., Middleton, K. M., & Crompton, A. W. (2015). Respiratory turbinates and the evolution of endothermy in mammals and birds. *Great transformations in vertebrate evolution*, 143-165.

Pang, B. (2017). A study of respiratory turbinal morphology in response to evolutionary pressure and development (Doctoral dissertation, UCLA).

Parsons, T. S. (1971). Anatomy of nasal structures from a comparative viewpoint. *Olfaction* (pp. 1-26). Springer, Berlin, Heidelberg.

Paulli, S. (1900a). Über die Pneumaticität des Schädels bei den Säugetieren. *Eine morphologische Studie. I. Über den Bau des Siebbeins. Über die Morphologie des Siebbeins und die Pneumaticität bei den Monotremen und den Marsupialiern, Morph. Jb*, *28*, 147-178.

Paulli, S. (1900b). Über die Pneumaticität des Schädels bei den Säugetieren. *Eine morphologische Studie. II. Über die Morphologie des Siebbeins und die Pneumaticität bei den Ungulaten und Prosbosciden, Morph. Jb., 28,* 179–251.

Paulli, S. (1900c). Über die Pneumaticität des Schädels bei den Säugetieren. *Eine morphologische Studie. III. Über die Morphologie des Siebbeins und die Pneumaticität bei den Insectivoren, Hyracoideen, Chiropteren, Carnivoren, Pinnipedien, Edentaten, Rodentiern, Prosimiern und Primaten, nebst einer zusammenfassenden Übersicht über die Morphologie des Siebbeins und die der Pneumaticität des Schädels bei den Säugetieren, Morph. Jb., 28,* 483–564.

Pauwels, E., Van Loo, D., Cornillie, P., Brabant, L., & Van Hoorebeke, L. (2013). An exploratory study of contrast agents for soft tissue visualization by means of high resolution X-ray computed tomography imaging. *Journal of microscopy*, *250*(1), 21-31.

Pihlström, H., Fortelius, M., Hemilä, S., Forsman, R., & Reuter, T. (2005). Scaling of mammalian ethmoid bones can predict olfactory organ size and performance. *Proceedings of the Royal Society B: Biological Sciences*, *272*(1566), 957-962.

Poncelet, G., & Shimeld, S. M. (2020). The evolutionary origins of the vertebrate olfactory system. *Open Biology*, *10*(12), 200330.

Porter, J., Craven, B., Khan, R. M., Chang, S. J., Kang, I., Judkewitz, B., ... & Sobel, N. (2007). Mechanisms of scent-tracking in humans. *Nature neuroscience*, *10*(1), 27-29.

Ray, S., Li, M., Koch, S. P., Mueller, S., Boehm-Sturm, P., Wang, H., ... & Naumann, R. K. (2020). Seasonal plasticity in the adult somatosensory cortex. *Proceedings of the National Academy of Sciences*, *117*(50), 32136-32144.

Reinbach, W. (1952a). Zur Entwicklung des Primordialcraniums von Dasypus novemcinctus Linné (Tatusia novemcincta Lesson) I. *Zeitschrift für Morphologie und Anthropologie*, (H. 3), 375-444.

Reinbach, W. (1952b). Zur Entwicklung des Primordialcraniums von Dasypus novemcinctus Linné (Tatusia novemcincta Lesson) II. *Zeitschrift für morphologie und anthropologie*, (H. 1), 1-72.

Reisz, R. R., & Müller, J. (2004). Molecular timescales and the fossil record: a paleontological perspective. *TRENDS in Genetics*, *20*(5), 237-241.

Ressler, K. J., Sullivan, S. L., & Buck, L. B. (1993). A zonal organization of odorant receptor gene expression in the olfactory epithelium. *Cell*, *73*(3), 597-609.

Ressler, K. J., Sullivan, S. L., & Buck, L. B. (1994). A molecular dissection of spatial patterning in the olfactory system. *Current opinion in neurobiology*, *4*(4), 588-596.

Ribeiro, P. F., Manger, P. R., Catania, K. C., Kaas, J. H., & Herculano-Houzel, S. (2014). Greater addition of neurons to the olfactory bulb than to the cerebral cortex of eulipotyphlans but not rodents, afrotherians or primates. *Frontiers in neuroanatomy*, *8*, 23.

Rivière, S., Challet, L., Fluegge, D., Spehr, M., & Rodriguez, I. (2009). Formyl peptide receptor-like proteins are a novel family of vomeronasal chemosensors. *Nature*, *459*(7246), 574-577.

Roppolo, D., Ribaud, V., Jungo, V. P., Lüscher, C., & Rodriguez, I. (2006). Projection of the Grüneberg ganglion to the mouse olfactory bulb. *European Journal of Neuroscience*, *23*(11), 2887-2894.

Rossie, J. B. (2006). Ontogeny and homology of the paranasal sinuses in Platyrrhini (Mammalia: Primates). *Journal of Morphology*, *267*(1), 1-40.

Rossie, J. B., & Smith, T. D. (2007). Ontogeny of the nasolacrimal duct in primates: functional and phylogenetic implications. *Journal of anatomy*, *210*(2), 195-208.

Rouby, C., Schaal, B., Dubois, D., Gervais, R., & Holley, A. (Eds.). (2002). *Olfaction, taste, and cognition*. New York: Cambridge University Press.

Rowe, T. B., Eiting, T. P., Macrini, T. E., & Ketcham, R. A. (2005). Organization of the olfactory and respiratory skeleton in the nose of the gray short-tailed opossum *Monodelphis domestica*. *Journal of Mammalian Evolution*, *12*(3), 303-336.

Rowe, T. B., Macrini, T. E., & Luo, Z. X. (2011). Fossil evidence on origin of the mammalian brain. *science*, *332*(6032), 955-957.

Ruben, J. A., Hillenius, W. J., Geist, N. R., Leitch, A., Jones, T. D., Currie, P. J., ... & Espe, G. (1996). The metabolic status of some Late Cretaceous dinosaurs. *Science*, *273*(5279), 1204-1207.

Ruben, J. A., & Jones, T. D. (2000). Selective factors associated with the origin of fur and feathers. *American Zoologist*, *40*(4), 585-596.

Ruf, I. (2004). Vergleichend-ontogenetische Untersuchungen an der Ethmoidalregion der Muroidea (Rodentia, Mammalia). *Ein Beitrag zur Morphologie und Systematik der Nagetiere*.

Ruf, I. (2014). Comparative anatomy and systematic implications of the turbinal skeleton in Lagomorpha (Mammalia). *The Anatomical Record*, *297*(11), 2031-2046.

Ruf, I., Maier, W., Rodrigues, P. G., & Schultz, C. L. (2014). Nasal anatomy of the non-mammaliaform cynodont *Brasilitherium riograndensis* (Eucynodontia, Therapsida) reveals new insight into mammalian evolution. *The Anatomical Record*, *297*(11), 2018-2030.

Ruf, I., Janßen, S., & Zeller, U. (2015). The ethmoidal region of the skull of *Ptilocerus lowii* (Ptiloceridae, Scandentia, Mammalia) - a contribution to the reconstruction of the cranial morphotype of primates. *Primate Biology*, *2*(1), 89-110.

Ruf, I. (2020). Ontogenetic transformations of the ethmoidal region in Muroidea (Rodentia, Mammalia): new insights from perinatal stages. *Vertebrate Zoology*, *70*(3), 383-415.

Salazar, I., & Sánchez-Quinteiro, P. (2009). The risk of extrapolation in neuroanatomy: the case of the mammalian vomeronasal system. *Frontiers in neuroanatomy*, *3*, 22.

Salazar, I., & Sánchez-Quinteiro, P. (2011). A detailed morphological study of the vomeronasal organ and the accessory olfactory bulb of cats. *Microscopy research and technique, 74(12)*, 1109-1120.

Scharff, C., Kirn, J. R., Grossman, M., Macklis, J. D., & Nottebohm, F. (2000). Targeted neuronal death affects neuronal replacement and vocal behavior in adult songbirds. *Neuron*, *25*(2), 481-492.

Schmidt-Nielsen, K., & Haines, H. B. (1964). Water balance in a carnivorous desert rodent the grasshopper mouse. *Physiological Zoology*, *37*(3), 259-265.

Schmidt-Nielsen, K. (1964). Desert animals: physiological problems of heat and water. Oxford: University Press.

Schmidt-Nielsen, K. (1969). The neglected interface: the biology of water as a liquid-gas system. *Quarterly reviews of biophysics*, *2*(3), 283-304.

Schmidt-Nielsen, K., Hainsworth, F. R., & Murrish, D. E. (1970). Counter-current heat exchange in the respiratory passages: effect on water and heat balance. *Respiration physiology*, *9*(2), 263-276.

Schmidt-Nielsen, K., Schroter, R. C., & Shkolnik, A. (1981). Desaturation of exhaled air in camels. *Proceedings of the Royal Society of London. Series B. Biological Sciences*, *211*(1184), 305-319.

Schreider, J. P., & Raabe, O. G. (1981). Anatomy of the nasal-pharyngeal airway of experimental animals. *The Anatomical Record*, *200*(2), 195-205.

Shinoda, K., Shiotani, Y., & Osawa, Y. (1989). “Necklace olfactory glomeruli” form unique components of the rat primary olfactory system. *Journal of Comparative Neurology*, *284*(3), 362-373.

Smadja, C., & Ganem, G. (2002). Subspecies recognition in the house mouse: a study of two populations from the border of a hybrid zone. *Behavioral Ecology*, *13*(3), 312-320.

Smadja, C., & Butlin, R. K. (2009). On the scent of speciation: the chemosensory system and its role in premating isolation. *Heredity*, *102*(1), 77-97.

Smith, R. M., & Hanna, J. M. (1975). Skinfolds and resting heat loss in cold air and water: temperature equivalence. *Journal of applied physiology*, *39*(1), 93-102.

Smith, T. D., Bhatnagar, K. P., Tuladhar, P., & Burrows, A. M. (2004). Distribution of olfactory epithelium in the primate nasal cavity: are microsmia and macrosmia valid morphological concepts?. *The Anatomical Record Part A: Discoveries in Molecular, Cellular, and Evolutionary Biology: An Official Publication of the American Association of Anatomists*, *281*(1), 1173-1181.

Smith, T. D., & Rossie, J. B. (2008). Nasal fossa of mouse and dwarf lemurs (Primates, Cheirogaleidae). *The Anatomical Record: Advances in Integrative Anatomy and Evolutionary Biology*, *291*(8), 895-915.

Smith, T. D., Eiting, T. P., & Bhatnagar, K. P. (2012). A quantitative study of olfactory, non-olfactory, and vomeronasal epithelia in the nasal fossa of the bat *Megaderma lyra*. *Journal of Mammalian Evolution*, *19*(1), 27-41.

Smith, T. D., Martell, M. C., Rossie, J. B., Bonar, C. J., & Deleon, V. B. (2016). Ontogeny and microanatomy of the nasal turbinals in lemuriformes. *The Anatomical Record*, *299*(11), 1492-1510.

Smith, T. D., Curtis, A., Bhatnagar, K. P., & Santana, S. E. (2020a). Fissures, folds, and scrolls: The ontogenetic basis for complexity of the nasal cavity in a fruit bat (*Rousettus leschenaultii*). *The Anatomical Record*.

Smith, T. D., Craven, B. A., Engel, S. M., Van Valkenburgh, B., & DeLeon, V. B. (2020b). “Mucosal maps” of the canine nasal cavity: Micro-computed tomography and histology. *The Anatomical Record*, *304*(1), 127-138.

Spatz, W. (1964). *Beitrag zur Kenntnis der Ontogenese des Cranium von Tupaia glis (DIARD 1820)* (Doctoral dissertation, Akad. Verlag-Ges. Geest & Portig).

Springer, M. S., & Gatesy, J. (2017). Inactivation of the olfactory marker protein (OMP) gene in river dolphins and other odontocete cetaceans. *Molecular phylogenetics and evolution*, *109*, 375-387.

Stathopoulos, S., Bishop, J. M., & O’Ryan, C. (2014). Genetic signatures for enhanced olfaction in the African mole-rats. *PLoS One*, *9*(4), e93336.

Stoddart, D. M. (1980). *The ecology of vertebrate olfaction*. Chapman & Hall, New York

Storan, M. J., & Key, B. (2006). Septal organ of Grüneberg is part of the olfactory system. *Journal of Comparative Neurology*, *494*(5), 834-844.

Tachibana, T., Fujiwara, N., & Nawa, T. (1990). The ultrastructure of the ganglionated nerve plexus in the nasal vestibular mucosa of the musk shrew (*Suncus murinus*, insectivora). *Archives of histology and cytology*, *53*(2), 147-156.

Tian, H., & Ma, M. (2004). Molecular organization of the olfactory septal organ. *Journal of Neuroscience*, *24*(38), 8383-8390.

Toller, S. V. (1999). Assessing the impact of anosmia: review of a questionnaire's findings. *Chemical senses*, *24*(6), 705-712.

Turner, W. (1890). The convolutions of the brain: a study in comparative anatomy. *Journal of anatomy and physiology*, *25*(Pt 1), 105.

Van Tuinen, M., & Hadly, E. A. (2004). Error in estimation of rate and time inferred from the early amniote fossil record and avian molecular clocks. *Journal of Molecular Evolution*, *59*(2), 267-276.

Van Valkenburgh, B., Theodor, J., Friscia, A., Pollack, A., & Rowe, T. (2004). Respiratory turbinates of canids and felids: a quantitative comparison. *Journal of Zoology*, *264*(3), 281-293.

Van Valkenburgh, B., Curtis, A., Samuels, J. X., Bird, D., Fulkerson, B., Meachen-Samuels, J., & Slater, G. J. (2011). Aquatic adaptations in the nose of carnivorans: evidence from the turbinates. *Journal of Anatomy*, *218*(3), 298-310.

Van Valkenburgh, B., Pang, B., Bird, D., Curtis, A., Yee, K., Wysocki, C., & Craven, B. A. (2014a). Respiratory and olfactory turbinals in feliform and caniform carnivorans: the influence of snout length. *The Anatomical Record*, *297*(11), 2065-2079.

Van Valkenburgh, B., Smith, T. D., & Craven, B. A. (2014b). Tour of a labyrinth: exploring the vertebrate nose. *The Anatomical Record*, *297*(11), 1975-1984.

Venter, J. C., Adams, M. D., Myers, E. W., Li, P. W., Mural, R. J., Sutton, G. G., ... & Kalush, F. (2001). The sequence of the human genome. *Science*, *291*(5507), 1304-1351.

Villamayor, P. R., Cifuentes, J. M., Fdz.-de-Troconiz, P., & Sanchez-Quinteiro, P. (2018). Morphological and immunohistochemical study of the rabbit vomeronasal organ. *Journal of anatomy*, *233*(6), 814-827.

Voit, M. (1909). Das Primordialcranium des Kaningchens. *Anatomische Hefte*, *38*(3), 425-616.

Voss, R. S., & Jansa, S. A. (2003). Phylogenetic studies on didelphid marsupials II. Nonmolecular data and new IRBP sequences: separate and combined analyses of didelphine relationships with denser taxon sampling. *Bulletin of the American Museum of Natural History*, *2003*(276), 1-82.

Wang, Z., Nudelman, A., & Storm, D. R. (2007). Are pheromones detected through the main olfactory epithelium?. *Molecular neurobiology*, *35*(3), 317-323.

Wagner, F., & Ruf, I. (2019). Who nose the borzoi? Turbinal skeleton in a dolichocephalic dog breed (*Canis lupus familiaris*). *Mammalian Biology*, *94*(1), 106-119.

Wagner, F., & Ruf, I. (2020). “Forever young”—Postnatal growth inhibition of the turbinal skeleton in brachycephalic dog breeds (*Canis lupus familiaris*). *The Anatomical Record*, *304*(1), 154-189.

Walker, J. E., & Wells, R. E. (1961). Heat and water exchange in the respiratory tract. *The American journal of medicine*, *30*(2), 259-267.

Watson, D. M. S. (1913). XXV.—Further notes on the skull, brain, and organs of special sense of Diademodon. *Annals and Magazine of Natural History*, *12*(68), 217-228.

Weibel, E. R. (2007). Obituary in memoriam Knut Schmidt-Nielsen 24 September 1915–25 January 2007.

Whittow, G. C. (1971) Comparative physiology of thermoregulation. Volume II. Academic Press, New York, New York, USA.

Wislocki, G. B. (1933). Location of the testes and body temperature in mammals. *The Quarterly Review of Biology*, *8*(4), 385-396.

Witmer, L. M. (1997). The evolution of the antorbital cavity of archosaurs: a study in soft-tissue reconstruction in the fossil record with an analysis of the function of pneumaticity. *Journal of Vertebrate Paleontology*, *17*(S1), 1-76.

Yazdanpanah, N., Saghazadeh, A., & Rezaei, N. (2020). Anosmia: a missing link in the neuroimmunology of coronavirus disease 2019 (COVID-19). *Reviews in the Neurosciences*, *1*(ahead-of-print).

Yee, K. K., Craven, B. A., Wysocki, C. J., & Van Valkenburgh, B. (2016). Comparative morphology and histology of the nasal fossa in four mammals: Gray squirrel, bobcat, coyote, and white-tailed deer. *The Anatomical Record*, *299*(7), 840-852.

Yohe, L. R., & Brand, P. (2018). Evolutionary ecology of chemosensation and its role in sensory drive. *Current zoology*, *64*(4), 525-533.

Yohe, L. R., & Dávalos, L. M. (2018). Strength of selection on the Trpc2 gene predicts accessory olfactory bulb form in bat vomeronasal evolution. *Biological Journal of the Linnean Society*, *123*(4), 796-804.

Yohe, L. R., Hoffmann, S., & Curtis, A. (2018). Vomeronasal and olfactory structures in bats revealed by DiceCT clarify genetic evidence of function. *Frontiers in neuroanatomy*, *12*, 32.

Yohe, L. R., Leiser-Miller, L. B., Kaliszewska, Z. A., Donat, P., Santana, S. E., & Dávalos, L. M. (2021) Diversity in olfactory receptor repertoires is associated with dietary specialization in a genus of frugivorous bat. *bioRxiv*, 2020-12.

Yoon, H., Enquist, L. W., & Dulac, C. (2005). Olfactory inputs to hypothalamic neurons controlling reproduction and fertility. *Cell*, *123*(4), 669-682.

Zhang, X., & Firestein, S. (2002). The olfactory receptor gene superfamily of the mouse. *Nature neuroscience*, *5*(2), 124-133.

Zhou, X., Sun, F., Xu, S., Fan, G., Zhu, K., Liu, X., ... & Yang, G. (2013). Baiji genomes reveal low genetic variability and new insights into secondary aquatic adaptations. *Nature communications*, *4*(1), 1-6.

↑ Back to summary ↑

Article 1 - Convergent evolution of an extreme dietary specialisation, the olfactory system of worm-eating rodents

SCIENTIFIC REPORTS

OPEN

Convergent evolution of an extreme dietary specialisation, the olfactory system of worm-eating rodents

Received: 11 June 2018
Accepted: 9 November 2018
Published online: 13 December 2018

Quentin Martinez[1], Renaud Lebrun[1], Anang S. Achmadi[2], Jacob A. Esselstyn[3,4], Alistair R. Evans[5,6], Lawrence R. Heaney[7], Roberto Portela Miguez[8], Kevin C. Rowe[6,9] & Pierre-Henri Fabre[1]

Turbinal bones are key components of the mammalian rostrum that contribute to three critical functions: (1) homeothermy, (2) water conservation and (3) olfaction. With over 700 extant species, murine rodents (Murinae) are the most species-rich mammalian subfamily, with most of that diversity residing in the Indo-Australian Archipelago. Their evolutionary history includes several cases of putative, but untested ecomorphological convergence, especially with traits related to diet. Among the most spectacular rodent ecomorphs are the vermivores which independently evolved in several island systems. We used 3D CT-scans (N = 87) of murine turbinal bones to quantify olfactory capacities as well as heat or water conservation adaptations. We obtained similar results from an existing 2D complexity method and two new 3D methodologies that quantify bone complexity. Using comparative phylogenetic methods, we identified a significant convergent signal in the rostral morphology within the highly specialised vermivores. Vermivorous species have significantly larger and more complex olfactory turbinals than do carnivores and omnivores. Increased olfactory capacities may be a major adaptive feature facilitating rats' capacity to prey on elusive earthworms. The narrow snout that characterises vermivores exhibits significantly reduced respiratory turbinals, which may reduce their heat and water conservation capacities.

Understanding how species have adapted to their environment is a major goal of evolutionary biology[1–3]. Salient examples of convergence, the evolution of a similar trait in independent evolutionary lineages[4], have demonstrated the importance of determinism through natural selection[3]. Recent advances in X-ray microtomography (X-ray μCT) provide the opportunity to quantify convergence in morphological structures that are otherwise inaccessible[5–7]. In mammals, the use of morphological proxies such as inner ears, braincase, floccular fossa, cribriform plate, and turbinal bones[5–11] have shed light on ecological and functional adaptations, especially for taxa that are difficult to observe directly in the wild[7].

Extensive studies of the mammalian olfactory subgenome revealed that mammals have a wide array of olfactory receptor genes that represent 1–6% of their genomes[12–14]. The huge mammalian olfactory subgenome has proven useful to illustrate dietary and other adaptions[12,15,16]. However, the nasal chamber of mammals has been relatively neglected by anatomists due to its internal position[17], and few studies have tested for an adaptive link between nasal morphology and olfactory capacities[18–20].

[1]Institut des Sciences de l'Evolution (ISEM, UMR 5554 CNRS-IRD-UM), Université de Montpellier, Place E. Bataillon - CC 064 - 34095, Montpellier Cedex 5, France. [2]Museum Zoologicum Bogoriense, Research Center For Biology, Indonesian Institute of Sciences (LIPI), Jl.Raya Jakarta-Bogor Km.46, Cibinong, 16911, Indonesia. [3]Museum of Natural Science, 119 Foster Hall, Louisiana State University, Baton Rouge, Louisiana, 70803, United States. [4]Department of Biological Sciences, Louisiana State University, Baton Rouge, Louisiana, 70803, United States. [5]School of Biological Sciences, 18 Innovation Walk, Monash University, Victoria, 3800, Australia. [6]Sciences Department, Museums Victoria, Melbourne, Victoria, 3001 Australia. [7]Field Museum of Natural History, 1400 S Lake Shore Drive, Chicago, 60605, United States. [8]Natural History Museum of London, Department of Life Sciences, Mammal Section, London, United Kingdom. [9]School of BioSciences, The University of Melbourne, Melbourne, Victoria, 3010, Australia. Correspondence and requests for materials should be addressed to Q.M. (email: quentinmartinezphoto@gmail.com)

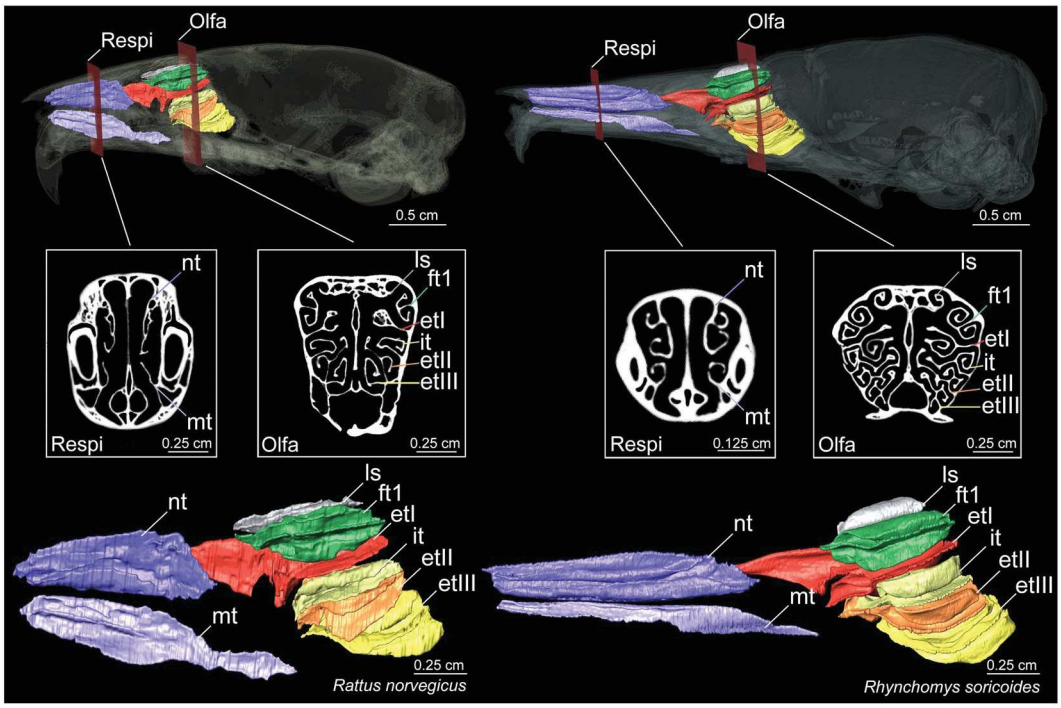

Figure 1. Coronal cross section and sagittal plane of skull and 3D representations of turbinal bones in *Rattus norvegicus* and *Rhynchomys soricoides*. Abbreviations: Respi = respiratory turbinals, Olfa = olfactory turbinals, nt = nasoturbinal, mt = maxilloturbinal, ls = lamina semicircularis, it = interturbinal, ft1 = frontoturbinal 1, etI = ethmoturbinal I, etII = ethmoturbinal II, and etIII = ethmoturbinal III.

In mammals, the nasal chambers contain bony plates called turbinals or turbinates, which are key structures involved in olfaction, thermoregulation, and water conservation. Because they bear the respiratory and olfactory epithelia[8,9,17,21–24], these turbinals have played a major role in the evolution of homeothermy and olfaction in mammals[25]. Anatomists and physiologists usually distinguish two major functional parts for turbinals: (1) the respiratory and (2) the olfactory components (Fig. 1). The respiratory turbinals, which are anterior to the olfactory turbinals, are further divided into maxilloturbinals (MT) and nasoturbinals (NT, Fig. 1). Maxilloturbinals link the naris and nasopharynx and are covered by respiratory epithelium, a vascularised mucosa. During inhalation, they moisten and warm the breath; at exhalation, they conserve moisture[17,23,26–29]. Nasoturbinals are located in the anterior portion of the nasal cavity, near the naris, and dorsal to the MT. They contribute to homeothermy, as suggested by their distal position from the olfactory bulbs, the presence of respiratory epithelium, airflow dynamics, and performance tests[21,22,27,29–33]. However, NT probably also serve, at least partly, as olfactory structures[34] because they are partially covered by olfactory epithelium in groups such as rodents[24]. As such, NT probably serve dual functions for olfaction and heat and water conservation[21,22]. The olfactory turbinals are primarily associated with the olfactory process. They are covered by a thick olfactory epithelium, innervated by several olfactory receptors and directly connected to the close cerebral olfactory bulbs via olfactory nerves[9,17,23,24,35–37]. In addition, olfactory turbinals are divided into several structures variably named lamina semicircularis (ls), frontoturbinals (ft), interturbinals (it), and ethmoturbinals (et, Fig. 1)[38–41].

Studies of carnivorans suggest a possible link between olfactory turbinal size and olfactory performance as well as between respiratory turbinal size and heat or moisture conservation performance[8,9,42]. The physiological importance of turbinal bones was thereby shown by the correlation between surface areas of these bones and species' ecological traits. These studies have especially demonstrated the correlation between dietary adaptations and the surface area of olfactory turbinals[23]. However, these types of studies are rare outside of carnivorans, leaving open the question of whether connections between ecological traits and turbinal surface areas is a general pattern.

Rodents of the family Muridae have migrated from mainland Asia to the many islands of the Indo-Australian Archipelago (IAA) multiple times since the Miocene[43,44]. These small to medium-sized mammals have spread over most of the IAA, where they occupy many terrestrial niches[43,44]. Included among this diversity are the "shrew-rats", carnivorous rodents (i.e., those that feed on metazoans) that evolved independently in New Guinea, the Philippines, and Sulawesi[44–47]. Shrew-rats are an ideal comparative system to study dietary specialisation because they have convergently evolved from an ancestral omnivorous diet toward carnivory[44]. This adaptation appeared at least five times in the highly diverse Murinae, with at least two origins of highly specialised carnivorous lineages: (1) the Sulawesi shrew-rats and (2) the Philippine shrew-rats. Several species of shrew-rats consume a wide-range of invertebrates, but others are earthworm specialists with spectacular changes to their rostrum morphology. In the most specialised vermivorous species (*Paucidentomys* and *Rhynchomys* genera), the snout is extremely long and narrow[44,45,48] and might have constrained the size and shape of turbinals. Additionally,

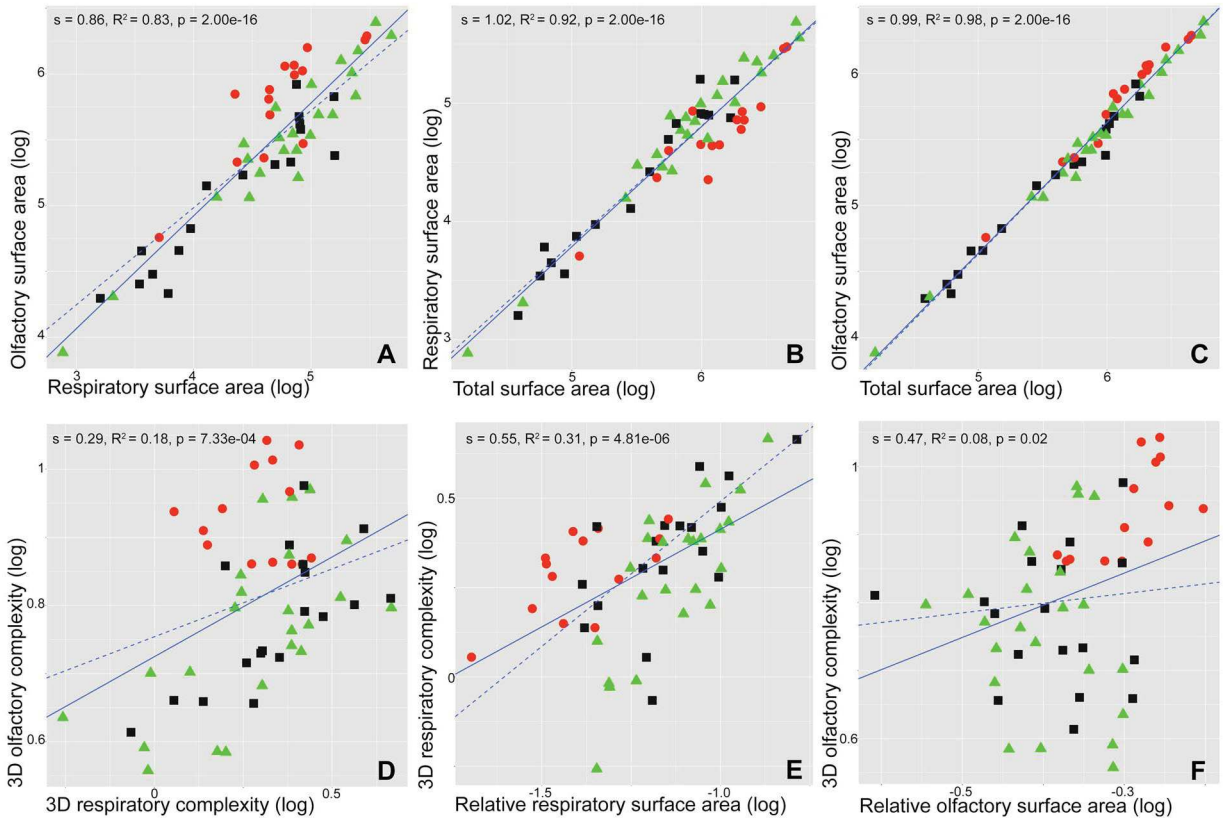

Figure 2. Log–log regressions (continuous line) and PGLS (dashed line) of (**A**) olfactory vs respiratory turbinal surface area, (**B**) respiratory vs total surface area, (**C**) olfactory vs total surface area, (**D**) olfactory vs respiratory 3D complexity (CHAR), (**E**) respiratory 3D complexity (CHAR) vs relative respiratory surface area, and (**F**) olfactory 3D complexity (CHAR) vs relative olfactory surface area. Colours and symbols: red dots = vermivorous, black squares = carnivorous, and green triangles = omnivorous.

the snout morphology of these vermivores might involve increased olfactory capacities to detect earthworms in leaf-litter.

Using comparative phylogenetic methods, we contrasted turbinal surface area and turbinal complexity between vermivorous, carnivorous and omnivorous species of Murinae to test hypothesised adaptations related to olfaction and heat and moisture conservation in the shrew-rats. We tested for convergence of the vermivorous pattern. In doing so, we propose two new indices of three dimensional (3D) complexity of turbinal bones, which we have implemented in the freeware MorphoDig[49].

Results

Turbinal surface area. There is a significant correlation between surface area of all turbinals and skull length (electronic supplementary material (ESM), Fig. S3A; slope (s) = 2.25, r squared (R^2) = 0.88, p-value (p) = 2.00e-16). The surface area of all turbinals show strong positive allometry (s = 2.25). The PGLS slope of vermivores is significantly different from the PGLS slope of carnivores and omnivores (p = 0.01 and 0.02, respectively; ESM, Fig. S3A). This indicates that when skull length increases, vermivores have a smaller increase in turbinal surface area than do carnivores and omnivores. This surface area difference could be explained by the smaller area of the respiratory turbinals (ESM, Fig. S3B). In fact, the PGLS slope of respiratory turbinal area and skull length in vermivores is significantly different from that of carnivores and omnivores (p = 0.01 in both cases; ESM, Fig. S3B). Furthermore, there are no PGLS slope differences between dietary categories for the correlation between olfactory turbinal surface area and skull length (p > 0.05; ESM, Fig. S3C). There is a significant correlation between olfactory and respiratory surface area (Fig. 2A; slope (s) = 0.86, R^2 = 0.83, p = 2.00e-16) and these variables display a negative allometry (s = 0.86). There are significant correlations between the surface area of respiratory or olfactory turbinals and the surface area of all turbinals (Fig. 2B and C; s = 1.02, R^2 = 0.92, p = 2.00e-16 and s = 0.99, R^2 = 0.98, p = 2.00e-16, respectively). PGLS slopes do not differ significantly between dietary categories for these two correlations (p > 0.3; Fig. 2B, C) and the relationship between these variables is isometric (s = 1.02 and s = 0.99; Fig. 2B, C). This suggests that sampled species exhibit the same relationship for these variables, thereby allowing comparisons of respiratory and olfactory turbinals between dietary categories.

ANOVA reveals that the residuals of PGLS (resPGLS) between olfactory and respiratory turbinals surface area is significantly affected by diet (p = 2.62e-07; ESM, Table S2). Indeed, vermivores have resPGLS between the

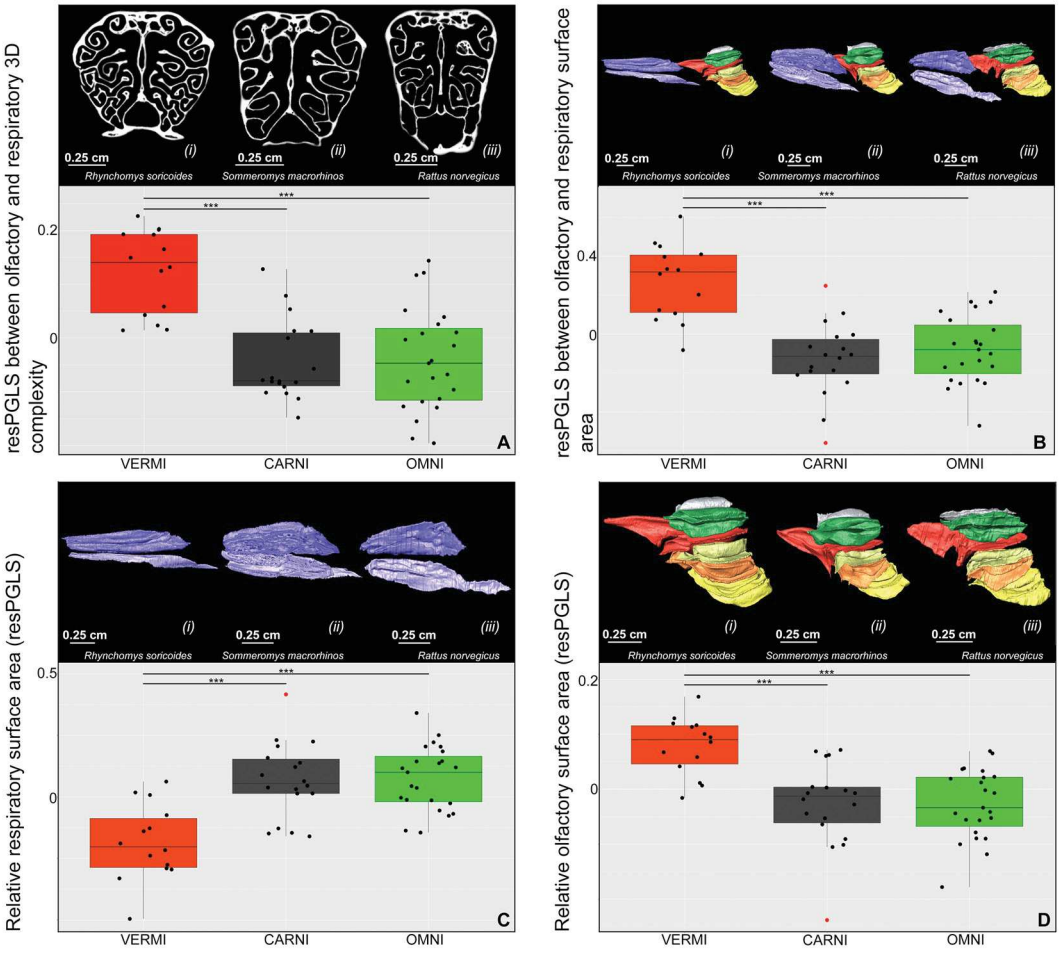

Figure 3. Boxplot with dietary categories: (**A**) residuals of PGLS (resPGLS) between olfactory and respiratory 3D complexity of turbinals (CHAR), (**B**) resPGLS between olfactory and respiratory surface area, (**C**) relative respiratory surface area, and (**D**) relative olfactory surface area. Significance codes are based on phylogenetic Tukey's HSD test. (i) *Rhynchomys soricoides*, (ii) *Sommeromys macrorhinos*, and (iii) *Rattus norvegicus*. Colours: red = vermivorous, black = carnivorous, and green = omnivorous. Red points are outliers.

surface area of olfactory and respiratory turbinals significantly higher than carnivores and omnivores (Fig. 3B; p = 1.00e-04; ESM, Table S3). Phylogenetic ANCOVA shows similar results with significant differences between vermivorous and carnivorous dietary categories (p = 1.43e-08; ESM, Table S6). Considering the nasoturbinal either as olfactory or as respiratory turbinals does not significantly change the results (ESM, Table S4). Moreover, slope differences between linear regressions and PGLS are small (ESM, Table S1). Differences between phylogenetic and non-phylogenetic Tukey's HSD tests are also small (ESM, Table S5).

ANOVA reveals that the relative surface area of olfactory turbinals is significantly affected by diet (p = 2.62e-07; ESM, Table S2). Indeed, vermivores have significantly higher relative surface area of olfactory turbinals as compared to carnivores and omnivores (Fig. 3D; p = 9.17e-05 and 8.40e-05, respectively; ESM, Table S3). Phylogenetic ANCOVA shows similar results with significant differences between vermivorous and carnivorous dietary categories (p = 8.46e-07; ESM, Table S6).

ANOVA reveals that the relative surface area of respiratory turbinals is significantly affected by diet (p = 4.11e-06; ESM, Table S2). Indeed, vermivores have significantly smaller relative respiratory turbinal surface area, relative nasoturbinal surface area, and relative maxilloturbinal surface area than do carnivores and omnivores (Fig. 3C; p = 1.18e-05, 1.00e-05, 2.67e-04, 2.19e-04, 4.47e-03, and 1.34e-03, respectively; ESM, Fig. S4A, B, Table S3). Phylogenetic ANCOVA shows similar results with significant differences between vermivorous and carnivorous dietary categories (p = 8.46e-07; ESM, Table S6).

Turbinal complexity. Olfactory and respiratory 3D complexity are significantly correlated (CHAR, Fig. 2 D; s = 0.29, R^2 = 0.18, p = 7.33e-04). Olfactory 3D complexity (CHAR) and skull length are also significantly correlated (ESM, Fig. S3E; s = 0.27, R^2 = 0.27, p = 2.60e-05). ANOVA reveals that resPGLS between olfactory and respiratory 3D complexity (CHAR) is significantly affected by diet (p = 3.59e-07; ESM, Table S2). Indeed, vermivores have a significantly higher resPGLS between the 3D complexity (CHAR) of olfactory and respiratory turbinals compared to carnivores and omnivores (Fig. 3A; p = 2.70e-06 and 1.60e-06, respectively). Phylogenetic

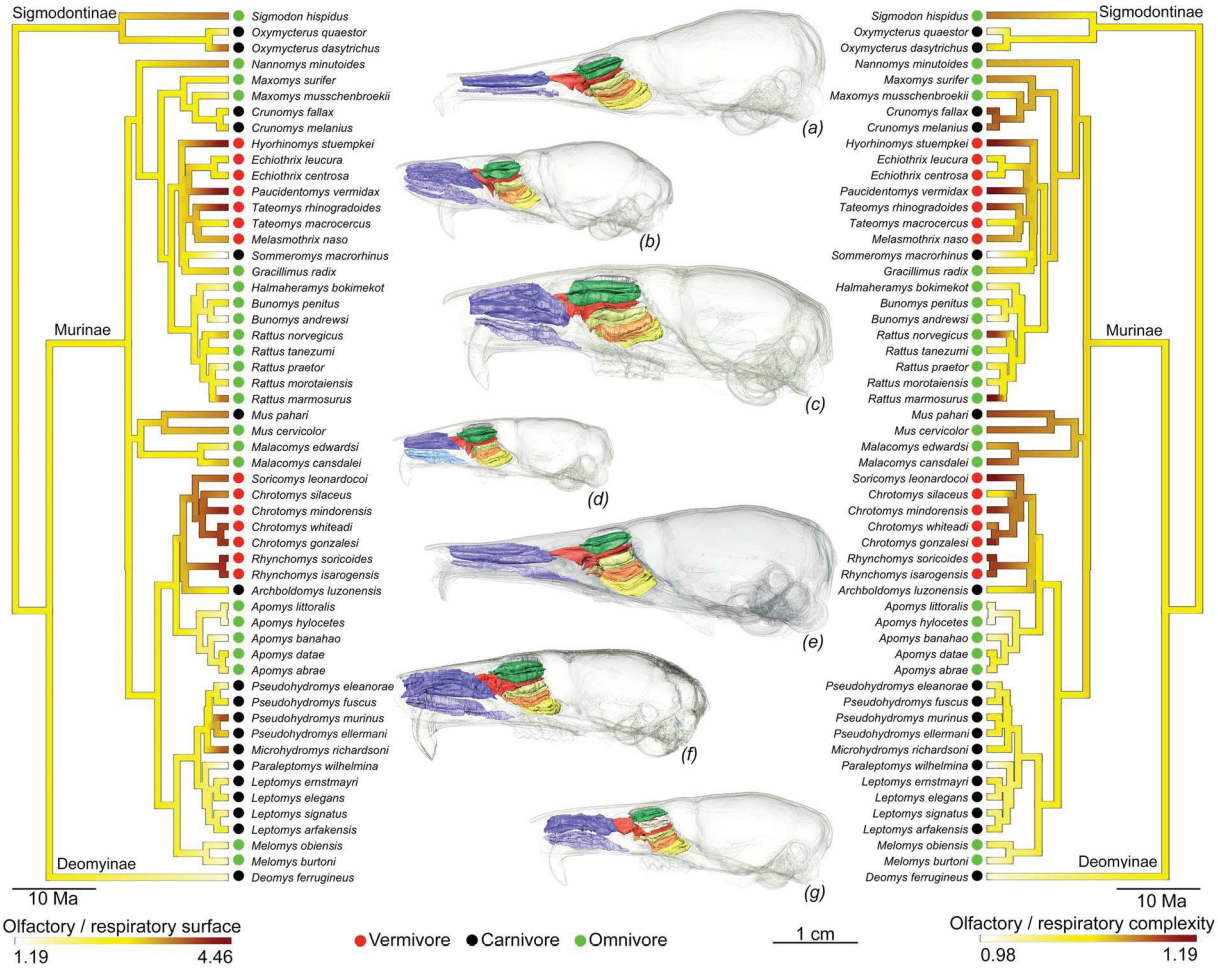

Figure 4. Continuous mapping of the ratio between olfactory and respiratory turbinal surface area (left) and of the ratio between olfactory and respiratory turbinal 3D complexity (CHAR, right) with phylogenetic relationships. (**a**) *Paucidentomys vermidax*, (**b**) *Sommeromys macrorhinos*, (**c**) *Bunomys penitus*, (**d**) *Mus pahari*, (**e**) *Rhynchomys soricoides*, (**f**) *Apomys banahao*, and (**g**) *Deomys ferrugineus*.

ANCOVA shows similar results with significant differences between vermivorous and carnivorous dietary categories ($p = 1.82e\text{-}03$, ESM, Table S6). Slope differences between linear regressions and PGLS are low (ESM, Table S1). 3D complexity (CHAR) of olfactory turbinals is significantly affected by diet ($p = 8.54e\text{-}05$). Indeed, vermivores and carnivores express a significantly higher olfactory turbinal complexity than omnivores ($p = 5.42e\text{-}05$ and $p = 0.05$, respectively; ESM, Table S3). Respiratory turbinals 3D complexity (CHAR) is not significantly affected by diet ($p = 0.14$; ESM, Table S2).

Results obtained with our two 3D complexity indices are similar to each other (ESM, Fig. S5 and Table S3) and to those obtained from 2D complexity (ESM, Fig. S5 and Table S3). This indicates that the 2D complexity signal from the middle slice of each turbinal group extracts the complexity of each turbinal group.

Turbinal surface area and turbinal complexity. There is a significant correlation between 3D complexity (CHAR) and relative surface area of respiratory turbinals (Fig. 2E; $s = 0.55$, $R^2 = 0.31$, $p = 4.81e\text{-}06$). Considering phylogeny, there is no significant correlation between the 3D complexity (CHAR) and the relative surface area of olfactory turbinals (Fig. 2F; PGLS $s = 0.14$, PGLS $p = 0.36$). The continuous phylogenetic mapping of the ratio between olfactory and respiratory surface areas and 3D complexity (CHAR) reveals similar patterns for both proxies (surface area and complexity; Fig. 4). However, four species display a different pattern between these two proxies: *Chrotomys silaceus*, *Maxomys surifer*, *Microhydromys richardsoni*, and *Pseudohydromys murinus* (Fig. 4). Even if patterns between surface area and 3D complexity (CHAR) are similar (Fig. 4), very low R^2 values in some PGLS (Fig. 2; ESM, Fig. S3, and Table S1) reveal that we need to consider both proxies to understand olfactory capacities.

Snout. Snout length and width differences are significantly affected by diet when vermivores are separated into two ecological subcategories: terrestrial and semi-fossorial vermivores ($p = 0.01$, $p = 1.09e\text{-}04$, respectively; ESM, Table S2). Indeed, semi-fossorial vermivores (*Chrotomys* spp.) have significantly shorter snouts than carnivores and terrestrial vermivores ($p = 0.04$, $p = 0.03$, respectively; ESM, Table S3). Terrestrial vermivores have

Model	(A) RespiSA/TotSA		(B) OlfaSA/TotSA		(C) OlfaSA/RespiSA		(D) OlfaCHAR		(E) OlfaCHAR/RespiCHAR	
	AICc	ΔAICc	AICc	ΔAICc	AICc	ΔAICc	AICc	ΔAICc	AICc	ΔAICc
BM	−132.63	34.35	−132.63	34.35	453.76	1127.27	−94.73	15.01	−127.42	62.83
OU1	−161.79	5.20	−161.79	5.29	−668.09	5.42	−107.18	2.56	−186.47	3.78
OU2	−166.99	0.00	−166.98	0.00	−673.51	0.00	−109.74	0.00	−190.25	0.00
OU3	−164.58	2.40	−164.59	2.40	−669.04	4.47	−107.50	2.25	−185.76	4.49

Table 1. Results of 1 000 simulations of single-rate BM and three alternative OU models with (A) the ratio between respiratory and total surface area, (B) the ratio between olfactory and total surface area, (C) the ratio between olfactory and respiratory surface area, (D) the 3D olfactory complexity (CHAR), and (E) the ratio between olfactory and respiratory 3D complexity (CHAR). BM and OU1 with omnivorous and all carnivorous dietary categories (carnivorous + vermivorous); OU2 with omnivorous, carnivorous, and vermivorous dietary categories; and OU3 with omnivorous, carnivorous, terrestrial vermivorous, and semi-fossorial vermivorous dietary categories. AICc = Akaike's information criterion corrected. ΔAICc = difference between AICc compared to minimum AICc.

Variables	C1	p-value	C2	p-value	C3	p-value
RelatOlfaSA + RelatRespiSA + OlfaCHAR + SNW	0.233	0.123	0.11	0.002	0.122	0.113
RelatOlfaSA + RelatRespiSA + OlfaCHAR	0.394	0.003	0.163	<1.000e-04	0.207	0.005
RelatOlfaSA + OlfaCHAR	0.408	0.009	0.165	<1.000e-04	0.217	0.003

Table 2. Results of the three convergence index tests as proposed by Stayton 2015[106] with: RelatOlfaSA = relative olfactory surface area, RelatRespiSA = relative respiratory surface area, OlfaCHAR = olfactory 3D complexity of the convex hull area ratio, and SNW = snout width.

significantly narrower snouts than omnivores and semi-fossorial vermivores (ESM, Fig. S6; p = 0.02 and 6.03e-05, respectively; ESM, Table S3). Semi-fossorial vermivores (*Chrotomys* spp.) have significantly larger relative snouts compared to omnivores, carnivores, and terrestrial vermivores (ESM, Fig. S6; p = 0.01, 2.00e-03, and 6.03e-05, respectively; ESM, Table S3).

Adaptation and convergence. The best-fitting model is OU2 (Table 1), a model with 3 adaptive optima: omnivorous, carnivorous, and vermivorous dietary categories for (A) relative respiratory surface area, (B) relative olfactory surface area, (C) olfactory and respiratory surface area, (D) 3D complexity (CHAR) of olfactory turbinals, and (E) 3D complexity (CHAR) of olfactory and respiratory turbinals. The best fitting model for the relative snout width is OU3 (ESM, Table S7), with 4 adaptive optima: omnivorous, carnivorous, terrestrial vermivorous, and semi-fossorial vermivorous diets and lifestyles.

Considering the C2 index, vermivorous murine convergence is highly significant when we test for global rostral pattern composed of relative olfactory and respiratory surface area, olfactory 3D complexity (CHAR), and snout width (Table 2). The convergence is not significant when we consider the C1 and C3 indices (Table 2). Considering the three indices (C1, C2, and C3), the convergence is highly significant when we test for the relative olfactory surface area, the respiratory surface area, and the olfactory 3D complexity (Table 2); or when we test for the relative olfactory surface area and the olfactory 3D complexity (Table 2).

Discussion

Olfactory capacities in vermivorous murines. Compared to carnivores and omnivores, vermivores should have significantly better olfactory capacities, based on both the larger surface area and higher complexity of their olfactory turbinals. We hypothesised that these bony specialisations are related to an improvement of their olfactory adaptations allowing them to detect prey that are underground or invisible within wet leaf litter (Heaney, pers. comm). Such prey may be especially elusive and difficult to detect for more generalist, opportunistic rats. Indeed, molecular odorants are especially difficult to detect underground as compared to on the surface[50]. Most of these insular vermivorous rats (*Melasmothrix*, *Soricomys*, and *Tateomys*) are terrestrial and display relatively long claws in order to dig into moss, bark, leaf litter, and damp soil, where these earthworms are most abundant[51]. Other earthworm specialists patrol runways (*Echiothrix* and *Rhynchomys*)[45,52] or dig underground (*Chrotomys*)[52] to find their prey. The wide and short snout of the semi-fossorial vermivorous *Chrotomys* (ESM, Table S3 and Fig. S6) might be a fossorial adaptation that is also found in other fossorial rodents like chisel-tooth diggers[53,54]. Following Heth & Todrank[50], the semi-fossorial vermivorous *Chrotomys* should have higher olfactory capacities than terrestrial ones, in order to detect molecular odorants from their underground prey. Based on turbinal complexity and surface area measurements some vermivores display the most derived morphology relative to the sampled murines with the highest olfactory capacities. This occurs with semi-fossorial species (*Chrotomys* spp.), with species that are patrolling along runways (*Rhynchomys isarogensis* and *R. soricoides*), that dig into bark (*Tateomys rhinogradoides*) and some with unknown feeding behaviours (*Hyorhinomys stuempkei* and *Paucidentomys vermidax*; Figs. 3 and 4). As our results show, the morphological diversity of these vermivores is quite large and we have a rather limited knowledge about their ecological diversity. Ecological studies of rodents are difficult due to most species' nocturnal activity, poor trapping success, and sometimes low abundance, especially in the case of the vermivores[55–57]. It will be important in the future to investigate in greater detail stomach

contents using metabarcoding if we are to understand the link between olfactory capacities and dietary behaviors of vermivorous rats. Different ecomorphs of earthworm specialists might occur in different underground and ground layers. Our results reveal a connection between dietary specialisations and surface area and complexity of olfactory turbinals, which suggests a functional link. However, these lines of morphological evidence are just a first step toward understanding the ecological and functional diversity of shrew-rats. While the link between the size of olfactory organs or the number of olfactory receptors and olfactory performance is debated[9,18–20,58,59], mammals show a strong correlation between the size of a morphological proxy for olfaction (the cribriform plate) and the repertoire of olfactory receptor genes (OR)[11].

To our knowledge, there is no study showing a clear relation between olfactory performances and the size of olfactory proxies such as turbinal bones, cribriform plate, olfactory bulb or vomeronasal organ. This lack of knowledge does not allow us to discriminate between acuity, sensitivity, and discrimination when we used olfactory turbinal proxies. However, our findings about the highly specialised vermivores suggest that an increasing in olfactory turbinal size is probably not correlated with odorant acuity, that is the ability to detect a wide array odorants[9]. Integrative studies of the olfactory system that include performance tests will further our understanding of these distinctive animals.

Heat and moisture conservation. In terrestrial vermivores, the distal part of the snout is narrow (ESM, Table S3 and Fig. S6), which is assumed to be a morphological adaptation to earthworm consumption[60–62]. Such snout morphology has profound consequences for the respiratory surface and complexity of turbinals. Under a trade-off hypothesis between olfactory and respiratory turbinals, respiratory turbinal reduction could be a consequence of the increased size of olfactory turbinals. Indeed, previous work on carnivorans[9] suggests a trade-off between olfactory and respiratory turbinal areas due to the limited rostral space and the need for other functions, such as vision or cranio-mandibular muscles. Additionally, the highly specialised cranio-mandibular apparatus of vermivores[48] might impact the evolution of their rostrum, and the narrowing trend has resulted in highly reduced surface of the naso- and maxilloturbinal bones (Fig. 3C and ESM, Table S3 and Fig. S4). Depending on the organism and their environmental conditions, the respiratory turbinals may be involved in water conservation (e.g., in salty or dry environments) or heat retention (e.g., in cool or aquatic environments)[8,17,26–32,63]. Despite wide altitudinal and thermal differences in the sampled murines, the reduction of heat and moisture conservation potential in vermivores may not present a major energetic constraint in their tropical and terrestrial environments. Under the trade-off hypothesis between respiratory and olfactory turbinals, respiratory turbinal reduction might have facilitated an increase of olfactory capacities as the novel cranio-mandibular specialisations developed in vermivorous lineages.

Vermivores convergence. Claims of convergence were previously proposed for vermivorous murines based on discrete character observations[44,51], or by the use of a common vernacular name: shrew-rats. Dietary convergences in both insular and continental murids were recently demonstrated with stomach content evidence[44]. Using a large-scale phylogenetical framework for murids, Rowe[44] inferred ancestral dietary state and recorded at least 7 shifts from an omnivorous to a carnivorous diet, with a potential reversal from carnivory to omnivory in *Gracilimus*[64]. Our results demonstrate a strong convergence footprint involving aspects of both the rostrum and turbinal morphologies (Tables 1, 2, and ESM, Table S7). Specifically, convergence among shrew-rats involves larger and more complex olfactory turbinals (Fig. 3A, B, D, 4, and ESM, Table S3), reduced respiratory turbinals (Fig. 3C and ESM, Table S3 and Fig. S4), and narrower snouts (ESM, Table S3 and Fig. S6). As explained in previous sections, these convergent patterns are probably related to dietary adaptations within the most specialised vermivorous forms.

Convergence among these shrew-rats might have been fostered by their replicated colonisation of islands in the Indo-Australian Archipelago, a hypothesis that is in accordance with the insular adaptive radiation theory[65,66]. However, colonisation of islands is not the only factor that might have led to the convergence of these lineages that are mainly found on the largest islands with mountainous landscapes[52,64]. Indeed, most IAA vermivores occur at relatively high elevation[47,52,67–69]. This distribution pattern coincides with an increase in earthworm density and abundance, demonstrated along elevation transects both in Luzon (Philippines) and Borneo (Malaysia)[55,70]. Rowe *et al.*[44] suggested that the altitudinal distribution of vermivores might be explained by increased earthworm abundance as well as the reduction of potential food competitors such as ants that are most abundant in the lowlands[55,71,72]. Richness and abundance of small mammals is also higher at high altitude in islands of the IAA[57,72–75]. Inter-specific interaction of small mammals is another hypothesis to explain the diversity of these vermivores, especially on islands. Both high species richness and high competition for resources in these small mammal communities might have fostered these convergences. In fact, their omnivorous ancestors independently took advantage of an ecological niche that was likely vacant, mainly in an insular context. Specialisation into shrew-rat ecomorphs (runner, digger, and fossorial) might have reduced food competition and allowed co-occurrence of several earthworm specialists that likely share diverse earthworm resources at mid- to high elevations on islands. The successful dietary specialisation of vermivores was associated with independent acquisitions of large and complex olfactory turbinal bones that presumably improved olfactory capacities. Beyond the morphological convergence of molar reduction[62] and turbinal bones, other convergent aspects will certainly be revealed by future anatomical and functional studies.

Conclusion

Despite recent studies about mammal olfaction[11,16,76,77] our knowledge in this field is rather limited. For example, the olfactory and respiratory epithelial covers are unknown or poorly described in most of non-model species. Comparative histology will help to refine the functional discrimination between olfactory and respiratory turbinals. Additionally, very few studies have been done concerning the complexity of turbinal bones[8,9,28,77,78].

Consequently, further studies will be necessary to understand the functional role of the complexity in nasal airflow and odorant deposition[79]. Despite this first evidence showing the possible trade-off between respiratory and olfactory turbinal bones (Fig. S3) further studies should use other variables than the skull length to test this hypothesis. Indeed, skull length might covary with nasal cavity and turbinal bones. Finally, other anatomical proxies should be further investigated such as the nasal septum, the cribriform plate, the olfactory bulb or the vomeronasal organ to understand multiple factors of murine olfaction.

Turbinal bones are important structures to understand how species that are challenging to study in the field have adapted to their environment. Consequently, museum specimens with undamaged turbinates are very valuable. Over the past few years there is an emerging trend to request samples of turbinal bones from museum specimens for molecular work (R. Portela Miguez in pers.). In light of the findings of our research, we recommend that the integrity of these nasal structures should be preserved so others can replicate this study or investigate other species applying similar methods.

Material and Methods

We borrowed 87 skulls belonging to 55 rodent species from: American Museum of Natural History (AMNH), Centre de Biologie et de Gestion des Populations (CBGP), Field Museum of Natural History (FMNH), Museums Victoria (NMV), Museum Zoologicum Bogoriense (MZB), Natural History Museum London (NHMUK), Natural History Museum of Paris (MNHN), Smithsonian Institution National Museum of Natural History (NMNH), and University of Montpellier (UM). These samples comprised 14 vermivorous (30 specimens), 18 carnivorous (28 specimens), and 23 omnivorous species (29 specimens (ESM, Tables S8 and S9)). All sampled species were considered terrestrial except for *Chrotomys*, a semi-fossorial genus[52,55,56]. For outgroups, we selected additional carnivorous and omnivorous genera in Cricetidae (*Oxymycterus* and *Sigmodon*) and Muridae (Deomyinae).

Digitising and measurement. Skulls were scanned using X-ray microtomography on a SkyScan 1076 (ISEM Institute, Montpellier), Nikon Metrology HMX ST 225 (NHMUK Natural History Museum, London), or SkyScan 1174v2 (The Evans Evolutionary Morphology Lab, Monash University, Melbourne). Acquired voxel size ranged from 18 to 36 μm. We digitised each left turbinal from each individual with Avizo Lite 9.0.1 software (VSG Inc., Burlington, MA, USA). This process was completed by semi-automatically selecting and delimiting each turbinal on each reconstructed virtual slice. Segmentation followed turbinal descriptions presented for Rodentia[80], Lagomorpha[38], and Marsupialia[81]. According to these references, we divided into 8 or 9 turbinals (Fig. 1 and ESM, Figs. S1 and S2) and followed anatomical terminology of ontogeny[38–41]. For the lamina semicircularis, we segmented only the homologous branching part (Fig. 1 and ESM, Figs. S1 and S2) that is covered by olfactory epithelium[24]. We identified an additional frontoturbinal (ft2) positioned between ft1 and etI (ESM, Fig. S2), which is only present in the outgroups (Deomyinae and Sigmodontinae). A second interturbinal (it) was also found in one individual of *Tateomys macrocercus* (Murinae). These additional turbinals were used in quantitative analyses of olfactory surfaces because they are located in the olfactory recess and should be covered by epithelial olfactory cells as are other olfactory turbinals[24]. Following previous comparative studies works that used turbinal bone surface area[9,23], we decide to not include other bone structures that are covered by epithelium other than turbinals. For example, the nasal septum is partially covered in sensory epithelium[17,24,82] but accurate delimitation is not possible with dry skulls. For all following quantitative measures and analyses, we took species averages for which we have multiple specimens (ESM, Table S8).

Skull length (SKL) was measured between the most anterior part of the nasal bone and the most posterior part of the occipital bone[83]. Snout length (SNL) was measured between the most anterior part of the nasal bone and the posterior-most portion of the naso-frontal suture. The snout width (SNW) was measured across the nasolacrimal capsules[83]. Length measurements were exported using Avizo Lite 9.0.1 software (VSG Inc., Burlington, MA, USA).

Turbinal surface area. We divided the turbinals into olfactory and respiratory regions to estimate the surface area available for these two functions and used the surface area as a proxy for olfactory or heat and moisture conservation capacities. Due to the impossibility of estimating the proportion of nasoturbinal that was involved in olfaction or in heat and moisture conservation, we performed separate surface area analyses including nasoturbinal either as respiratory or as olfactory turbinals (ESM, Table S4). Within turbinal regions, we assumed that the different epithelial cells and receptors were evenly distributed and as such, greater surface area indicates greater capacity. We sized turbinal surface areas by the total surface area of all turbinals. The surface area of segmented turbinals were exported using Avizo Lite 9.0.1 software (VSG Inc., Burlington, MA, USA).

Turbinal complexity. In addition to surface area, we also used turbinal complexity as a proxy for olfactory and heat or moisture conservation capacities. We interpret complexity as the degree of details in a predefined area. Following the principles of fluid dynamics, proportionally more fluid volume will come in contact with the edge of a narrow pipe than in a larger pipe. We assume that the same rule applies to air as it passes by the turbinals. As such, turbinals should be more efficient for surface exchange in complex structures than in simpler ones. As an example, a species with a high olfactory turbinal complexity is hypothesised to have good olfactory capacities.

To measure 2D turbinal complexity, we used the box counting method[84,85]. The complexity value (Db) was based on the number of boxes placed into a grid and necessary to cover the shape border, changing box size from large to small. It is a ratio between the details and the total scale, quantifying the fractal dimension of the bone. To simplify the process of 2D complexity acquisition, we measured turbinal complexity for each respiratory and olfactory turbinal group. We considered that all anteriorly positioned turbinals (respiratory turbinals) were involved in heat and moisture conservation, while posterior ones (olfactory turbinals) participated in

olfaction. Using ImageJ software[86], we extracted scanned images corresponding to the middle of the total number of slices composing each turbinal group. We converted the turbinal shape into a single pixel-wide binary contour using skeletonisation. The image was then scaled and centered onto a 300 × 300-pixel black square with Adobe Photoshop CS6 software. Images were converted to grayscale and binary formats. The 2D complexity value was obtained with ImageJ plugin FracLac[87]. Slice surface area was used as a size proxy to scale complexity values.

To measure 3D turbinal complexity we propose two indices implemented in the freeware MorphoDig[49]. These indices both make use of 3D convex hulls. A convex hull is the smallest convex envelope that contains the studied shape, in our case the turbinal bones.

Firstly, the convex hull area ratio (CHAR) is the ratio between the turbinal surface area (SA) and the surface area of the corresponding convex hull (CHSA):

$$CHAR = \frac{SA}{CHSA}$$

Secondly, the convex hull normalised shape index (CHNSI) measures how much turbinal surface area (SA) can be enclosed within the volume defined by the convex hull of the turbinal (CHV). It is defined as:

$$CHNSI = F\frac{\sqrt{SA}}{\sqrt[3]{CHV}}$$

where F is a constant defined so that spherical shapes express a CHNSI index equal to 1, as the 3D convex hull of a given:

$$F = \frac{\sqrt[3]{\frac{4}{3}\pi}}{2\sqrt{\pi}}$$

Quantitative analyses. We performed phylogenetic generalized least squares (PGLS) using R v.3.2.4[88], with ape[89], nlme[90], and phytools[91]. The phylogeny used for the following analyses was adapted from Fabre *et al.*, Rowe *et al.*, and Steppan & Schenk ([43,44,92], ESM, legend S1). To determine if slopes were significantly different between dietary groups and to compare allometric effects, we performed analysis of covariance (ANCOVA) following Claude[93]. We also performed analysis of variance (ANOVA) based on the residuals of PGLS (resPGLS) to test for dietary influence on turbinal surface area, turbinal complexity, snout length, and snout width. To test for group differences, we performed the multiple comparison test of Tukey's HSD based on the residuals of the PGLS with the R package multcomp[94]. To compare differences without phylogeny we also performed Tukey's HSD tests based on the residuals of linear regressions. For all analyses based on PGLS we performed model fitting with: a model without phylogeny, Brownian (BM), Ornstein–Uhlenbeck (OU), and Grafen models in order to adapt the phylogenetic model to our data[95,96].

Because methodological studies pointed out some biased results when residuals are treat as data[97–99], we compared our residual approach with phylogenetic ANCOVA (ESM, Table S6). We contrasted three models: a model without dietary categories (H0), a model with omnivorous and carnivorous dietary categories (Carni), and a model with omnivorous, carnivorous, and vermivorous dietary categories (Vermi). Models were compared using the Akaike information criterion (AIC) and the Likelihood-ratio test (LRT).

Adaptation and convergence tests. To test for associations between dietary categories and turbinal surface area, turbinal complexity, snout length, and snout width, we fit Brownian motion (BM) and Ornstein–Uhlenbeck (OU) models[96,100,101]. We computed 1,000 simulations of single-rate BM and three alternative OU models: BM and OU1 with omnivorous and all carnivorous dietary categories (carnivorous + vermivorous); OU2 with omnivorous, carnivorous, and vermivorous dietary categories; and OU3 with omnivorous, carnivorous, terrestrial vermivorous, and semi-fossorial vermivorous dietary categories. Model fits were compared using differences in the Akaike information criterion (ΔAIC). If earthworm consumption had a deterministic impact on the evolution of one of our measured traits, the best-fitted models should be OU2 or OU3. We ran these analyses with R packages: ape[89], corpcor[102], mvMORPH[100], phytools[91], and subplex[103].

To visualize a pattern of convergence in surface area and complexity states, we separately mapped the ratio between olfactory and respiratory turbinal surface area and complexity on the phylogeny. Using maximum likelihood (ML)[104], we estimated ancestral states at internal nodes and interpolated the states along each edge of the phylogeny[105].

To quantify convergence among dietary groups in turbinal surface area, turbinal complexity, snout length, and snout width, we used three measures proposed by Stayton[106]. Firstly, C1 is the inverse of the ratio between the phenotypic distance between convergent tips (Dtip) and the maximum distance between any pair of taxa in those two lineages (Dmax). Secondly, C2 is the difference between Dmax and Dtip. Thirdly, C3 is the ratio between C2 and the sum of all phenotypic distances from ancestors to descendants (Ltot.clade). Contrary to C2 and C3, C1 compares phenotypic similarities and phylogenetic relationships without taking into account the absolute amount of evolution that has occurred during convergence[106]. We ran these analyses with a modified R package convevol[107,108], performing 1,000 simulations.

Data Availability Statement

Raw data are available in the electronic supplementary material (ESM). The CT-scan surfaces could be requested to the corresponding author.

References

1. Gould, S. J. & Lewontin, R. C. The spandrels of San Marco and the Panglossian paradigm: a critique of the adaptationist programme. *Proceedings of the Royal Society of London. Series B, Biological sciences* **205**, 581–98 (1979).
2. Reeve, H. K. & Sherman, P. W. Adaptation and the Goals of Evolutionary Research. *The Quarterly Review of Biology* **68**, 1–32 (1993).
3. McGhee, G. R. *Convergent evolution: limited forms most beautiful*. (MIT Press, 2011).
4. Losos, J. B. Convergence, adaptation, and constraint. *Evolution* **65**, 1827–1840 (2011).
5. Van Valkenburgh, B., Theodor, J., Friscia, A., Pollack, A. & Rowe, T. Respiratory turbinates of canids and felids: a quantitative comparison. *Journal of Zoology* **264**, 281–293 (2004).
6. Brusatte, S. L. *et al*. The Braincase and Neurosensory Anatomy of an Early Jurassic Marine Crocodylomorph: Implications for Crocodylian Sinus Evolution and Sensory Transitions. *The Anatomical Record* **299**, 1511–1530 (2016).
7. Pfaff, C., Martin, T. & Ruf, I. Bony labyrinth morphometry indicates locomotor adaptations in the squirrel-related clade (Rodentia, Mammalia). *Proceedings. Biological sciences* **282**, 20150744 (2015).
8. Van Valkenburgh, B., Smith, T. D. & Craven, B. A. Tour of a Labyrinth: Exploring the Vertebrate Nose. *The Anatomical Record* **297**, 1975–1984 (2014).
9. Van Valkenburgh, B. *et al*. Aquatic adaptations in the nose of carnivorans: evidence from the turbinates. *Journal of Anatomy* **218**, 298–310 (2011).
10. Ferreira-Cardoso, S. *et al*. Floccular fossa size is not a reliable proxy of ecology and behaviour in vertebrates. *Scientific Reports* **7**, 2005 (2017).
11. Bird, D. J. *et al*. Olfaction written in bone: cribriform plate size parallels olfactory receptor gene repertoires in Mammalia. *Proceedings. Biological sciences* **285**, 20180100 (2018).
12. Hayden, S. *et al*. Ecological adaptation determines functional mammalian olfactory subgenomes. *Genome research* **20**, 1–9 (2010).
13. Zarzo, M. The sense of smell: molecular basis of odorant recognition. *Biological Reviews* **82**, 455–479 (2007).
14. Lindblad-Toh, K. *et al*. Genome sequence, comparative analysis and haplotype structure of the domestic dog. *Nature* **438**, 803–819 (2005).
15. Hayden, S. *et al*. A Cluster of Olfactory Receptor Genes Linked to Frugivory in Bats. *Molecular Biology and Evolution* **31**, 917–927 (2014).
16. Hughes, G. M. *et al*. The Birth and Death of Olfactory Receptor Gene Families in Mammalian Niche Adaptation. *Molecular Biology and Evolution* **35**, 1390–1406 (2018).
17. Negus, V. The Comparative Anatomy and Physiology of the Nose and Paranasal Sinuses Livingstone. *Edinburgh and London* (1958).
18. Laska, M., Genzel, D. & Wieser, A. The Number of Functional Olfactory Receptor Genes and the Relative Size of Olfactory Brain Structures Are Poor Predictors of Olfactory Discrimination Performance with Enantiomers. *Chemical Senses* **30**, 171–175 (2005).
19. Frasnelli, J. *et al*. Neuroanatomical correlates of olfactory performance. *Experimental Brain Research* **201**, 1–11 (2010).
20. Seubert, J., Freiherr, J., Frasnelli, J., Hummel, T. & Lundstrom, J. N. Orbitofrontal Cortex and Olfactory Bulb Volume Predict Distinct Aspects of Olfactory Performance in Healthy Subjects. *Cerebral Cortex* **23**, 2448–2456 (2013).
21. Smith, T. D., Eiting, T. P. & Rossie, J. B. Distribution of Olfactory and Nonolfactory Surface Area in the Nasal Fossa of Microcebus murinus: Implications for Microcomputed Tomography and Airflow Studies. *The Anatomical Record: Advances in Integrative Anatomy and Evolutionary Biology* **294**, 1217–1225 (2011).
22. Rowe, T. B., Eiting, T. P., Macrini, T. E. & Ketcham, R. A. Organization of the Olfactory and Respiratory Skeleton in the Nose of the Gray Short-Tailed Opossum Monodelphis domestica. *Journal of Mammalian Evolution* **12**, 303–336 (2005).
23. Green, P. A. *et al*. Respiratory and olfactory turbinal size in canid and arctoid carnivorans. *Journal of Anatomy* **221**, 609–621 (2012).
24. Barrios, A. W., Núñez, G., Quinteiro, P. S., Salazar, I. & Chamero, P. Anatomy, histochemistry, and immunohistochemistry of the olfactory subsystems in mice. https://doi.org/10.3389/fnana.2014.00063 (2014).
25. Ruben, J. A. *et al*. The Metabolic Status of Some Late Cretaceous Dinosaurs. *Science* **273**, 1204–1207 (1996).
26. Schmidt-Nielsen, K., Hainsworth, F. R. & Murrish, D. E. Counter-current heat exchange in the respiratory passages: Effect on water and heat balance. *Respiration Physiology* **9**, 263–276 (1970).
27. Hillenius, W. J. The evolution of nasal turbinates and mammalian endothermy. *Paleobiology* **18**, 17–29 (1992).
28. Craven, B. A. *et al*. Reconstruction and Morphometric Analysis of the Nasal Airway of the Dog (Canis familiaris) and Implications Regarding Olfactory Airflow. *The Anatomical Record: Advances in Integrative Anatomy and Evolutionary Biology* **290**, 1325–1340 (2007).
29. Craven, B. A., Paterson, E. G. & Settles, G. S. The fluid dynamics of canine olfaction: unique nasal airflow patterns as an explanation of macrosmia. *Journal of the Royal Society, Interface* **7**, 933–43 (2010).
30. Morgan, K. T., Kimbell, J. S., Monticello, T. M., Patra, A. L. & Fleishman, A. Studies of inspiratory airflow patterns in the nasal passages of the F344 rat and rhesus monkey using nasal molds: Relevance to formaldehyde toxicity. *Toxicology and Applied Pharmacology* **110**, 223–240 (1991).
31. Kimbell, J. S. *et al*. Computer Simulation of Inspiratory Airflow in All Regions of the F344 Rat Nasal Passages. *Toxicology and Applied Pharmacology* **145**, 388–398 (1997).
32. Lester, C. W. & Costa, D. P. Water conservation in fasting northern elephant seals (Mirounga angustirostris). *The Journal of experimental biology* **209**, 4283–94 (2006).
33. Eiting, T. P., Smith, T. D., Perot, J. B. & Dumont, E. R. The role of the olfactory recess in olfactory airflow. *The Journal of experimental biology* **217**, 1799–803 (2014).
34. Allison, A. C. The morphology of the olfactory system in the vertebrates. *Biological Reviews* **28**, 195–244 (1953).
35. Ressler, K. J., Sullivan, S. L. & Buck, L. B. A zonal organization of odorant receptor gene expression in the olfactory epithelium. *Cell* **73**, 597–609 (1993).
36. Van Valkenburgh, B. *et al*. Respiratory and Olfactory Turbinals in Feliform and Caniform Carnivorans: The Influence of Snout Length. *The Anatomical Record* **297**, 2065–2079 (2014).
37. Firestein, S. How the olfactory system makes sense of scents. *Nature* **413**, 211–218 (2001).
38. Ruf, I. Comparative Anatomy and Systematic Implications of the Turbinal Skeleton in Lagomorpha (Mammalia). *The Anatomical Record* **297**, 2031–2046 (2014).
39. Maier, W. & Ruf, I. Morphology of the Nasal Capsule of Primates-With Special Reference to *Daubentonia* and *Homo*. *The Anatomical Record* **297**, 1985–2006 (2014).
40. Reinbach, W. Zur Entwicklung des Primordialcraniums von Dasypus novemcinctus Linné (Tatusia novemcincta Lesson) I. *Zeitschrift für Morphologie und Anthropologie* 375–444, https://doi.org/10.2307/25753216 (1952).
41. Reinbach, W. Zur Entwicklung des Primordialcraniums von Dasypus novemcinctus Linné (Tatusia novemcincta Lesson) II. *Zeitschrift für Morphologie und Anthropologie* 1–72, https://doi.org/10.2307/25753226 (1952).
42. Yee, K. K., Craven, B. A., Wysocki, C. J. & Van Valkenburgh, B. Comparative Morphology and Histology of the Nasal Fossa in Four Mammals: Gray Squirrel, Bobcat, Coyote, and White-Tailed Deer. *The Anatomical Record* **299**, 840–852 (2016).
43. Fabre, P.-H. *et al*. A new genus of rodent from Wallacea (Rodentia: Muridae: Murinae: Rattini), and its implication for biogeography and Indo-Pacific Rattini systematics. *Zoological Journal of the Linnean Society* **169**, 408–447 (2013).

44. Rowe, K. C., Achmadi, A. S. & Esselstyn, J. A. Repeated evolution of carnivory among Indo-Australian rodents. *Evolution* **70**, 653–665 (2016).
45. Musser, G. G. & Durden, L. A. Morphological and Geographic Definitions of the Sulawesian Shrew Rats *Echiothrix leucura and E. centrosa* (Muridae, Murinae), and Description of a New Species of Sucking Louse (Phthiraptera: Anoplura). *Bulletin of the American Museum of Natural History* **391**, 1–87 (2014).
46. Balete, D. S. *et al*. Archboldomys (Muridae: Murinae) Reconsidered: A New Genus and Three New Species of Shrew Mice from Luzon Island, Philippines. *American Museum Novitates* **3754**, 1–60 (2012).
47. Esselstyn, J. A., Achmadi, A. S. & Rowe, K. C. Evolutionary novelty in a rat with no molars. *Biology letters* **8**, 990–3 (2012).
48. Samuels, J. Cranial morphology and dietary habits of rodents. *Zoological Journal of the Linnean Society* **156**, 864–888 (2009).
49. Lebrun, R. MorphoDig, an open-source 3d freeware dedicated to biology. *available at* http://morphomuseum.com/morphodig (2018).
50. Heth, G. & Todrank, J. In *Subterranean Rodents* 85–96, https://doi.org/10.1007/978-3-540-69276-8_8 (Springer Berlin Heidelberg, 2007).
51. Musser, G. G. Crunomys and the small-bodied shrew rats native to the Philippine Islands and Sulawesi (Celebes). *Bulletin of the AMNH* **174**, (1982).
52. Heaney, L. R., Balete, D. S. & Rickart, E. A. *The mammals of Luzon Island: biogeography and natural history of a Philippine fauna*. (Johns Hopkins University Press, Baltimore., 2016).
53. McIntosh, A. F. & Cox, P. G. The impact of digging on craniodental morphology and integration. *Journal of Evolutionary Biology* **29**, 2383–2394 (2016).
54. Gomes Rodrigues, H., Šumbera, R. & Hautier, L. Life in Burrows Channelled the Morphological Evolution of the Skull in Rodents: the Case of African Mole-Rats (Bathyergidae, Rodentia). *Journal of Mammalian Evolution* **23**, 175–189 (2016).
55. Rickart, E. A., Heaney, L. R. & Utzurrum, R. C. B. Distribution and Ecology of Small Mammals along an Elevational Transect in Southeastern Luzon, Philippines. *Journal of Mammalogy* **72**, 458–469 (1991).
56. Heaney, L. R., Balete, D. S., Rosell-Ambal, R. G. B., Veluz, M. J. & Rickart, E. A. The Small Mammals of Mt. Banahaw - San cristobal national Park, Luzon, Philippines: elevational distribution and ecology of a highly endemic Fauna. *National Museum of the Philippines: Journal of Natural History* **1**, 49–64 (2013).
57. Rickart, E. A., Heaney, L. R., Balete, D. S. & Tabaranza, B. R. Small mammal diversity along an elevational gradient in northern Luzon, Philippines. *Mammalian Biology - Zeitschrift für Säugetierkunde* **76**, 12–21 (2011).
58. McGann, J. P. Poor human olfaction is a 19th-century myth. *Science (New York, N.Y.)* **356**, eaam7263 (2017).
59. Laska, M. & Seibt, A. Olfactory sensitivity for aliphatic alcohols in squirrel monkeys and pigtail macaques. *Journal of Experimental Biology* **205**, (2002).
60. Musser, G. G. Sulawesi Rodents: Species Traits and Chromosomes of Haeromys minahassae and Echiothrix leucura (Muridae: Murinae). *American Museum Novitates* **2989**, 1–18 (1990).
61. Musser, G. G. & Lunde, D. P. Systematic Reviews of New Guinea Coccymys and 'Melomys' Albidens (Muridae, Murinae) with Descriptions of New Taxa. *Bulletin of the American Museum of Natural History* **329**, 1–139 (2009).
62. Charles, C., Solé, F., Rodrigues, H. G. & Viriot, L. Under pressure? Dental adaptations to termitophagy and vermivory among mammals. *Evolution* **67**, 1792–1804 (2013).
63. Jackson, D. C. & Schmidt-Nielsen, K. Countercurrent heat exchange in the respiratory passages. *Proceedings of the National Academy of Sciences of the United States of America* **51**, 1192–7 (1964).
64. Rowe, K. C., Achmadi, A. S. & Esselstyn, J. A. A new genus and species of omnivorous rodent (Muridae: Murinae) from Sulawesi, nested within a clade of endemic carnivores. *Journal of Mammalogy* **97**, 978–991 (2016).
65. Muschick, M., Indermaur, A. & Salzburger, W. Convergent Evolution within an Adaptive Radiation of Cichlid Fishes. *Current Biology* **22**, 2362–2368 (2012).
66. Losos, J. B. & Ricklefs, R. E. Adaptation and diversification on islands. *Nature* **457**, 830–836 (2009).
67. Esselstyn, J. A., Achmadi, A. S., Handika, H. & Rowe, K. C. A hog-nosed shrew rat (Rodentia: Muridae) from Sulawesi Island, Indonesia. *Journal of Mammalogy* **96**, 895–907 (2015).
68. Musser, G. G. Crunomys and the small-bodied shrew rats native to the Philippine Islands and Sulawesi (Celebes). Bulletin of the AMNH; v. 174, article 1. (1982).
69. Musser, G. G. Results of the Archbold Expeditions. No. 91 A New Genus and Species of Murid Rodent from Celebes, with a Discussion of its Relationships. *American Museum Novitates* (1969).
70. Collins, N. M. The Distribution of Soil Macrofauna on the West Ridge of Gunung (Mount) Mulu, Sarawak. *Oecologia* **44**, 263–275 (1980).
71. Samson, D. A., Rickart, E. A. & Gonzales, P. C. Ant Diversity and Abundance along an Elevational Gradient in the Philippines. *Biotropica* **29**, 349–363 (1997).
72. Heaney, L. R. Small mammal diversity along elevational gradients in the Philippines: an assessment of patterns and hypotheses. *Global Ecology and Biogeography* **10**, 15–39 (2001).
73. Heaney, L. R. Mammalian species richness on islands on the Sunda Shelf, Southeast Asia. *Oecologia (Berlin)* **61**, 11–17 (1984).
74. Nor, S. M. Elevational diversity patterns of small mammals on Mount Kinabalu, Sabah, Malaysia. *Global Ecology and Biogeography* **10**, 41–62 (2001).
75. Balete, D. S., Heaney, L. R., Josefa Veluz, M. & Rickart, E. A. Diversity patterns of small mammals in the Zambales Mts., Luzon, Philippines. *Mammalian Biology - Zeitschrift für Säugetierkunde* **74**, 456–466 (2009).
76. Yohe, L. R., Hoffmann, S. & Curtis, A. Vomeronasal and Olfactory Structures in Bats Revealed by DiceCT Clarify Genetic Evidence of Function. *Frontiers in neuroanatomy* **12**, 32 (2018).
77. Wagner, F. & Ruf, I. Who nose the borzoi? Turbinal skeleton in a dolichocephalic dog breed (Canis lupus familiaris). *Mammalian Biology*, https://doi.org/10.1016/J.MAMBIO.2018.06.005 (2018).
78. Schreider, J. P. & Raabe, O. G. Anatomy of the nasal-pharyngeal airway of experimental animals. *The Anatomical Record* **200**, 195–205 (1981).
79. Rygg, A. D., Van Valkenburgh, B. & Craven, B. A. The Influence of Sniffing on Airflow and Odorant Deposition in the Canine Nasal Cavity. *Chemical Senses* **42**, 683–698 (2017).
80. Ruf, I. Vergleichend-ontogenetische Untersuchungen an der Ethmoidalregion der Muroidea (Rodentia, Mammalia). Ein Beitrag zur Morphologie und Systematik der Nagetiere. (2004).
81. Macrini, T. E. Comparative Morphology of the Internal Nasal Skeleton of Adult Marsupials Based on X-ray Computed Tomography. *Bulletin of the American Museum of Natural History* **365**, 1–91 (2012).
82. Smith, T. D., Rossie, J. B. & Bhatnagar, K. P. Evolution of the nose and nasal skeleton in primates. *Evolutionary Anthropology: Issues, News, and Reviews* **16**, 132–146 (2007).
83. Musser, G. G. A Systematic Review of Sulawesi *Bunomys* (Muridae, Murinae) with the Description of Two New Species. *Bulletin of the American Museum of Natural History* **392**, 1–313 (2014).
84. Smith, T. G., Lange, G. D. & Marks, W. B. Fractal methods and results in cellular morphology–dimensions, lacunarity and multifractals. *Journal of neuroscience methods* **69**, 123–36 (1996).
85. Karperien, A. L., Jelinek, H. F., Buchan, A. M. & Karperien, A. Box-counting analysis of microglia form in schizophrenia, Alzheimer's disease and affective disorder. *Fractals* **16**, 103–107 (2008).

86. Rasband, W. S. ImageJ: Image processing and analysis in Java. *Astrophysics Source Code Library, record ascl:1206.013* (2012).
87. Karperien, A. User's guide for FracLac for ImageJ, version 2.5. (2012).
88. Team R-Core. R: A language and environment for statistical computing. *R Foundation for Statistical Computing, Vienna, Austria*. (2017).
89. Paradis, E., Claude, J. & Strimmer, K. APE: Analyses of Phylogenetics and Evolution in R language. *Bioinformatics* **20**, 289–290 (2004).
90. Pinheiro, J., Bates, D., DebRoy, S., Sarkar, D. & Team, R. C. nlme: linear and nonlinear mixed effects models. *R package version* **3**, 1–117 (2014).
91. Revell, L. J. phytools: an R package for phylogenetic comparative biology (and other things). *Methods in Ecology and Evolution* **3**, 217–223 (2012).
92. Steppan, S. J. & Schenk, J. J. Muroid rodent phylogenetics: 900-species tree reveals increasing diversification rates. *PLOS ONE* **12**, e0183070 (2017).
93. Claude, J. *Morphometrics with R*. (Springer, 2008).
94. Hothorn, T. *et al*. Package 'multcomp'. (2017).
95. Grafen, A. The phylogenetic regression. *Philosophical transactions of the Royal Society of London. Series B, Biological sciences* **326**, 119–57 (1989).
96. Butler, M. A. & King, A. A. Phylogenetic Comparative Analysis: A Modeling Approach for Adaptive Evolution. *The American Naturalist* **164**, 683–695 (2004).
97. García-Berthou, E. On the misuse of residuals in ecology: testing regression residuals vs. the analysis of covariance. *Journal of Animal Ecology* **70**, 708–711 (2001).
98. Freckleton, R. P. The seven deadly sins of comparative analysis. *Journal of Evolutionary Biology* **22**, 1367–1375 (2009).
99. Freckleton, R. P. On the misuse of residuals in ecology: regression of residuals vs. multiple regression. *Journal of Animal Ecology* **71**, 542–545 (2002).
100. Clavel, J., Escarguel, G. & Merceron, G. mv morph: an r package for fitting multivariate evolutionary models to morphometric data. *Methods in Ecology and Evolution* **6**, 1311–1319 (2015).
101. Hansen, T. F. Stabilizing Selection and the Comparative Analysis of Adaptation. *Evolution* **51**, 1341 (1997).
102. Schaefer, J. *et al*. corpcor: Efficient estimation of covariance and (partial) correlation. *R package version* **1**, (2013).
103. King, A. & King, M. Package 'subplex'. (2016).
104. Felsenstein, J. Phylogenies and the Comparative Method. *The American Naturalist* **125**, 1–15 (1985).
105. Revell, L. J. Two new graphical methods for mapping trait evolution on phylogenies. *Methods in Ecology and Evolution* **4**, 754–759 (2013).
106. Stayton, C. T. The definition, recognition, and interpretation of convergent evolution, and two new measures for quantifying and assessing the significance of convergence. *Evolution* **69**, 2140–2153 (2015).
107. Stayton, A. C. T. & Stayton, M. C. T. Package 'convevol': Analysis of Convergent Evolution. (2017).
108. Zelditch, M. L., Ye, J., Mitchell, J. S. & Swiderski, D. L. Rare ecomorphological convergence on a complex adaptive landscape: Body size and diet mediate evolution of jaw shape in squirrels (Sciuridae). *Evolution* **71**, 633–649 (2017).

Acknowledgements

We thank: S. Cardoso, M. Wright, J. Clavel, I. Ruf, R. Allio, J. Claude, L. Hautier, C. Molinier, F. Delsuc, M. Orliac, and G.G. Musser. 3D data acquisitions were performed using the μ-CT facilities of the MRI platform member of the national infrastructure France-BioImaging supported by the French National Research Agency (ANR-10-INBS-04, «Investments for the future»), and of the Labex CEMEB (ANR-10-LABX-0004) and NUMEV (ANR-10-LABX-0020). Thanks to F. Ahmed, B. Clark, and V. Fernandez for access to the CT-scan facilities at the Natural History Museum (NHMUK, London). We are grateful to the following people and institutions for granting access to specimens: S. Morand with ANR 07 BDIV 012 CERoPath, S. Ginot, J. Claude, F. Veyrunes, F. Bonhomme, and J. J. Duquesne (UM2); Y. Chaval and N. Charbonnel (CBGP); P. Jenkins, S. Oxford, and K. Dixey (NHMUK, London); D. Wilson, L. Gordon, and D. Lunde (USNM, Washington, D.C.); E. Westwig, M. Surovy, N. Duncan, C. Grohé, and R. S. Voss (AMNH, New York); K. Roberts and K. M.C. Rowe (NMV, Melbourne); D. S. Balete, A. Ferguson, and W. T. Stanley (FMNH, Chicago); G. Véron, V. Nicolas, and C. Denys (MNHN, Paris); S. van Der Mije (RMNH, Leiden). Likewise, we thank the Research Center for Biology, Indonesian Institute of Sciences (RCB-LIPI) and the Museum Zoologicum Bogoriense for providing staff, and support to carry out fieldwork in the Wallacea. This research received support from: SYNTHESYS Project which is financed by the European Community Research Infrastructure Action (FP7: GB-TAF-5737, GB-TAF-6945 to the NHM UK), Agence Nationale de la Recherche (Défi des autres savoirs, DS10, ANR-17-CE02-0005 RHINOGRAD 2017), PEPS ADAPTATION ADAPTABILITE (SHREWNOSE), Negaunee Foundation, Field Museum's Barbara Brown Fund for Mammal Research National Science Foundation (DEB-1441634, DEB-1343517, OISE-0965856), and National Geographic Society (9025-11). This is contribution of ISEM SUD N°2018-243, Univ Montpellier, CNRS, EPHE, IRD, Montpellier, France.

Author Contributions

Q.M. and P.H.F. designed the study, collected most of CT-scan data, performed analyses, and drafted the first manuscript. A.S.A., K.C.R., L.R.H. and J.A.E. collected most Sulawesi and Philippines specimens. A.R.E. made available half of Sulawesi CT-scan data. R.L. designed the 3D complexity method and implemented it in the freeware MorphoDig. A.R.E., A.S.A., K.C.R., L. R. H., J.A.E., R.L. and R.P.M. significantly and critically improved the manuscript. Authors gave final approval for publication.

Additional Information

Supplementary information accompanies this paper at https://doi.org/10.1038/s41598-018-35827-0.

Competing Interests: The authors declare no competing interests.

Publisher's note: Springer Nature remains neutral with regard to jurisdictional claims in published maps and institutional affiliations.

↑ Back to summary ↑

Article 2 - Convergent evolution of olfactory and thermoregulatory capacities in small amphibious mammals

Convergent evolution of olfactory and thermoregulatory capacities in small amphibious mammals

Quentin Martinez[a,1], Julien Clavel[b,c], Jacob A. Esselstyn[d,e], Anang S. Achmadi[f], Camille Grohé[g,h], Nelly Pirot[i,j], and Pierre-Henri Fabre[a,k]

[a]Institut des Sciences de l'Évolution de Montpellier (ISEM), CNRS, Institut de recherche pour le développement (IRD), Université de Montpellier (UM), UMR 5554, 34095 Montpellier, France; [b]Department of Life Sciences, The Natural History Museum, SW7 5DB London, United Kingdom; [c]Univ. Lyon Laboratoire d'Ecologie des Hydrosystèmes Naturels et Anthropisés, UMR CNRS 5023, Université Claude Bernard Lyon 1, École Nationale des Travaux Publics de l'État (ENTPE), F-69622 Villeurbanne, Cedex, France; [d]Museum of Natural Science, Louisiana State University, Baton Rouge, LA 70803; [e]Department of Biological Sciences, Louisiana State University, Baton Rouge, LA 70803; [f]Museum Zoologicum Bogoriense, Research Center for Biology, Indonesian Institute of Sciences (LIPI), 16911 Cibinong, Indonesia; [g]Division of Paleontology, American Museum of Natural History, New York, NY 10024; [h]Laboratoire Paléontologie Évolution Paléoécosystèmes Paléoprimatologie (PALEVOPRIM, UMR 7262, CNRS-Institut écologie et environnement [INEE]), Université de Poitiers, 86073 Poitiers, Cedex 9, France; [i]Institut de Recherche en Cancérologie de Montpellier (IRCM), INSERM, U1194 UM, Institut du Cancer de Montpellier (ICM), F-34298 Montpellier, Cedex 5, France; [j]Réseau d'Histologie Expérimentale de Montpellier, UMS3426 CNRS-US009 INSERM-UM, 34298 Montpellier, France; and [k]Mammal Section, Department of Life Sciences, The Natural History Museum, SW7 5DB London, United Kingdom

Edited by David B. Wake, University of California, Berkeley, CA, and approved February 28, 2020 (received for review October 11, 2019)

Olfaction and thermoregulation are key functions for mammals. The former is critical to feeding, mating, and predator avoidance behaviors, while the latter is essential for homeothermy. Aquatic and amphibious mammals face olfactory and thermoregulatory challenges not generally encountered by terrestrial species. In mammals, the nasal cavity houses a bony system supporting soft tissues and sensory organs implicated in either olfactory or thermoregulatory functions. It is hypothesized that to cope with aquatic environments, amphibious mammals have expanded their thermoregulatory capacity at the expense of their olfactory system. We investigated the evolutionary history of this potential trade-off using a comparative dataset of three-dimensional (3D) CT scans of 189 skulls, capturing 17 independent transitions from a strictly terrestrial to an amphibious lifestyle across small mammals (Afrosoricida, Eulipotyphla, and Rodentia). We identified rapid and repeated loss of olfactory capacities synchronously associated with gains in thermoregulatory capacity in amphibious taxa sampled from across mammalian phylogenetic diversity. Evolutionary models further reveal that these convergences result from faster rates of turbinal bone evolution and release of selective constraints on the thermoregulatory-olfaction trade-off in amphibious species. Lastly, we demonstrated that traits related to vital functions evolved faster to the optimum compared to traits that are not related to vital functions.

olfaction | thermoregulation | heat loss | aquatic habitat | turbinal bones

The adaptive radiation of mammals is characterized by the colonization of a variety of habitats in association with morphological innovations (1, 2). Among the most spectacular patterns of mammalian evolution is the multiple invasions of aquatic habitats (3). Several mammalian lineages, including the ancestors of whales and manatees, became fully aquatic (3), whereas several groups of rodents, afrotherians, carnivorans, and others evolved an amphibious lifestyle. These amphibious mammals are adapted to live both in water and on land, a circumstance that is predicted to lead to evolutionary trade-offs (3). For instance, aquatic habitats are a challenge to mammalian thermoregulation because warm organisms lose heat quicker in water than in air due to the high thermal inertia of water (4, 5). Similarly, olfaction is particularly inefficient underwater because it requires inhalation (3, 6).

In mammals, the rostrum contains bony structures named turbinals that contribute to heat conservation and olfaction (7). Anteriorly, the respiratory turbinals are lined with a vascular epithelium that helps conserve heat during respiration (7). Posteriorly, the olfactory turbinals are covered by olfactory receptors and connected to the olfactory bulb, representing a critical component of mammalian olfaction (7–9). This anteroposterior functional partitioning has been documented in histological, airflow dynamic, and performance test studies (9–13). It was previously hypothesized that the number and the shape of turbinal bones are conserved across species while their relative size and complexity are more labile, with variation related to species ecology (14–23). For example, dietary specializations are correlated with relative turbinal surface area in some Carnivora and Rodentia (19, 22).

Important functions such as thermoregulation should be under strong selective pressure in amphibious organisms. Indeed, Van Valkenburgh et al. (16) demonstrated that some aquatic Carnivora have huge respiratory turbinal bones that limit heat loss. In contrast, because mammals usually do not smell underwater (6), olfaction should be under relaxed selective pressures. It was previously shown that some amphibious mammals have a reduced

Significance

In the evolutionary history of mammals, invasion of aquatic habitats is associated with profound morphological changes. Because mammalian systems of olfaction and thermoregulation are challenged by aquatic environments, it was previously hypothesized that amphibious mammals have reduced olfactory capacity but enhanced thermoregulatory capacity. Using newly acquired three-dimensional (3D) computed tomography (CT) scans of nasal cavities from terrestrial and amphibious mammals, we found strong statistical support for this hypothesis. Our results show a strong trade-off between olfactory and thermoregulatory capacities in amphibious mammals, with morphological changes that occurred 5.4 times faster than the background rate. The rapid rate of morphological change and convergent patterns we identified demonstrate the adaptation experienced by mammals during the many transitions to amphibious habits.

Author contributions: Q.M. and P.-H.F. designed research; Q.M., J.C., J.A.E., N.P., and P.-H.F. performed research; J.C. and N.P. contributed new reagents/analytic tools; Q.M., J.C., and P.-H.F. analyzed data; Q.M., J.C., J.A.E., A.S.A., C.G., and P.-H.F. wrote the paper; A.S.A. provided museum specimens; and C.G. provided 3D CT scans.

The authors declare no competing interest.

This article is a PNAS Direct Submission.

Data deposition: The 3D CT scan surfaces are available via MorphoSource (https://www.morphosource.org/Detail/ProjectDetail/Show/project_id/974).

[1]To whom correspondence may be addressed. Email: quentinmartinezphoto@gmail.com.

This article contains supporting information online at https://www.pnas.org/lookup/suppl/doi:10.1073/pnas.1917836117/-/DCSupplemental.

First published April 6, 2020.

olfactory bulb and cribriform plate, two components of olfaction, compared to their terrestrial relatives (24–26). Aquatic vertebrates also have a smaller repertoire of functional olfactory receptor (OR) genes than terrestrial vertebrates (27–32). Nevertheless, how pervasive, consistent, and strong these putative convergences and trade-offs are remains unknown.

We analyzed turbinal morphology in amphibious mammals to test for consistent anatomical adaptations enhancing heat conservation and for simultaneous release from selective pressures on olfactory structures. In total, we compared 17 independently derived amphibious lineages to their close terrestrial relatives in order to illuminate the evolution of thermoregulatory-olfactory trade-offs during major mammalian land-to-water transitions.

Results

Adaptation and Convergence. The relative surface area of olfactory and respiratory turbinals is significantly associated with ecological lifestyle ($P < 0.0001$ in both cases; *SI Appendix*, Table S1). Most amphibious species have reduced olfactory turbinals and expanded respiratory turbinals as compared to their close terrestrial relatives (Fig. 1). The relative reduction of olfactory surface area is affected by the relative reduction of some olfactory turbinals (Figs. 1 and 2) and by the loss of other olfactory turbinals, as seen in *Myocastor coypus*, which lost two frontoturbinals (Fig. 2*A*). The relative increase of respiratory surface area is driven by a relative expansion of the size of respiratory turbinals (Figs. 1 and 2), an increase in complexity (Fig. 2*B*), and the emergence of a new respiratory turbinal (Fig. 2*A*).

The best-fitted model of morphological evolution for the relative surface area of respiratory turbinals is based on an Ornstein–Uhlenbeck process (OUM) that describes the evolution toward distinct optimal values for species with terrestrial and amphibious lifestyles (Table 1). This is also the case for size-corrected estimates of the relative surface area of the respiratory turbinals

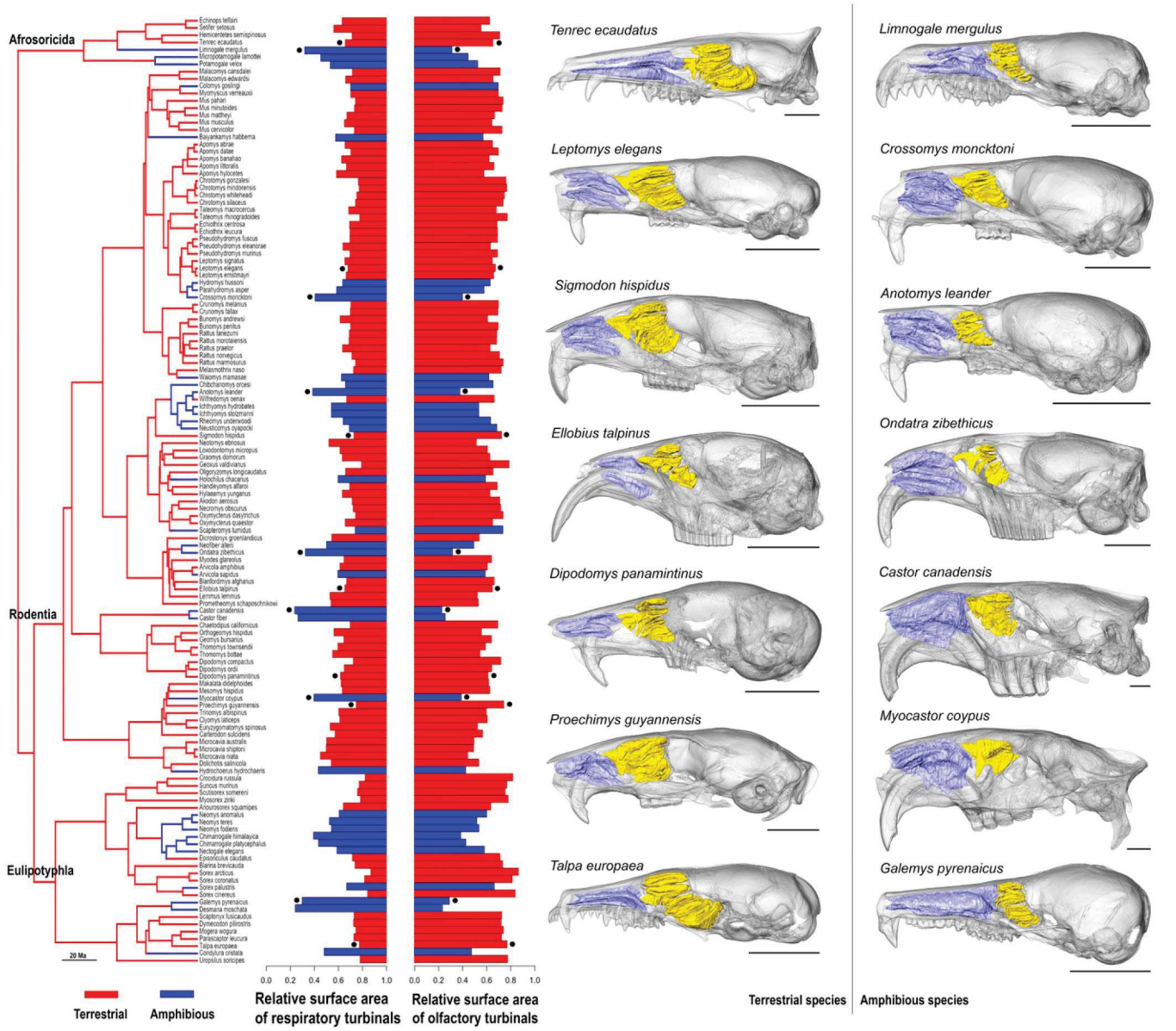

Fig. 1. Loss of olfactory and gain of thermoregulatory capacities in amphibious mammals. Phylogeny of the sampled species with barplots of the relative surface area of olfactory and respiratory turbinals based on ratios; blue = amphibious; red = terrestrial. Black circles highlight illustrated species. Respiratory turbinals are blue and olfactory turbinals are yellow. (Scale bars, 1 cm.)

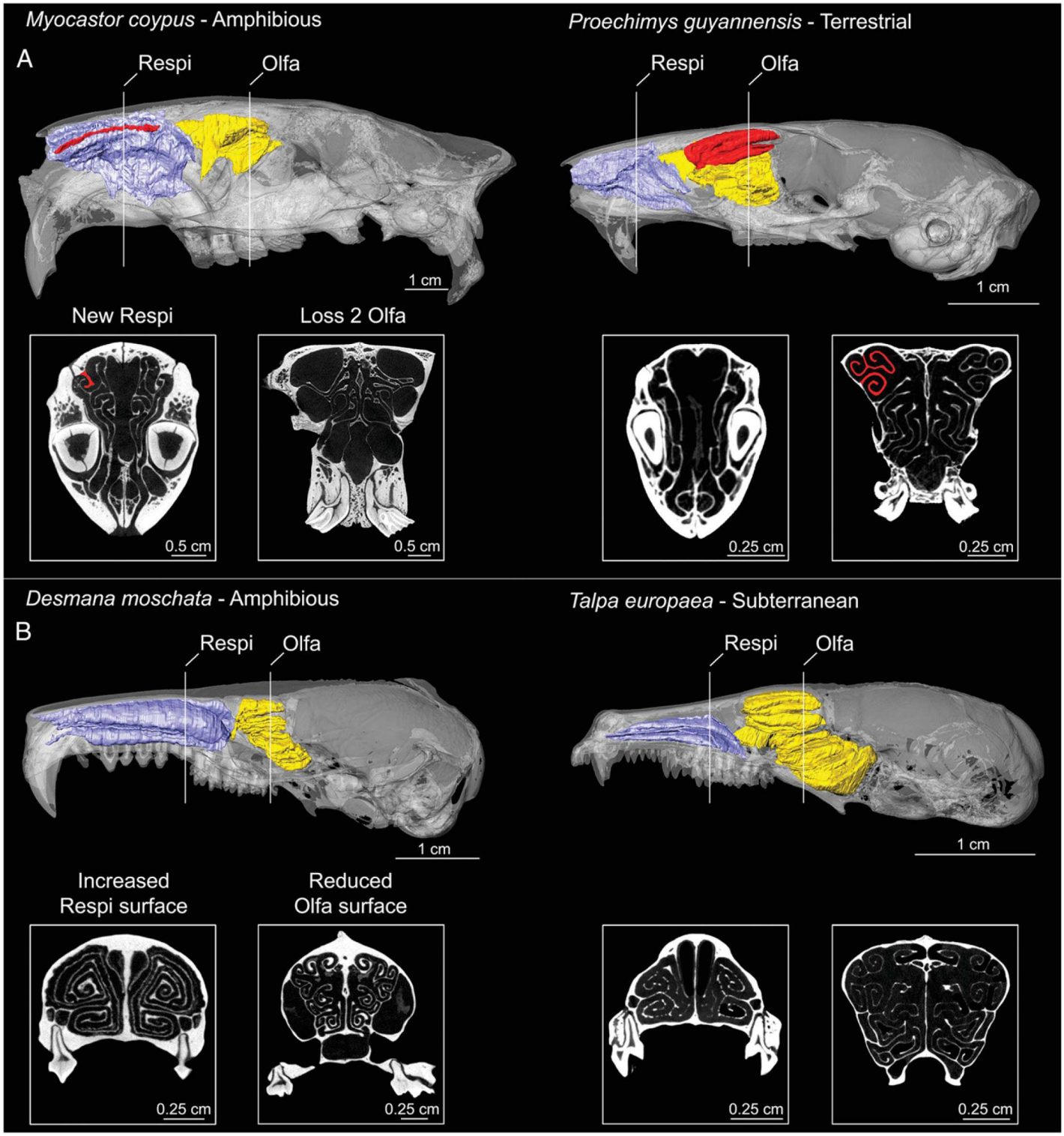

Fig. 2. Loss and gain of anatomical structures. 3D representations of turbinal bones and coronal cross section showing two mechanisms of adaptation to the amphibious environment: (*A*) emergence of new respiratory turbinals and loss of some olfactory turbinals as seen in the amphibious *Myocastor coypus* and its close terrestrial relative *Proechimys guyannensis*. (*B*) Increase in surface area and complexity of respiratory turbinals and reduction in olfactory turbinals, as seen in the amphibious *Desmana moschata* and its close terrestrial relative *Talpa europaea*. Respi = respiratory turbinals, Olfa = olfactory turbinals. Red = turbinals not shared between amphibious and terrestrial relatives; blue = respiratory turbinals; yellow = olfactory turbinals.

(*SI Appendix*, Table S2), indicating that this pattern is not driven by allometric effects. In contrast, the best model for the evolution of the relative surface area of the olfactory turbinals is a Brownian motion model with multirate and multiselective regimes (BMMm), which illustrates mean phenotype and evolutionary rate differences between amphibious and terrestrial lineages (Table 1). The estimated rates of the BMMm model further show that the amphibious lineages were evolving faster than their terrestrial relatives (see below). The second-best–fitted model (but also the best model for the size-corrected relative surface area of olfactory turbinals; *SI Appendix*, Table S2) is an ecological release (ER) model consistent with a release of selective pressures on olfactory turbinals associated

Table 1. Mean results from models of turbinal bone evolution fitted to 100 stochastic character maps of amphibious and terrestrial lifestyles

	Relative olfactory turbinal surface area		Relative respiratory turbinal surface area		Bivariate model: relative olfactory and respiratory surface area	
Model	AIC	AICw	AIC	AICw	AIC	AICw
BM1	−60.353	0.000	30.554	0.000	−273.975	0
BMM	−104.670	0.000	23.697	0.000	−367.927	0
BM1m	−96.136	0.000	−4.240	0.286	−309.068	0
BMMm	−124.436	0.980	−3.504	0.192	−395.461	1
OU1	−66.957	0.000	20.143	0.000	−289.787	0
OUM	−99.446	0.005	−5.390	0.501	−319.622	0
ER	−103.035	0.015	7.958	0.020	−351.664	0

Model fits were compared using differences in the AIC. See *SI Appendix*, Table S2 for size-free results.

with colonization of the aquatic environment (Table 1). This scenario is also supported by bivariate models of correlated evolution between the relative surface area of respiratory and olfactory turbinals that favor the BMMm and the ER model (Table 1). These models show a strong negative association between the respiratory and olfactory turbinal surface area, typical of evolutionary trade-offs (average correlation of −0.92) and favoring a scenario with release from selection on this trade-off in amphibious mammals.

Convergence in the relative surface area of olfactory and respiratory turbinals in amphibious taxa is supported by three of four of Stayton's (33) convergence indices (C1: $P = 0.003$, C2: 0.001, C3: $P = 0.005$, and C4: $P = 0.188$; *SI Appendix*, Table S3). Phenograms for the relative surface area of olfactory and respiratory turbinals show convergences in most clades, with amphibious species evolving toward a lower relative surface area of olfactory turbinals (Fig. 3, *Left*) and a greater relative surface area of respiratory turbinals (Fig. 3, *Right*).

Phylogenetic Half-Life and Evolutionary Rates. The phylogenetic half-life of the total turbinal surface area and that of the relative surface area of olfactory and respiratory turbinals were estimated under the best-fitted OU models (respectively, 0.88, 0.15, and 0.18; *SI Appendix*, Table S4). They are all lower than that of skull length (1.41; *SI Appendix*, Table S4), indicating that the turbinal bone surface area evolved faster than skull length, a body-size–related trait that is itself associated with features of species ecology.

The evolutionary rate of the relative surface area of olfactory turbinals is 5.4 times faster in amphibious species than in terrestrial ones (likelihood ratio test [LRT]: $P < 0.001$; Table 2 and *SI Appendix*, Tables S5 and S6). The evolutionary rate of the relative surface area of respiratory turbinals is 1.4 times faster in amphibious species as compared to terrestrial ones (LRT: $P < 0.001$; Table 2 and *SI Appendix*, Tables S5 and S6).

Discussion

Convergent Olfactory Losses in Small Amphibious Mammals. Olfaction is a key function for mammals which was hypothesized to be under strong selective pressure (16, 17). Mammals usually do not smell underwater (6), suggesting that olfaction may be less important to amphibious species than to their terrestrial relatives. Our results show that amphibious mammals adapted to the aquatic environment through at least two types of morphological changes in their olfactory system: 1) the reduction of the relative surface area of the olfactory turbinals and 2) the loss of some olfactory turbinals (Fig. 2).

Using turbinal bones and phylogenetic comparative methods, we report that 17 lineages of small amphibious mammals convergently experienced a reduction of their olfactory turbinal bones (Figs. 1 and 3), suggesting relaxed selective pressures on olfactory anatomical structures in amphibious placentals. We found reduced olfactory turbinals in all three studied orders (Afrosoricida, Eulipotyphla, and Rodentia; Fig. 1). In Afrosoricida, the amphibious *Microgale mergulus* has less than half the olfactory turbinal surface area of its terrestrial counterpart, *Tenrec ecaudatus* (Fig. 1). The largest quantitative differences between an amphibious lineage and its close terrestrial relatives are found within the Talpidae (Eulipotyphla). Both amphibious desman species (*Desmana* and *Galemys*) have, respectively, less than a third and less than half of the relative olfactory turbinal surface area compared to the subterranean mole *Talpa europaea* (Figs. 1 and 2*B*). This is somewhat surprising given that some Eulipotyphla, such as the star-nosed mole (*Condylura cristata*), water shrews (*Sorex palustris*), and the Russian desman (*Desmana moschata*), are known to sniff and smell underwater (34–36). However, the large difference may be partially related to the earthworm dietary specializations of subterranean moles. In rodents, earthworm specialists have significantly larger and more complex olfactory turbinals than do carnivores and omnivores (22). A similar pattern of olfactory turbinal reduction was also found in Rodentia. For example, the amphibious North American beaver (*Castor canadensis*) has less than half the olfactory turbinal surface area of its close terrestrial relative, the panamint kangaroo rat (*Dipodomys panamintinus*, Fig. 1).

Most small mammals in our sampling have relatively conserved turbinal morphology, consisting of a set of six to eight olfactory turbinals and two to three respiratory turbinals (Fig. 1 and *SI Appendix*, Fig. S1). The amphibious coypu (*Myocastor coypus*) is an exception. This species lost two olfactory turbinals, and we showed the presence of a new respiratory turbinal bone not seen in its close terrestrial relatives such as *Proechimys guyannensis* (Fig. 2*A*). The relative surface area of the olfactory turbinals in the coypu also decreased, and this species has about half of the relative surface area of olfactory turbinals measured in the terrestrial *Proechimys guyannensis* (Fig. 1). Further studies should assess the role and significance of both the reduction of the surface area of the olfactory turbinals and the loss of some olfactory turbinals (Fig. 2).

Our results are consistent with those of studies on the olfactory bulb brain, another major component of olfaction. Indeed, the olfactory bulb of some amphibious mammals is smaller compared to their terrestrial relatives (24). This organ is involved in detection and discrimination of odor molecules (37). Our results are also consistent with histological studies in eulipotyphlan water shrews. *Neomys fodiens* and *Sorex palustris* water shrews have a lower relative number of olfactory receptors than their closely related terrestrial species (38), and we quantified that these two species also have reduced olfactory turbinals (Fig. 1). Our observation of repeated reduction of olfactory surface area is also consistent with convergent enrichment in pseudogenes as well as reduction of the number of functional OR genes in amphibious and aquatic vertebrate genomes (26–31, 39). We demonstrated that small amphibious mammals convergently lost a part of their olfactory capacities. Altogether, our observations suggest that olfactory turbinal bones can be used as reliable proxies for olfactory capacities in mammals and used to infer that the ecology of fossil mammals provides critical information on the timing and onset of aquatic transitions.

Efficient Heat Conservation Capacities in Small Amphibious Mammals. Olfactory turbinal bone reduction might result from a trade-off between the sizes of the respiratory and olfactory turbinals (16, 22). We found strong support for this hypothesis, indicated by the negative association between the respiratory and olfactory turbinals (see *Results*) for the ecological release model.

Respiratory turbinal bones are essential to moisten and warm the air before it enters the lungs (7, 40). We showed that small amphibious species convergently evolved larger respiratory turbinals

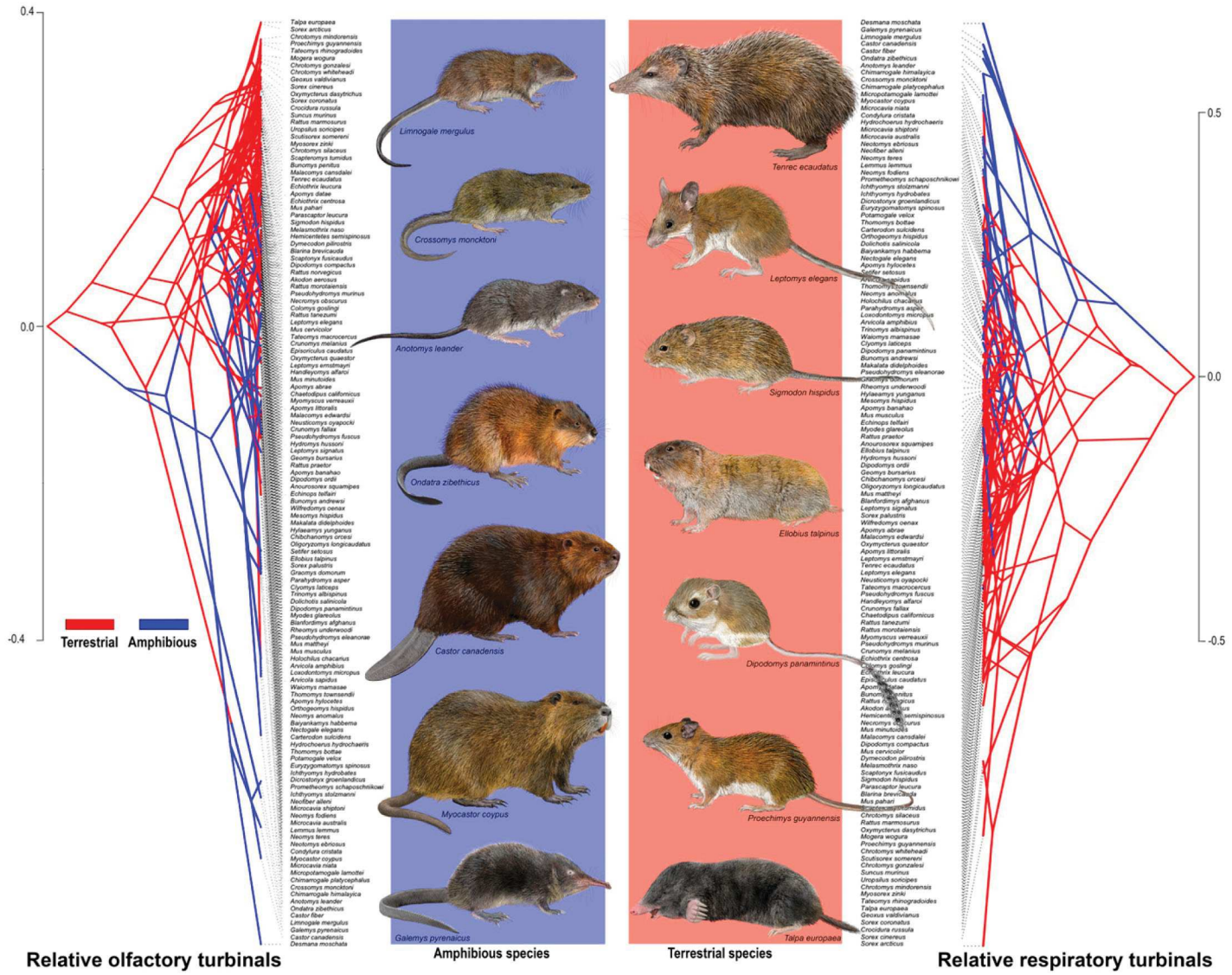

Fig. 3. Convergent loss of olfactory and gain of thermoregulatory capacities in amphibious mammals. Phenograms based on the residual of phylogenetic generalized least squares regressions for the relative surface area of olfactory and respiratory turbinals. Phenograms with branches crossing and concentrating in a given area indicate convergent lineages. Blue = amphibious; red = terrestrial. Illustrations by Toni Llobet and Lynx Editions. Reprinted with permission from refs. 73–75.

compared to their terrestrial relatives (Figs. 1–3), an adaptation that minimizes heat loss in the aquatic environment. Due to the great thermal conductivity of water (41), heat loss is about two to four times higher in water than in air for the same temperature (5). This factor is even more important in small amphibious mammals than in fully aquatic mammals because the former generally paddle at the air-water interface, an energetically demanding form of locomotion (42–44). To respond to the energetic and thermal constraints of the aquatic environment, some small amphibious mammals developed many anatomical, physiological, and behavioral features compared to their terrestrial relatives, such as (1) a larger body size (6, 45), (2) a higher metabolic rate (45–47), (3) denser fur and fat (45, 48), (4) Hardarian glands to waterproof the fur (45, 49), and (5) an energy-rich carnivorous diet (45).

Our evidence for the enlargement of respiratory turbinals in amphibious mammals is consistent with histological studies showing a thickening of the epithelium of respiratory turbinals in amphibious shrews (38) and of the bony structures of the respiratory turbinals in extinct aquatic mammals (50, 51). Our results also show a gradient of increasing relative surface area of respiratory turbinals with greater aquatic specialization. For instance, within Talpidae, this gradient increases from the nonamphibious (*Dymecodon*, *Mogera*, *Parascaptor*, *Scaptonyx*, *Talpa*, and *Uropsilus*) to the occasionally amphibious (*Condylura*) and finally to the fully amphibious (*Desmana* and *Galemys*; Fig. 1 and *SI Appendix*, Fig. S2).

Our results also suggest that temperature may contribute to the size of respiratory turbinals. For example, the Russian desman (*Desmana moschata*) lives in colder water and has a larger relative respiratory turbinal surface area (Fig. 1) than the Pyrenean desman (*Galemys pyrenaicus*). The importance of temperature was previously suggested via a respiratory turbinal comparison between the leopard seal (*Hydrurga leptonyx*) and the extinct tropical

Table 2. Fast morphological evolution of small amphibious mammals

Variables	Observed rate ratio	TER rate	AMP rate	LRT
Relative olfactory turbinal surface area	5.425	0.001	0.004	<0.001
Relative respiratory turbinal surface area	1.426	0.003	0.004	<0.001

AMP = amphibious; LRT = likelihood-ratio test; TER = terrestrial.

monk seal (*Monachus tropicalis*), two species existing different thermal environments (16). However, the importance of temperature in the relative size of turbinals has never been tested using convergent species. In Rodentia, the Ecuadorian fish-eating rat (*Anotomys leander*) lives in cold-water torrents at high elevation (up to 4,000 m) and has relatively larger respiratory turbinals than the Oyapock's fish-eating rat (*Neusticomys oyapocki*; Fig. 1 and *SI Appendix*, Fig. S3), which lives in lowland streams (below 500 m, refs. 52 and 53). We found a similar example in Australo-Papuan murinae with the earless water rat (*Crossomys moncktoni*) that lives and dives in cold-water torrents up to 3,500 m (54) and has relatively larger respiratory turbinals than the western water rat (*Hydromys hussoni*; Fig. 1 and *SI Appendix*, Fig. S3) that lives below 1,800 m (55). Hence, the convergent evolution of relative surface area of respiratory turbinals reveals fine ecological variation.

Fast Evolution of the Turbinals in Small Amphibious Mammals. We demonstrated that small amphibious mammals convergently reduced their olfactory turbinal bones and increased their respiratory turbinal bones, producing differential olfactory and thermoregulatory capacities. We hypothesized that differential evolutionary rates between amphibious and terrestrial species reflect the relaxed selective pressures for the relative size of olfactory turbinals and the strong selection for respiratory turbinals. Indeed, we demonstrated that the evolutionary rates of olfactory and respiratory turbinals were 5.4 and 1.4 times faster in amphibious species than in terrestrial ones. Rapid evolution in this case was likely fostered by a trade-off in which relaxed selection on a previously important trait (olfactory turbinals) provided physical space within the nasal cavity for expansion of a newly important trait (respiratory turbinals). Furthermore, because the shift between foraging in water and in terrestrial environments is abrupt, we suggest that the morphological changes occurred quickly to adapt to new sensorial and physiological environments. Indeed, vertebrates can evolve faster when they are confronted with rapid environmental modifications (56–58). The consistent (17 times) and highly convergent loss of olfactory capacities and the gain of thermoregulatory capacities at the order level is surprising. We showed that morphological traits related to vital functions such as olfaction and thermoregulation evolved faster to the selective optimum—the average phenotype expected to be optimal for both amphibious and terrestrial lineages—compared to morphological traits unrelated to vital functions such as skull length. Together, these results demonstrate that the shift to the aquatic environment played an important role in the morpho-anatomical shaping of small amphibious mammals.

Materials and Methods

Data Acquisition. Undamaged skulls belonging to 130 species of Afrosoricida, Eulipotyphla, and Rodentia were selected from the following: American Museum of Natural History (AMNH), Centre de Biologie et de Gestion des Populations (CBGP), Field Museum of Natural History (FMNH), Museums Victoria (NMV), Museum Zoologicum Bogoriense (MZB), Natural History Museum London (NHMUK), Natural History Museum of Paris (MNHN), Naturalis Biodiversity Center of Leiden (RMNH), Royal Museum for Central Africa (RMCA), Smithsonian Institution National Museum of Natural History (NMNH), and University of Montpellier (UM). In total, our sample included 17 evolutionarily independent colonizations of the aquatic environment framed by closely related terrestrial species. Skulls were scanned using X-ray microtomography (*SI Appendix*, Table S7). We segmented left turbinals from each individual with Avizo Lite 9.0.1 (VSG Inc.). Segmentation followed turbinal descriptions presented for Rodentia (14, 22), Lagomorpha (15), and Marsupialia (18). Following Martinez et al. (22), we segmented the branching of the lamina semicircularis that is covered by the olfactory epithelium (9). Based on morphological, histological, airflow dynamic, and performance tests, we partitioned the turbinal bones into two functional parts: thermoregulatory and olfactory (Fig. 1 and *SI Appendix*, Fig. S2). To refine this functional partitioning, we performed turbinal bone histology on representative specimens of the following species: *Tenrec ecaudatus* (Afrosoricida), *Suncus murinus* (Eulipotyphla), *Talpa europaea* (Eulipotyphla), and *Mus musculus domesticus* (Rodentia, *SI Appendix*, Figs. S4 and S5).

Adaptation and Convergence. We computed phylogenetic ANCOVA (analysis of covariance) to determine if differences between amphibious and terrestrial lifestyles explain the variation in olfactory and respiratory turbinal surface using the total surface area of the turbinals as a covariate. We used the residuals of the phylogenetic generalized least squares (PGLS) regression of the olfactory and thermoregulatory turbinal surface area on the total surface area as relative surface area measures in downstream comparative analyses (respectively, the relative surface area of olfactory and respiratory turbinals). To consider another proxy of size, we also used residuals from a PGLS regression of the olfactory and thermoregulatory turbinal surface areas on skull length (see results in *SI Appendix*, Tables S1, S3, and S5 and Figs. S6 and S7). In order to obtain size-free estimates of relative surface area for both respiratory and olfactory turbinals, we also computed the residuals of a linear model (generalized least squares [GLS]) with the olfactory surface or respiratory surface area as the response variable and skull length and total surface area as covariates (see results in *SI Appendix*, Table S6 and Fig. S8). Prior to comparative analyses, data averages were taken when multiple individuals were available. The PGLS regressions were performed using the "gls" function in the R package *nlme* and the "corBrownian" structure in the R package *ape* (59). We used a maximum clade credibility (MCC) phylogeny obtained from 1,000 trees sampled in the posterior distribution of Upham et al. (60) and pruned to match the species in our dataset. The MCC tree was constructed in TreeAnnotator v.1.8.2 (61).

To assess the evolution of the turbinal surface area in relation to ecological lifestyles, and to investigate the potential changes in evolutionary dynamics of the olfactory and thermoregulatory turbinal surface area, we used univariate and bivariate phylogenetic models of trait evolution. We focused on two models, Brownian motion (BM) and Ornstein–Uhlenbeck (OU, refs. 62–64), both implemented in the R package *mvMORPH* (ref. 64, functions "mvBM" and "mvOU"). BM processes describe the accumulation of infinitesimal phenotypic change along the branches of a phylogenetic tree (with the amount of change controlled by the rate parameter σ); OU processes describe selection toward an optimal trait value (parameter θ, or two optima associated with terrestrial or amphibious lifestyles—hereafter called selective regimes) and add to the BM process an extra parameter (α) that describes the strength of selection toward the optimal trait value (62, 63). The macroevolutionary optimum estimated by these models can be seen as the average phenotype toward which the lineages have evolved in both the amphibious and terrestrial species. More specifically, we applied a single-rate BM model (BM1), a model with regime-specific rates (BMM), an OU model with a single selective regime (OU1), and an OU model with regime-specific optima (OUM) to our trait data. We also considered BM models (BM1m and BMMm) that allow different ancestral states for the different lifestyles (using the option "smean=FALSE" in the function "mvBM"). BM1m has distinct trait means per regime but a single rate, while BMMm has distinct means and rates (65–67). In addition, we considered an ER model (using "mvSHIFT" in *mvMORPH*) which combines BM and OU processes. In the ER process function, the terrestrial species evolve under selective pressures to maintain the evolutionary trade-off (modeled by an OU process) while amphibious species are released from these pressures (modeled by a BM process). This scenario matched our expectation that olfactory turbinals are not valuable underwater and that thermoregulation becomes more important. The reconstructed history of the terrestrial and amphibious selective regimes on which BMM, OUM, and the ER model were fitted was obtained from 100 stochastic character maps using the function "make.simmap" in the R package *phytools* (68). Model fits were compared using the Akaike information criterion.

We quantified the level of convergences in turbinal surface area for the amphibious species using the C indexes proposed by Stayton (33). We ran these analyses with the R package *convevol* (69, 70), performing 1,000 simulations. Finally, we mapped the evolution of relative olfactory and respiratory surface areas on the branches of the phylogeny using the "phenogram" function in *phytools* (68). This phenogram projects the phylogeny related to a phenotype trait. Phenograms with branches crossing and concentrating in a given area indicate convergent evolution.

Evolutionary Rates and Phylogenetic Half-Life. We compared the rates of morphological evolution ($\sigma 2$) estimated from the BMM and BMMm fit for the relative surface area of turbinals between amphibious and terrestrial species. The significance of the difference in rates between the amphibious and terrestrial species was assessed by comparing the fit of BMM to a model with a common rate for the two lifestyles (BM1 and BM1m) using both the Akaike information criterion and likelihood ratio tests.

We found that an OU model best fit the relative surface area of the respiratory turbinals (*SI Appendix*, Table S5); thus, interpreting the difference in rates of phenotypic evolution estimated by the BM model can be misleading

EVOLUTION

because young clades may appear to evolve more quickly than older ones under a homogeneous OU process (67, 71). To assess if the differences in evolutionary rates were not artifactual and could be interpreted biologically, we ran simulations under the best-fit OU model maximum likelihood parameter estimates to compute a null distribution of expected rate differences. This null distribution of rate differences between terrestrial and amphibious species obtained from 100 simulated traits (in the OU model) was then compared to the rate differences estimated on the empirical data (*SI Appendix*, Table S5).

To test if turbinal bones evolved faster to the optimal trait value associated with each lifestyle as compared to skull length—a size-related trait that often correlates with multiple features of species ecology and life history—we estimated the phylogenetic half-life from the Ornstein-Uhlenbeck process that describes the time necessary for our morphological trait to evolve halfway from the ancestral state to the primary optimum (62). Compared to the evolutionary rates we obtained from the BM models described previously, this measure could be interpreted as a rate of "adaptation" to the different lifestyles (62, 72). We estimated the phylogenetic half-life, with the function "halflife" in *mvMORPH* (64).

ACKNOWLEDGMENTS. We thank the editor and two anonymous reviewers for their helpful and constructive reviews. We thank R. Allio, S. Ferreira-Cardoso, J. Claude, F. Condamine, F. Delsuc, E. Eveque, L. Hautier, R. Lebrun, C. Molinier, K.C. Rowe, I. Ruf, and N. Upham for different types of support, including interesting discussions. Three-dimensional data acquisitions were performed using the micro-computed tomography (μ-CT) facilities of the MRI platform member of the national infrastructure France-BioImaging supported by the French National Research Agency (Grant ANR-10-INBS-04, "Investments for the future"), and those of the Laboratoire d'Excellence Centre Méditerranéen de l'Environnement et de la Biodiversité (LabEx CeMEB, ANR-10-LABX-0004), LabEx Centre d'étude de la biodiversité amazonienne (CEBA, ANR-10-LABX-25-01), and Digital and Hardware Solutions and Modeling for the Environment and Life Sciences (NUMEV, ANR-10-LABX-0020). We acknowledge the Réseau d'Histologie Expérimentale de Montpellier (RHEM) facility supported by a Sites de Recherche Intégrée sur le Cancer (SIRIC) Montpellier Cancer Grant (Institut National Du Cancer [INCa] Inserm Direction générale de l'offre de soins [DGOS] 12553), the European Regional Development Foundation, and the Occitanian Region (Grant FEDER-FSE 2014-2020 Languedoc Roussillon) for processing our animal tissues, histology technics, and expertise. Thanks to M. Broyon, Y. Glasson, and F. Abella from the RHEM MRI platform for slide digitalization, and to F. Ahmed, B. Clark, V. Fernandez, and R. P. Miguez for access to the computed tomography facilities at the Natural History Museum London. A. Evans and M. McCurry helped with CT scanning at Monash University. We are grateful to the following people for granting access to specimens: S. Agret, F. Bonhomme, F. Catzeflis, J. Claude, F. Darinot, J. J. Duquesne, R. Gibert, S. Ginot, G. Le Minter, F. Poitevin, P. Tortosa, N. Simmons, N. Vazzoler-Antoine, and F. Veyrunes. We thank T. Llobet and Lynx Edicions for use of their illustrations. Funding was provided by the Synthesis of Systematic Resources (SYNTHESYS) Project, which is financed by European Community Research Infrastructure Action (FP7: Grants GB-TAF-5737 and GB-TAF-6945 to the National History Museum London), by Agence Nationale de la Recherche (Défi des autres savoirs, Grants DS10, ANR-17-CE02-0005 RHINOGRAD 2017), "Projets Exploratoires Premier Soutien (PEPS), adaptation, adaptabilite (shrewnose)," by a Frick postdoctoral fellowship, the National Science Foundation (Grants DEB-1754393 and DEB-1257572), and SHREWNOSE (Grant ANR-10-LABX-0025-01). This is a contribution of ISEM 2020-035 SUD, Université de Montpellier, CNRS, École Pratique des Hautes Études (EPHE), IRD, Montpellier, France.

1. K. V. Kardong, "Introduction" in *Vertebrates: Comparative Anatomy, Function, Evolution*, D. W. C. Brown, Ed. (McGraw-Hill, 1998), chap. 1, pp. 1–47.
2. G. R. McGhee, *Convergent Evolution: Limited Forms Most Beautiful* (MIT Press, 2011).
3. J. G. M. Thewissen, S. Nummela, *Sensory Evolution on the Threshold: Adaptations in Secondarily Aquatic Vertebrates* (University of California Press, 2008).
4. G. W. Molnar, Survival of hypothermia by men immersed in the ocean. *J. Am. Med. Assoc.* **131**, 1046–1050 (1946).
5. R. M. Smith, J. M. Hanna, Skinfolds and resting heat loss in cold air and water: Temperature equivalence. *J. Appl. Physiol.* **39**, 93–102 (1975).
6. H. Pihlström, "Comparative anatomy and physiology of chemical senses in aquatic mammals" in *Sensory Evolution on the Threshold: Adaptations in Secondarily Aquatic Vertebrates* (University of California Press, Berkeley, 2008), pp. 95–109.
7. V. Negus, *The Comparative Anatomy and Physiology of the Nose and Paranasal Sinuses* (Livingstone, 1958).
8. H. Breer, J. Fleischer, J. Strotmann, The sense of smell: Multiple olfactory subsystems. *Cell. Mol. Life Sci.* **63**, 1465–1475 (2006).
9. A. W. Barrios, G. Núñez, P. Sánchez Quinteiro, I. Salazar, P. Chamero, Anatomy, histochemistry, and immunohistochemistry of the olfactory subsystems in mice. *Front. Neuroanat.* **8**, 63 (2014).
10. K. J. Ressler, S. L. Sullivan, L. B. Buck, A zonal organization of odorant receptor gene expression in the olfactory epithelium. *Cell* **73**, 597–609 (1993).
11. H. Pihlström, M. Fortelius, S. Hemilä, R. Forsman, T. Reuter, Scaling of mammalian ethmoid bones can predict olfactory organ size and performance. *Proc. Biol. Sci.* **272**, 957–962 (2005).
12. J. R. Harkema, S. A. Carey, J. G. Wagner, The nose revisited: A brief review of the comparative structure, function, and toxicologic pathology of the nasal epithelium. *Toxicol. Pathol.* **34**, 252–269 (2006).
13. B. A. Craven, E. G. Paterson, G. S. Settles, The fluid dynamics of canine olfaction: Unique nasal airflow patterns as an explanation of macrosmia. *J. R. Soc. Interface* **7**, 933–943 (2010).
14. I. Ruf, "Vergleichend-ontogenetische Untersuchungen an der Ethmoidalregion der Muroidea (Rodentia, Mammalia). Ein Beitrag zur Morphologie und Systematik der Nagetiere," PhD dissertation, Universität Tübingen, Tübingen, Germany (2004).
15. I. Ruf, Comparative anatomy and systematic implications of the turbinal skeleton in Lagomorpha (Mammalia). *Anat. Rec. (Hoboken)* **297**, 2031–2046 (2014).
16. B. Van Valkenburgh *et al.*, Aquatic adaptations in the nose of carnivorans: Evidence from the turbinates. *J. Anat.* **218**, 298–310 (2011).
17. P. A. Green *et al.*, Respiratory and olfactory turbinal size in canid and arctoid carnivorans. *J. Anat.* **221**, 609–621 (2012).
18. T. E. Macrini, Comparative morphology of the internal nasal skeleton of adult marsupials based on X-ray computed tomography. *Bull. Am. Mus. Nat. Hist.* **365**, 1–91 (2012).
19. B. Van Valkenburgh *et al.*, Respiratory and olfactory turbinals in feliform and caniform carnivorans: The influence of snout length. *Anat. Rec. (Hoboken)* **297**, 2065–2079 (2014).
20. K. K. Yee, B. A. Craven, C. J. Wysocki, B. Van Valkenburgh, Comparative morphology and histology of the nasal fossa in four mammals: Gray squirrel, bobcat, coyote, and white-tailed deer. *Anat. Rec. (Hoboken)* **299**, 840–852 (2016).
21. A. A. Curtis, N. B. Simmons, Unique turbinal morphology in horseshoe bats (Chiroptera: Rhinolophidae). *Anat. Rec. (Hoboken)* **300**, 309–325 (2017).
22. Q. Martinez *et al.*, Convergent evolution of an extreme dietary specialisation, the olfactory system of worm-eating rodents. *Sci. Rep.* **8**, 17806 (2018).
23. I. K. Lundeen, E. C. Kirk, Internal nasal morphology of the Eocene primate *Rooneyia viejaensis* and extant Euarchonta: Using μCT scan data to understand and infer patterns of nasal fossa evolution in primates. *J. Hum. Evol.* **132**, 137–173 (2019).
24. M. R. Sánchez-Villagra, R. J. Asher, Cranio-sensory adaptations in small faunivorous semiaquatic mammals, with special reference to olfaction and the trigeminal system. *Mammalia* **66**, 93–109 (2002).
25. D. J. Bird, A. Amirkhanian, B. Pang, B. Van Valkenburgh, Quantifying the cribriform plate: Influences of allometry, function, and phylogeny in Carnivora. *Anat. Rec. (Hoboken)* **297**, 2080–2092 (2014).
26. D. J. Bird *et al.*, Olfaction written in bone: cribriform plate size parallels olfactory receptor gene repertoires in Mammalia. *Proc. Biol. Sci.* **285**, 20180100 (2018).
27. T. Kishida, S. Kubota, Y. Shirayama, H. Fukami, The olfactory receptor gene repertoires in secondary-adapted marine vertebrates: Evidence for reduction of the functional proportions in cetaceans. *Biol. Lett.* **3**, 428–430 (2007).
28. Y. Niimura, On the origin and evolution of vertebrate olfactory receptor genes: Comparative genome analysis among 23 chordate species. *Genome Biol. Evol.* **1**, 34–44 (2009).
29. T. Kishida, T. Hikida, Degeneration patterns of the olfactory receptor genes in sea snakes. *J. Evol. Biol.* **23**, 302–310 (2010).
30. T. Kishida *et al.*, Loss of olfaction in sea snakes provides new perspectives on the aquatic adaptation of amniotes. *Proc. Biol. Sci.* **286**, 20191828 (2019).
31. A. C. Beichman *et al.*, Aquatic adaptation and depleted diversity: A deep dive into the genomes of the sea otter and giant otter. *Mol. Biol. Evol.* **36**, 2631–2655 (2019).
32. A. Liu *et al.*, Convergent degeneration of olfactory receptor gene repertoires in marine mammals. *BMC Genomics* **20**, 977 (2019).
33. C. T. Stayton, The definition, recognition, and interpretation of convergent evolution, and two new measures for quantifying and assessing the significance of convergence. *Evolution* **69**, 2140–2153 (2015).
34. K. C. Catania, Olfaction: Underwater "sniffing" by semi-aquatic mammals. *Nature* **444**, 1024–1025 (2006).
35. K. C. Catania, J. F. Hare, K. L. Campbell, Water shrews detect movement, shape, and smell to find prey underwater. *Proc. Natl. Acad. Sci. U.S.A.* **105**, 571–576 (2008).
36. Y. F. Ivlev, M. V. Rutovskaya, O. S. Luchkina, The use of olfaction by the Russian desman (*Desmana moschata* L.) during underwater swimming. *Dokl. Biol. Sci.* **452**, 280–283 (2013).
37. S. Firestein, How the olfactory system makes sense of scents. *Nature* **413**, 211–218 (2001).
38. R. Larochelle, G. Baron, Comparative morphology and morphometry of the nasal fossae of four species of North American shrews (Soricinae). *Am. J. Anat.* **186**, 306–314 (1989).
39. S. Hayden *et al.*, Ecological adaptation determines functional mammalian olfactory subgenomes. *Genome Res.* **20**, 1–9 (2010).
40. M. L. Noback, K. Harvati, F. Spoor, Climate-related variation of the human nasal cavity. *Am. J. Phys. Anthropol.* **145**, 599–614 (2011).
41. T. J. Dawson, F. D. Fanning, Thermal and energetic problems of semiaquatic mammals: A study of the Australian water rat, including comparisons with the platypus. *Physiol. Zool.* **54**, 285–296 (1981).
42. F. E. Fish, R. V. Baudinette, Energetics of locomotion by the Australian water rat (*Hydromys chrysogaster*): A comparison of swimming and running in a semi-aquatic mammal. *J. Exp. Biol.* **202**, 353–363 (1999).
43. T. M. Williams, The evolution of cost efficient swimming in marine mammals: Limits to energetic optimization. *Philos. Trans. R. Soc. B Biol. Sci.* **354**, 193–201 (1999).

44. F. E. Fish, Mechanics, power output and efficiency of the swimming muskrat (*Ondatra zibethicus*). *J. Exp. Biol.* **110**, 183–201 (1984).
45. N. Dunstone, "Adaptations to the semi-aquatic habit and habitat" in *Behaviour and Ecology of Riparian Mammals*, N. Dunstone, M. L. Gorman, Eds. (Cambridge University Press, Cambridge, UK, 1998), pp. 1–16.
46. P. J. Stephenson, Resting metabolic rate and body temperature in the aquatic tenrec *Limnogale mergulus* (Insectívora: Tenrecidae). *Acta Theriol. (Warsz.)* **39**, 89–92 (1994).
47. R. W. Gusztak, "Diving physiology and aquatic thermo-regulation of the American water shrew (*Sorex palustris*)," M.S. thesis, University of Manitoba, Winnipeg, MB, Canada (2008).
48. W. J. Hamilton, Habits of the star-nosed mole, *Condylura cristata*. *J. Mammal.* **12**, 345 (1931).
49. H. J. Harlow, The influence of Hardarian gland removal and fur lipid removal on heat loss and water flux to and from the skin of muskrats, *Ondatra zibethicus*. *Physiol. Zool.* **57**, 349–356 (1984).
50. E. Amson, G. Billet, C. de Muizon, Evolutionary adaptation to aquatic lifestyle in extinct sloths can lead to systemic alteration of bone structure. *Proc. Biol. Sci.* **285**, 20180270 (2018).
51. E. Peri, P. D. Gingerich, G. Aringhieri, G. Bianucci, Reduction of olfactory and respiratory turbinates in the transition of whales from land to sea: The semiaquatic middle Eocene *Aegyptocetus tarfa*. *J. Anat.* **236**, 98–104 (2020).
52. R. S. Voss, *Systematics and Ecology of Ichthyomyine Rodents (Muroidea) : Patterns of Morphological Evolution in a Small Adaptive Radiation* (Bulletin of the American Museum of Natural History Series, vol. 188, American Museum of National History, 1988).
53. R. S. Voss, *Tribe Ichthyomyini Vorontsov, 1959. Mammals of South America. Vol. 2 Rodents 2* (The University of Chicago Press, 2015), pp. 279–291.
54. K. M. Helgen, "A taxonomic and geographic overview of the mammals of Papua" in *The Ecology of Papua,* A. J. Marshall, B. M. Beehler, Eds. (Periplus Editions, 2007), pp. 689–749.
55. G. G. Musser, E. Piik, A new species of *Hydromys* (Muridae) from western New Guinea (Irian Jaya). *Zool. Meded.* **56**, 153–166 (1982).
56. R. M. Bonett, A. L. Blair, Evidence for complex life cycle constraints on salamander body form diversification. *Proc. Natl. Acad. Sci. U.S.A.* **114**, 9936–9941 (2017).
57. E. K. Baken, D. C. Adams, Macroevolution of arboreality in salamanders. *Ecol. Evol.* **9**, 7005–7016 (2019).
58. V. Millien, Morphological evolution is accelerated among island mammals. *PLoS Biol.* **4**, e321 (2006).
59. E. Paradis, J. Claude, K. Strimmer, APE: Analyses of phylogenetics and evolution in R language. *Bioinformatics* **20**, 289–290 (2004).
60. N. S. Upham, J. A. Esselstyn, W. Jetz, Inferring the mammal tree: Species-level sets of phylogenies for questions in ecology, evolution, and conservation. *PLoS Biol.* **17**, e3000494 (2019).
61. A. J. Drummond, M. A. Suchard, D. Xie, A. Rambaut, Bayesian phylogenetics with BEAUti and the BEAST 1.7. *Mol. Biol. Evol.* **29**, 1969–1973 (2012).
62. T. F. Hansen, Stabilizing selection and the comparative analysis of adaptation. *Evolution* **51**, 1341–1351 (1997).
63. M. A. Butler, A. A. King, Phylogenetic comparative analysis: A modeling approach for adaptive evolution. *Am. Nat.* **164**, 683–695 (2004).
64. J. Clavel, G. Escarguel, G. Merceron, mvMORPH : an R package for fitting multivariate evolutionary models to morphometric data. *Methods Ecol. Evol.* **6**, 1311–1319 (2015).
65. B. C. O'Meara, C. Ané, M. J. Sanderson, P. C. Wainwright, Testing for different rates of continuous trait evolution using likelihood. *Evolution* **60**, 922–933 (2006).
66. G. H. Thomas, R. P. Freckleton, T. Székely, Comparative analyses of the influence of developmental mode on phenotypic diversification rates in shorebirds. *Proc. Biol. Sci.* **273**, 1619–1624 (2006).
67. S. Joly *et al.*, Greater pollination generalization is not associated with reduced constraints on corolla shape in Antillean plants. *Evolution* **72**, 244–260 (2018).
68. L. J. Revell, phytools: An R package for phylogenetic comparative biology (and other things). *Methods Ecol. Evol.* **3**, 217–223 (2012).
69. A. C. T. Stayton, M. C. T. Stayton, convevol: Analysis of convergent evolution. R package version 1.3. https://cran.r-project.org/web/packages/convevol/convevol.pdf. Accessed 23 March 2020.
70. M. L. Zelditch, J. Ye, J. S. Mitchell, D. L. Swiderski, Rare ecomorphological convergence on a complex adaptive landscape: Body size and diet mediate evolution of jaw shape in squirrels (Sciuridae). *Evolution* **71**, 633–649 (2017).
71. S. A. Price, J. J. Tavera, T. J. Near, P. C. Wainwright, Elevated rates of morphological and functional diversification in reef-dwelling Haemulid fishes. *Evolution* **67**, 417–428 (2013).
72. T. F. Hansen, *Adaptive Landscape and Macroevolutionary Dynamics. The Adaptive Landscape in Evolutionary Biology* (Oxford University Press, 2012).
73. D. E. Wilson, T. E. Lacher Jr., R. A. Mittermeier, Eds., "Lagomorphs and rodents I" in *Handbook of the Mammals of the World* (Lynx Editions, Barcelona, 2016), vol. 6.
74. D. E. Wilson, T. E. Lacher Jr., R. A. Mittermeier, Eds., "Rodents II" in *Handbook of the Mammals of the World* (Lynx Editions, Barcelona, 2017), vol. 7.
75. D. E. Wilson, T. E. Lacher Jr., R. A. Mittermeier, Eds., "Insectivores, sloths and colugos" in *Handbook of the Mammals of the World* (Lynx Editions, Barcelona, 2018), vol. 8.

↑ Back to summary ↑

Article 3 - in preparation -

The mammalian maxilloturbinal evolution: when maxilloturbinal does not reflect thermal abilities

The mammalian maxilloturbinal evolution: when maxilloturbinal does not reflect thermal abilities

Quentin Martinez 1, Radim Šumbera 2, Jan Okrouhlík 2, Mark Wright 1, 3, Stan Braude 4, Thomas B. Hildebrandt 5, Susanne Holtze 5, Irina Ruf 6 , and Pierre-Henri Fabre 1, 7

1 Institut des Sciences de l'Évolution (ISEM, UMR 5554 CNRS-IRD-UM), Université de Montpellier, Place E. Bataillon - CC 064 - 34095, Montpellier Cedex 5, France
2 Department of Zoology, Faculty of Science, University of South Bohemia, 37005 České Budějovice, Czech Republic
3 Department of Organismic and Evolutionary Biology & Museum of Comparative Zoology, Harvard University, Cambridge, MA, 02138, USA
4 Biology Department, Washington University, St. Louis, MO 63130, USA
5 Department of Reproduction Management, Leibniz-Instiute for Zoo and Wildlife Research, 10315 Berlin, Germany
6 Abteilung Messelforschung und Mammalogie, Senckenberg Forschungsinstitut und Naturmuseum Frankfurt, 60325 Frankfurt am Main, Germany
7 Mammal Section, Department of Life Sciences, The Natural History Museum, SW7 5DB London, United Kingdom

Abstract

The evolution of endothermy in vertebrates has been extensively studied in recent decades. The ability of mammals to maintain constant and high body temperature was considered as a key innovation, enabling them to successfully colonize new areas. In mammals, the anterior nasal cavity houses the maxilloturbinal, a bony system supporting an epithelium involved in heat and moisture conservation. The presence of the maxilloturbinal was previously used to infer the ancestral homeothermic conditions and the basal metabolic rates of extinct vertebrates. Using a comprehensive dataset spanning most mammalian orders, we demonstrated that such inferences are hazardous. Indeed, we demonstrated that neither basal metabolic rate (BMR) nor body temperature (Tb) significantly correlated with the relative surface area of the maxilloturbinal (Maxillo RSA). Along the mammalian phylogeny, we identified important variations in the relative surface area, morpho-anatomy, and complexity of the maxilloturbinal.

Introduction

Among environmental conditions, temperature is often considered a major driver of diversification that has shaped vertebrate diversity (Figueirido et al. 2012; Davis et al. 2016). Indeed, both the ecological and evolutionary success of mammals may be partially explained by their ability to maintain a high and stable body temperature in a wide range of habitats (Hillenius and Ruben 2004; Lovegrove 2012). Temperature has also constrained and shaped vertebrate morphological and physiological evolution (Bicego et al. 2007). However, few anatomical structures have been shown to be relevant to diagnose and date the origin of their endothermy (e.g. Hillenius and Ruben 2004). Respiratory turbinals (turbinates) are still considered to be among the rare structures that may provide some evidence for potential endothermic and metabolic adaptations within extant and extinct vertebrates (Hillenius 1992, 1994). Indeed, at least in mammals, turbinals are ossified structures that may be preserved in fossils (Hillenius and Ruben 2004; Owerkowicz et al. 2014).

Respiratory turbinals support an epithelium that participates in heat and moisture conservation. During inhalation, the air is usually warmed up at contact with the vascularised anterior part of the maxilloturbinal and is simultaneously moistened by mucus glands. During subsequent exhalation, this air is cooled down by the anterior portion of the respiratory turbinals which were previously cooled down by inspired air. This process condenses water from the nasal cavity and therefore conserves, on average, 66% of the humidity of the exhaled air (Negus 1958; Walker and Wells 1961; Jackson and Schmidt-Nielsen 1964; Schmidt-Nielsen et al. 1970; Collins et al. 1971; Hillenius 1992; Ruben et al. 1996; Hillenius and Ruben 2004). Respiratory turbinals are present in mammals and birds and are, in mean, three times larger in the former clade (Owerkowicz et al. 2014). The presence of respiratory turbinals-like are highly debated in other groups such as in crocodilians (Parsons 1971; Hillenius 1994; Owerkowicz et al. 2014) where they are mostly involved in olfaction (Parsons 1971).

Among respiratory turbinals, the maxilloturbinal is shared by all extant terrestrial mammals and plays a significant role in maintaining body temperature (Hillenius 1994). Functionally, the relative size of the maxilloturbinal is related to heat and moisture conservation capacities and its presence has been used to infer the potential ancestral homeothermic conditions and basal metabolic rates of extinct species (Hillenius 1992, 1994; Ruben et al. 1996; Hillenius and Ruben 2004). However, mammalian species differ by their thermal and metabolic conditions. As an example, some anteaters, marsupials, monotremes, Xenarthra and subterranean rodents present poor temperature regulation, low body temperature and for some, low rates of metabolism (Martin 1903; Wislocki 1933; Enger 1957; McNab 1966; Šumbera 2019). This is also the case of some mammals that do different forms of dormancy (e.g. hibernation, aestivation and daily torpor,

Geiser and Ruf 1995; Wilz and Heldmaier 2000). In this study, we explored the anatomical diversity of maxilloturbinal in major mammalian orders on the basis of relative surface area, morphology and complexity. We also test the potential relation between basal metabolic rates (BMR) and the relative surface area of the maxilloturbinal (Maxillo RSA) as well as between body temperatures (Tb) and Maxillo RSA.

Results

Surface area

There is a significant correlation between maxilloturbinal surface area and skull length (Fig. 2A, $s = 2.60$, $R^2 = 0.87$, $p = 2.20e\text{-}16$). These variables display a negative allometry ($s = 2.60$) meaning that large species have higher maxilloturbinal surface area than small ones. However, some species deviated from the general trend (Fig. 1, 2A). Mammalian species with highest values of the relative surface area of the maxilloturbinal (Maxillo RSA) are generally aquatic and amphibious species. This is for example the case of *Castor*, *Chironectes, Galemys*, *Ornithorhynchus*, and *Zalophus* (Fig. 1, 2A SI 3). They respectively have 448, 275, 329, 306, and 611% of the predicted Maxillo RSA (SI 3). The second species with the highest predicted Maxillo RSA (463%) is *Rangifer tarandus* (Fig. 1, 2A SI 3). Also, some carnivores have among the highest values of Maxillo RSA such as *Felis*, *Ursus*, and *Zalophus* that have respectively 350, 430, and 611% of the predicted Maxillo RSA (Fig. 1, 2A, SI 3). However, there exist some discrepancies with for example *Hyaena* and *Proteles* that have respectively 58 and 30% of the predicted Maxillo RSA (Fig. 1, 2A, SI 3). In addition, some genus such as *Hystrix*, *Manis*, *Pteronotus*, and *Setifer* have among the highest values of predicted Maxillo RSA (respectively 286, 357, 377, and 312%, Fig. 1, 2A SI 3) without any noticeable explanatory patterns. The naked mole-rat (*Heterocephalus glaber*) is the sampled mammalian species with the lowest value of predicted Maxillo RSA (6%, mean of 17 individuals, Fig. 1, 2A, SI 3). Other species with low thermoregulatory capacities such as *Bradypus* and *Tachyglossus* have 310% and 55% of the predicted Maxillo RSA, respectively (Fig. 1, 2A SI 3). Elephants (genera *Elephas* and *Loxodonta*) have the lowest predicted Maxillo RSA after *Heterocephalus glaber* (both 7%, Fig. 1, 2A, SI 3). Worm-eating rodents such as *Paucidentomys vermidax* and *Rhynchomys soricoides* have some of the lowest predicted Maxillo RSA among mammals (16 and 22%, Fig. 1, 2A SI 3). Other species with highly elongated rostrum such as *Myrmecophaga*, and *Tachyglossus* also presented low values of predicted Maxillo RSA (28% and 55%, Fig. 1, 2A, SI 3).

There is no significant correlation between basal metabolic rates (BMR) and Maxillo RSA (Fig. 2 B, $s = 0.18$, $R^2 = -3.75e\text{-}3$, $p = 0.43$) nor between body temperatures (Tb) and Maxillo RSA (Fig. 2 C, $s = 2.69e\text{-}3$, $R^2 = -0.01$, $p = 0.75$).

Among species that do different forms of dormancy, the European ground squirrel (*Spermophilus citellus*) is an obligate hibernator (Ramos-Lara et al. 2014) that has lower predicted Maxillo RSA than the red squirrel (*Sciurus vulgaris*, 70 *vs* 106%, Fig. 1, 2A SI 3) that doesn't hibernate or only exceptionally (Lurz et al. 2005; Wilson et al. 2016). The brown bear (*Ursus arctos*) is known to hibernate between 5 to 6 months per year (Stenvinkel et al. 2012) and has lower predicted Maxillo RSA than its close aquatic relative, *Zalopus* (430 *vs* 611%, Fig. 1, 2A, SI 3). *Ursus* has higher predicted Maxillo RSA than the two sampled species of foxes that didn't hibernate (430 *vs* 166 and 184%, Mittermeier and Wilson 2009, Fig. 1, 2A, SI 3). The fat-tailed dwarf lemur (*Cheirogaleus medius*) can aestivate for the longest period of time (up to 70 days, McKechnie and Mzilikazi 2011) and has the same predicted Maxillo RSA than this closely related *Eulemur collaris* that is not known to aestivate (158%, Fig. 1, 2A, SI 3). Finally, the edible dormouse (*Glis glis*) is capable of daily torpor during diet restriction and low ambient temperature, as well as hibernation and aestivation (Wilz and Heldmaier 2000). All sampled Gliridae are known to either hibernate, aestivate or capable of daily torpor (McKechnie and Mzilikazi 2011). As a comparison with more phylogenetically distant species, *Glis glis* has lower predicted Maxillo RSA than the red squirrel (79 *vs* 106%, Fig. 1, 2A, SI 3).

Morphology

Among mammals, the maxilloturbinal is generally positioned ventrally in the nasal cavity, however in some species where the maxilloturbinal is highly developed, it also occupied the dorsal part. This is for example the case of *Castor* and *Zalophus* where it extends to the nasal roof (Fig. 1 n 7, 18). It doesn't extend as dorsally in *Pteronotus*, *Manis*, and *Rangifer* despite their high development (Fig. 1 n 15, 20, 16). The antero-posterior position of the maxilloturbinal also varied considerably. Maxilloturbinal anteriorly reaches the rostrum nasal opening in several species such as in *Acerodon*, *Castor*, *Didelphis*, *Pedetes*, *Procavia*, *Rangifer*, and *Tympanoctomys* (Fig. 1 n 14, 7, 29, 6, 28, 16, 33). A gap exists between the anterior part of the maxilloturbinal and the rostrum opening in *Elephas*, *Equus*, *Fukomys*, *Heterocephalus*, *Manis*, *Notoryctes*, *Orycteropus*, *Pteronotus*, and *Tarsius*. This gap is very important and distinctive in monotremes (genera *Ornithorhynchus* and *Tachyglossus*, Fig. 1 n 31, 32). This gap is supposed to be occupied by the outer nasal cartilage and the cartilaginous margino- and atrio-turbinals (e.g. Maier 2020; Ruf 2020). These structures are not, or only very slightly covered by blood vessels and mucus glands. Therefore, the implication of the margino- and atrio-

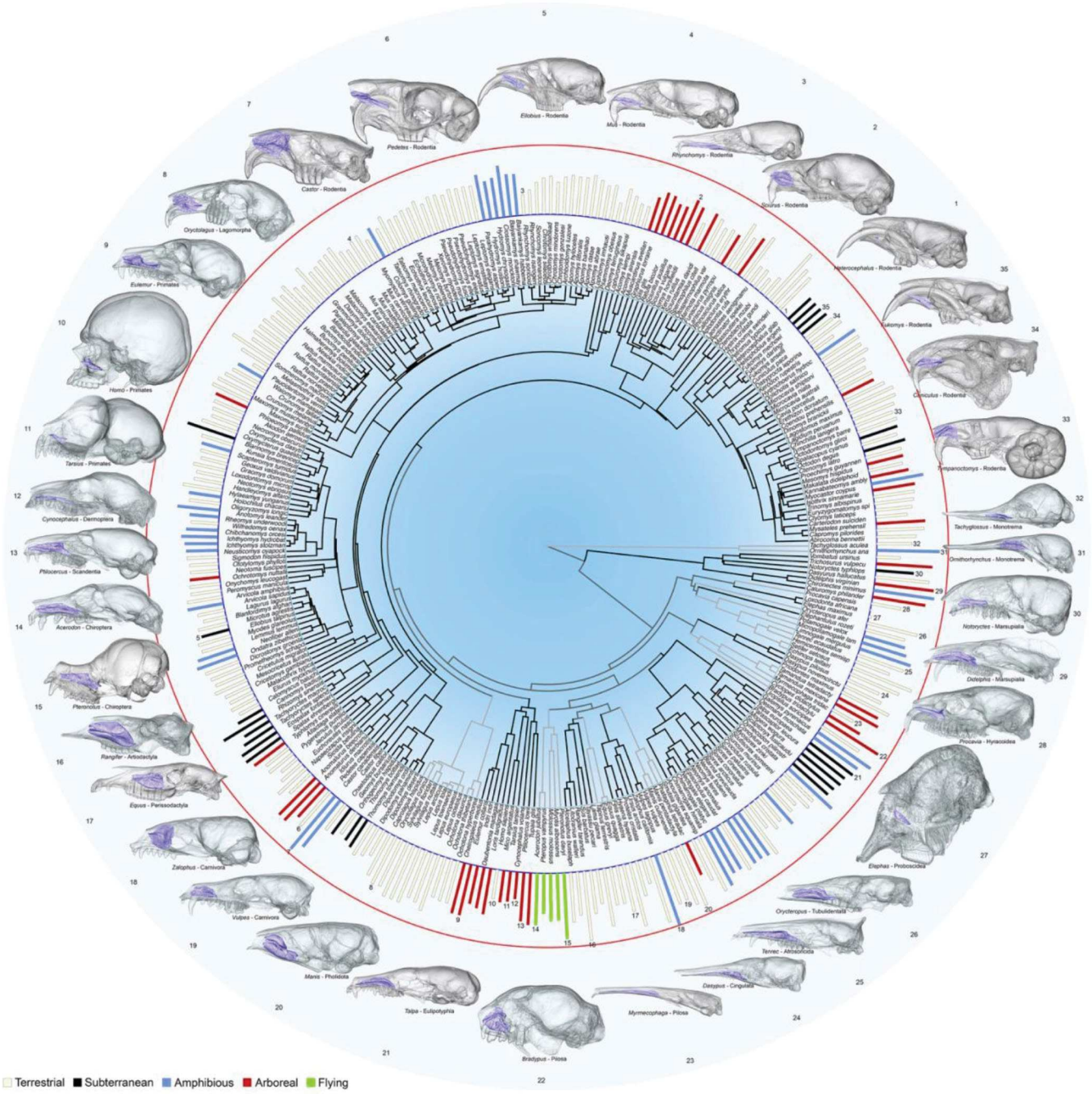

Figure 1: Important variations of the relative surface area and shape of maxilloturbinal between mammalian species. Barplots represent the relative surface area of maxilloturbinal in 310 species. Blue and red circles respectively represent the minimum and the maximum values from the naked mole rat (*Heterocephalus glaber*) and the California sea lion (*Zalophus californianus*). 3D representations of the skull and the maxilloturbinal in several species. Barplots: beige = terrestrial, red = arboreal, blue = amphibious, black = subterranean, and yellow = flying species.

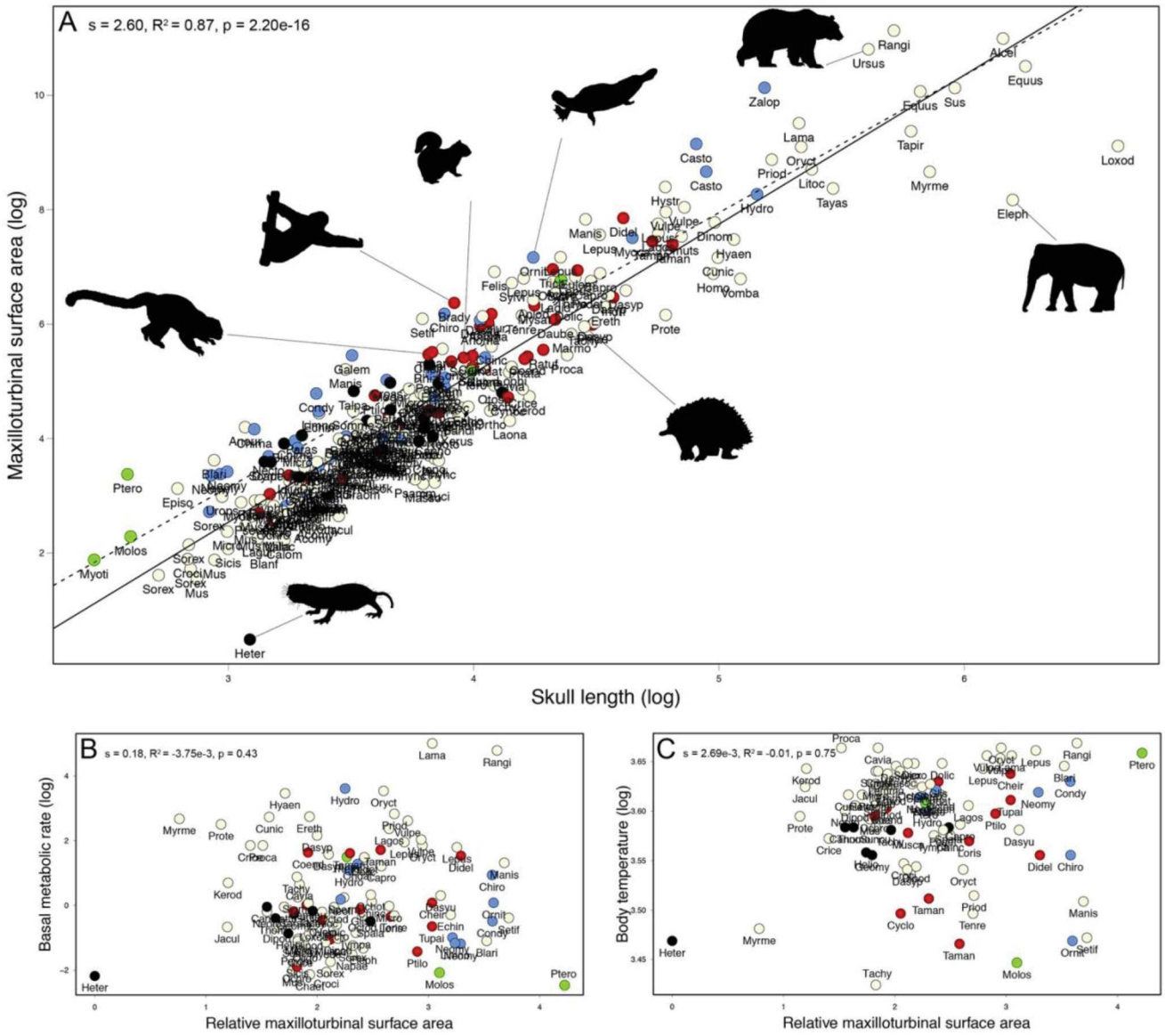

Figure 2: Maxilloturbinal may not always reflect thermal and metabolic conditions. (A) Log–log regression (continuous line) and PGLS (dashed line) of maxilloturbinal surface area on skull length. (B) Linear regression between basal metabolic rates (BMR) and the relative surface area of the maxilloturbinal (Maxillo RSA) and (C) between body temperatures (Tb) and Maxillo RSA. Barplots: beige = terrestrial, red = arboreal, blue = amphibious, black = subterranean, and yellow = flying species. Species silhouettes come from http://phylopic.org.

turbinals in heat and moisture conservation may be limited. In general, the maxilloturbinal morphology varied with skull shape. As an example some species with an elongated rostrum present an elongated maxilloturbinal. This is the case of *Dasypus*, *Myrmecophaga*, *Rhynchomys*, and *Tenrec* (Fig. 1 n 24, 23, 3, 25). The maxilloturbinal of some species formed a recessus with the most derived forms found in lineages such as *Hystrix*, *Manis*, *Orycteropus*, and *Rangifer* (Fig. 1 n 20, 26, 16). The maximum height of the maxilloturbinal may be higher than the rostrum opening in *Castor*, *Bradypus*, *Manis*, *Ornithorhynchus* and *Zalophus* (Fig. 1 n 7, 22, 20, 31, 18). In most species, this is the opposite pattern with a maximum difference in *Cynocephalus*, *Elephas*, *Heterocephalus*, and *Pedetes* (Fig. 1 n 12, 27, 1, 6).
No common morphological pattern is found among species that present particular BMR, Tb or that do different forms of dormancy (Fig. 1, 2).

Complexity

We identified that maxilloturbinal complexity widely varied among mammals and might have convergently evolved according to ecological lifestyle or phylogenetic relationships (Fig. 4). As an example, the European rabbit (*Oryctolagus cuniculus*), North American beaver (*Castor canadensis*), red squirrel (*Sciurus vulgaris*), Californian sea lion (*Zalophus californianus*), red fox (*Vulpes vulpes*), North American opossum (*Didelphis virginiana*), and platypus (*Ornithorhynchus anatinus*) developed numerous lamellae and folding in their maxilloturbinal resulting in a dendritic pattern in cross-section (Fig. 3, 4). Other species present two symmetrical and scrolled branches with a variable number of windings that originated from a single main branch (e. g. double scroll pattern, Fig. 4). This is the case in the collared brown lemur (*Eulemur collaris*), reindeer (*Rangifer tarandus*), Chinese pangolin (*Manis pentadactyla*), European mole (*Talpa europaea*), giant anteater (*Myrmecophaga tridactyla*), hairy long-nosed armadillo (*Dasypus pilosus*), and aardvark (*Orycteropus afer*, Fig. 4). Other species present a non-complex but well-developed lamella such as humans (*Homo sapiens*), Philippine flying lemur (*Cynocephalus volans*), and Asian elephant (*Elephas maximus*, Fig. 4). Lastly, when present, the maxilloturbinal of the naked mole-rat is a vestigial and non-complex lamina that is anteriorly attached to the medial side of the incisor alveolus (ia, Fig. 3, 4). Posteriorly, this lamina extends ventrally and merges with the canal housing the nasolacrimal duct (nld, Fig. 3). As with morphology, no common pattern of complexity is found among species that present particular BMR, Tb or that do different forms of dormancy (Fig. 4).

Discussion

Body temperature and metabolic conditions

We demonstrated that neither basal metabolic rate (BMR) nor body temperature (Tb) significantly correlated with the relative surface area of the maxilloturbinal (Maxillo RSA, Fig. 2B, C, SI 1A, B). These results challenged the long standing hypothesis that assumed that respiratory turbinals may reflect thermal and metabolic conditions (Hillenius 1992, 1994; Ruben et al. 1996; Hillenius and Ruben 2004). As an example, in synapsids,

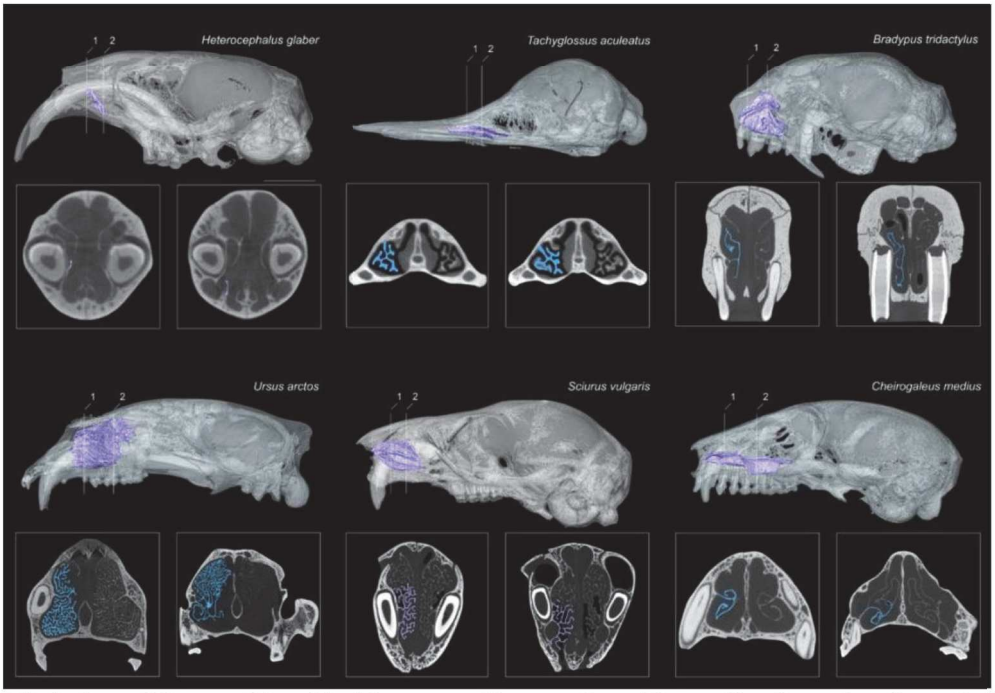

Figure 3: Detailed view of the maxilloturbinal in mammalian species with peculiar thermal and metabolic conditions. 3D representations and coronal cross sections of the maxilloturbinal.

bony scars are interpreted as potential respiratory turbinals in the upper Permian therapsid *Glanosuchus* (~ 260 Mya, Hillenius 1992, 1994). Based on these evidences, Hillenius (1992, 1994) infers that this genus may be the earliest known tetrapod with a partially warm-blooded system and therefore some internal thermoregulatory adaptations. Since BMR are significantly correlated with field metabolic rates FMR (White and Seymour 2004), our results also challenged the relation found between FMR and the residuals between respiratory turbinal surface area and body mass (Owerkowicz et al. 2014). This difference may be explained by the sample size of Owerkowicz et al. (2014) that is only based on ten mammal species. Another explanation may be that they also quantified another respiratory turbinal, the nasoturbinal. However, at the mammalian scale the epithelial cover of the nasoturbinal may vary between species. Indeed, in some species, a portion of the nasoturbinal is covered with olfactory epithelium and therefore plays a role in olfaction (Smith et al. 2004, 2012; Smith and Rossie 2008; Yee et al. 2016; Herbert et al. 2018).

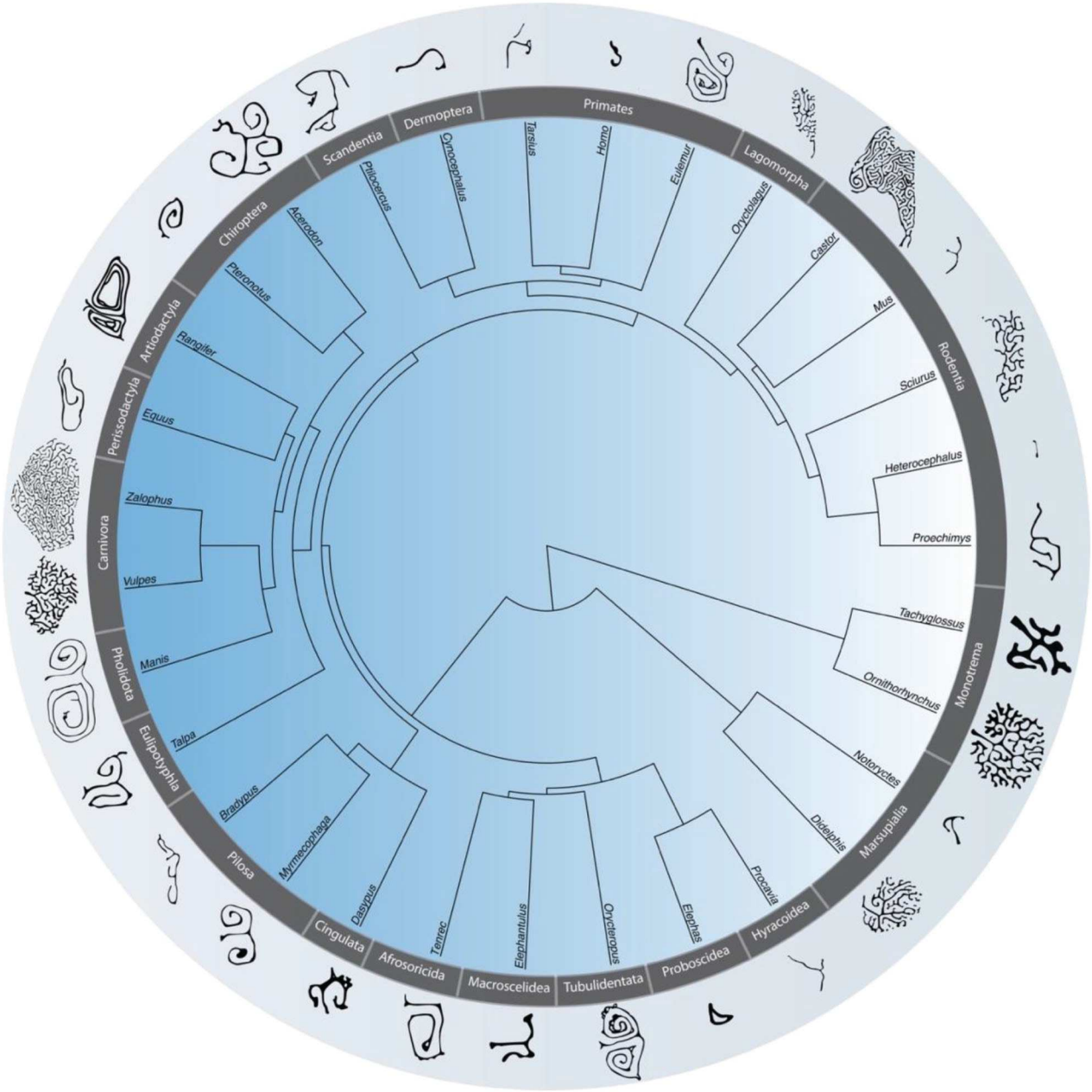

Figure 4: Important variations of the maxiloturbinal complexity between mammalian species. Silhouette of the maxilloturbinal coronal cross section across mammalian major clades.

The naked mole-rat is the sampled mammalian species with the lowest value of predicted Maxillo RSA (6%, mean of 17 individuals, Fig. 1, 2A, SI 3). Therefore, this species may match with the past hypothesis that Maxillo RSA correlated with thermal and metabolic conditions (e.g. Hillenius 1992, 1994; Ruben et al. 1996; Owerkowicz et al. 2014). Indeed, the naked mole-rat is a poorly thermoregulating endotherm with low basal rates of metabolism and has been described by some authors as the only known obligatory poikilotherm mammal (McNab 1966; Withers and Jarvis 1980; Buffenstein and Yahav 1991; Hislop and Buffenstein 1994; but see Braude et al. 2021). However, Marsupials, Monotremes, Xenarthra, some anteaters, and some subterranean rodents also present poor temperature regulation, low body temperature and for some, low basal rates of metabolism (Martin 1903; Wislocki 1933; Enger 1957; McNab 1966; Šumbera 2019). For example, after the naked mole rat, echidnas (genus *Tachyglossus*) have the lowest thermoregulatory capacities among terrestrial mammals (Martin 1903). Similarly, sloths have low basal rates of metabolism and also face significant body temperature variations (Cliffe et al. 2018). However, *Bradypus* has among the highest values of the predicted Maxillo RSA in the sampled mammals (310%, Fig. 1, 2A, SI 3) whereas *Tachyglossus* has intermediate values (55%, Fig. 1, 2A, SI 3).

The body temperature variation referred to as the poikilothermy may be also found in other mammals during various periods of time: (1) during hibernation in winter conditions, (2) during aestivation (= estivation) in hot and dry conditions, and (3) during daily torpor (Geiser and Ruf 1995; Wilz and Heldmaier 2000). These forms of dormancy are also associated with a decrease of metabolic rates. The European ground squirrel (*Spermophilus citellus*) is an obligate hibernator that hibernates for 4 to 7 months (Ramos-Lara et al. 2014). This species has lower predicted Maxillo RSA than the red squirrel (*Sciurus vulgaris*, 70 *vs* 106%, Fig. 1, 2A, SI 3) that doesn't hibernate or only exceptionally (Lurz et al. 2005; Wilson et al. 2016). The brown bear (*Ursus arctos*) is known to hibernate between 5 to 6 months per year (Stenvinkel et al. 2012). However, in this species, hibernation has little effect on the body temperature in comparison to other hibernating mammals (Stenvinkel et al. 2012). *Ursus* has lower predicted Maxillo RSA than its close aquatic relative, *Zalopus* (430 *vs* 611%, Fig. 1, 2A, SI 3). *Ursus* has higher predicted Maxillo RSA than the two sampled species of foxes that didn't hibernate (430 *vs* 166 and 184%, Mittermeier and Wilson 2009, Fig. 1, 2A, SI 3). In our sample, the fat-tailed dwarf lemur (*Cheirogaleus medius*) is the species that can aestivate for the longest period of time (up to 70 days, McKechnie and Mzilikazi 2011). However, this species has the same predicted Maxillo RSA than this closely related *Eulemur collaris* that is not known to aestivate (158%, Fig. 1, 2A, SI 3). Finally, in our sample, the edible dormouse (*Glis glis*) is capable of daily torpor during diet restriction and low ambient temperature, as well as hibernation and aestivation (Wilz and Heldmaier 2000). All sampled Gliridae are known to either hibernate, aestivate or capable of daily torpor (McKechnie and Mzilikazi 2011). However, as a comparison with more phylogenetically distant species, *Glis glis* has lower predicted Maxillo RSA than the red squirrel (79 *vs* 106%, Fig. 1, 2A, SI 3). Therefore, our results didn't match with a consistent pattern of hibernation, aestivation nor of daily torpor.

Overall, our results demonstrated that maxilloturbinal are not necessarily associated with thermal and metabolic conditions of the species. Therefore, we challenged previous hypotheses on thermal and metabolic inferences of extinct species. In the light of our result we recommend being prudent within such interpretations.

Environmental conditions

Mammalian species with highest values of the relative surface area of the maxilloturbinal (Maxillo RSA) are generally aquatic and amphibious species. This is for example the case of *Castor*, *Chironectes, Galemys*, *Ornithorhynchus*, and *Zalophus* (Fig. 1, 2A, SI 3). They respectively have 448, 275, 329, 306, and 611% of the predicted Maxillo RSA (Fig. 1, 2A, SI 3). This pattern had been interpreted as an adaptation to limit heat loss due to the high thermal inertia of water (Valkenburgh et al. 2011; Martinez et al. 2020). There, we demonstrated that this pattern is convergent across whole mammals (Fig. 1, 2A, SI 3). The increase of Maxillo RSA in aquatic and amphibious species is also associated with an increase in turbinal complexity (Fig. 4). For example, in monotrema, the maxilloturbinal complexity between the amphibious platypus (*Ornithorhynchus anatinus*) and the terrestrial short-beaked echidna (*Tachyglossus aculeatus*) strongly differ (Fig. 4). Platypus has a very complex maxilloturbinal with several small lamellae originating from the main three branches, being similar to some carnivores, aquatic or amphibious species (Fig. 4, e.g. Valkenburgh et al. 2011; Martinez et al. 2020). In contrast, echidna has no additional lamellae to the main three branches but an unusual thickening that is proportionally thicker than pachyostosis turbinals found in giant and amphibious sloths (Fig. 4, Amson et al. 2018). To date, the increasing turbinal complexity is described as the development of infolding and small lamellae called epiturbinals and resulting from repetitive mesenchymal growth (e.g. Valkenburgh et al. 2014a; Ruf 2020). From a statistical perspective, turbinal complexity is often described as the degree of details in a predefined area (e.g. Craven et al. 2007; Martinez et al. 2018; Wagner and Ruf 2019). Based on fluid dynamic principles, Martinez et al. (2018) hypothesised that the increase in turbinal

complexity may increase the proportion of air in contact with mucus gland and epithelium. Therefore, the increase in turbinal complexity may facilitate heat and moisture conservation performances. In rodents, they demonstrated that there is a significant correlation between complexity and surface area (Martinez et al. 2018). These results support the functional significance of most turbinal studies that only used the surface area proxy.

Some studies suggested that temperature and altitude may have constrained the development and the complexity of maxilloturbinal (Valkenburgh et al. 2011; supplementary results in Martinez et al. 2020). In this study, the second species with the highest predicted Maxillo RSA (463%) is *Rangifer tarandus* (Fig. 1, 2A, SI 3). This may be an adaptation of this arctic species that is known to have efficient heat and moisture conservation capacities (Langman 1985). Finally, for arctic or marine species it is complicated to differentiate the origins of the selective pressure for improving heat or moisture conservation. As an example, sea lions and elephant seals have extremely complex and well developed maxilloturbinal (Fig. 1, 2A, SI 3, Valkenburgh et al. 2011; Mason et al. 2020). This may be associated with high efficiency in their heat conservation capacities due to the high thermal inertia of water and / or to efficient moisture conservation capacities resulting in an adaptation to a salty environment (Lester and Costa 2006).

Water conservation

Another major role of maxilloturbinal is water conservation that on average allows to conserve 66% of the humidity of the exhaled air (Negus 1958; Walker and Wells 1961; Jackson and Schmidt-Nielsen 1964; Schmidt-Nielsen et al. 1970; Collins et al. 1971; Hillenius 1992; Ruben et al. 1996; Hillenius and Ruben 2004). Experimental studies demonstrated the importance of nasal breathing and respiratory turbinals in water conservation. Indeed, mammals with plugged nares that are obligated to breath with mouth significantly increased evaporative water loss (EWL, Hillenius 1992). The naked mole-rat is the sampled mammalian species with the lowest value of predicted Maxillo RSA (6%, Fig. 1, 2A SI 3). In birds, when respiratory turbinals are lost or reduced, longer trachea can compensate for heat and moisture conservation (Owerkowicz et al. 2014). Apparently, this is not the case with the naked mole-rat. Indeed, this species has the highest EWL recorded in mammals (Buffenstein and Yahav 1991, but see also Buffenstein and Jarvis 1985). As an example, in experimental conditions, the naked mole-rat has a water evaporation rate up to 10 times higher than *Gerbillus pusillus*, a terrestrial rodent of comparable body mass that co-occurs in the same habitat (Buffenstein and Jarvis 1985; Buffenstein and Yahav 1991). Elephants (genera *Elephas* and *Loxodonta*) have the lowest predicted Maxillo RSA after the naked mole-rat (both 7%, Fig. 1, 2A, SI 3). However, the maxilloturbinal of adult elephants is merged with other nasal structures and difficult to delineate (SI 2). In addition, these species have a highly modified respiratory system comprising a trunk that may differentially operate in comparison to other mammals. However, other species with a trunk such as *Elephantulus rozeti*, present normal predicted Maxillo RSA (78%, Fig. 1, 2A, SI 3).

Methods

Undamaged specimens of 424 individuals belonging to 310 species were selected from museums (SI3) and scanned using high-resolution X-ray micro-computed tomography. From these 424 individuals, 32 were downloaded from Morphosource (Boyer et al. 2017) and 6 from DigiMorph (SI3). Left maxilloturbinal was segmented following Martinez et al. (2018, 2020) with AvizoLite 2020.1 (VSG Inc.). Mean values were used for interspecific comparison when multiple individuals of a species were sampled. Maxilloturbinal surface areas were standardized by skull length. The named "*relative surface area of maxilloturbinal*" (Maxillo RSA) is based on the residuals of the phylogenetic generalized least squares (PGLS) regression between maxilloturbinal surface area and skull length (Fig. 1, 2A, SI3). This was performed with the *gls* function from the package nlme (Pinheiro et al. 2006). To avoid negative values, we added the lowest residual value (2.77, SI3) to all residuals. We used the following equation to estimate how Maxillo RSA deviates from the prediction (see also SI3): *(e^[(residuals of the model)+(prediction of the model)]*100) / e^(prediction of the Model)*. The model is the PGLS regression between maxilloturbinal surface area and skull length. The predicted values were obtained with the *Predict* function from the package car (Fox et al. 2012) and were named "*Predicted Maxillo RSA*". Mammalian basal metabolic rates (BMR) and body temperatures (Tb) were extracted from (Clarke et al. 2010). We performed PGLS between BMR and Maxillo RSA (Fig. 2B) and between Tb and Maxillo RSA (Fig. 2C). For Maxillo RSA, to avoid negative values, we added the lowest residual value, 2.64 and 2,67 respectively. These 2 PGLS comprised 99 and 89 species respectively. We also performed linear regressions between BMR and the relative surface area of the maxilloturbinal based on body mass (SI 1A) as well as between Tb and the relative surface area of the maxilloturbinal based on body mass (SI 1B). The Phylogenetic figures were performed with the R package phytools (Revell 2012). We used a maximum clade credibility (MCC) phylogeny obtained from 10,000 trees sampled in the posterior distribution of Upham et al. (2019) and pruned to match the species in our dataset. The MCC consensus tree was inferred using TreeAnnotator v.1.8.2 (Drummond et al. 2012) with a 25% burn-in.

Creative commons silhouettes were downloaded from http://phylopic.org. According to the phylopic guidelines we credited Anthony Caravaggi and T. Michael Keesey for the use of their silhouettes and provided the link to the licence: https://creativecommons.org/licenses/by-nc-sa/3.0/. All raw data and R script are available in the supplementary information (SI 2, 4).

Acknowledgements

We thank P. G. Cox, F. Delsuc, B. Dubourguier, S. Ferreira-Cardoso, L. Hautier, L. Kerber, R. Lebrun, M. Lovy, and H. G. Rodrigues for different types of support, including interesting discussions. We thank A. C. Fabre, V. Fernandez, A. Goswami, and S. Renaud for providing some scans that were not included in the final version of this study. Thanks to B. Clark, V. Fernandez, and R. P. Miguez for access to the mammal collections and the computed tomography facilities at the Natural History Museum London. We thank the 3D data repositories morphosource, DigiMorph and their contributors (see SI 2). Three-dimensional data acquisitions were performed using the micro-computed tomography (µCT) facilities of the MRI platform member of the national infrastructure France-BioImaging supported by the French National Research Agency (Grant ANR-10-INBS-04, "Investments for the future"), and those of the Laboratoire d'Excellence Centre Méditerranéen de l'Environnement et de la Biodiversité (LabEx CeMEB, ANR10-LABX-0004). We acknowledge the Réseau d'Histologie Expérimentale de Montpellier (RHEM) facility supported by a Sites de Recherche Intégrée sur le Cancer (SIRIC) Montpellier Cancer Grant (Institut National Du Cancer [INCa] Inserm Direction générale de l'offre de soins [DGOS] 12553), the European Regional Development Foundation, and the Occitanian Region (Grant FEDER-FSE 2014-2020 Languedoc Roussillon) for processing our animal tissues, histology techniques, and expertise. Funding was provided by the Synthesis of Systematic Resources (SYNTHESYS) project, which is financed by European Community Research Infrastructure Action (FP7: Grants GB-TAF-5737 and GB-TAF-6945 to the National History Museum London), by Agence Nationale de la Recherche (Défi des autres savoirs, Grants DS10, ANR-17-CE02-0005 RHINOGRAD 2017), PEPS, adaptation, adaptabilite SHREWNOSE (Grant ANR-10- LABX-0025-01), and Czech Science Foundation project GAČR [n.20-10222S]. This is a contribution of ISEM X, Univ Montpellier, CNRS, EPHE, IRD, Montpellier, France.

References

Amson, E., G. Billet, and C. de Muizon. 2018. Evolutionary adaptation to aquatic lifestyle in extinct sloths can lead to systemic alteration of bone structure. Proc. R. Soc. B Biol. Sci. 285:20180270.

Bicego, K. C., R. C. H. Barros, and L. G. S. Branco. 2007. Physiology of temperature regulation: Comparative aspects. Comp. Biochem. Physiol. A. Mol. Integr. Physiol. 147:616–639.

Boyer, D., G. Gunnell, S. Kaufman, and T. McGeary. 2017. Morphosource: Archiving and sharing 3-d digital specimen data. Paleontol. Soc. Pap. 22:157–181.

Braude, S., S. Holtze, S. Begall, J. Brenmoehl, H. Burda, P. Dammann, D. del Marmol, E. Gorshkova, Y. Henning, A. Hoeflich, A. Höhn, T. Jung, D. Hamo, A. Sahm, Y. Shebzukhov, R. Šumbera, S. Miwa, M. Y. Vyssokikh, T. von Zglinicki, O. Averina, and T. B. Hildebrandt. 2021. Surprisingly long survival of premature conclusions about naked mole-rat biology. Biol. Rev. 96:376–393.

Buffenstein, R., and J. U. M. Jarvis. 1985. Thermoregulation and metabolism in the smallest African gerbil, Gerbillus pusillus. J. Zool. 205:107–121.

Buffenstein, R., and S. Yahav. 1991. Is the naked mole-rat Hererocephalus glaber an endothermic yet poikilothermic mammal? J. Therm. Biol. 16:227–232. Elsevier Limited.

Clarke, A., P. Rothery, and N. J. B. Isaac. 2010. Scaling of basal metabolic rate with body mass and temperature in mammals. J. Anim. Ecol. 79:610–619.

Cliffe, R. N., D. M. Scantlebury, S. J. Kennedy, J. Avey-Arroyo, D. Mindich, and R. P. Wilson. 2018. The metabolic response of the Bradypus sloth to temperature. PeerJ 6:e5600. PeerJ Inc.

Collins, J. C., T. C. Pilkington, and K. Schmidt-Nielsen. 1971. A Model of Respiratory Heat Transfer in a Small Mammal. Biophys. J. 11:886–914.

Craven, B. A., T. Neuberger, E. G. Paterson, A. G. Webb, E. M. Josephson, E. E. Morrison, and G. S. Settles. 2007. Reconstruction and Morphometric Analysis of the Nasal Airway of the Dog (Canis familiaris) and Implications Regarding Olfactory Airflow. Anat. Rec. 290:1325–1340.

Davis, K. E., J. Hill, T. I. Astrop, and M. A. Wills. 2016. Global cooling as a driver of diversification in a major marine clade. Nat. Commun. 7:13003.

Drummond, A., M. A. Suchard, D. Xie, and A. Rambaut. 2012. Bayesian phylogenetics with BEAUti and the BEAST 1.7. Mol Biol Evol 22:1185–1192.

Enger, P. S. 1957. Heat Regulation and Metabolism in some Tropical Mammals and Birds. Acta Physiol. Scand. 40:161–166.

Figueirido, B., C. M. Janis, J. A. Perez-Claros, M. De Renzi, and P. Palmqvist. 2012. Cenozoic climate change influences mammalian evolutionary dynamics. Proc. Natl. Acad. Sci. 109:722–727.

Fox, J., D. Adler, G. Bates, S. Ellison, D. Firth, M. Friendly, G. Gorjanc, S. Graves, R. Heiberger, R. Laboissiere, G. Monette, D. Murdoch, H. Nilsson, D. Ogle, B. Ripley, W. Venables, D. Winsemius, A. Zeileis, and R-Core. 2012. Package 'car.'

Geiser, F., and T. Ruf. 1995. Hibernation versus Daily Torpor in Mammals and Birds: Physiological Variables and Classification of Torpor Patterns. Physiol. Zool. 68:935–966.

Herbert, R. A., K. S. Janardhan, A. R. Pandiri, M. F. Cesta, and R. A. Miller. 2018. Nose, Larynx, and Trachea. Boormans Pathol. Rat 391–435.

Hillenius, W. J. 1992. The evolution of nasal turbinates and mammalian endothermy. Paleobiology 18:17–29.

Hillenius, W. J. 1994. Turbinates in Therapsids: Evidence for Late Permian Origins of Mammalian Endothermy. Evolution 48:207–229.

Hillenius, W. J., and J. A. Ruben. 2004. The Evolution of Endothermy in Terrestrial Vertebrates: Who? When? Why? Physiol. Biochem. Zool. 77:1019–1042.

Hislop, M. S., and R. Buffenstein. 1994. Noradrenaline induces

nonshivering thermogenesis in both the naked mole-rat (Heterocephalus glaber) and the Damara mole-rat (Cryptomys damarensis) despite very different modes of thermoregulation. J. Therm. Biol. 19:25–32.
Jackson, D. C., and K. Schmidt-Nielsen. 1964. Countercurrent heat exchange in the respiratory passages. Proc. Natl. Acad. Sci. U. S. A. 51:1192–1197.
Langman, V. A. 1985. Nasal heat exchange in a northern ungulate, the reindeer (Rangifer tarandus). Respir. Physiol. 59:279–287.
Lester, C. W., and D. P. Costa. 2006. Water conservation in fasting northern elephant seals (Mirounga angustirostris). J. Exp. Biol. 209:4283–4294.
Lovegrove, B. G. 2012. The evolution of endothermy in Cenozoic mammals: a plesiomorphic-apomorphic continuum. Biol. Rev. 87:128–162.
Lurz, P. W. W., J. Gurnell, and L. Magris. 2005. Sciurus vulgaris. Mamm. Species 2005:1–10. American Society of Mammalogists.
Maier, W. 2020. A neglected part of the mammalian skull: The outer nasal cartilages as progressive remnants of the chondrocranium. , doi: 10.26049/VZ70-3-2020-09. Senckenberg Gesellschaft für Naturforschung.
Martin, C. J. 1903. I. Thermal adjustment and respiratory exchange in monotremes and marsupials.—A study in the development of homæothermism. Philos. Trans. R. Soc. Lond. Ser. B Contain. Pap. Biol. Character 195:1–37. Royal Society.
Martinez, Q., J. Clavel, J. A. Esselstyn, A. S. Achmadi, C. Grohé, N. Pirot, and P.-H. Fabre. 2020. Convergent evolution of olfactory and thermoregulatory capacities in small amphibious mammals. Proc. Natl. Acad. Sci. 117:8958–8965. National Academy of Sciences.
Martinez, Q., R. Lebrun, A. S. Achmadi, J. A. Esselstyn, A. R. Evans, L. R. Heaney, R. P. Miguez, K. C. Rowe, and P.-H. Fabre. 2018. Convergent evolution of an extreme dietary specialisation, the olfactory system of worm-eating rodents. Sci. Rep. 8:17806. Nature Publishing Group.
Mason, M. J., L. M. D. Wenger, Ø. Hammer, and A. S. Blix. 2020. Structure and function of respiratory turbinates in phocid seals. Polar Biol. 43:157–173.
McKechnie, A., and N. Mzilikazi. 2011. Heterothermy in Afrotropical Mammals and Birds: A Review. Integr. Comp. Biol. 51:349–63.
McNab, B. K. 1966. The Metabolism of Fossorial Rodents: A Study of Convergence. Ecology 47:712–733.
Mittermeier, R. A., and D. E. Wilson. 2009. Carnivores Handbook of the mammals of the world. Lynx Editions. Barcelona.
Negus, V. 1958. The Comparative Anatomy and Physiology of the Nose and Paranasal Sinuses. E. & S. Livingstone, London.
Owerkowicz, T., C. Musinsky, K. M. Middleton, and A. W. Crompton. 2014. Respiratory Turbinates and the Evolution of Endothermy in Mammals and Birds. University of Chicago Press.
Parsons, T. S. 1971. Anatomy of Nasal Structures from a Comparative Viewpoint. Pp. 1–26 *in* J. E. Amoore, M. G. J. Beets, J. T. Davies, T. Engen, J. Garcia, R. C. Gesteland, P. P. C. Graziadei, K.-E. Kaissling, R. A. Koelling, J. LeMagnen, P. MacLeod, D. G. Moulton, M. M. Mozell, D. Ottoson, T. S. Parsons, S. F. Takagi, D. Tucker, B. M. Wenzel, and L. M. Beidler, eds. Olfaction. Springer, Berlin, Heidelberg.
Pinheiro, J., D. Bates, S. DebRoy, D. Sarkar, and R. C. Team. 2006. Linear and nonlinear mixed effects models.
Ramos-Lara, N., J. Koprowski, B. Krystufek, and I. Hoffmann. 2014. Spermophilus citellus (Rodentia: Sciuridae). Mamm. Species 913:71–87.
Revell, L. J. 2012. phytools: an R package for phylogenetic comparative biology (and other things). Methods Ecol. Evol. 3:217–223.
Ruben, J. A., W. J. Hillenius, N. R. Geist, A. Leitch, T. D. Jones, P. J. Currie, J. R. Horner, and G. Espe. 1996. The Metabolic Status of Some Late Cretaceous Dinosaurs. Science 273:1204–1207. American Association for the Advancement of Science.
Ruf, I. 2020. Ontogenetic transformations of the ethmoidal region in Muroidea (Rodentia, Mammalia): new insights from perinatal stages. , doi: 10.26049/VZ70-3-2020-10. Senckenberg Gesellschaft für Naturforschung.
Schmidt-Nielsen, K., F. R. Hainsworth, and D. E. Murrish. 1970. Counter-current heat exchange in the respiratory passages: Effect on water and heat balance. Respir. Physiol. 9:263–276.
Smith, T. D., K. P. Bhatnagar, P. Tuladhar, and A. M. Burrows. 2004. Distribution of olfactory epithelium in the primate nasal cavity: Are microsmia and macrosmia valid morphological concepts? Anat. Rec. A. Discov. Mol. Cell. Evol. Biol. 281A:1173–1181.
Smith, T. D., T. P. Eiting, and K. P. Bhatnagar. 2012. A Quantitative Study of Olfactory, Non-Olfactory, and Vomeronasal Epithelia in the Nasal Fossa of the Bat Megaderma lyra. J. Mamm. Evol. 19:27–41.
Smith, T. D., and J. B. Rossie. 2008. Nasal Fossa of Mouse and Dwarf Lemurs (Primates, Cheirogaleidae). Anat. Rec. 291:895–915.
Stenvinkel, P., A. Jani, and R. Johnson. 2012. Hibernating bears (Ursidae): Metabolic magicians of definite interest for the nephrologist. Kidney Int. 83.
Šumbera, R. 2019. Thermal biology of a strictly subterranean mammalian family, the African mole-rats (Bathyergidae, Rodentia) - a review. J. Therm. Biol. 79:166–189.
Upham, N. S., J. A. Esselstyn, and W. Jetz. 2019. Inferring the mammal tree: Species-level sets of phylogenies for questions in ecology, evolution, and conservation. PLOS Biol. 17:e3000494. Public Library of Science.
Valkenburgh, B. V., A. Curtis, J. X. Samuels, D. Bird, B. Fulkerson, J. Meachen-Samuels, and G. J. Slater. 2011. Aquatic adaptations in the nose of carnivorans: evidence from the turbinates. J. Anat. 218:298–310.
Valkenburgh, B. V., T. D. Smith, and B. A. Craven. 2014. Tour of a Labyrinth: Exploring the Vertebrate Nose. Anat. Rec. 297:1975–1984.
Wagner, F., and I. Ruf. 2019. Who nose the borzoi? Turbinal skeleton in a dolichocephalic dog breed (Canis lupus familiaris). Mamm. Biol. 94:106–119.
Walker, J. E. C., and R. E. Wells. 1961. Heat and water exchange in the respiratory tract. Am. J. Med. 30:259–267.
White, C. R., and R. S. Seymour. 2004. Does Basal Metabolic Rate Contain a Useful Signal? Mammalian BMR Allometry and Correlations with a Selection of Physiological, Ecological, and Life-History Variables. Physiol. Biochem. Zool. 77:929–941. The University of Chicago Press.
Wilson, D. E., T. E. Lacher Jr, and R. A. Mittermeier. 2016. Lagomorphs and rodents I Handbook of the Mammals of the World. Lynx Editions. Barcelona.
Wilz, M., and G. Heldmaier. 2000. Comparison of hibernation, estivation and daily torpor in the edible dormouse, Glis glis. J. Comp. Physiol. [B] 170:511–521.
Wislocki, G. B. 1933. Location of the Testes and Body Temperature in Mammals. Q. Rev. Biol. 8:385–396. The University of Chicago Press.
Withers, P. C., and J. U. M. Jarvis. 1980. The effect of huddling on thermoregulation and oxygen consumption for the naked mole-rat. Comp. Biochem. Physiol. A Physiol. 66:215–219.
Yee, K. K., B. A. Craven, C. J. Wysocki, and B. V. Valkenburgh. 2016. Comparative Morphology and Histology of the Nasal Fossa in Four Mammals: Gray Squirrel, Bobcat, Coyote, and White-Tailed Deer. Anat. Rec. 299:840–852.

↑ Back to summary ↑

Supplementary informations – Article 1

Electronic supplementary material (ESM) for:

Convergent evolution of an extreme dietary specialisation, the olfactory system of worm-eating rodents

Quentin Martinez[1*], Renaud Lebrun[1], Anang S. Achmadi[2], Jacob A. Esselstyn[3,4], Alistair R. Evans[5,6], Lawrence R. Heaney[7], Roberto Portela Miguez[8], Kevin C. Rowe[6,9], and Pierre-Henri Fabre[1]

[1] Institut des Sciences de l'Evolution (ISEM, UMR 5554 CNRS-IRD-UM), Université de Montpellier, Place E. Bataillon - CC 064 - 34095 Montpellier Cedex 5, France

[2] Museum Zoologicum Bogoriense, Research Center For Biology, Indonesian Institute of Sciences (LIPI), Jl.Raya Jakarta-Bogor Km.46 Cibinong 16911, Indonesia

[3] Museum of Natural Science, 119 Foster Hall, Louisiana State University, Baton Rouge, Louisiana 70803, United States

[4] Department of Biological Sciences, Louisiana State University, Baton Rouge, Louisiana 70803, United States

[5] School of Biological Sciences, 18 Innovation Walk, Monash University, Victoria 3800, Australia

[6] Sciences Department, Museums Victoria, Melbourne, Victoria, 3001, Australia

[7] Field Museum of Natural History, 1400 S Lake Shore Drive, Chicago, 60605, United States

[8] Natural History Museum, London, Department of Life Sciences, Mammal Section, United Kingdom, London

[9] School of BioSciences, The University of Melbourne, Melbourne, Victoria, 3010, Australia

*Corresponding author (quentinmartinezphoto@gmail.com).

Figure S1. Coronal cross section and sagittal plane of skull and 3D representations of turbinal bones in *Rattus norvegicus*, Rhynchomys soricoides, and *Paucidentomys vermidax*. Abbreviations: see Table S1.

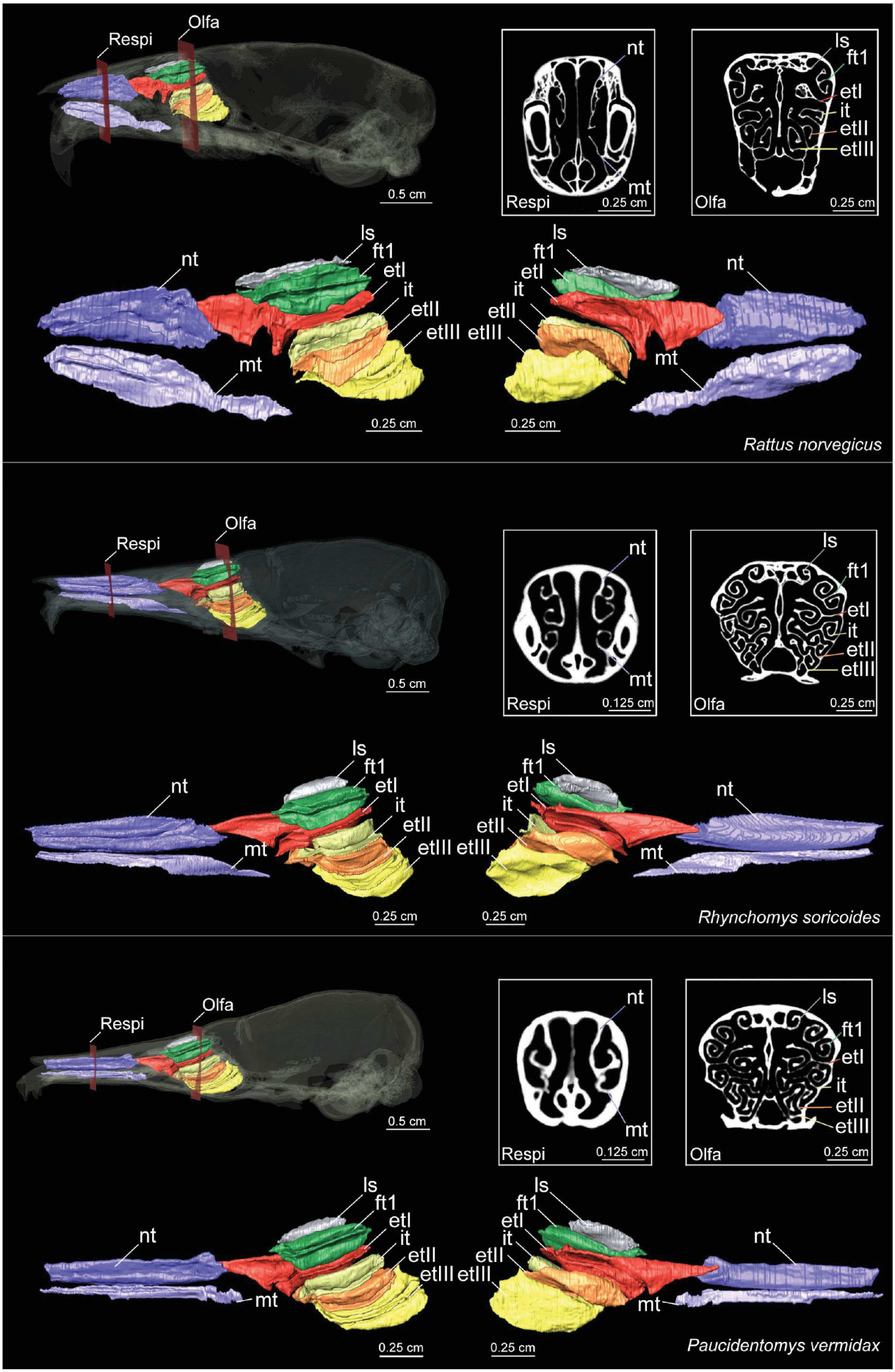

Figure S2. Coronal cross section and sagittal plane of skull and 3D representations of turbinal bones in *Sommeromys macrorhinos*, *Deomys ferrugineus*, and *Mus cervicolor*. Abbreviations: see Table S1.

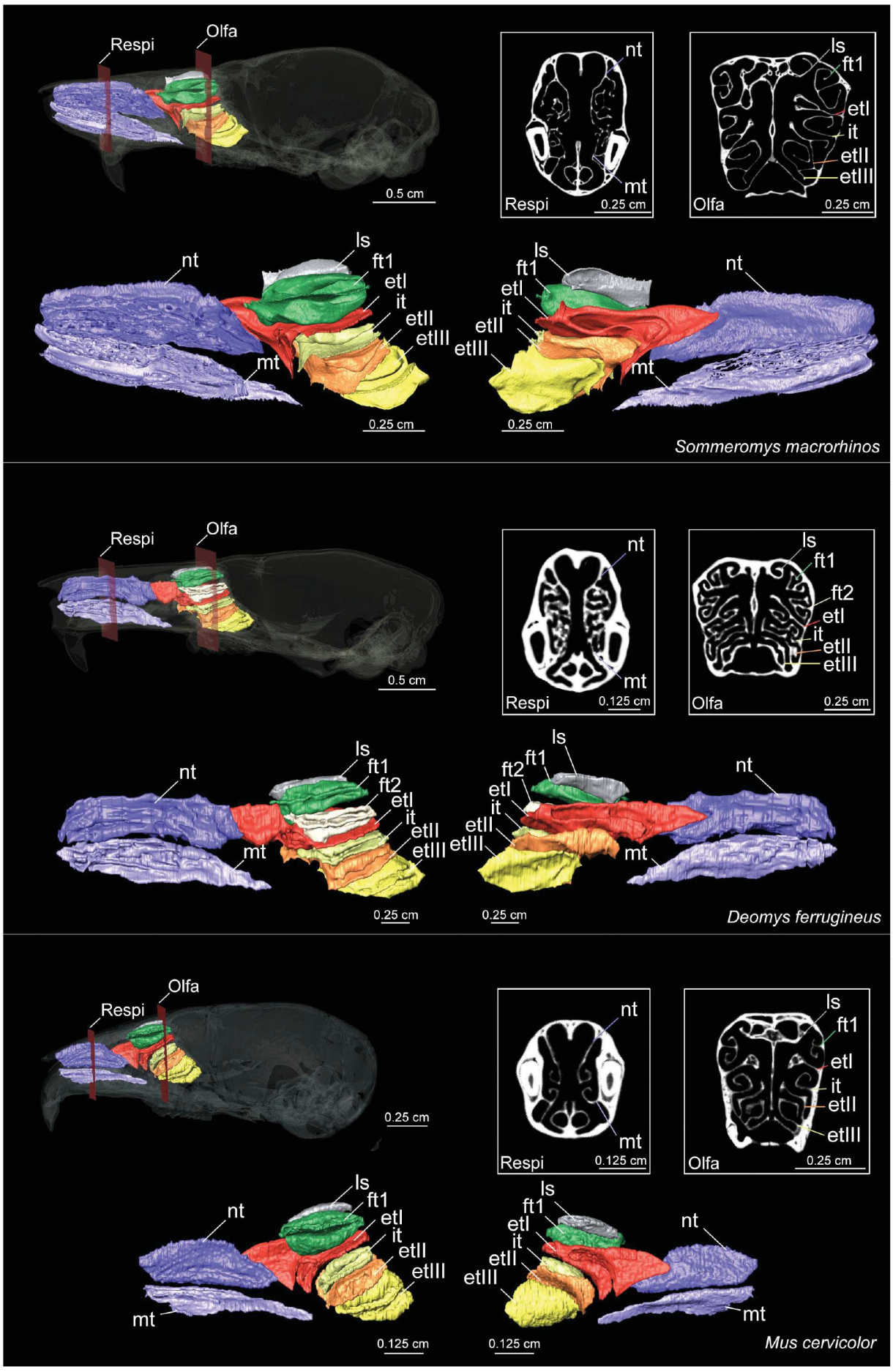

Figure S3. Linear regressions (continuous line) and PGLS (dashed line) of (A) total surface area of turbinals against skull length, (B) respiratory turbinals surface area against skull length, (C) olfactory turbinals surface area against skull length, (D) 3D respiratory complexity (CHAR) against skull length, and (E) 3D olfactory complexity (CHAR) against skull.

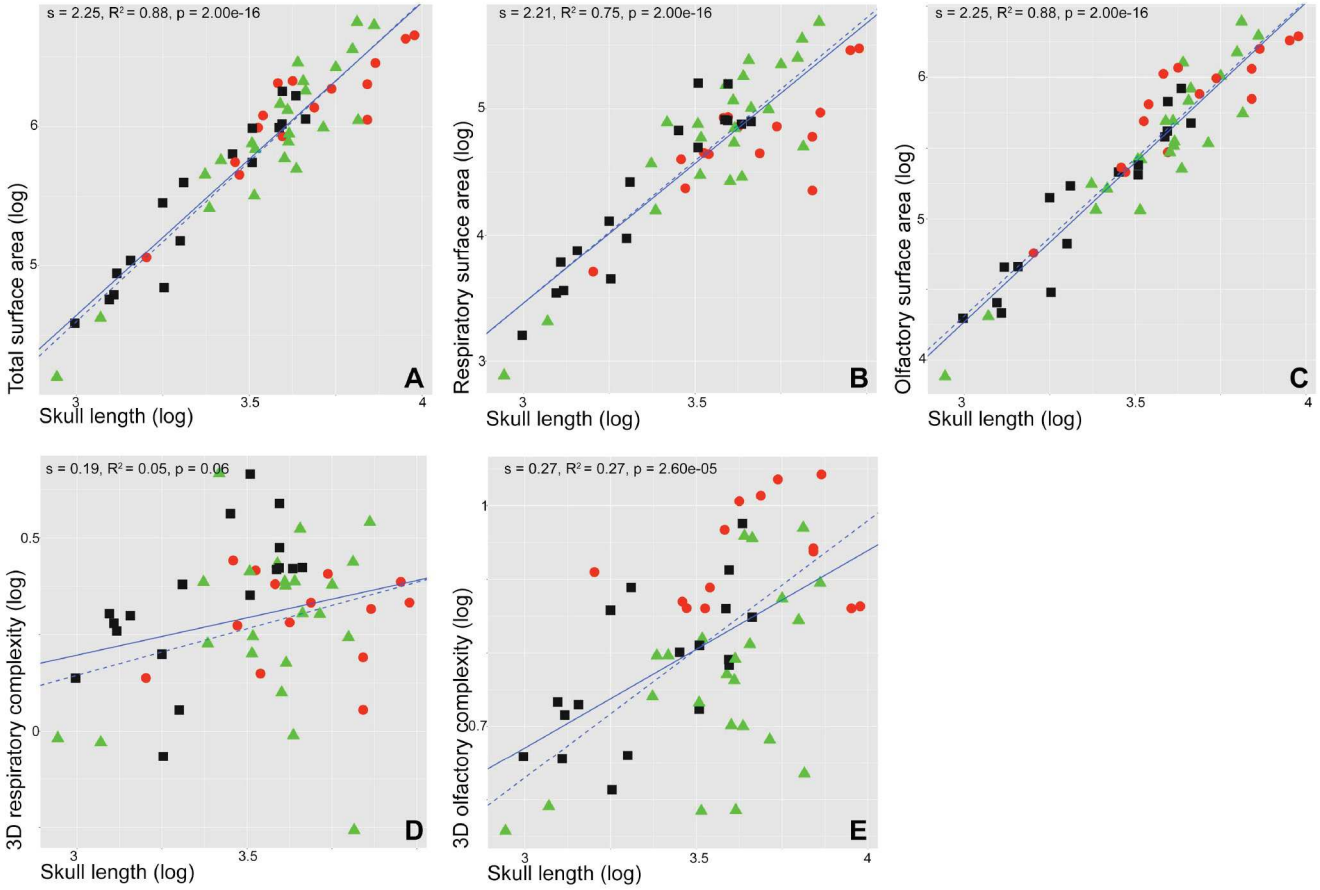

Figure S4. Boxplot with dietary categories: (A) relative nasoturbinal surface area and (B) relative maxilloturbinal surface area. Boxplot are based on PGLS residuals. Significance code are based on phylogenectic Tukey's HSD test. (i) *Rhynchomys soricoides*, (ii) *Sommeromys* macrorhinos, and (iii) *Rattus norvegicus*. Red points are outliers.

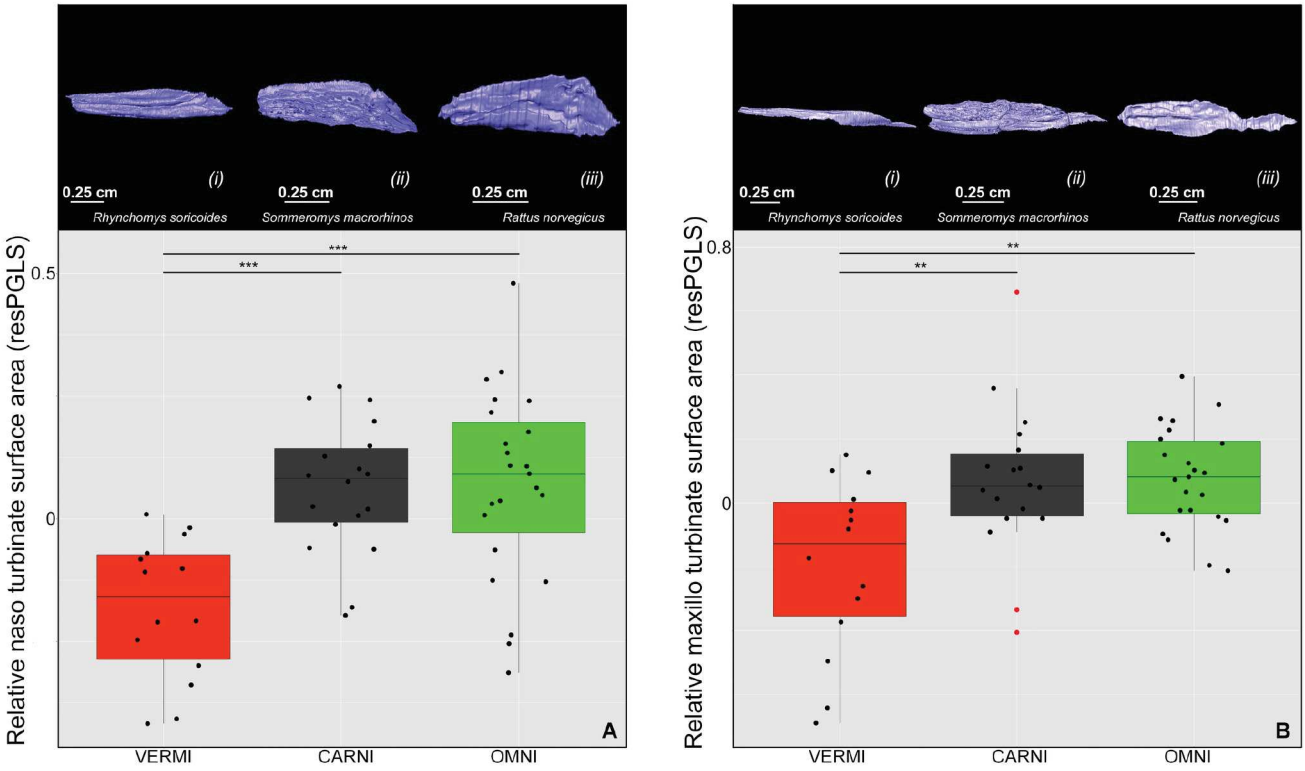

Figure S5. Boxplot of the residuals of PGLS (resPGLS) between olfactory and respiratory complexity with dietary categories: (A) 2D complexity method, (B) 3D complexity method (CHAR), and 3D complexity method (CHNSI).

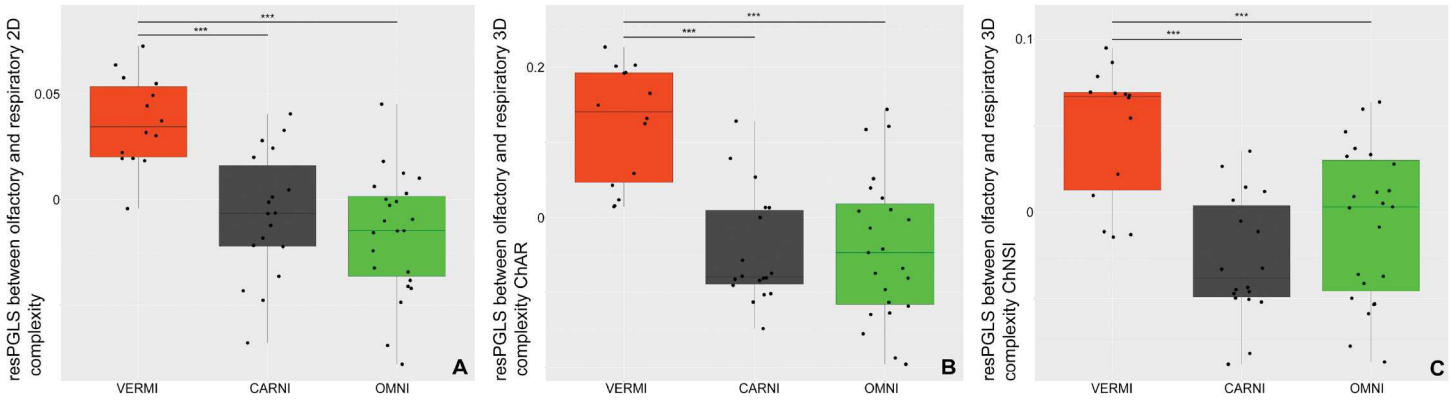

Figure S6. Boxplot of snout width (SNW) with dietary categories. Boxplot are based on PGLS residuals. Significance code are based on phylogenectic Tukey's HSD test. (i) *Rhynchomys isarogensis,* (ii) *Leptomys elegans,* (iii) *Malacomys cansdalei,* and (iiii) *Chrotomys silaceus.*

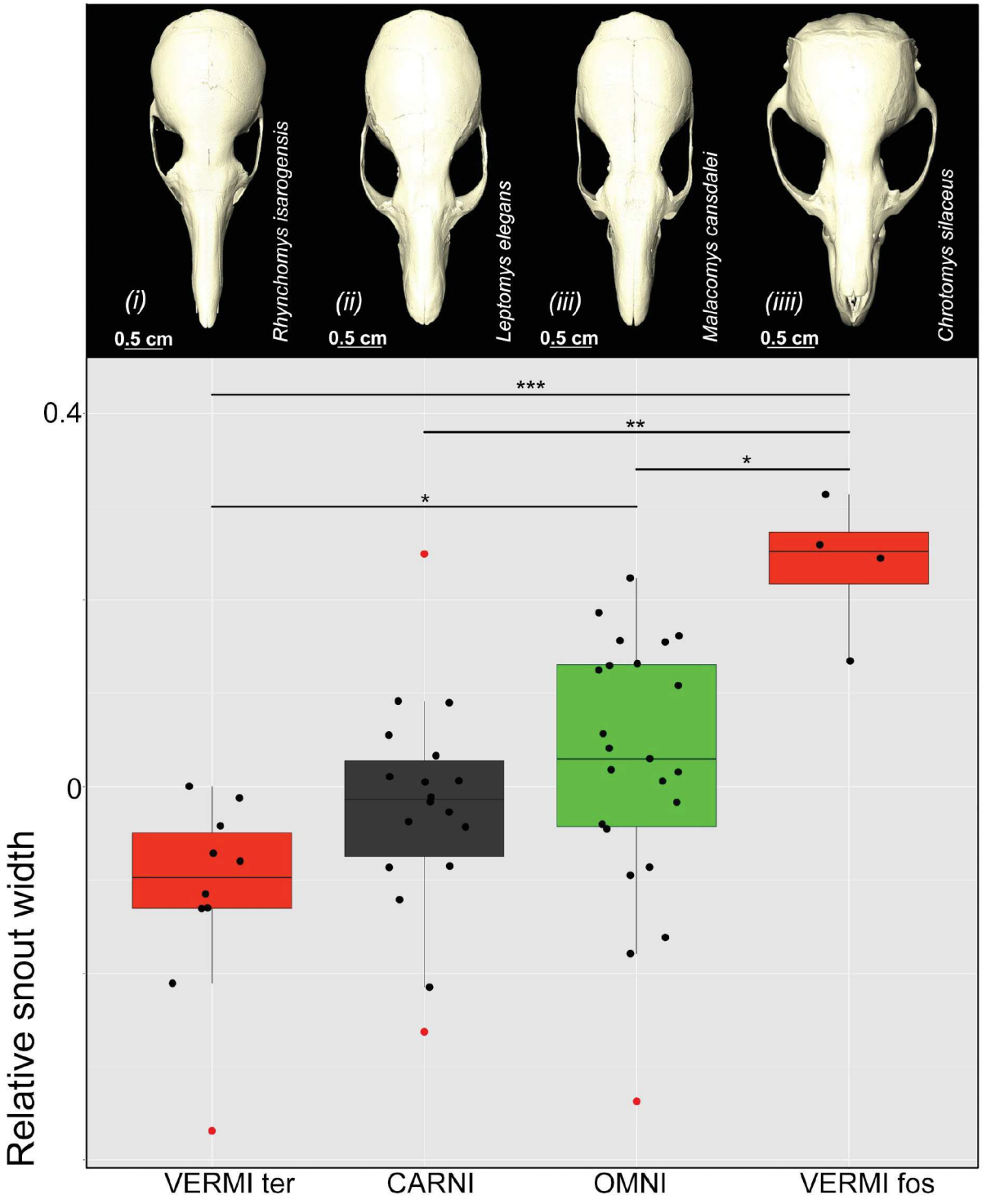

Legend S1. In order to implement phylogenetic comparative analyses to our turbinal dataset, we build a composite phylogenetic tree. Concerning the murinae we used the phylogenetic tree from Rowe et al. (2016). We subsequently used the dated tree from Steppan & Schenk (2017) for the divergence among Cricetidae and the basal split between Muridae and Cricetidae. A species of *Crunomys*, a *Malacomys*, 2 species of *Pseudohydromys*, 3 species of *Leptomys* were missing from these phylogenies. We constrained missing species to their assigned genus, thereby assuming monophyly at the genus level, respectively. We subsequently used the PASTIS R package (Thomas *et al.* 2013) to randomly incorporate them in our composite tree following Maestri *et al.* (2016) protocol.

Table S1. PGLS and linear regression results. Abbreviations: SA = surface area, TotSA = total surface area of turbinals, Relat = relative, Cor = corrected, NoCor = non-corrected, CHAR = convex hull area ratio, CHNSI = convex hull normalized shape index, Respi = respiratory, Olfa = olfactory, NT = nasoturbinal, MT = maxilloturbinal, LS = lamina semicircularis, FT1 = frontoturbinal 1, FT1 bis = frontoturbinal 1 bis, FT2 = frontoturbinal 2, ET1 = ethmoturbinal 1, ET2 = ethmoturbinal 2, and ET3 = ethmoturbinal 3, SKL = skull length, SNW = snout width, SNL = snout length, NaRe = nasoturbinal considered as respiratory turbinal, and NaOl = nasoturbinal considered as olfactory turbinal.

Variables	Slope	P-value	Signif-code	R-squared	PGLS slope	PGLS p-value
TotSA/SKL	2.25	2.00e-16	***	0.88	2.30	<0.01
RespiSA/SKL	2.21	2.00e-16	***	0.75	2.26	<0.01
OlfaSA/SKL	2.25	2.00e-16	***	0.88	2.33	<0.01
OlfaSA/RespiSA	0.86	2.00e-16	***	0.83	0.74	<0.01
OlfaSA/TotSA	0.99	2.00e-16	***	0.98	1.00	<0.01
RespiSA/TotSA	1.02	2.00e-16	***	0.92	0.99	<0.01
2DNoCorOlfa/2DNoCorRespi	0.37	2.00e-16	***	0.19	0.33	2.00E-04
2DCorOlfa/SKL	0.34	1.52e-03	**	0.16	0.25	0.08
2DCorRespi/SKL	0.28	0.03	*	0.07	0.21	0.38
2DCorOlfa/RelatOlfaSA	0.41	0.22	-	0.01	0.34	0.16
2DCorRespi/RelatRespiSA	0.48	0.01	**	0.12	0.55	4.00e-03
OlfaCHAR/RespiCHAR	0.29	7.33e-04	***	0.18	0.19	2.80e-03
OlfaCHAR/SKL	0.27	2.60e-05	***	0.27	0.35	1.00e-04
RespiCHAR/SKL	0.19	0.06	-	0.05	0.24	0.18
OlfaCHAR/OlfaSA	0.15	8.21e-10	***	0.50	0.18	<0.01
OlfaCHAR/RelatOlfaSA	0.47	0.02	*	0.08	0.14	0.36
RespiCHAR/RespiSA	0.18	5.33e-07	***	0.36	0.31	<0.01
RespiCHAR/RelatRespiSA	0.55	4.81e-06	***	0.31	0.81	<0.01
OlfaCHNSI/RespiCHNSI	0.40	6.99e-06	***	0.30	0.19	0.01
OlfaCHNSI/SKL	0.17	3.13e-09	***	0.47	0.19	<0.01
RespiCHNSI/SKL	0.15	7.42e-04	***	0.18	0.16	0.06
OlfaCHNSI/OlfaSA	0.08	5.91e-16	***	5.90e-16	0.10	<0.01
OlfaCHNSI/RelatOlfaSA	0.18	0.06	-	0.05	0.10	0.15
RespiCHNSI/RespiSA	0.09	2.55e-09	***	0.48	0.14	<0.01
RespiCHNSI/RelatRespiSA	0.19	4.78e-04	***	0.19	0.35	<0.01

Table S2. Analysis of variance (ANOVA) results for dietary variables. Abbreviations: see Table S1.

Variable	Sum Sq	Mean Sq	F value	Pr(>F)	Signif-code
OlfaSA/TotSA	0.11	0.06	13.04	2.57e-05	***
RespiSA/TotSA	0.67	0.34	15.90	4.11e-06	***
OlfaSA/RespiSA	1.42	0.71	20.57	2.62e-07	***
MT/TotSA	0.73	0.37	7.61	1.25e-03	**
NT/TotSA	0.63	0.31	11.66	6.57e-05	***
2DCorOlfa/SKL	0.66	0.33	15.54	5.11e-06	***
2DCorRespi/SKL	0.18	0.09	1.86	0.17	-
2DNoCorOlfa/2NoDCorRespi	0.03	0.01	17.50	1.54e-06	***
SNL/SKL	0.01	0.01	1.31	0.28	-
SNL/SKL_VERMI_fos_ter	0.04	0.01	3.83	0.01	*
SNW/SNL	0.02	0.01	0.57	0.57	-
SNW/SNL_VERMI_fos_ter	0.38	0.13	8.52	1.09e-04	***
OlfaCHAR/RespiCHAR	0.29	0.15	20.01	3.59e-07	***
OlfaCHAR/SKL	0.18	0.09	11.28	8.54e-05	***
RespiCHAR/SKL	0.12	0.06	2.04	0.14	-
OlfaCHNSI/RespiCHNSI	0.04	0.02	13.66	1.71e-05	***
OlfaCHNSI/SKL	0.02	0.01	6.13	4.08e-03	**
RespiCHNSI/SKL	0.01	0.01	1.32	0.27	-

Table S3. Phylogenetic Tukey's HSD results. Abbreviations: see Table S1.

Variables	Comparison	p-value	Signif-code
RespiSA/TotSA	OMNI/CARNI	0.99	-
RespiSA/TotSA	VERMI/CARNI	1.18e-05	***
RespiSA/TotSA	VERMI/OMNI	1.00e-05	***
OlfaSA/TotSA	OMNI/CARNI	0.97	-
OlfaSA/TotSA	VERMI/CARNI	9.17e-05	***
OlfaSA/TotSA	VERMI/OMNI	8.40e-05	***
OlfaSA/RespiSA	OMNI/CARNI	0.64	-
OlfaSA/RespiSA	VERMI/CARNI	1.00e-04	***
OlfaSA/RespiSA	VERMI/OMNI	1.00e-04	***
MTSA/TotSA	OMNI/CARNI	0.98	-
MTSA/TotSA	VERMI/CARNI	4.47e-03	**
MTSA/TotSA	VERMI/OMNI	1.34e-03	**
NTSA/TotSA	OMNI/CARNI	0.98	-
NTSA/TotSA	VERMI/CARNI	2.67e-04	***
NTSA/TotSA	VERMI/OMNI	2.19e-04	***
SNL/SKL	OMNI/CARNI	0.32	-
SNL/SKL	VERMIter/CARNI	0.94	-
SNL/SKL	VERMIfos/CARNI	0.04	*
SNL/SKL	VERMIter/OMNI	0.19	-
SNL/SKL	VERMIfos/OMNI	0.30	-
SNL/SKL	VERMIter/VERMIfos	0.03	*
SNW/SNL	OMNI/CARNI	0.65	-
SNW/SNL	VERMIter/CARNI	0.21	-
SNW/SNL	VERMIfos/CARNI	2.00e-03	**
SNW/SNL	VERMIter/OMNI	0.02	*
SNW/SNL	VERMIfos/OMNI	0.01	*
SNW/SNL	VERMIter/VERMIfos	6.03e-05	***
2DCorOlfa/SKL	OMNI/CARNI	2.67e-04	***
2DCorOlfa/SKL	VERMI/CARNI	0.31	-
2DCorOlfa/SKL	VERMI/OMNI	1.00e-04	***
2DCorRespi/SKL	OMNI/CARNI	0.07	-
2DCorRespi/SKL	VERMI/CARNI	0.29	-
2DCorRespi/SKL	VERMI/OMNI	0.88	-
2DNoCorOlfa/2NoDCorRespi	OMNI/CARNI	0.52	-
2DNoCorOlfa/2NoDCorRespi	VERMI/CARNI	1.00e-04	***
2DNoCorOlfa/2NoDCorRespi	VERMI/OMNI	1.00e-04	***
OlfaCHAR/RespiCHAR	OMNI/CARNI	0.99	-
OlfaCHAR/RespiCHAR	VERMI/CARNI	2.70e-06	***
OlfaCHAR/RespiCHAR	VERMI/OMNI	1.60e-06	***
OlfaCHAR/SKL	OMNI/CARNI	0.05	*
OlfaCHAR/SKL	VERMI/CARNI	0.06	-
OlfaCHAR/SKL	VERMI/OMNI	5.42e-05	***
OlfaCHNSI/RespiCHNSI	OMNI/CARNI	0.25	-
OlfaCHNSI/RespiCHNSI	VERMI/CARNI	1.36e-05	***
OlfaCHNSI/RespiCHNSI	VERMI/OMNI	8.26e-04	***
OlfaCHNSI/SKL	OMNI/CARNI	0.39	
OlfaCHNSI/SKL	VERMI/CARNI	0.09	-
OlfaCHNSI/SKL	VERMI/OMNI	2.73e-03	**

Table S4. Phylogenetic Tukey's HSD differences between considering the nasoturbinal whether as olfactory whether as respiratory turbinals. Abbreviations: see Table S1.

Variables	Comparison	NaRe p-value	NaOl p-value
RespiSA/TotSA	OMNI/CARNI	0.76	0.83
RespiSA/TotSA	VERMI/CARNI	0.01	0.03
RespiSA/TotSA	VERMI/OMNI	0.00	0.00
OlfaSA/TotSA	OMNI/CARNI	0.90	1.00
OlfaSA/TotSA	VERMI/CARNI	0.01	0.03
OlfaSA/TotSA	VERMI/OMNI	0.00	0.04
OlfaSA/RespiSA	OMNI/CARNI	0.86	0.75
OlfaSA/RespiSA	VERMI/CARNI	0.00	0.00
OlfaSA/RespiSA	VERMI/OMNI	0.00	0.00

Table S5. Comparison between the results of phylogenetic Tukey's HSD and non-phylogenetic Tukey's HSD. Abbreviations: see Table S1.

Variables	Comparison	PhyloTukey p-value	Tukey p-value
RespiSA/TotSA	OMNI/CARNI	0.76	0.94
RespiSA/TotSA	VERMI/CARNI	0.01	0.00
RespiSA/TotSA	VERMI/OMNI	0.00	0.00
OlfaSA/TotSA	OMNI/CARNI	0.90	0.98
OlfaSA/TotSA	VERMI/CARNI	0.01	0.00
OlfaSA/TotSA	VERMI/OMNI	0.00	0.00
OlfaSA/RespiSA	OMNI/CARNI	0.86	0.44
OlfaSA/RespiSA	VERMI/CARNI	0.00	0.00
OlfaSA/RespiSA	VERMI/OMNI	0.00	0.00

Table S6. Results of phylogenetic ANCOVA. Three models were contrasted: a model without dietary categories (H0), a model with omnivorous and carnivorous dietary categories (Carni), and a model with omnivorous, carnivorous, and vermivorous dietary categories (Vermi). Model were compared using the Akaike information criterion (AIC) and the Likelihood-ratio test.

	AIC	**Lr test likelihood**	**Lr test p-value**		
	RespiSA/TotSA		H0	Carni	Vermi
H0	512.34	-253.17	-	2.12e-04	6.02e-09
Carni	499.42	-244.71	-	-	8.46e-07
Vermi	477.17	-232.58	-	-	-

	AIC	**Lr test likelihood**	**Lr test p-value**		
	OlfaSA/TotSA		H0	Carni	Vermi
H0	512.34	-253.17	-	2.12e-04	6.02e-09
Carni	499.42	-244.71	-	-	8.46e-07
Vermi	477.17	-232.58	-	-	-

	AIC	**Lr test likelihood**	**Lr test p-value**		
	OlfaSA/RespiSA		H0	Carni	Vermi
H0	636.07	-315.03	-	3.20e-06	2.06e-12
Carni	614.76	-302.38	-	-	1.43e-08
Vermi	584.62	-286.31	-	-	-

	AIC	**Lr test likelihood**	**Lr test p-value**		
	RespiSKL		H0	Carni	Vermi
H0	565.52	-279.76	-	1.55e-05	5.06e-09
Carni	591.67	-290.84	-	-	1.47e-15
Vermi	530.00	-259.00	-	-	-

	AIC	**Lr test likelihood**	**Lr test p-value**		
	OlfaSKL		H0	Carni	Vermi
H0	636.07	-315.03	-	3.10e-11	2.48e-12
Carni	591.67	-290.84	-	-	3.22e-03
Vermi	585.00	-286.50	-	-	-

	AIC	**Lr test likelihood**	**Lr test p-value**		
	OlfaCHAR/RespiCHAR		H0	Carni	Vermi
H0	59.32	-26.66	-	9.84e-13	4.98e-14
Carni	8.03	0.99	-	-	1.82e-03
Vermi	0.31	5.85	-	-	-

Table S7. Results of 1.000 simulations of single-rate BM and three alternative OU models with the ratio between snout width (SNW) and snout length (SNL). BM and OU1 with omnivorous and all carnivorous dietary categories (carnivorous + vermivorous); OU2 with omnivorous, carnivorous, and vermivorous dietary categories; and OU3 with omnivorous, carnivorous, terrestrial vermivorous, and semi-fossorial vermivorous dietary categories. AICc = Akaike's information criterion corrected. ΔAICc = difference between AICc compared to minimum AICc.

	SNW/SNL	
Model	AICc	ΔAICc
BM	-90.22	27.60
OU1	-104.65	13.17
OU2	-104.60	13.21
OU3	-117.82	00.00

Table S8. Dataset used for quantitative analyses. Abbreviations: see Table S1. American Museum of Natural History (AMNH), Centre de Biologie et de Gestion des Populations (CBGP), Field Museum of Natural History (FMNH), Museums Victoria (NMV), Museum Zoologicum Bogoriense (MZB), Natural History Museum London (NHMUK previously BMNH), Natural History Museum of Paris (MNHN), Smithsonian Institution National Museum of Natural History (NMNH), and University of Montpellier (UM).

Taxa	MUSEUM	VOUCHER	Taxa_2	DIET	Sexe	mtSA	ntSA	lsSA	ft1SA	etlSA	ft2SA	etllSA	etlIISA	TotSA	SKL	SNL	SNW	2DRespi	2DOlfa	2DCorRespi	2DCorOlfa	ChARRespi	ChAROlfa	ChNSIRespi	ChNSIOlfa
Apomys_abrae	AMNH	242099,00	APOabra	OMNI	-	45,86	112,45	25,73	54,49	73,22	36,87	50,99	54,84	454,45	37,00	13,40	6,09	1,47	1,52	2498,64	3683,00	1,47	2,14	1,54	1,72
Apomys_banahao	CBGP	P0045	APObana	OMNI	-	71,18	93,17	22,40	55,86	84,52	40,42	50,63	62,37	480,56	36,51	13,08	6,50	1,53	1,53	2768,21	4242,00	1,48	2,29	1,59	1,76
Apomys_banahao	CBGP	P0067	APObana	OMNI	-	51,74	82,52	21,15	41,47	66,34	32,26	35,17	43,19	373,83	33,74	12,16	5,65	-	-	-	-	1,48	2,03	1,55	1,63
Apomys_banahao	CBGP	P0066	APObana	OMNI	-	95,83	141,24	27,78	60,51	89,26	39,57	43,07	71,20	568,47	38,38	13,30	6,81	-	-	-	-	1,67	2,17	1,66	1,70
Apomys_datae	FMNH	252475,00	APOdata	OMNI	F	57,64	143,09	42,91	80,95	126,60	60,02	69,49	88,33	669,03	38,48	14,26	7,62	1,56	1,56	3277,09	5127,00	1,62	2,74	1,65	1,89
Apomys_datae	FMNH	188256,00	APOdata	OMNI	M	72,04	110,79	31,89	82,47	117,05	55,07	59,41	80,02	608,73	37,73	13,95	6,54	-	-	-	-	1,32	2,48	1,49	1,83
Apomys_hylocetes	USNM	125244,00	APOhylo	OMNI	F	39,44	93,68	13,59	32,53	54,47	18,96	28,01	36,11	316,78	30,51	11,02	5,40	1,48	1,46	2500,00	3709,00	1,95	2,22	1,84	1,71
Apomys_littoralis	USNM	458755,00	APOlitt	OMNI	M	35,44	60,65	13,42	32,47	58,77	20,12	29,07	35,99	285,94	29,14	9,34	5,21	1,46	1,42	2191,68	3197,00	1,47	2,10	1,58	1,69
Archboldomys_luzonensis	USNM	573840,00	ARCluzo	INSEC	F	33,27	48,03	15,44	38,81	52,07	19,01	26,29	33,29	266,21	26,67	9,10	5,13	1,46	1,53	2695,39	3935,00	1,51	2,45	1,58	1,79
Archboldomys_luzonensis	USNM	573837,00	ARCluzo	INSEC	M	32,78	52,09	12,07	38,71	54,39	19,37	27,30	37,88	274,58	28,10	9,90	4,93	-	-	-	-	1,42	2,42	1,56	1,79
Bunomys_andrewsi	NMV	36977,00	BUNandr	OMNI	-	62,54	132,80	21,63	59,70	80,96	45,31	50,49	66,65	520,08	36,68	15,55	6,63	1,43	1,46	2083,80	2979,00	1,68	2,32	1,72	1,77
Bunomys_andrewsi	NMV	36982,00	BUNandr	OMNI	-	88,70	150,71	34,02	64,89	100,92	43,97	53,13	61,15	597,48	40,75	16,13	7,04	-	-	-	-	1,70	2,18	1,74	1,72
Bunomys_penitus	NMV	36984,00	BUNpeni	OMNI	-	77,80	179,94	42,61	105,51	137,21	86,21	115,81	109,92	855,00	45,23	18,67	8,31	1,53	1,58	2296,93	3512,00	1,55	2,64	1,67	1,86
Chrotomys_gonzalesi	USNM	458955,00	CHRgonz	WORM	F	50,11	53,48	24,36	80,38	78,84	37,79	51,63	60,37	436,95	34,45	12,00	7,49	1,36	1,52	2238,40	3044,00	1,16	2,43	1,43	1,80
Chrotomys_mindorensis	FMNH	222107,00	CHRmind	WORM	F	43,34	85,29	38,74	94,64	91,61	49,60	70,22	86,33	559,77	37,54	12,52	8,19	1,36	1,55	2010,33	2725,00	1,32	2,74	1,50	1,88
Chrotomys_silaceus	NHMUK	97.5.2.16	CHRsila	WORM	M	47,19	61,08	24,81	68,76	75,60	38,55	51,14	49,98	417,10	34,62	11,06	6,91	1,48	1,53	2644,03	3924,00	1,50	2,33	1,58	1,71
Chrotomys_silaceus	NHMUK	97.5.2.39	CHRsila	WORM	F	41,72	59,29	18,89	56,20	61,89	37,46	51,64	56,79	383,87	33,31	11,21	6,02	-	-	-	-	1,53	2,40	1,63	1,77
Chrotomys_whiteadi	NHMUK	95.8.2.20	CHRwhit	WORM	F	49,03	76,45	28,03	82,65	105,97	51,56	62,95	90,61	547,26	35,29	12,30	7,68	1,42	1,60	2683,92	3805,00	1,57	2,88	1,62	1,95
Chrotomys_whiteadi	NHMUK	95.8.2.19	CHRwhit	WORM	M	64,47	85,89	38,71	94,05	92,76	56,15	67,34	91,50	590,87	36,84	12,12	7,59	-	-	-	-	1,44	2,53	1,55	1,85
Chrotomys_whiteadi	NHMUK	97.5.2.17	CHRwhit	WORM	F	57,88	80,57	33,00	80,92	83,95	47,17	53,42	79,17	516,08	35,78	12,24	7,73	-	-	-	-	1,38	2,48	1,56	1,82
Crunomys_fallax	NHMUK	97.4.8.4	CRUfall	INSEC	-	15,78	22,72	9,17	16,24	24,17	9,69	12,78	16,09	126,63	25,89	8,82	4,06	1,28	1,43	1256,45	1606,00	0,94	1,85	1,35	1,56
Crunomys_melanius	NHMUK	7.2.2.14	CRUmela	INSEC	M	23,39	29,81	8,93	23,20	35,78	13,63	19,14	24,01	177,89	27,12	9,24	6,61	1,37	1,39	1841,28	2515,00	1,06	1,94	1,38	1,57
Deomys_ferrugineus	MNHN	1620,00	DEOferr	INSEC	-	46,18	100,29	13,22	24,11	79,92	29,51	39,54	41,62	374,38	37,05	16,04	5,22	1,45	1,56	2271,12	3282,00	1,62	2,23	1,62	1,73
Deomys_ferrugineus	MNHN	1622,00	DEOferr	INSEC	-	49,53	81,63	14,48	23,50	63,38	22,92	36,12	34,94	326,49	35,84	15,29	5,07	-	-	-	-	1,60	2,15	1,61	1,70
Echiothrix_centrosa	NHMUK	40.385	ECHcent	WORM	F	95,13	152,01	39,44	106,40	142,58	62,49	81,37	112,51	791,92	51,82	21,44	7,19	1,45	1,55	2520,53	3653,00	1,54	2,32	1,71	1,83
Echiothrix_centrosa	AMNH	153013,00	ECHcent	WORM	M	91,34	132,22	42,59	93,33	143,38	56,80	70,30	94,85	724,82	52,29	22,83	6,75	-	-	-	-	1,40	2,41	1,63	1,83
Echiothrix_leucura	NHMUK	97.1.2.46	ECHleuc	WORM	M	96,81	159,22	46,65	101,20	152,26	55,06	82,46	90,03	783,69	53,68	22,50	6,95	1,43	1,56	2420,25	3452,00	1,39	2,36	1,68	1,82
Echiothrix_leucura	NHMUK	97.1.2.45	ECHleuc	WORM	M	93,01	128,75	41,30	107,86	126,19	68,16	86,23	119,37	770,86	53,13	22,54	7,12	-	-	-	-	1,40	2,38	1,66	1,80
Gracilimus_radix	NMV	36995,00	GRAradi	OMNI	-	24,73	41,67	12,16	29,49	54,12	17,93	24,24	20,35	224,69	29,51	10,00	5,12	1,38	1,47	1876,77	2583,00	1,25	2,22	1,43	1,68
Halmaheramys_bokimekot	MZB	33266,00	HALboki	OMNI	-	116,12	178,48	50,38	103,91	149,48	68,35	85,72	82,56	834,99	47,52	18,26	8,43	1,49	1,53	2475,95	3681,00	1,72	2,45	1,71	1,83
Hyorhinomys_stuempkei	NMV	C37198	HYOstue	WORM	-	45,62	73,22	24,02	82,33	98,39	58,87	73,39	91,13	546,97	46,59	18,35	7,15	1,29	1,49	1898,19	2450,00	1,21	2,57	1,45	1,80
Leptomys_arfakensis	NHMUK	29.5.27.22	LEParf	INSEC	F	47,48	86,64	21,57	53,28	81,39	38,61	46,87	50,30	426,14	38,98	14,31	6,43	1,44	1,56	2234,15	3225,00	1,53	2,34	1,53	1,75
Leptomys_elegans	NHMUK	5.11.28.22	LEPeleg	INSEC	M	51,69	91,06	26,38	49,94	71,44	35,71	41,03	54,68	421,91	36,79	13,93	6,32	1,50	1,52	2490,17	3738,00	1,55	2,19	1,62	1,76
Leptomys_elegans	NHMUK	50.1254	LEPeleg	INSEC	M	51,95	75,32	27,63	47,17	66,37	34,68	41,22	55,87	400,20	36,01	12,74	6,17	-	-	-	-	1,50	2,22	1,56	1,74
Leptomys_ernstmayri	NHMUK	50.1252	LEPerns	INSEC	M	60,87	92,89	26,08	56,28	76,00	42,67	44,16	49,29	448,22	36,67	13,70	6,30	1,48	1,54	2848,95	4221,00	1,64	2,46	1,60	1,79
Leptomys_ernstmayri	AMNH	190936,00	LEPerns	INSEC	F	46,29	71,36	24,83	41,69	59,80	29,08	35,72	44,07	353,33	35,55	11,91	6,22	-	-	-	-	1,40	2,26	1,51	1,73
Leptomys_signatus	AMNH	105370,00	LEPsign	INSEC	F	44,43	64,80	17,93	32,67	56,63	26,42	30,50	38,62	312,00	33,40	12,02	5,62	1,46	1,47	2384,04	3490,00	1,42	2,06	1,54	1,66
Malacomys_cansdalei	USNM	486151,00	MALcans	OMNI	M	57,40	91,74	29,17	78,86	84,95	42,11	62,43	74,79	521,46	38,98	15,14	6,70	1,41	1,58	2271,92	3210,00	1,36	2,60	1,62	1,88
Malacomys_edwardsi	USNM	467226,00	MALedwa	OMNI	F	37,65	80,22	15,26	50,81	61,99	21,35	31,80	44,34	343,43	33,69	13,41	5,18	1,45	1,54	2206,53	3203,00	1,28	2,27	1,53	1,78
Maxomys_musschenbroekii	NMV	37009,00	MAXmuss	OMNI	-	89,41	121,07	26,45	77,42	102,55	41,92	62,22	96,41	617,44	42,53	16,11	6,17	1,48	1,55	2262,00	3355,00	1,46	2,40	1,56	1,82
Maxomys_surifer	CBGP	6369,00	MAXsuri	OMNI	F	117,11	91,74	35,17	87,11	109,53	52,84	67,63	90,47	651,60	44,98	16,59	7,50	1,46	1,49	2493,32	3641,00	1,38	2,14	1,61	1,73
Maxomys_surifer	CBGP	C0119	MAXsuri	OMNI	F	115,37	119,17	39,25	108,19	137,39	53,23	81,92	98,94	753,47	44,29	17,64	7,30	1,33	1,47	1986,61	2640,00	1,17	2,52	1,50	1,86
Mayermys_ellermani	AMNH	53278,00	MAYelle	INSEC	M	11,77	18,40	6,14	14,23	19,11	8,45	11,68	10,37	100,15	21,40	6,84	4,54	1,33	1,47	1986,61		1,39	2,00	1,48	1,59
Mayermys_ellermani	NHMUK	53280,00	MAYelle	INSEC	M	16,30	22,38	6,82	19,28	25,57	13,02	14,40	14,55	132,32	22,79	6,58	5,08	-	-	-	-	1,32	2,16	1,46	1,65
Melasmothrix_naso	AMNH	225092,00	MELnaso	WORM	F	32,23	45,41	14,56	39,27	47,34	24,26	28,20	37,01	268,29	31,87	11,49	5,29	1,44	1,55	2426,67	3483,00	1,29	2,28	1,57	1,70
Melasmothrix_naso	AMNH	225101,00	MELnaso	WORM	M	30,17	50,35	18,44	48,13	48,91	29,94	34,06	43,01	303,01	32,50	12,59	5,18	-	-	-	-	1,34	2,45	1,60	1,76
Melomys_burtoni	MZBM	33533,00	MELburt	OMNI	M	53,59	99,89	18,23	50,88	58,27	24,89	34,72	53,77	394,25	34,23	10,97	7,14	1,47	1,47	2285,68	3354,00	1,62	2,07	1,39	1,69
Melomys_burtoni	MZBM	33552,00	MELburt	OMNI	M	41,35	67,88	18,06	46,42	51,18	19,97	27,58	48,18	320,62	32,53	10,34	5,79	-	-	-	-	1,40	2,09	1,51	1,72
Melomys_obiensis	MZB	YS394	MELobie	OMNI	-	37,06	50,77	15,71	31,96	32,59	18,73	22,56	36,30	245,66	33,60	10,19	4,60	1,38	1,44	1957,81	2710,00	1,22	1,79	1,51	1,59
Microhydromys_richardsoni	AMNH	198790,00	MICrich	INSEC	M	10,74	13,92	6,31	13,65	17,89	9,90	11,63	14,01	98,04	20,00	6,26	4,20	1,33	1,47	1703,44	2270,00	1,15	1,93	1,41	1,58
Mus_cervicolor	CBGP	7314,00	MUScerv	OMNI	M	11,91	15,54	5,47	14,79	18,78	7,54	8,85	18,89	101,77	21,54	7,25	4,19	1,32	1,41	1492,22	1966,00	0,97	1,81	1,34	1,55
Mus_pahari	CBGP	7226,00	MUSpaha	INSEC	-	25,81	35,12	18,50	39,10	37,61	18,78	22,19	36,29	233,40	25,78	9,54	4,80	1,40	1,55	1753,60	2461,00	1,22	2,36	1,56	1,75
Nannomys_minutoides	UM	–	NANminu	OMNI	F	6,55	11,37	3,90	8,14	11,92	3,91	7,48	13,27	66,55	18,98	6,69	3,09	1,28	1,35	1384,58	1776,00	0,98	1,75	1,33	1,54
Oxymycterus_dasytrichus	MNHN	CG1468NZ002	OXYdasy	INSEC	-	37,93	93,26	25,30	50,03	88,44	40,81	53,83	66,45	456,06	37,89	15,18	6,05	1,48	1,57	2882,11	4271,00	1,52	2,65	1,68	1,86
Oxymycterus_quaestor	MNHN	272,00	OXYquae	INSEC	-	55,83	124,73	22,21	46,87	88,37	39,28	50,28	50,04	477,62	36,44	13,29	6,76	1,40	1,57	2145,41	3004,00	1,80	2,49	1,70	1,79
Paraleptomys_wilhelmina	AMNH	150546,00	PARwilh	INSEC	F	57,60	74,97	17,80	42,13	55,68	26,06	33,33	41,38	348,95	31,62	11,87	5,55	1,48	1,50	3054,22	4512,00	1,90	2,33	1,71	1,74
Paraleptomys_wilhelmina	AMNH	150536,00	PARwilh	INSEC	M	51,18	66,10	11,64	38,81	49,72	26,21	31,53	38,95	314,13	31,47	10,82	5,67	-	-	-	-	1,61	2,13	1,61	1,67
Paucidentomys_vermidax	FMNH	213102,00	PAUverm	WORM	-	30,11	61,40	23,37	58,34	102,36	57,30	64,13	90,87	487,88	53,37	21,50	5,73	1,33	1,59	2013,04	2687,00	0,94	2,50	1,37	1,82
Paucidentomys_vermidax	MZB	35001,00	PAUverm	WORM	-	21,62	45,13	19,46	53,52	79,97	44,82	54,04	69,93	388,50	42,26	17,30	4,96	-	-	-	-	1,16	2,60	1,56	1,88
Paucidentomys_vermidax	NMV	HH766	PAUverm	WORM	-	24,35	50,44	19,47	47,67	72,53	48,15	55,21	77,46	395,29	44,16	17,93	4,55	-	-	-	-	1,07	2,56	1,49	1,86
Pseudohydromys_ekanorae	NHMUK	50.1734	PSEelea	INSEC	F	18,39	25,56	7,33	12,66	21,41	10,48	12,89	11,36	120,08	22,39	7,42	4,65	1,37	1,42	2059,68	2823,00	1,32	1,93	1,47	1,55
Pseudohydromys_fuscus	NHMUK	53.296	PSEfusc	INSEC	M	19,31	28,79	9,20	25,30	33,70	10,50	19,30	23,00	169,10	23,92	8,30	5,13	1,44	1,46	2286,55	3302,00	1,32	2,18	1,50	1,67
Pseudohydromys_fuscus	NHMUK	501.733	PSEfusc	INSEC	M	18,44	29,80	8,04	16,72	23,98	10,84	15,01	15,50	138,32	23,06	7,65	4,19	-	-	-	-	1,43	2,00	1,53	1,61
Pseudohydromys_murinus	NHMUK	53.290	PSEmuri	INSEC	F	11,88	23,17	9,30	19,12	30,93	12,61	17,54	15,68	140,23	22,57	6,90	4,71	1,35	1,45	1763,01	2382,00	1,30	2,05	1,42	1,62
Rattus_marmosurus	NMV	37018,00	RATmarm	OMNI	-	52,67	57,23	31,67	48,28	88,67	33,32	51,49	58,98	422,30	45,38	15,75	8,39	-	-	-	-	0,77	1,89	1,22	1,62
Rattus_morotaiensis	MZB	33229,00	RATmoro	OMNI	F	48,40	78,74	21,88	44,03	71,04	29,49	34,87	54,81	383,27	37,16	12,39	6,75	1,41	1,48	1664,89	2343,00	1,19	1,80	1,53	1,65
Rattus_norvegicus	CBGP	C0304	RATnorv	OMNI	M	38,80	47,79	16,51	30,78	51,76	31,74	34,42	46,00	297,79	37,95	12,70	6,88	1,34	1,49	1690,10	2272,00	0,99	2,01	1,40	1,67
Rattus_praetor	CBGP	-	RATprae	OMNI	-	55,63	92,05	23,12	47,66	95,30	27,36	32,94	26,46	400,52	41,02	14,20	7,68	1,41	1,49	2080,65	2941,00	1,35	1,98	1,55	1,65
Rattus_tanezumi	CBGP	R5422	RATtane	OMNI	F	42,37	70,92	16,96	40,14	75,38	26,89	38,30	50,74	361,69	37,09	13,06	6,30	1,39	1,50	2081,78	2897,00	1,46	2,21	1,60	1,78
Rhynchomys_isarogensis	USNM	573576,00	RHYisar	WORM	M	31,54	80,86	17,16	46,29	80,29	41,99	54,23	70,10	422,47	39,24	15,77	6,50	1,44	1,59	2767,72	3975,00	1,56	2,68	1,69	1,84
Rhynchomys_isarogensis	USNM	573585,00	RHYisar	WORM	M	40,66	98,02	24,71	76,79	119,08	71,19	78,65	102,74	611,84	43,85	17,16	7,18	-	-	-	-	1,44	3,02	1,66	1,96
Rhynchomys_isarogensis	FMNH	573913,00	RHYisar	WORM	M	36,87	98,84	27,58	64,62	106,67	58,57	63,64	97,24	554,02	42,93	16,83	6,98	-	-	-	-	1,50	2,75	1,67	1,87
Rhynchomys_soricoides	NHMUK	95.8.2.18	RHYsori	WORM	M	35,07	91,22	21,90	60,24	95,80	53,69	67,30	75,87	501,09	45,25	17,69	6,82	1,36	1,58	1887,43	2572,00	1,31	2,63	1,63	1,86
Rhynchomys_soricoides	NHMUK	97.5.2.18	RHYsori	WORM	M	38,10	128,98	37,71	100,52	161,78	73,10	91,00	119,72	750,92	48,69	19,46	7,31	-	-	-	-	1,43	3,08	1,74	2,02
Rhynchomys_soricoides	FMNH	193833,00	RHYsori	WORM	F	31,63	97,66	24,63	83,05	110,40	60,88	67,45	107,07	582,76	48,58	19,72	6,25	-	-	-	-	1,34	2,72	1,67	1,92
Rhynchomys_soricoides	NHMUK	95.8.2.17	RHYsori	WORM	M	38,30	114,72	29,58	99,90	143,69	71,95	86,70	127,29	712,12	48,24	19,55	7,12	-	-	-	-	1,41	2,92	1,68	1,97
Sigmodon_hispidus	MNHN	CG2007N335	SIGhisp	OMNI	-	38,14	45,59	12,51	32,67	75,33	21,20	30,43	40,74	296,61	36,67	13,40	7,28	1,34	1,43	1477,09	1979,00	1,11	2,02	1,37	1,66
Sommeromys_macrorhinus	NMV	KCR2644	SOMmacr	INSEC	-	91,09	93,97	16,48	48,25	53,70	22,76	27,44	45,22	398,91	33,37	13,03	5,27	1,51	1,54	2936,30	4425,00	2,03	2,28	1,84	1,72
Sommeromys_macrorhinus	NMV	37074,00	SOMmacr	INSEC	-	75,86	79,84	16,41	36,97	38,70	18,95	20,12	35,56	322,41	31,94	12,30	5,23	-	-	-	-	1,85	2,10	1,75	1,63
Sommeromys_macrorhinus	AMNH	M226956	SOMmacr	INSEC	M	77,99	109,36	19,34	53,91	72,19	31,13	39,05	56,11	459,08	35,07	13,35	5,72	-	-	-	-	1,85	2,39	1,77	1,76
Sommeromys_macrorhinus	NMV	KCR2596	SOMmacr	INSEC	-	105,82	92,89	16,25	50,93	54,00	22,34	27,04	45,58	414,85	33,29	11,84	5,09	-	-	-	-	2,04	2,22	1,84	1,70
Soricomys_leonardocoi	FMNH	190966,00	SORleon	WORM	F	15,59	25,13	8,74	24,40	31,06	12,57	17,87	21,89	157,25	24,60	7,83	4,55	1,37	1,54	1446,52	1980,00	1,15	2,48	1,37	1,77
Tateomys_macrocercus	AMNH	225073,00	TATmacr	WORM	F	43,04	61,86	20,19	39,24	51,62	24,43	30,55	43,83	314,76	30,65	10,73	5,28	1,42	1,57	2304,43	3261,00	1,66	2,47	1,67	1,77
Tateomys_macrocercus	AMNH	225072,00	TATmacr	WORM	F	44,58	58,75	18,66	42,76	51,51	26,38	31,43	42,85	316,92	32,29	11,42	5,34	-	-	-	-	1,46	2,28	1,60	1,71
Tateomys_macrocercus	NMV	37081,00	TATmacr	WORM	-	37,62	52,46	16,56	40,72	53,10	24,52	30,87	45,85	301,69	32,43	12,13	5,23	-	-	-	-	1,55	2,41	1,58	1,76
Tateomys_rhinogradoides	NMV	KCR2634	TATrhin	WORM	-	41,81	58,63	24,99	61,80	86,40	46,39	60,70	68,54	449,26	39,85	16,88	5,16	1,38	1,59	1823,98	2518,00	1,34	2,60	1,58	1,84
Tateomys_rhinogradoides	AMNH	M225117	TATrhin	WORM	M	38,90	69,21	31,62	67,80	104,74	38,92	59,16	65,53	475,86	40,09	14,16	5,63	-	-	-	-	1,45	2,91	1,62	1,93

Table S9. List of references for dietary categorizations.

Species	DIET	Region	Reference
APOabra	OMNI	PHIL	Heaney et. al. 2016
APObana	OMNI	PHIL	Heaney et. al. 2016
APOdata	OMNI	PHIL	Heaney et. al. 2016
APOhylo	OMNI	PHIL	L. Heaney pers. comm.; IUCN red list
APOlitt	OMNI	PHIL	Based on other Apomys
ARCluzo	CARNI	PHIL	Rickart et. al. 1991; Heaney et. al. 1999; Balete et. al. 2012
BUNandr	OMNI	SULAW	Musser 2014
BUNpeni	OMNI	SULAW	Musser 2014
CHRgonz	VERMI	PHIL	Rickart et. al. 1991; Heaney et. al. 1999
CHRmind	VERMI	PHIL	Rickart et. al. 1991; Heaney et. al. 1999; Heaney et. al. 2016
CHRsila	VERMI	PHIL	Heaney et. al. 2010; Rickart et. al. 2011
CHRwhit	VERMI	PHIL	Heaney et. al. 2010; Rickart et. al. 2011
CRUfall	CARNI	PHIL	-
DEOferr	CARNI	AFRIC	Happold 2013
CRUmela	CARNI	PHIL	Musser & Durden 2002
ECHcent	VERMI	SULAW	Musser & Durden 2014
ECHleuc	VERMI	SULAW	Musser 1990
GRAradi	OMNI	SULAW	Rowe et. al. 2016
HALboki	OMNI	MOLUC	Fabre et. al. 2013
HYOstue	VERMI	SULAW	Esselstyn et. al. 2015
LEParf	CARNI	PAPUA	Musser et. al. 2008
LEPeleg	CARNI	PAPUA	Musser et. al. 2008
LEPerns	CARNI	PAPUA	Musser et. al. 2008
LEPsign	CARNI	PAPUA	Musser et. al. 2008
MALedwa	OMNI	AFRIC	Happold 1987; Cole 1975
MAXmuss	OMNI	SULAW	Musser 1982
MAXsuri	OMNI	ORIEN	Pimsai et. al. 2014
MELburt	OMNI	MOLUC	Kerle 2008
MELobie	OMNI	MOLUC	Pers. Data.
MELnaso	VERMI	SULAW	Musser 1982
MICrich	CARNI	PAPUA	Helgen et. al. 2010
MUScerv	OMNI	ORIEN	Francis 2008; Lekagul & McNeely 1988
MUSpaha	CARNI	ORIEN	Smith & Xie 2008
NANminu	OMNI	AFRIC	Happold 2013
OXYdasy	CARNI	AMERI	Based on other Oxymycterus species; Wilson et. al. 2017
OXYquae	CARNI	AMERI	Based on other Oxymycterus species; Wilson et. al. 2017
PARwilh	CARNI	PAPUA	Musser et. al. 2008
PAUverm	VERMI	SULAW	Esselstyn et. al. 2012
PSEelea	CARNI	PAPUA	Based on other Pseudohydromys
PSEelle	CARNI	PAPUA	Based on other Pseudohydromys
PSEfusc	CARNI	PAPUA	Wilson et. al. 2017
PSEmuri	CARNI	PAPUA	Wilson et. al. 2017
RATmarm	OMNI	SULAW	Musser 1982
RATmoro	OMNI	MOLUC	Pers. Comm.
RATnorv	OMNI	ORIEN	Francis 2008; Zhang et. al. 2005
RATprae	OMNI	PAPUA	Taylor et. al. 1982; Flannery 1995
RATtane	OMNI	ORIEN	Pimsai et. al. 2014
RHYisar	VERMI	PHIL	Rickart et. Al. 1991; Heaney et. al. 1999; Rickart et. al. 2011; Balete et. al. 2009
RHYsori	VERMI	PHIL	Rickart et. Al. 1991; Heaney et. al. 1999; Rickart et. al. 2011; Balete et. al. 2009
SIGhisp	OMNI	AMERI	Cameron & Spencer 1981
SOMmacr	CARNI	SULAW	Musser & Durden 2002; Achmadi et. al. 2014
SORleon	VERMI	PHIL	Balete et. al. 2012
TATmacr	VERMI	SULAW	Musser 1982
TATrhin	VERMI	SULAW	Musser 1982

↑ Back to summary ↑

Supplementary informations – Article 2

Supporting information for:

Convergent evolution of olfactory and thermoregulatory capacities in small amphibious mammals

Quentin Martinez[1*], Julien Clavel[2,3], Jacob A. Esselstyn[4,5], Anang S. Achmadi[6], Camille Grohé[7,8], Nelly Pirot[9,10] and Pierre-Henri Fabre[1,11]

[1]Institut des Sciences de l'Evolution (ISEM, UMR 5554 CNRS-IRD-UM), Université de Montpellier, Place E. Bataillon - CC 064 - 34095 Montpellier Cedex 5, France
[2]Department of Life Sciences, The Natural History Museum, London SW7 5DB, United Kingdom
[3]Univ. Lyon. Laboratoire d'Ecologie des Hydrosystèmes Naturels et Anthropisés, UMR CNRS 5023, Université Claude Bernard Lyon 1, ENTPE, Boulevard du 11 Novembre 1918 F-69622 Villeurbanne Cedex, France
[4]Museum of Natural Science, 119 Foster Hall, Louisiana State University, Baton Rouge, Louisiana 70803
[5]Department of Biological Sciences, Louisiana State University, Baton Rouge, Louisiana 70803
[6]Museum Zoologicum Bogoriense, Research Center for Biology, Indonesian Institute of Sciences (LIPI), JI. Raya Jakarta-Bogor Km 46 Cibinong 16911 Indonesia
[7]Division of Paleontology, American Museum of Natural History, Central Park West at 79th Street, New York, NY, 10024, USA
[8]Laboratoire Paléontologie Évolution Paléoécosystèmes Paléoprimatologie (PALEVOPRIM, UMR 7262, CNRS-INEE), Université de Poitiers, Bât B35, 6 rue Michel Brunet - TSA 51106 - 86073 Poitiers Cedex 9, France
[9]IRCM, INSERM, U1194 Univ Montpellier, ICM, 208, rue des Apothicaires, F-34298, Montpellier, Cedex 5, France
[10]Réseau d'Histologie Expérimentale de Montpellier, BioCampus, UMS3426 CNRS-US009 INSERM-UM, Montpellier, France
[11]Mammal Section, Department of Life Sciences, The Natural History Museum, Cromwell Road, London

*Corresponding author (quentinmartinezphoto@gmail.com).

www.pnas.org/cgi/doi/10.1073/pnas.1917836117

Table S1. Results of phylogenetic ANCOVA to test if our data are significantly affected by ecology. Because the total surface area may also show an allometric relationship, we used either the total surface area of turbinals or the skull length as covariate. Olfa = olfactory surface area, Respi = respiratory surface area, Skull = skull length, Tot = total surface area

Variables	Ecology F-value	Ecology p-value	Tot F-value	Tot p-value
Olfa ~ Ecology + Tot	75.591	<0.0001	1870.654	<0.0001
Respi ~ Ecology + Tot	233.512	<0.0001	4824.108	<0.0001
Variables	**Ecology F-value**	**Ecology p-value**	**Skull F-value**	**Skull p-value**
Olfa ~ Ecology + Skull	22.387	<0.0001	682.904	<0.0001
Respi ~ Ecology + Skull	31.985	<0.0001	418.390	<0.0001

Table S2. Mean results from models of turbinal bone evolution fitted to 100 stochastic character maps of the amphibious and terrestrial lifestyles, based on size-free data. (A) model fit on the relative olfactory surface area, (B) on the relative respiratory surface area, and (C) bivariate model fit on both the relative olfactory and respiratory surface area. Model fits were compared using differences in the Akaike information criterion (AIC). See "Adaptation and convergence" section and SI appendix 15 for the material and methods.

	(A) Relative surface area of olfactory turbinals – size-free		(B) Relative surface area of respiratory turbinals – size-free		(C) Bivariate model: relative olfactory and respiratory surface area – size-free	
Model	**AIC**	**AICw**	**AIC**	**AICw**	**AIC**	**AICw**
BM1	-59.290	0.000	31.615	0.000	-273.172	0.000
BMM	-97.818	0.001	27.831	0.000	-370.081	0.002
BM1m	-84.588	0.000	9.6319	0.000	-296.555	0.000
BMMm	-110.869	0.292	10.593	0.000	-387.383	0.861
OU1	-71.308	0.000	9.2175	0.000	-305.685	0.000
OUM	-103.508	0.099	-21.459	0.953	-336.486	0.000
ER	-114.349	0.608	-2.972	0.047	-366.752	0.137

Table S3. Results of C indexes proposed by Stayton (2015, 1). Abbreviations: see SI appendix 1.

Variables	C1	p-value	C2	p-value	C3	p-value	C4	p-value
Residual PGLS Olfa/Tot + Respi/Tot	0.403	0.003	0.282	0.000	0.193	0.005	0.005	0.188
Residual PGLS Olfa/Skull + Respi/Skull	0.266	0.053	0.272	0.003	0.119	0.103	0.002	0.248

Table S4. Results of phylogenetic half-life estimated from Ornstein-Uhlenbeck models. Phylogenetic half-life is expressed as a percentage of the total tree height. A relatively high-phylogenetic half-life value indicates slow evolution towards the optimum. Abbreviations: see SI appendix 1.

Variables	Phylogenetic half-life
Residual PGLS Olfa/Tot	0.15
Residual PGLS Respi/Tot	0.18
Total turbinal surface area	0.88
Skull length	1.41

Table S5. Rates of turbinal evolution based on PGLS residuals between: (A) olfactory and total surface area, (B) respiratory and total surface area, (C) olfactory and skull length, (D) respiratory and skull length. AMP = amphibious, LRT = likelihood-ratio test, TER = terrestrial. For OUM fits: (*) differences observed are significantly larger than expected under a homogeneous OU process and can thus be interpreted confidently.

Variables	Observed rate ratio	TER rate	AMP rate	LRT	Best fitted model	Result of simulations
(A) Relative surface area of olfactory turbinals (based on total surface area)	5.425	0.001	0.004	< 0.001	BMM	-
(B) Relative surface area of respiratory turbinals (based on total surface area)	1.426	0.003	0.004	< 0.001	OUM	0.024*
(C) Relative surface area of olfactory turbinals (based on skull length)	1.314	0.006	0.007	-	BM1	-
(D) Relative surface area of respiratory turbinals (based on skull length)	1.272	0.007	0.009	< 0.005	OUM	0.132

Table S6. Comparison of rates of turbinal evolution with and without size correction. PGLS residuals between: (A) olfactory and total surface area, (B) respiratory and total surface area, (C) olfactory and total surface area corrected by size, and (D) respiratory and total surface area corrected by size. AMP = amphibious, LRT = likelihood-ratio test, TER = terrestrial. For OUM fits: (*) differences observed are significantly larger than expected under a homogeneous OU process and can thus be interpreted with confidence. See "Phylogenetic half-life and evolutionary rates" section and SI appendix 15 for the material and methods.

Variables	Size-free	Observed rate ratio	TER rate	AMP rate	LRT	Best fitted model	Resul of simulations
(A) Relative surface area of olfactory turbinals	No	5.43	0.001	0.004	< 0.001	OUM	0.004*
(B) Relative surface area of respiratory turbinals	No	1.43	0.003	0.004	< 0.001	OUM	0.271
(C) Relative surface area of olfactory turbinals	Yes	5,20	0.0009	0.005	< 0.001	BMM	-
(D) Relative surface area of respiratory turbinals	Yes	1,38	0.005	0.003	< 0.001	OUM	0.0956

Figure S1. Morphological variation of the ethmoturbinal I (etI) in some Afrosoricida and Eulipotyphla. The anteroposterior functional partitioning is based on histological evidence (SI appendix 11, 12). This figure illustrates the turbinal reduction between the anterior (in blue) and the posterior etI (in yellow). Scale bars represent one centimeter.

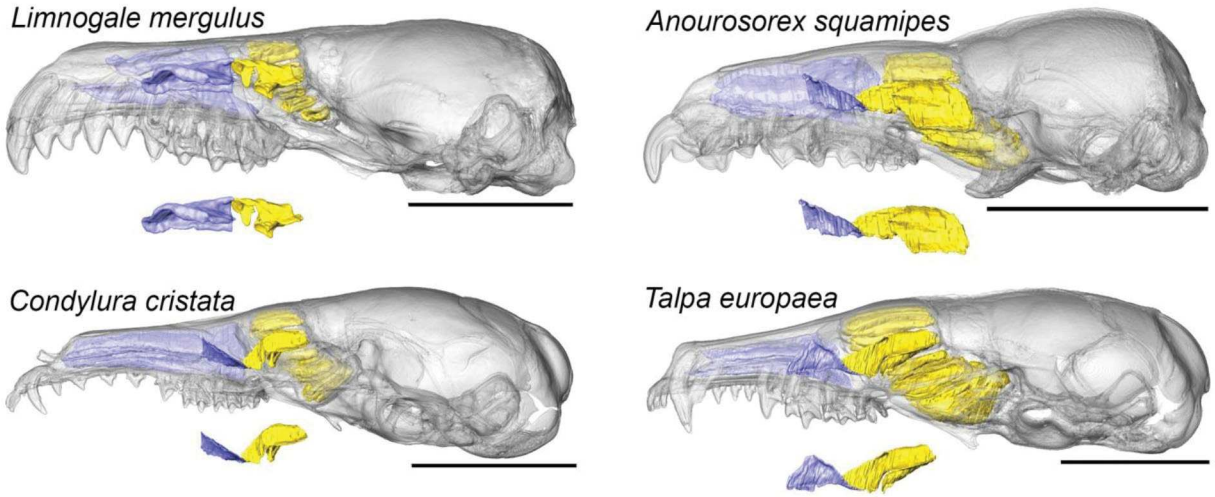

Figure S2. 3D representations of turbinal bones and coronal cross-section showing a gradient pattern of increasing relative surface of respiratory turbinals with increasing degree of aquatic specialization in Talpidae: (A) the amphibious *Desmana moschata*, (B) the sub-amphibious *Condylura cristata*, (C) the subterranean *Talpa europaea.* Panel D shows the phylogeny of the sampled species with barplots of the relative surface area of respiratory turbinals. Abbreviations: Respi = respiratory turbinals, Olfa = olfactory turbinals. Turbinal colors: blue = respiratory turbinals, yellow = olfactory turbinals. Colors of barplots: blue = amphibious and red = terrestrial species.

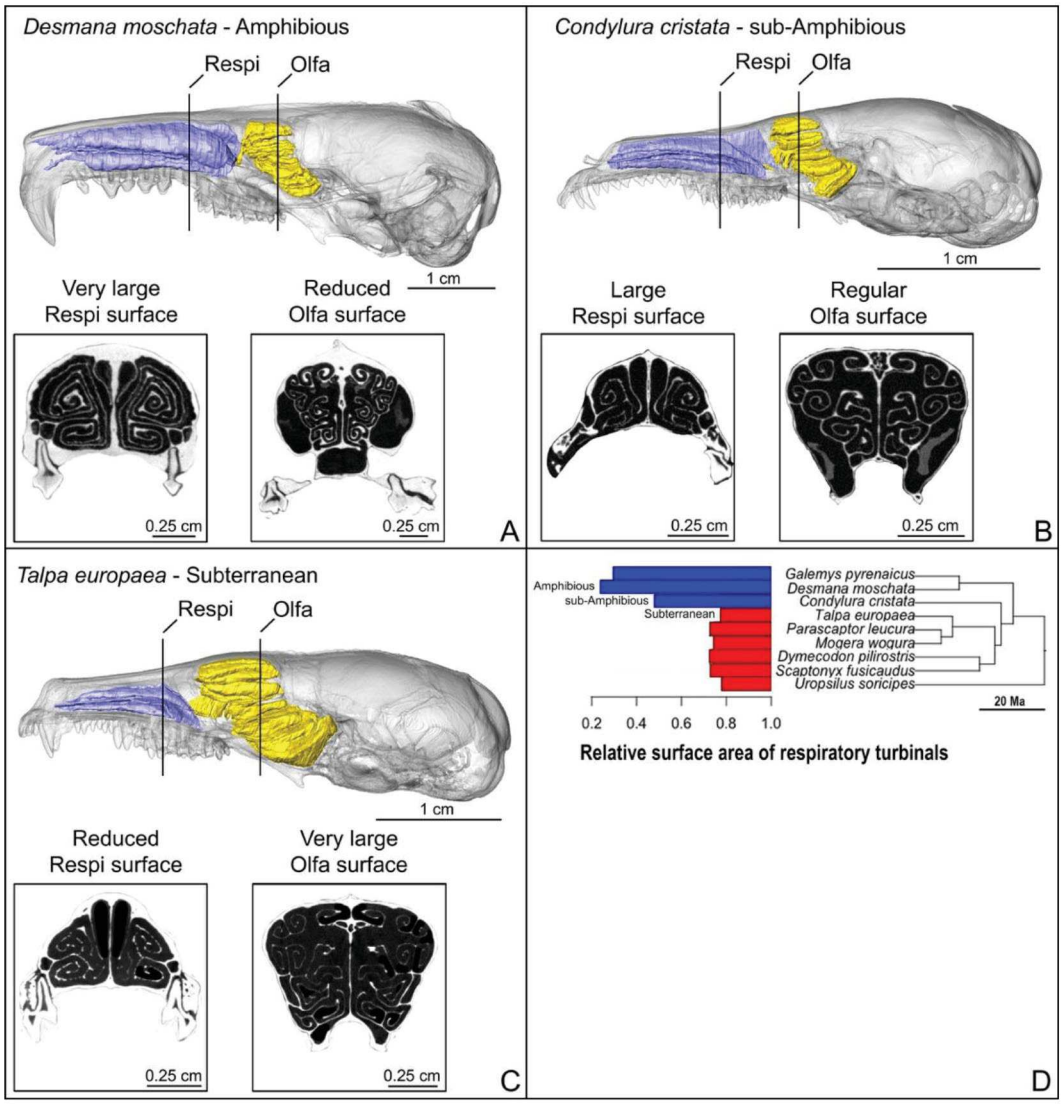

Figure S3. 3D representations of turbinal bones and barplots of the relative surface area of respiratory turbinals suggest that temperature mediated by altitude in this case is an important driver of the evolution of the size of respiratory turbinals. Examples in (A) Cricetidae and (B) Muridae.

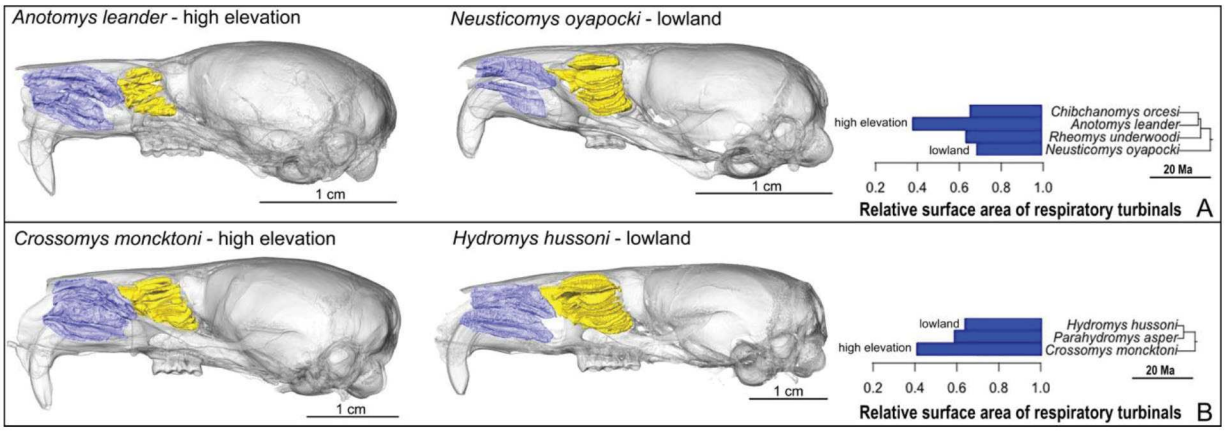

Table S7. Skulls were scanned using the following X-ray microtomographs.

CT-scan	Facilities
SkyScan 1076	ISEM Institute, Montpellier
Nikon Metrology HMX ST 225	NHMUK Natural History Museum, London
SkyScan 1174v2	The Evans Evolutionary Morphology Lab, Monash University, Melbourne
GE Phoenix v|tome|x s 240	Microscopy and Imaging Facility, American Museum of Natural History, N. Y.

Figure S4. Haematoxilin-Eosin-Saffron (HES) stained histology of coronal (transverse) sections of (A) the anterior part of the ethmoturbinal I (etI), (B) the maxilloturbinal (mt), (C) the frontoturbinal 1 (ft1), and (D) the posterior part of the ethmoturbinal I (etI), in European mole (*Talpa europaea*). The specimen was fixed 48 hours in 10% formaldehyde then stored in 70% ethanol. It was subsequently decalcified during 25 days in TBD-2 solution (Decalcifier Thermo Scientific). The HES was performed by the Institut de Recherche en Cancérologie de Montpellier (Inserm U1194). Based on Harkema et al. (2006, 2), Barrios et al. (2014, 3), and Herbert et al. (2018, 4), this figure illustrates the difference in epithelium type and thickness, where it is thicker posteriorly than anteriorly, as expected for olfactory and respiratory tissues, respectively. These results give new evidences that (A) the anterior part of the etI may be involved in heat conservation whereas (D) the posterior part of the etI may be involved in the olfactory process. Arrows show epithelium thickness.

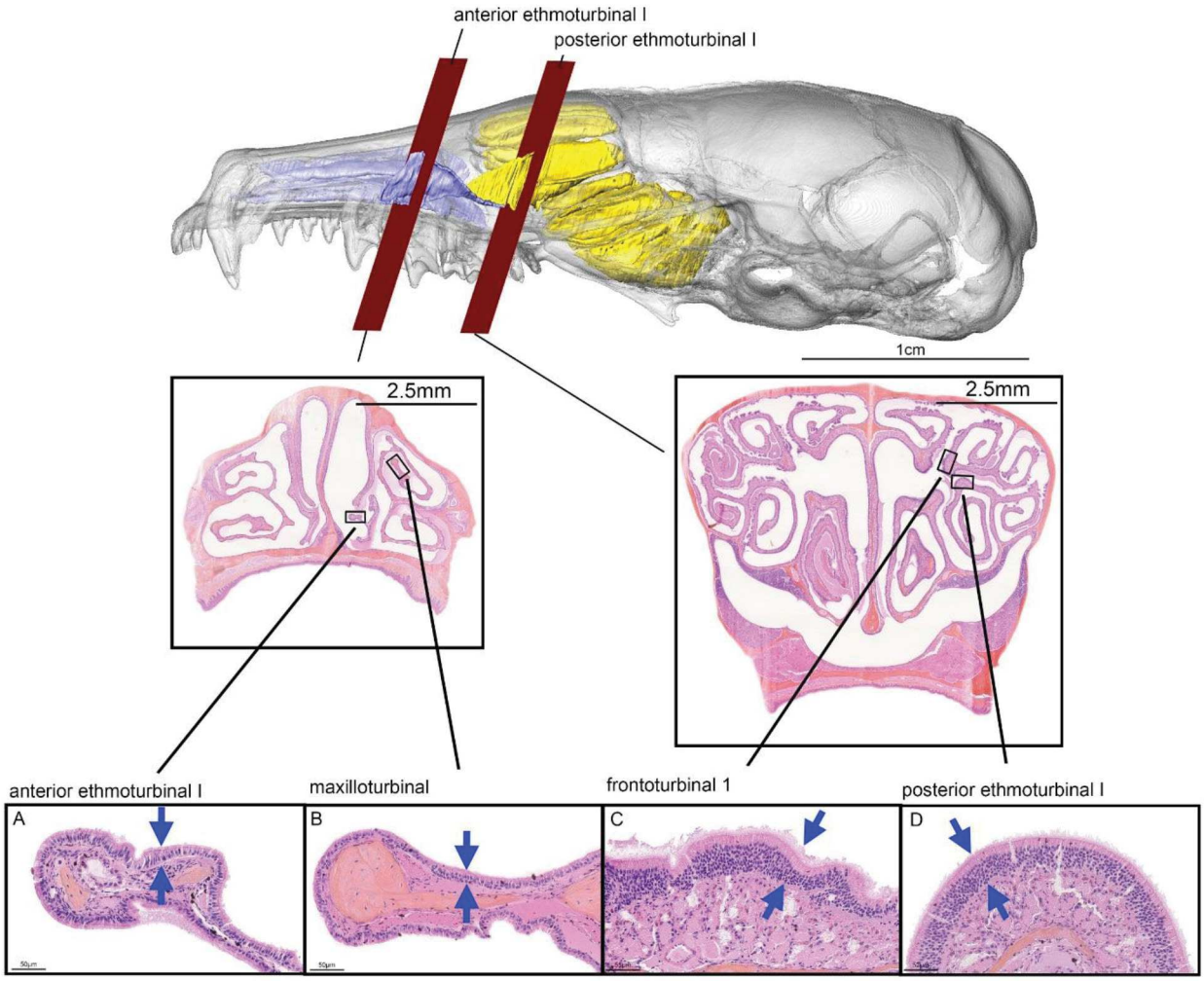

Figure S5. Haematoxilin-Eosin-Saffron (HES) stained histology of coronal nasal cavity sections: (A) *Suncus murinus* (Eulipotyphla), (B) *Talpa europaea* (Eulipotyphla), (C) *Tenrec ecaudatus* (Afrosoricida), and (D) *Mus musculus domesticus* (Rodentia). See SI appendix 11 for the histological protocol. These histological results allow accurate anteroposterior functional delimitation in some Afrosoricida and Eulipotyphla where we identified an ethmoturbinal I (etI) with both an anterior part and a posterior part (SI appendix 7). Based on both epithelial thickness and types (2-4), we identified anteroposterior functional partitioning between respiratory (in blue, A1, A2, B1, B2, C1, C2, D1) and olfactory turbinals (in yellow, A3, B3, B4, C3, D2, D3). Respiratory turbinals are covered with squamous, transitional and respiratory epithelium whereas olfactory turbinals are mostly covered by olfactory epithelium (2-4). In *Suncus murinus* (Eulipotyphla), *Talpa europaea* (Eulipotyphla), and *Tenrec ecaudatus* (Afrosoricida), histological sections indicate that the etI anterior part is likely involved into heat conservation (A2, B2, C2) whereas the etI posterior part might be involved in the olfactory process (A3, B3, C3). Arrows show epithelium thickness.

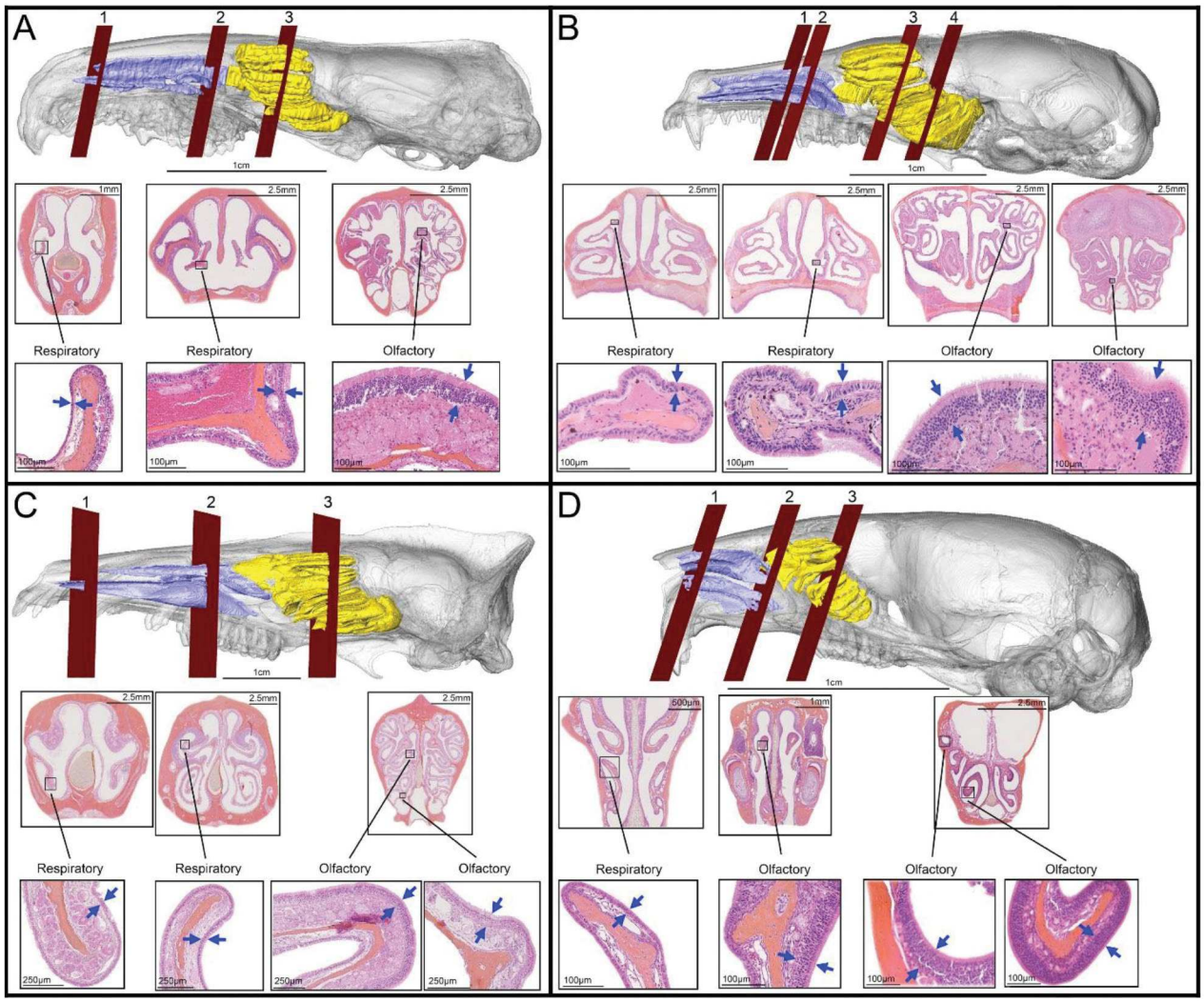

Figure S6. Phylogeny of the sampled species with barplot of (A) the relative surface area of olfactory turbinals (based on skull length), and (B) the relative surface area of respiratory turbinals (based on skull length). Colors of barplots: blue = amphibious species, red = terrestrial species.

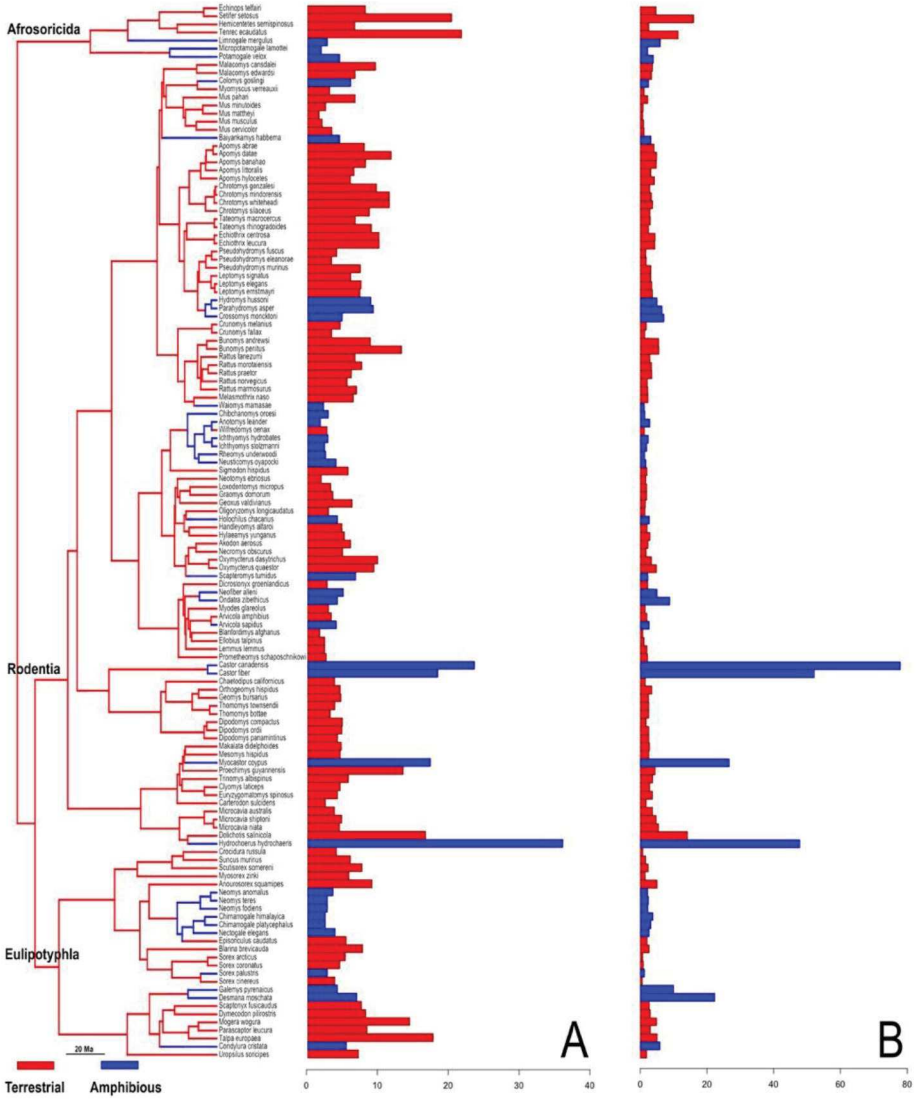

Figure S7. Phenograms based on the residuals of phylogenetic generalized least squares (PGLS) of: (A) the relative surface area of olfactory turbinals (based on skull length), and (B) the relative surface area of respiratory turbinals (based on skull length). Phenograms with branches crossing and concentrating in a given area indicate convergent evolution. Colors: blue = amphibious species, red = terrestrial species.

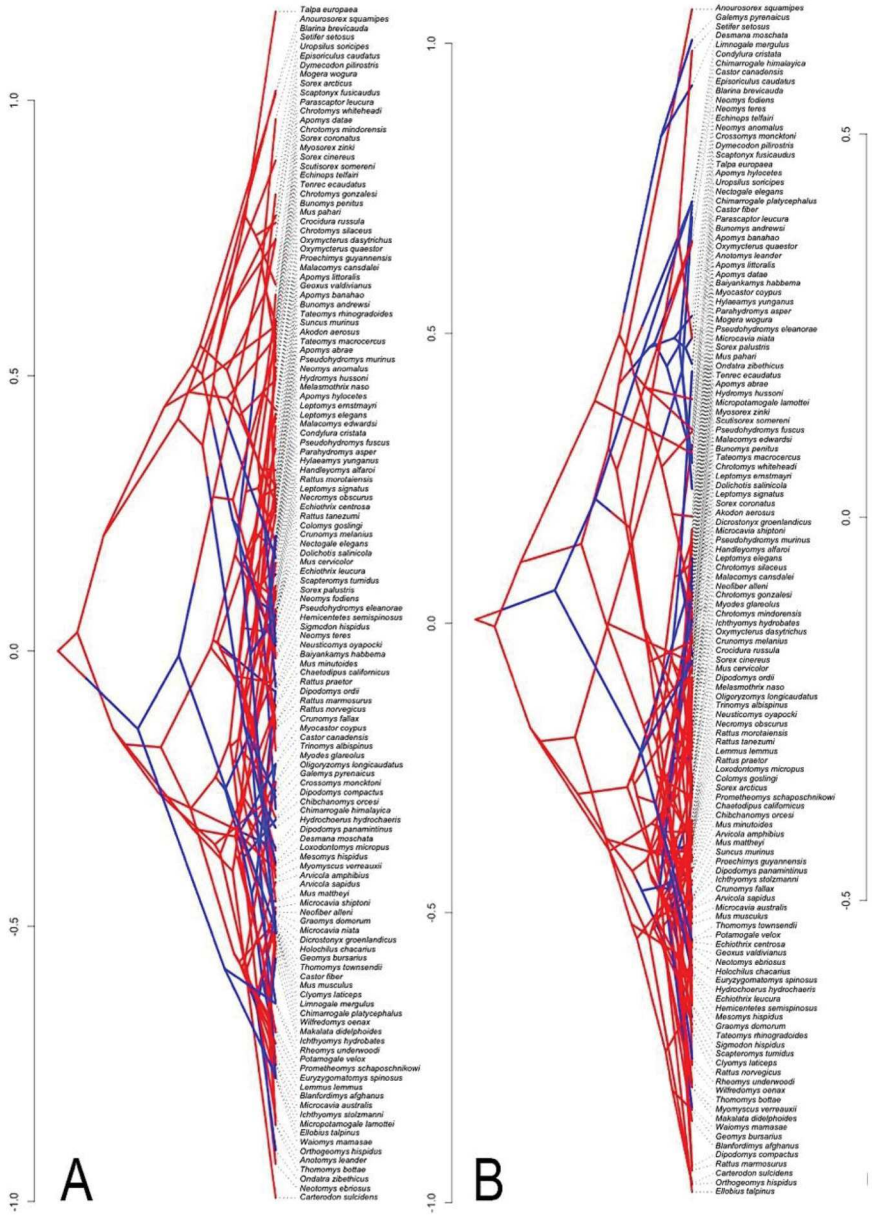

Figure S8. In order to obtain size-free estimates of relative surface area for both the respiratory and olfactory turbinals, we computed the residuals of a linear model (GLS - Generalized Least Squares) with the olfactory surface or respiratory surface area as the response variable, and the skull length and the total surface area as covariates. Plots of the residuals against skull length (used as a size proxy) show an allometric trend in the relative surface area for both the olfactory and respiratory turbinals (A, B), which is removed once we accounted for it (C, D).

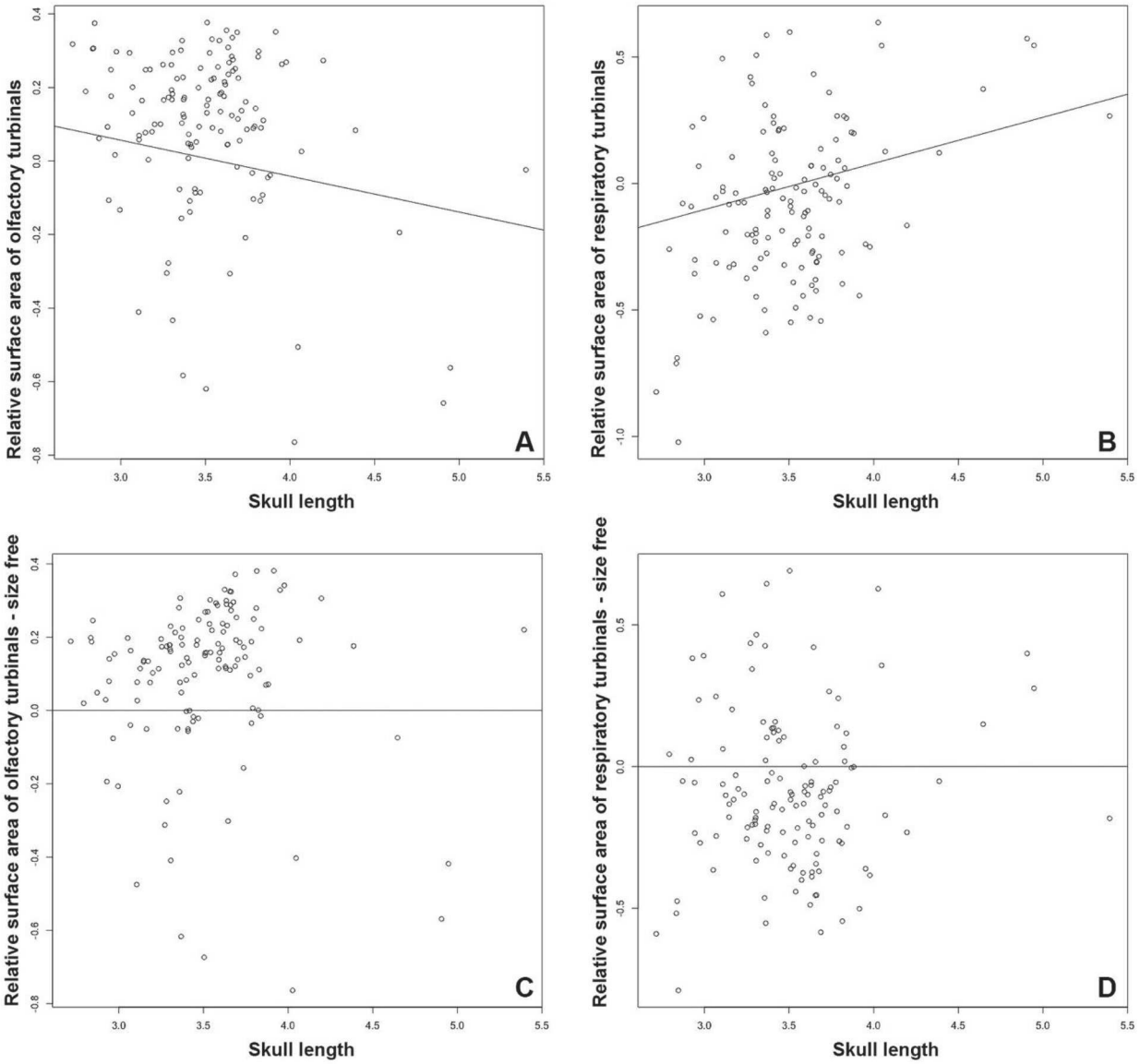

Figure S9. Log–log phylogenetic generalized least squares (PGLS) regressions to test allometric relationships between amphibious and terrestrial species. PGLS of: (A) the total turbinal surface area on the skull length, (B) olfactory on respiratory turbinal surface area, (C) olfactory on total turbinal surface area, (D) respiratory on total turbinal surface area, (E) olfactory turbinal surface area on skull length, and (F) respiratory turbinal surface area on skull length. Colors: blue = amphibious, black = terrestrial species.

We performed phylogenetic generalized least squares regressions (PGLS) with R packages ape (5), nlme (6), and ggplot2 (7). We performed an analysis of covariance (ANCOVA, 8), to test for differences in the slopes of the allometric relationships between amphibious and terrestrial species.
There is a strong positive allometric relationship between the total surface area of turbinals and skull length (slope (s) = 2.35, r squared (R^2) = 0.81, p-value (p) < 0.001, and the PGLS regression slopes estimated for the amphibious and terrestrial species are not significantly different (p = 0.16). There is a significant correlation between olfactory and respiratory surface area of turbinals (s = 0.70, R^2 = 0.76, p < 0.001), and again the PGLS slopes of amphibious and terrestrial species are not significantly different (p = 0.95). For a given size of respiratory turbinals, most amphibious species have smaller olfactory turbinals than do terrestrial species. These variables show a negative allometry (s = 0.70). There is a significant correlation between olfactory and total surface area of turbinals (s = 0.94, R^2 = 0.94, p < 0.001). The PGLS slopes of this correlation for amphibious and terrestrial species are not significantly different (p = 0.17). For a given size of turbinals, most amphibious species have smaller olfactory turbinals than do terrestrial species. These variables are nearly isometric (s = 0.94). There is a significant correlation between respiratory and total surface area of turbinals (s = 1.03, R^2 = 0.93, p < 0.001). For this model, the test for the PGLS slopes of amphibious and terrestrial species is not significant (p = 0.63). For a given size of turbinals, most amphibious species have larger respiratory turbinals than do terrestrial species. These variables display an isometric relationship (s = 1.03).

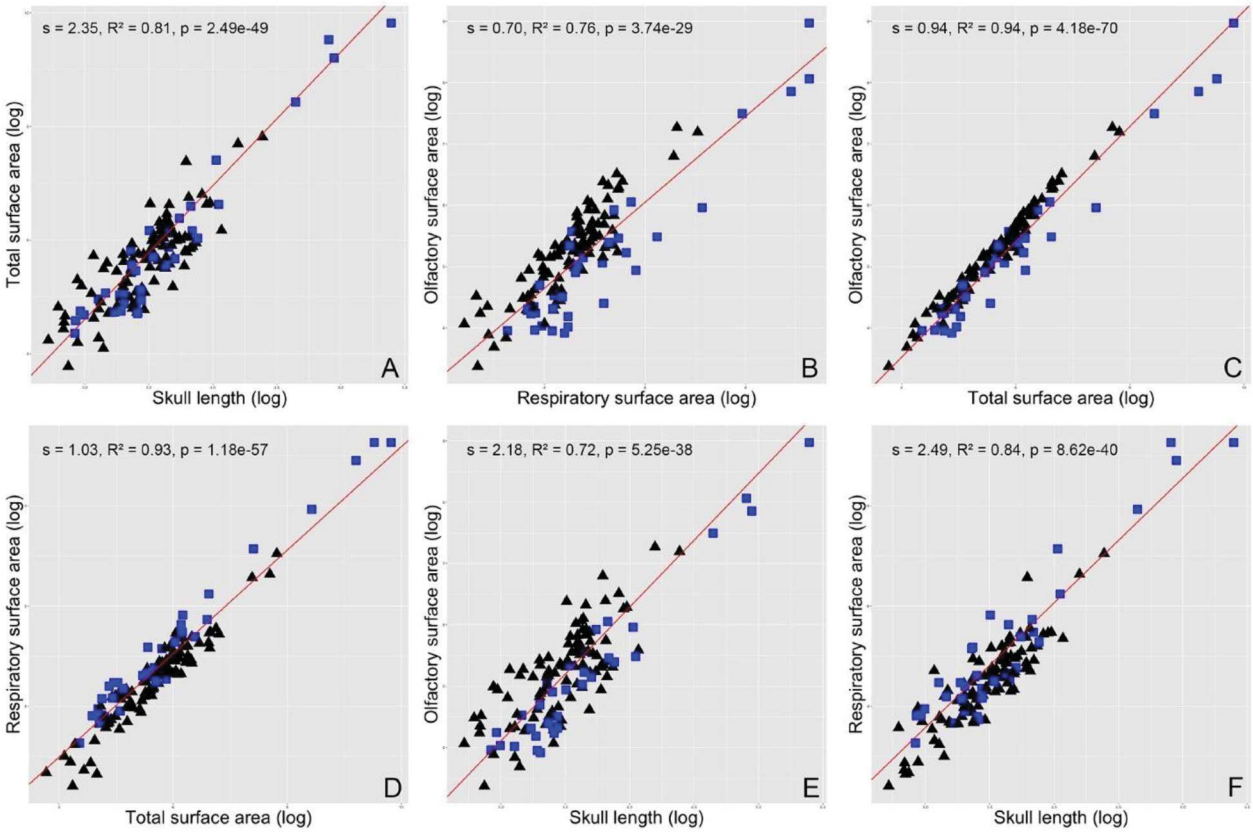

Table S8. Data set used for quantitative analyses. Abbreviations: see SI appendix 1. American Museum of Natural History (AMNH), Centre de Biologie et de Gestion des Populations (CBGP), Field Museum of Natural History (FMNH), Museums Victoria (NMV), Museum Zoologicum Bogoriense (MZB), Natural History Museum London (NHMUK), Natural History Museum of Paris (MNHN), Naturalis Biodiversity Center of Leiden (RMNH), Royal Museum for Central Africa (RMCA), Smithsonian Institution National Museum of Natural History (NMNH), and University of Montpellier (UM). AMP = amphibious, Ecol = ecology, TER = terrestrial.

Species	Museum	Voucher	Ecol	Respi	Olfa	Skull	Species	Museum	Voucher	Ecol	Respi	Olfa	Skull
Akodon aerosus	NHMUK	54580	TER	71,42	176,02	29,02	*Loxodontomys micropus*	NHMUK	37924	TER	62,87	98,15	29,92
Anotomys leander	NHMUK	51171	AMP	83,85	61,85	27,2	*Makalata didelphoides*	UM	V1566	TER	136,57	221,87	46,65
Anotomys leander	AMNH	66202	AMP	57,35	34,43	26,42	*Malacomys cansdalei*	NMNH	486151	TER	149,14	372,32	38,98
Anotomys leander	NHMUK	34910176	AMP	102,8	54,21	28,28	*Malacomys edwardsi*	NMNH	467226	TER	117,88	225,55	33,69
Anourosorex squamipes	NHMUK	3341157	TER	110,76	194,74	21,5	*Melasmothrix naso*	AMNH	225092	TER	77,64	190,65	31,87
Apomys abrae	AMNH	242099	TER	158,31	296,14	37	*Melasmothrix naso*	AMNH	225101	TER	80,52	222,5	32,5
Apomys banahao	CBGP	P0067	TER	134,26	239,57	33,74	*Mesomys hispidus*	UM	V953	TER	109,07	184,71	40,15
Apomys banahao	UM	P0045	TER	164,35	316,2	36,51	*Microcavia australis*	NHMUK	26101187	TER	174,29	173,15	45,8
Apomys banahao	CBGP	P0066	TER	237,07	331,4	38,38	*Microcavia niata*	NHMUK	9831619	TER	233,88	187,94	41,97
Apomys datae	FMNH	252475	TER	200,73	468,31	38,48	*Microcavia shiptoni*	NHMUK	3411498	TER	215,3	210,71	43,99
Apomys datae	FMNH	188256	TER	182,83	425,9	37,73	*Micropotamogale lamottei*	MNHN	CG1980N52	AMP	70,54	49,49	26,47
Apomys hylocetes	NMNH	125244	TER	133,11	183,66	30,51	*Micropotamogale lamottei*	MNHN	CG1980N57	AMP	56,76	54,31	26,76
Apomys littoralis	NMNH	458755	TER	96,09	189,85	29,14	*Mogera wogura*	NHMUK	259329	FOS	193,69	556,87	38,84
Arvicola amphibius	UM	QM857	TER	67,72	105,65	31,39	*Mus cervicolor*	UM	7314	TER	27,46	74,31	21,54
Arvicola sapidus	UM	QM932	AMP	105,75	152,99	37,79	*Mus mattheyi*	UM	2	TER	14,45	29,08	17,66
Baiyankamys habbema	AMNH	110056	AMP	80,38	109,56	27,51	*Mus minutoides*	UM	NA	TER	17,92	48,63	18,98
Baiyankamys habbema	AMNH	191441	AMP	120,88	159,95	32,4	*Mus musculus*	UM	R089V150FG1	TER	23,28	40,86	22,01
Blanfordimys afghanus	NHMUK	47425	TER	20	39,86	23,23	*Mus musculus*	UM	R089V152MP2	TER	27,58	52	22,75
Blarina brevicauda	NHMUK	951712	TER	52,84	147,02	18,95	*Mus pahari*	UM	7226	TER	60,93	172,46	25,78
Bunomys andrewsi	NMV	36977	TER	195,35	324,73	36,68	*Myocastor coypus*	UM	NA	AMP	2345,11	1604,42	92,28
Bunomys andrewsi	NMV	36982	TER	239,41	358,07	40,75	*Myocastor coypus*	NHMUK	707971	AMP	2585,22	1727,91	103,4
Bunomys penitus	NMV	36984	TER	257,73	597,27	45,23	*Myocastor coypus*	NHMUK	1610385	AMP	3427,73	2060,94	117,14
Carterodon sulcidens	NHMUK	79212	FOS	82,17	97,39	39,28	*Myodes glareolus*	CBGP	1	TER	39,06	72,91	24,28
Carterodon sulcidens	NHMUK	79213	FOS	70,6	104,16	40,61	*Myodes glareolus*	CBGP	2	TER	40,27	70,23	24,05
Castor canadensis	NHMUK	4966	AMP	10544,31	3168,24	135,24	*Myomyscus verreauxii*	NHMUK	544813	TER	39,29	91,41	29,26
Castor fiber	NHMUK	362261	AMP	7357,11	2574,74	140,87	*Myosorex zinki*	NHMUK	87760	TER	34,39	122,76	21,16
Chaetodipus californicus	UM	738N	FOS	44,61	101,66	26,64	*Necromys obscurus*	NHMUK	6462	TER	53,73	137,83	28,02
Chibchanomys orcesi	NHMUK	2816	AMP	39,08	74,56	25,4	*Nectogale elegans*	NHMUK	50497	AMP	65,9	92,47	23,65
Chimarrogale himalayica	NHMUK	50494	AMP	87,31	55,41	22,32	*Neofiber alleni*	NHMUK	9011141	AMP	238,17	235,34	46,45
Chimarrogale platycephalus	NHMUK	803209	AMP	87,28	65,81	26,36	*Neomys anomalus*	NHMUK	68381	AMP	45,77	69,49	19,42
Chrotomys gonzalesi	NMNH	458955	TER	103,59	333,36	34,45	*Neomys fodiens*	NHMUK	666465	AMP	55,85	49,31	19,04
Chrotomys mindorensis	FMNH	222107	TER	128,62	431,14	37,54	*Neomys fodiens*	UM	4	AMP	39,74	53,97	18,54
Chrotomys silaceus	NHMUK	975216	TER	108,27	308,83	34,62	*Neomys fodiens*	UM	5	AMP	39,62	54,29	18,57
Chrotomys silaceus	NHMUK	975239	TER	101,01	282,87	33,31	*Neomys teres*	NHMUK	1926224	AMP	51,72	56,28	19,99
Chrotomys whiteheadi	NHMUK	958220	TER	125,48	421,78	35,29	*Neotomys ebriosus*	NHMUK	2661254	TER	54,56	58,36	30,23
Chrotomys whiteheadi	NHMUK	958219	TER	150,36	440,51	36,84	*Neusticomys oyapocki*	MNHN	CG1995N3234	AMP	49,69	109,27	27,19
Chrotomys whiteheadi	NHMUK	975217	TER	138,45	377,63	35,78	*Oligoryzomys longicaudatus*	NHMUK	3411426	TER	38,15	72,92	24,54
Clyomys laticeps	NHMUK	79226	FOS	142,05	226,8	45,32	*Ondatra zibethicus*	NHMUK	36730121	AMP	675,32	308,84	59,26
Clyomys laticeps	NHMUK	79230	FOS	117,88	177,38	42,6	*Ondatra zibethicus*	NHMUK	3673010	AMP	577,68	239,81	58,43
Colomys goslingi	RMCA	7153	AMP	89,76	208,51	34,31	*Ondatra zibethicus*	NHMUK	19772750	AMP	311,68	201,62	55,67
Condylura cristata	NHMUK	921253	AMP	184,31	173,3	29,68	*Ondatra zibethicus*	UM	NA	AMP	485	213,2	55,6
Condylura cristata	NHMUK	85940	AMP	161,15	141,33	27,83	*Orthogeomys hispidus*	NHMUK	52162	FOS	210,99	267,57	58,45
Crocidura russula	UM	NA	TER	15,2	69,12	17,01	*Oxymycterus dasytrichus*	MNHN	CG1468N2002	TER	131,19	372,84	37,89
Crossomys moncktoni	NHMUK	501775	AMP	336,69	202,77	38,47	*Oxymycterus quaestor*	MNHN	272	TER	180,57	339,72	36,44
Crossomys moncktoni	RMNH	11650	AMP	217,86	169,73	38,12	*Parahydromys asper*	NHMUK	471366	AMP	277,01	410,11	46,03
Crunomys fallax	NHMUK	97484	TER	38,5	88,13	25,89	*Parahydromys asper*	NHMUK	471371	AMP	336,1	441,02	45,99
Crunomys melanius	NHMUK	72214	TER	53,2	124,69	27,12	*Parascaptor leucura*	NHMUK	361226444	FOS	85,69	226,93	27,1
Desmana moschata	NHMUK	NA	AMP	1243,5	460,32	57,11	*Potamogale velox*	NHMUK	A7004S2M4T24	AMP	203,7	281,9	55,41
Desmana moschata	NHMUK	71112	AMP	1159,58	332,78	54,57	*Potamogale velox*	NHMUK	E5425B	AMP	110,34	143,39	35,95
Desmana moschata	NHMUK	8911121	AMP	1373,15	371,01	56,53	*Potamogale velox*	MNHN	CG1892N2064	AMP	273,89	233,53	54,31
Dicrostonyx groenlandicus	NHMUK	3711327	TER	67,25	79,33	28,44	*Proechimys guyannensis*	UM	NA	TER	284,02	885,6	56,03
Dipodomys compactus	UM	NA	TER	73,69	190,39	38,97	*Proechimys guyannensis*	UM	V1648	TER	176,09	460,82	44,35
Dipodomys ordii	UM	726N	TER	88,69	161,48	33,41	*Prometheomys schaposchnikowi*	NHMUK	19666687	FOS	89,05	94,79	33,84
Dipodomys panamintinus	UM	727N	TER	96,54	153,47	36,28	*Prometheomys schaposchnikowi*	NHMUK	19666729	FOS	59,79	75,63	30,41
Dolichotis salinicola	NHMUK	34114171	TER	1148,77	1332,63	80,43	*Pseudohydromys eleanorae*	NHMUK	501734	TER	43,95	76,12	22,39
Dymecodon pilirostris	NHMUK	614445	FOS	74,81	195,18	23,88	*Pseudohydromys fuscus*	AMNH	53278	TER	30,16	69,99	21,4
Echinops telfairi	NHMUK	921164	TER	140,34	236,45	29,05	*Pseudohydromys fuscus*	NHMUK	53280	TER	38,68	93,64	22,79
Echiothrix centrosa	NHMUK	40385	TER	247,14	544,79	51,82	*Pseudohydromys fuscus*	NHMUK	501733	TER	48,23	90,09	23,06
Echiothrix centrosa	AMNH	153013	TER	223,57	501,25	52,29	*Pseudohydromys fuscus*	NHMUK	53296	TER	49,68	121,2	23,87
Echiothrix leucura	NHMUK	971246	TER	256,03	527,66	53,68	*Pseudohydromys murinus*	NHMUK	53291	TER	193,05	410,41	46,96
Echiothrix leucura	NHMUK	971245	TER	221,76	549,11	53,13	*Pseudohydromys murinus*	NHMUK	53290	TER	36,1	105,58	22,68
Ellobius talpinus	NHMUK	3421127	FOS	46,53	89,48	39,28	*Rattus marmosurus*	NMV	37018	TER	109,9	312,4	45,38
Ellobius talpinus	NHMUK	3421130	FOS	36,23	64,23	24,57	*Rattus morotaiensis*	MZB	33229	TER	127,14	256,13	37,16
Episoriculus caudatus	NHMUK	7587	TER	35,55	88,43	16,32	*Rattus morotaiensis*	MZB	33254	TER	155,15	358,53	43,33
Euryzygomatomys spinosus	NHMUK	9111930	FOS	180,91	202,14	47,89	*Rattus norvegicus*	UM	C0304	TER	86,58	211,21	37,95
Galemys pyrenaicus	NHMUK	713839	AMP	192,69	109,48	31,5	*Rattus praetor*	CBGP	NA	TER	147,68	252,85	41,02
Galemys pyrenaicus	MNHN	CG1961N751	AMP	351,02	143,06	33,33	*Rattus tanezumi*	UM	R5422	TER	113,28	248,41	37,09
Galemys pyrenaicus	MNHN	CG1961N752	AMP	418,08	150,23	33,97	*Rheomys underwoodi*	NHMUK	75305	AMP	44,21	77,12	30,02
Galemys pyrenaicus	MNHN	CG1961N750	AMP	350,06	149,92	33,76	*Scapteromys tumidus*	NHMUK	671657	AMP	93,66	262,31	38,71
Galemys pyrenaicus	MNHN	CG1961N749	AMP	372,03	145,99	33,68	*Scaptonyx fusicaudus*	NHMUK	321117	FOS	66,26	176,52	23,27
Geomys bursarius	NHMUK	60537	FOS	116,26	209,52	44,56	*Scutisorex somereni*	NHMUK	19633241	TER	67,44	209,12	27,27
Geoxus valdivianus	NHMUK	2751101	FOS	48,25	181,1	28,87	*Setifer setosus*	NHMUK	19391616	TER	712,38	895,96	44,31
Graomys domorum	NHMUK	22253	TER	72,53	122,92	34,53	*Sigmodon hispidus*	NHMUK	58504	TER	69,88	169,98	34,67
Handleyomys alfaroi	NHMUK	33350	TER	59,06	131,75	27,26	*Sigmodon hispidus*	MNHN	CG2007N335	TER	83,73	237,5	36,67
Hemicentetes semispinosus	NHMUK	13391606	TER	106,43	262,16	39,52	*Sorex arcticus*	NHMUK	2621	TER	14,07	91,69	17,22
Holochilus chacarius	NHMUK	201715	AMP	117,64	171,65	40,56	*Sorex cinereus*	NHMUK	96183	TER	11,07	58,12	15,11
Hydrochoerus hydrochaeris	UM	NA	AMP	10532,88	7884,29	220,16	*Sorex coronatus*	UM	NA	TER	17,55	77,36	17,09
Hydromys hussoni	RMNH	12585	AMP	71,13	139,01	29	*Sorex palustris*	NHMUK	1113914	AMP	26,14	52,06	18,58
Hydromys hussoni	MZB	YS391	AMP	250,86	441,28	50	*Suncus murinus*	UM	QM200	TER	51,48	172,56	28,66
Hydromys hussoni	CBGP	PA0024	AMP	330,97	540,55	47,06	*Talpa europaea*	UM	QM	FOS	174,41	590,68	33,47
Hylaeamys yunganus	NHMUK	81472	TER	88,53	150,38	28,83	*Tateomys macrocercus*	AMNH	225073	TER	104,91	214,69	30,65
Ichthyomys hydrobates	MNHN	CG1932N1951	AMP	89,78	96,65	33,82	*Tateomys macrocercus*	AMNH	225072	TER	103,34	213,58	32,29
Ichthyomys hydrobates	MNHN	CG1932N2950	AMP	91,66	109,53	33,07	*Tateomys macrocercus*	NMV	37081	TER	90,08	211,62	32,43
Ichthyomys hydrobates	MNHN	CG1900N562	AMP	51,51	64,48	26,46	*Tateomys rhinogradoides*	NMV	KCR2634	TER	100,44	348,82	39,85
Ichthyomys stolzmanni	NHMUK	948614	AMP	64,36	74,86	31,21	*Tateomys rhinogradoides*	AMNH	M225117	TER	108,1	367,76	40,09
Lemmus lemmus	NHMUK	3010416	TER	56,14	69,63	30,15	*Tenrec ecaudatus*	UM	QM201	TER	570,35	1123,15	59,3
Lemmus lemmus	NHMUK	3010424	TER	74,53	75,46	30,28	*Tenrec ecaudatus*	NHMUK	19391593	TER	949,06	1748,14	73,64
Leptomys elegans	AMNH	2952722	TER	134,12	292,01	38,98	*Thomomys bottae*	NHMUK	52327	FOS	115,72	139,93	43,7
Leptomys elegans	AMNH	501254	TER	127,27	272,94	36,01	*Thomomys townsendii*	NHMUK	8232028	FOS	100,81	159,09	37,79
Leptomys elegans	NHMUK	5112822	TER	142,75	279,17	36,79	*Thomomys townsendii*	NHMUK	9831131	FOS	98,96	131,49	37,65
Leptomys ernstmayri	NHMUK	501252	TER	153,75	294,47	36,67	*Trinomys albispinus*	NHMUK	571283	TER	162,67	243,5	42,33
Leptomys ernstmayri	AMNH	194936	TER	118,14	235,19	35,55	*Uropsilus soricipes*	NHMUK	38418	FOS	40,09	139,9	19,58
Leptomys signatus	AMNH	105370	TER	109,22	202,77	33,4	*Waiomys mamasae*	NMV	32027	AMP	41,75	68,66	30,33
Limnogale mergulus	MNHN	CG1984N921	AMP	214,48	88,75	30,35	*Wilfredomys oenax*	NHMUK	88113010	TER	40,56	80,93	29,19
Limnogale mergulus	MNHN	CG1952N2511	AMP	139,75	74,43	27,67							

References for SI appendix.

1. C. T. Stayton, The definition, recognition, and interpretation of convergent evolution, and two new measures for quantifying and assessing the significance of convergence. Evolution 69, 2140–2153 (2015).

2. J. R. Harkema, S. A. Carey, J. G. Wagner, The nose revisited: a brief review of the comparative structure, function, and toxicologic pathology of the nasal epithelium. Toxicol. Pathol. 34, 252–269 (2006).

3. A. W. Barrios, G. Núñez, P. S. Quinteiro, I. Salazar, P. Chamero, Anatomy, histochemistry, and immunohistochemistry of the olfactory subsystems in mice. Front. Neuroanat. 8, 63 (2014).

4. R. A. Herbert, K. S. Janardhan, A. R. Pandiri, M. F. Cesta, R. A. Miller, Nose, larynx, and trachea. In Boorman's Pathology of the Rat (pp. 391-435) (2018).

5. E. Paradis, J. Claude, K. Strimmer, APE: analyses of phylogenetics and evolution in R language. Bioinformatics 20, 289–290 (2004).

6. J. Pinheiro, et al., R Core Team nlme: linear and nonlinear mixed effects models. R package version 3.1-118. R Foundation for Statistical Computing, Vienna (2014).

7. H. Wickham, ggplot2: elegant graphics for data analysis. Springer (2016).

8. J. Claude, Morphometrics with R. Springer Science & Business Media (2008).

↑ Back to summary ↑

Supplementary informations – Article 3

Supplementary Information for:

The mammalian maxilloturbinal evolution: when maxilloturbinal does not reflect thermal abilities

Quentin Martinez [1], Radim Šumbera [2], Jan Okrouhlík [2], Mark Wright [1, 3], Stan Braude [4], Thomas B. Hildebrandt [5], Susanne Holtze [5], Irina Ruf [6], and Pierre-Henri Fabre [1, 7]

1 Institut des Sciences de l'Évolution (ISEM, UMR 5554 CNRS-IRD-UM), Université de Montpellier, Place E. Bataillon - CC 064 - 34095, Montpellier Cedex 5, France
2 Department of Zoology, Faculty of Science, University of South Bohemia, 37005 České Budějovice, Czech Republic
3 Department of Organismic and Evolutionary Biology & Museum of Comparative Zoology, Harvard University, Cambridge, MA, 02138, USA
4 Biology Department, Washington University, St. Louis, MO 63130, USA
5 Department of Reproduction Management, Leibniz-Instiute for Zoo and Wildlife Research, 10315 Berlin, Germany
6 Abteilung Messelforschung und Mammalogie, Senckenberg Forschungsinstitut und Naturmuseum Frankfurt, 60325 Frankfurt am Main, Germany
7 Mammal Section, Department of Life Sciences, The Natural History Museum, SW7 5DB London, United Kingdom

Supplementary Information 1: (A) Linear regression between basal metabolic rates (BMR) and the relative surface area of the maxilloturbinal based on body mass. (B) Linear regression between body temperatures (Tb) and the relative surface area of the maxilloturbinal based on body mass. Barplots: beige = terrestrial, red = arboreal, blue = amphibious, black = subterranean, and yellow = flying species.

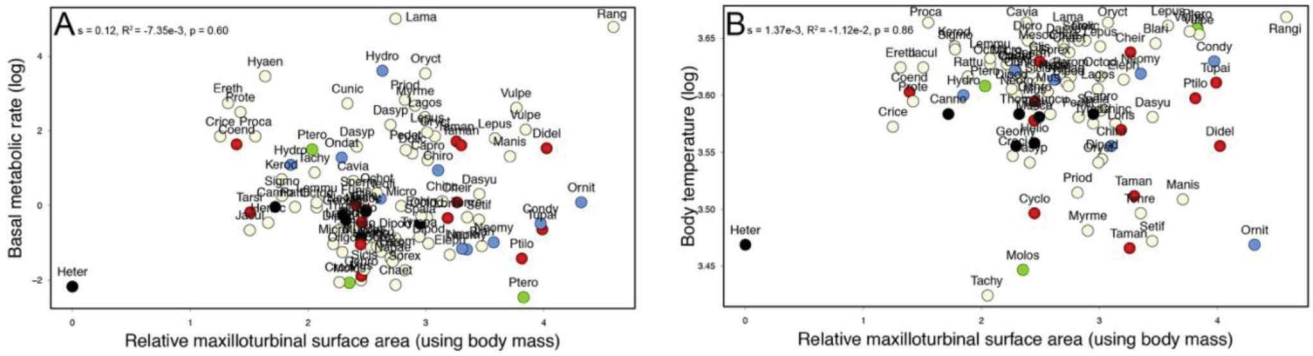

Supplementary Information 2: Detailed view of the maxilloturbinal of the African bush elephant (*Loxodonta africana*).

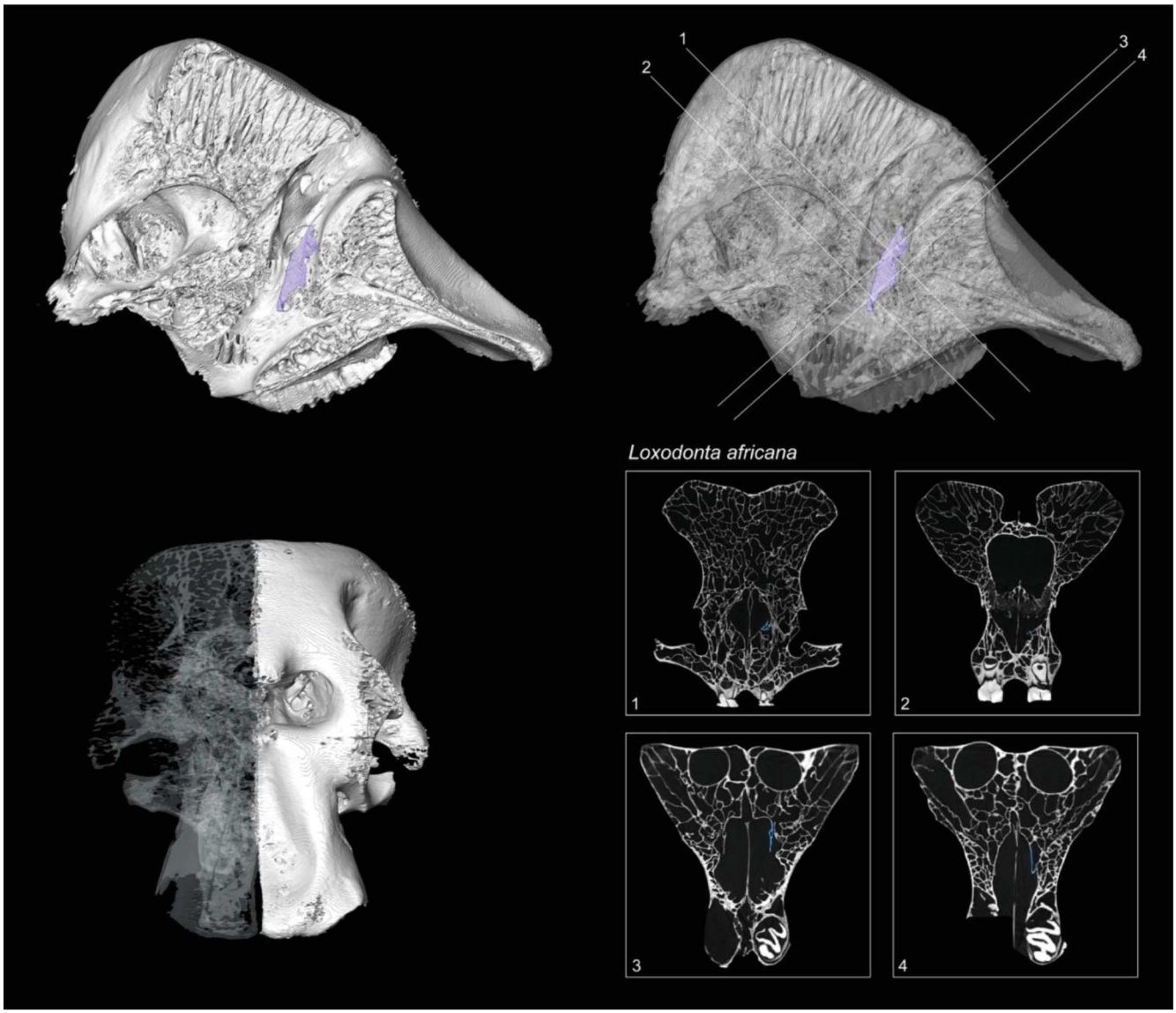

Supplementary Information 3: Data set used for quantitative analyses. Sheet 1: Ordered values from smallest to largest for percentage of the predicted value of maxilloturbinal (see method section). Sheet 2: Raw data of the 424 individuals used in this study. Museum abbreviations: American Museum of Natural History, New York, New York, USA (AMNH), Centre de Biologie et de Gestion des Populations (CBGP), Duke University, Evolutionary Anthropology, Durham, NC, USA (DU), Field Museum of Natural History (FMNH), University of Hull UK (Hull), Leibniz Institute for Zoo and Wildlife Research (IZW), Natural History Museum of Los Angeles County, Los Angeles, CA, USA (LACM), Museu de Ciências Naturais da Fundação Zoobotânica do Rio Grande do Sul, Porto Alegre, Brazil (MCN), Museum of Comparative Zoology, Harvard University, Cambridge, MA, USA (MCZ), Natural History Museum of Paris (MNHN), Museum of Vertebrate Zoology, UC Berkeley (MVZ), Museum Zoologicum Bogoriense (MZB), Natural History Museum London (NHMUK previously BMNH), Museums Victoria (NMV), Naturhistoriska riksmuseet, Stockholm, Sweden (NRM), Palaeontological Institute and Museum of the University of Zurich, Switzerland (PIMUZ), Royal Museum for Central Africa (RMCA), Naturalis Biodiversity Center of Leiden (RMNH), University of Texas, Vertebrate Paleontology Laboratory, Austin, TX, USA (TMM), University of Montpellier (UM), University of Michigan Museum of Zoology (UMMZ), University Museum of Zoology, Cambridge, United Kingdom (UMZC), University of South Bohemia in Ceske Budejovice, Czech Republic (USB), National Museum of Natural History, Washington, DC, USA (USNM), Yale Peabody Museum, New Haven, CT, USA (YPM), Museum für Naturkunde Berlin, Berlin, York Zooarchaeology Laboratory, York, UK (YZL), Berlin, Germany (ZMB), and Centrum für Naturkunde, Hamburg, Germany (ZMH-S).

Supplementary Information 4: R script, CSV file and nexus phylogeny needed to perform analyses and figures presented in this study.

↑ Back to summary ↑

Scientific contribution

Scientific publications

[10] Vacher, J.-P., Chave, J., Ficetola, F., Sommeria-Klein, G., Tao S., Thébaud, C., Blanc, M., ... **Martinez Q.**, ... & Fouquet, A. (2020). Large-scale DNA-based survey of frogs in Amazonia suggests a vast underestimation of species richness and endemism. *Journal of Biogeography, 47(8)*, 1781-1791.

[9] Martinez, Q., Clavel, J., Esselstyn, J. A., Achmadi, A. S., Grohé, C., Pirot, N., & Fabre, P. H. (2020). Convergent evolution of olfactory and thermoregulatory capacities in small amphibious mammals. *Proceedings of the National Academy of Sciences*, *117*(16), 8958-8965.

[8] Privet, K., Vedel, V., Fortunel, C., Orivel, J., **Martinez, Q.**, Cerdan, A., ... & Petillon, J. (2020). Relative efficiency of pitfall trapping vs. nocturnal hand collecting in assessing soil-dwelling spider diversity along a structural gradient of Neotropical habitats. *Diversity, 12(2)*, 81.

[7] Martinez, Q., Lebrun, R., Achmadi, A. S., Esselstyn, J. A., Evans, A. R., Heaney, L. R., Portela Miguez, R., Rowe, C. K., & Fabre, P. H. (2018). Convergent evolution of an extreme dietary specialisation, the olfactory system of worm-eating rodents. *Scientific reports, 8(1)*, 17806.

[6] Vacher J.-P., Kok P.J.R. , Rodrigues M.T., Dias Lima J., Lorenzini A., **Martinez Q.**, Fallet M., Courtois E.A., Blanc M., Gaucher P., Dewynter M., Jairam R., Ouboter P., Thébaud C. & Fouquet A. (2017). Cryptic diversity in Amazonian frogs: integrative taxonomy of the genus *Anomaloglossus* (Amphibia: Anura: Aromobatidae) reveals a unique case of diversification within the Guiana Shield. *Molecular Phylogenetics and Evolution, 112*, 158-173.

[5] Courtois E.A., Michel E., **Martinez Q.**, Pineau K., Dewynter M., Ficetola F. & Fouquet A. (2016). Taking the lead on climate change: Modeling and monitoring the fate of an Amazonian frog. *Oryx, 50(03),* 450–459.

[4] Fouquet A., **Martinez Q.**, Zeidler L., Courtois E.A., Gaucher P., Blanc M., Dias Lima J., Marques Souza S., Rodrigues M. & Kok P.J.R. (2016). Cryptic diversity in the *Hypsiboas semilineatus* species group (Amphibia, Anura) with the description of a new species from the eastern Guiana Shield. *Zootaxa. 4084 (1): 079*–104.

[3] Fouquet A., Orrico V. Dill, Ernst R., Blanc M., **Martinez Q.**, Vacher J.-P., Rodrigues M.T., Ouboter P., Jairam R., Ron S. (2015). A new *Dendropsophus* Fitzinger, 1843 (Anura: Hylidae) of the parviceps group from the lowlands of the Guiana Shield. *Zootaxa, 4052 (1), 39*-64.

[2] Vedel, V., Cerdan, A., **Martinez, Q.**, Baraloto, C., Petitclerc, F., Orivel J., & Fortunel, C. (2015). Day-time vs. night-time sampling does not affect estimates of spider diversity across a land use gradient in the Neotropics. *Journal of Arachnology, 43(3)*, 413–416.

[1] Fouquet A., **Martinez Q.**, Courtois E.A., Dewynter M., Pineau K., Gaucher P., Blanc M., Marty C. & Kok P.J.R. (2013). A new species of the genus *Pristimantis* (Amphibia, Craugastoridae) associated with the moderately elevated massifs of French Guiana. *Zootaxa, 3750 (5), 569*–586.

Scientific communications

[7] Martinez, Q., Clavel, J., Esselstyn, J. A., Achmadi, A. S., Grohé, C., Pirot, N., & Fabre, P. H. (2020). Convergent evolution of olfactory and thermoregulatory capacities in small amphibious mammals. ISEM meetings. Montpellier, France. [Talk]

[6] Martinez, Q., Clavel, J., Esselstyn, J. A., Achmadi, A. S., Grohé, C., Pirot, N., & Fabre, P. H. (2020). Convergent evolution of olfactory and thermoregulatory capacities in small amphibious mammals. Journée des doctorants. Montpellier, France. [Talk]

[5] Martinez, Q., & Fabre, P. H. (2019). Convergent evolution of olfactory and thermoregulatory capacities in small amphibious mammals. 99th Annual Meeting of the American Society of Mammalogy (ASM). Washington, DC, USA. [Talk]

[4] Hautier, L., Garland, K., Ferreira-Cardoso, S., Wright, M., **Martinez, Q.**, Fabre, P. H., ... & Delsuc, F. (2019). Sniffing out Covariation Patterns in the Olfactory System of Myrmecophagous Mammals. International Congress of Vertebrate Morphology (ICVM). Prague, Czech Republic. [Talk]

[3] Fabre, P. H., & **Martinez, Q.** (2019). Convergent evolution of olfactory and thermoregulatory capacities in small amphibious mammals. International Congress of Vertebrate Morphology (ICVM). Prague, Czech Republic. [Talk]

[2] Martinez, Q., Lebrun, R., Achmadi, A. S., Esselstyn, J. A., Evans, A. R., Heaney, L. R., ... & Fabre, P. H. (2018). Convergent evolution of an extreme dietary specialisation: a study of olfactory system in rodents. II Joint Congress on Evolutionary Biology. Montpellier, France. [Poster]

[1] Fabre, P. H., & **Martinez, Q.** (2016). Investigating the carnivorous rat nose through its olfactory turbinate bones. 96th Annual Meeting of the American Society of Mammalogy (ASM). Minneapolis, USA. [Poster]

Non peer publication

[1] Dewynter, M., Marty, C., Courtois, E. A., Blanc, M., Gaucher, P., **Martinez, Q.**, & Fouquet, A. (2016). L'identification des rainettes des genres *Osteocephalus* et *Trachycephalus* (Hylidae: Lophyohylinae) en Guyane. Les cahiers de la fondation Biotope, 7, 1–16.

Teaching

98 hours of graduate teaching (Bachelor 3) - Vertebrate evolution, Embryonic development and Genetics

Data-acquisition

- 3D µCT-scan, classical and iodine staining (ISEM lab and NHM UK)
- Biting force, running and jumping performances in small mammals
- Live trap, collecting, and handling: mammals and herps
- DNA, RNA, and specimen sampling (including non-invasive and swab methods) with lived, anesthetized, and road-killed (1190 collected samples since 2014)
- Specimen preparation: skulls, fluids, skins and vouchering (mammals and herps)
- Camera trap: home-made high-resolution DSLR camera trap for terrestrial and underwater environments

Fieldwork missions

2019 Malaysia (Borneo Gunung Murud) - Scientific mission. Co-Investigator.

2018 French Guiana (Gaa Kaba) - Scientific mission. Principal Investigator.

2013-14 French Guiana (different localities) - Scientific missions. Co-Investigator.

↑ Back to summary ↑

Acknowledgements / Remerciements

Beyond the scientific production and life experience of achieving a PhD, the most important thing to me is to thank all those people who during the last years trust in me, help me, inspire me and help me to learn and grow.

Merci à ma sœur, ma mère et mon père qui m'ont toujours soutenu dans mes passions et projets parfois envahissants. Également à ma famille plus élargie ainsi qu'à ma belle-famille.

Merci à mes amis sans qui le quotidien ne serait pas le même, notamment : Loic Nouet, Rémi Allio, Sergio Ferreira Cardosso, Emmanuel Pontet, Arnaud Aguilar, Vincent Goanec, Gopal Billy, Maxime Goineau, Chrystale Giraud, Celestine Roder. Une pensée toute particulière pour Loic, Rémi, Sergio, Manu et Vincent sans qui cette thèse n'aurait pas eu le même goût.

I would like to thank my previous supervisors who always transmit me their unconditional passion for their respective fields: Vincent Vedel, Jean-Pierre Vacher and Antoine Fouquet. A particular thanks to Antoine Fouquet who clearly influenced my career choice and actively introduced me to the research. A thought to Philippe Gaucher, star of the FR3 documentary "Les grenouilles des cimes" who inspired me when I was ten years old and who later became a friend.

Thanks to the ISEM lab that was a wonderful place to work. In this lab all people can interact and collaborate without any hierarchical and social barriers between students, technicians and permanent researchers. Thanks to Nicolas Galtier, head of the ISEM lab who tries to give a new dynamic to the research carried out in the lab by promoting open and ethical science while caring for the future of young researchers. A special thanks for some lab members such as: Renaud Lebrun, Lionel Hautier, Marie-Ka Tilak, Frédéric Delsuc, Julien Claude, François Bonhomme, François Catzeflis, Carole Smadja, and Ricardo Araújo.

I am grateful to all the students I have the chance to supervised or co-supervised on various topics such as Benjamin Dubourguier, Mark Wright, Theo Corbet, Elodie Conte, Emilie Eveque, Soraya Bengattat, Elisa Emily Davis, and, Arthur Naas.

Thanks to Marie-Ka Tilak and Remi Allio for their patience and their invaluable work for our super integrative project!

Thanks to Emmanuel Douzery and Maxime Courcelle for their interesting discussions, with the hope that we will finish our ongoing project.

Thanks to Nelly Pirot for her help and interest in our exotic project. Despite surprises and setbacks, I believe that we will eventually make it work. Thanks to all the team from "Réseau d'Histologie Expérimentale de Montpellier (RHEM)" with a special thought to Morgane Broyon for her incredible skills and patience.

Thanks to all our collaborators. A special thought to Renaud Lebrun, Julien Clavel, Jake Esselstyn and Radim Sumbera.

Thanks to Roberto Portela Miguez, from the Natural History Museum London (NHMUK) for his help and trust. Similarly, Vincent Fernandez for his help with for example the "tours infernales".

We are grateful to all these people who welcome us in their lab or houses: Anne-Claire Fabre, Louise Emmons, Radim Sumbera, Lawrence Heaney, Roberto Portela Miguez, and Steve Goodman.

Subterranean rodents from Radim Sumbera's lab: *Heterocephalus glaber*; *Fukomys anselli*; *Heliophobius argenteocinereus*; and *Fukomys darlingi*. Pictures: Quentin Martinez.

I also thank Sci-Hub (e.g. www.sci-hub.se), zlibrary (e.g. www.b-ok.cc) and all the initiatives that work for what science should be: an open resource for humanity.

Alexandra Elbakyan; Sci-Hub and; zlibrary.

Thanks to Cecile Molinier and Vincent Goanec for their unfailing motivation in our very tough field work in Gaa Kaba Mountain. Thanks to Benoît de Thoisy, Pierre-Henri Fabre, and Anthony Herrel for their logistic support.

Gaa Kaba mission (French Guiana): Vincent Goanec, Quentin Martinez, and Cécile Molinier; *Proechimys cuvieri*; *Philander opossum*; Cécile Molinier inspecting a young *Oecomys sp.*; Quentin Martinez holding a young *Oecomys sp.* for biting force measurements; Vincent Goanec inspecting a trap; and a young *Oecomys sp.* Pictures: Quentin Martinez.

Thanks to Jon Nations, Heru Handika, Amsyari Morni, Finaz, Syam and all other members of the Gunung Murud mission. A special thought for the weird church camp! Thanks to Jake Esselstyn and Pierre-Henri Fabre who let me be part of this mission.

Gunung Murud mission (Malaysia): Jon Nations inspecting a *Maxomys whiteheadi*; Heru Handika, Jon Nations, Syam, Finaz, Amsyari Morni, Quentin Martinez and local guides; Amsyari Morni inspecting a *Megaerops ecaudatus*; Heru Handika with a *Maxomys whiteheadi*; *Megaerops ecaudatus*; *Crocidura sp.* eating an Orthoptera; *Hylomys suillus*; and Maxomys whiteheadi. Pictures: Quentin Martinez.

Thanks to all the people who contributed to the mouse project. François Bonhomme for his trust and because the project started from his work. Anthony Herrel for his expertise, trust, logistic support, and without whom the project could not have been restarted. Cecile Molinier who accepted and helped the less fun parts of this project and who was an invaluable support for it. Julien Claude and Pierre-Henri Fabre for their logistic support. Remi Allio and Sergio Cardoso for their constant support and trust in the project. Thanks to all our catchers: Sebastien Puechmaille and his family, Severine Berard, Cecile Molinier, Remi Allio, Fabien Condamine, Emmanuel Pontet, Sergio Cardoso, and some anonymous people from Minerve. A very special thought to Anthony Herrel, Remi Allio, and Cecile Molinier who significantly contributed that this project was not abandoned.

Some additional thanks to Sabrina Renaud, Irina Ruf, Fabrice Darinot, Eliane Ramuz, Françoise Poitevin, Emmanuel Desouhant, and Bruno Guinand.

Unconditional thanks to Cecile Molinier, my awesome, adventurer-scientist-partner who has been an unfailing support over the last few years. For five years, we shared field work, wildlife photography and scientific projects. Hopefully, it is just the beginning of a long journey.

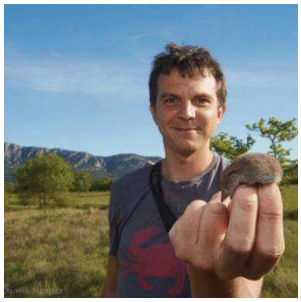

How would it be possible to finish my PhD without mentioning my incredible PhD supervisor? In spite of the false brutality of his language and anarchic discourses which may surprise at first sight, Pierre-Henri Fabre is a humanist who altruistically contributed to science and ecology by: participatory science, data collection, financial and logistical support for projects that he does not always co-sign, opening access to these data and giving its time to these students.

In the ISEM lab, Pierre-Henri is a key element who has the intellectual background and the research experience to collaborate and make bridges between two teams and two fields that were before rivals: morphology and genetics. Besides his inspirational integrative scientific work, Pierre-Henri contributed to a variety of scientific fields including biogeography, molecular evolution, phylogeny, taxonomy, paleontology, anatomy, sensory ecology and ecology (and in various organisms such as birds, mammals, and insects). Increasingly rare fact (especially in Europe), he collected raw data during his own scientific expeditions, in sometimes difficult conditions. In 2018, Pierre-Henri almost died in Peru at high elevation. Taxonomy being dear to him, to date, Pierre-Henri described several rodent new species, one new genus and one new subfamily. During a plenary talk given by Pierre-Henri for the Centennial Celebration of the American Society of Mammalogists (ASM), two mammalogists were discussing. Scott J. Steppan asked Jon Nations: "*Is this guy even sleeping?*".

Since we met for a bachelor project, and thanks to his unfailing enthusiasm I slowly turned my back on the amphibian world for these beloved rodents. Spoiler alert, rodents are one of the most difficult animal orders to study in the wild. During my PhD, Pierre-Henri gave me all the liberty and the support that I needed to develop the projects that I want, explore different leads and start collaborations with different students, researchers and teams. To date Pierre-Henri became a friend much more than a PhD supervisor and I will always be grateful to him for the trust he has placed in me. Hopefully we will do some field work together one day!

Finally, I apologize for all those whom I forgot or did not have the space to bring here and yet who mattered to me at one time or another.

Enfin, un remerciement et quelques excuses aux personnes que je n'ai pas eu la place de nommer ou que j'ai pu oublier.

Crocidura suaveolens eating goat moth caterpillar (*Cossus cossus*); shrew caravaning (*Crocidura russula*); *Mus pahari* eating a *Locusta sp.*; *Crocidura russula* and its cubs; *Mus caroli* and its cubs; *Arvicola amphibius* (fossorial morph) eating some roots; wild *Myocastor coypus* diving; and *Micromys minutus*. Pictures: Quentin Martinez and Cécile Molinier.

↑ Back to summary ↑

Extended abstract in French / Résumé étendu en français :

Capacités olfactives et thermorégulatrices des petits mammifères terrestres : une étude des turbines nasale

1. Contexte relatif à l'étude des turbines

a. Les turbines osseuses

Les mammifères ont dans leur cavité nasale, des rouleaux osseux que l'on appelle les turbines (= turbinaux, Fig. 1). Ces structures participent aux processus olfactifs, à la conservation de la chaleur et de l'humidité, ainsi qu'à la protection des voies respiratoires (p. ex. Negus 1958). Les premiers travaux sur les turbines font probablement référence à la médecine humaine où les turbines étaient nommées conques (= conces, p. ex. Bourgery & Jacob 1831). Au cours des dernières décennies, les turbines ont été largement sous-étudiées par rapport aux autres parties du crâne (Rowe *et al.* 2005). En effet, étant de fines plaques osseuses perforées, les turbines sont très fragiles et difficiles à extraire du crâne. Les anatomistes des siècles passés ont rivalisé d'ingéniosité afin de pouvoir accéder à ces structures. Ils ont notamment inventé de fastidieux protocoles de découpe du crâne, réalisés des projections sur transparents, des moulages en plastique ou en métaux ou encore des modèles en carton (p. ex. Watson 1913, Dawes 1952, Negus 1958, Folkow *et al.* 1988, Morgan & Monticello 1990). Dans ce contexte, nous pouvons saluer les éminents travaux de Simon Paulli et de Sir Victor Negus (Paulli 1900 a, b, c, Negus 1958) qui sont devenus des références pour le domaine.

Inventée dans les années 80, la tomographie à rayons X (= scanner à rayons X, micro-CT, µCT) est un système d'imagerie qui permet de révéler des objets de forte densité (p. ex. os). Cette technologie était dans un premier temps extrêmement coûteuse et uniquement consacrée à des projets d'exception. Par la suite, les avancées technologiques et leurs démocratisations ont permis une chute des coûts d'utilisation. La tomographie à rayons X a complètement révolutionné le domaine de l'écologie sensorielle et notamment dans le cas des études sur les turbines. Dans un contexte de diminution drastique de la biodiversité, les spécimens de musées sont devenus rares et de grandes valeurs. Par conséquent, la tomographie à rayons X qui est un processus non destructif, permet d'acquérir des données à partir de spécimens rares. C'est notamment le cas pour

les holotypes (= spécimens de référence servant à la description d'une espèce) ou des spécimens d'espèces menacées voire éteintes. Il est également possible d'effectuer des scans à rayons X sur des animaux vivants anesthésiés ou en mouvement (cinéradiographie). L'un des premiers travaux sur les turbines utilisant la microtomographie à rayons X est probablement celui de Ruben *et al.* (1996) qui a étudié les turbines respiratoires chez les oiseaux, les crocodiliens et les théropodes. Depuis, le nombre de publications relatives aux turbines a augmenté de façon exponentielle.

Cependant, la cavité nasale (et donc les turbines) est probablement encore la région la moins étudiée du crâne, et ce, en dépit de la grande proportion qu'elle y occupe (Rowe *et al.* 2005). Van Valkenburg et son équipe ont largement participé à la démocratisation des analyses quantitatives basées sur les turbines (p. ex. Van Valkenburg *et al.* 2004, 2011, 2014 a, Green *et al.* 2012). Aujourd'hui, la contrainte majeure reste le temps nécessaire pour traiter les données informatiques générées par les tomographes à rayons X. C'est notamment le cas pour la segmentation (= isolement d'une zone d'intérêt). En effet, chez les mammifères, il faut entre une demi-journée et plusieurs jours pour extraire correctement toutes les turbines d'un côté. Ce processus est encore plus long dans le cas d'images bruitées, pour des scans de fossiles, ou d'espèces ayant des turbines très complexes (p. ex. les espèces amphibies). Dans les prochaines années, les algorithmes informatiques de type "*deep learning*" pourraient considérablement réduire le temps de segmentation. À ce jour, certains logiciels (p. ex. Biomedisa, Losel *et al.* 2020) réalisent déjà d'exceptionnels travaux d'interpolation dans des structures telles que les endocastes (= moulages d'une structure osseuse creuse). Cependant, ces logiciels ne sont pas encore adaptés à des structures aussi complexes et fines que les turbines.

Ces dernières années, le nombre d'études liées aux turbines de mammifères n'a cessé de croître. Cependant, ces études restent rares chez d'autres tétrapodes (p. ex. oiseaux ou lézards) où la plupart de leurs turbines sont cartilagineuses et donc non visibles aux tomographes à rayons X. Le récent développement de méthodes de colorations (p. ex. iode ou acide) permet d'améliorer le contraste des tissus mous et donc de les rendre visibles aux tomographes à rayons X (Pauwels *et al.* 2013, Gignac *et al.* 2016).

b. Les turbines chez les mammifères

Parmi les tétrapodes actuels, les mammifères ont en moyenne les turbines les plus développées (p. ex. Negus 1958, Parson 1971). Malgré quelques études chez les primates, les carnivores, les chauves-souris, les lagomorphes ainsi que les rongeurs, l'homologie des turbines reste floue au sein de certains groupes (Hillenius 1994). La difficulté à déterminer l'homologie des turbines est principalement associée aux turbines olfactives (= turbines intervenant dans la détection des odeurs). En effet, l'augmentation de la complexité (= augmentation du nombre de détails pour une surface donnée) des turbines résulte en l'augmentation du nombre de petites lamelles indépendantes. Même chez les rongeurs, l'homologie des turbines olfactives est parfois

incertaine (Martinez *et al.* in prep. c, Fig. 4). Ce constat traduit l'importance des études développementales permettant l'identification des turbines homologues. Cependant, ce type d'étude reste rare et limité à certaines familles de mammifères (p. ex. Ruf 2004, 2020, Smith *et al.* 2016, 2020 a, Smith & Rossie 2008, Wagner & Ruf 2020).

Les turbines sont généralement divisées en deux catégories : les turbines respiratoires et olfactives. Les turbines respiratoires participent à la conservation de la chaleur et de l'humidité alors que les turbines olfactives interviennent dans les processus de détection des odeurs. Cette discrimination correspond souvent à une localisation antéro-postérieure dans la cavité nasale (Fig. 3).

Les turbines respiratoires sont impliquées dans la conservation de la chaleur et de l'humidité. Lors de l'inhalation, l'air est réchauffé à la température du corps par contact avec la partie antérieure des turbines respiratoires qui est recouverte d'un épithélium densément vascularisé. Simultanément, l'air en contact avec le mucus nasal est humidifié. Lors de l'expiration, cet air précédemment réchauffé est désormais refroidi par la partie antérieure des turbines respiratoires qui a été précédemment refroidi par l'air inspiré (Fig. 6). Ce processus condense l'eau des fosses nasales et conserve en moyenne 66 % de l'humidité de l'air expiré (Negus 1958, Walker & Wells 1961, Jackson & Schmidt-Nielsen 1964, Schmidt-Nielsen *et al.* 1970, Collins *et al.* 1971, Hillenius 1992, Ruben *et al.* 1996, Hillenius & Ruben 2004). Les turbines respiratoires sont également impliquées dans la protection des voies respiratoires profondes et du neuro-épithélium (= épithélium composé de neurones) des turbines olfactives localisées postérieurement. En effet, les turbines respiratoires filtrent, absorbent et éliminent des éléments macro et microscopiques mais également les composés volatils pouvant provoquer des lésions (p. ex. Morgan & Monticello 1990, Harkema *et al.* 2006). Ces processus sont rendus possibles grâce à la morphologie ciliée de l'épithélium respiratoire mais aussi du fait de ses propriétés d'absorption et de régénération.

Les turbines olfactives participent à la détection des odeurs. En effet, elles sont recouvertes d'un épithélium olfactif composé de neurones (Ressler *et al.* 1993, 1994, Harkema *et al.* 2006, Barrios *et al.* 2014, Herbert *et al.* 2018). Ces neurones olfactifs sont prolongés ventralement par des axones qui se ramifient et rejoignent des faisceaux de nerfs. Ces nerfs traversent la plaque cribriforme perforée pour rejoindre les glomérules du bulbe cérébral olfactif (Fig. 5). Ainsi, quand une molécule odorante est inspirée, elle est détectée via des récepteurs olfactifs localisés sur les turbines olfactives avant d'être analysée postérieurement par le cerveau.

c. Pressions sélectives affectant les turbines

Il a été largement admis que le nombre et la forme des turbines sont conservés en fonction du degré d'apparentement entre les espèces. En revanche, la taille relative et la complexité des turbines pourraient être plus labiles et varier en fonction de l'écologie des espèces (p. ex. Van

Valkenburg *et al.* 2011, 2014 a, b, Green *et al.* 2012, Macrini 2012, Ruf 2014, 2020, Yee *et al.* 2016, Curtis & Simmons 2017, Martinez *et al.* 2018, 2020, Lundeen & Kirk 2019, Wagner & Ruf 2019). Cependant, peu d'études abordent la question en utilisant des approches statistiques, de morphométrie géométrique ou via des modèles d'évolution.

A une échelle taxonomique relativement large, les turbines sont supposées être porteuses d'un signal phylogénétique. Plusieurs études ont identifié dans les turbines, des caractères potentiellement informatifs pour inférer les relations de parentés entre espèces (Paulli 1900 a, b, c, Negus 1958). Cependant, dans certains cas, ces caractères se sont révélés erronés par la suite (Gardiner 1982). D'autres études ont tenté de coder certains caractères morphologiques à l'aide des turbines de mammifères adultes (p. ex. Voss & Jansa 2003, Macrini 2012, Ruf 2014, 2020, Lundeen & Kirk 2019). Cependant, au moins chez les rongeurs, l'histoire pourrait être plus compliquée que prévu. En effet, les potentiels caractères identifiés se sont avérés faux ou présentant de nombreuses exceptions dès lors que l'échantillonnage devenait exhaustif (Martinez *et al.* in prep. c).

Les contraintes développementales sont également supposées avoir un impact sur l'évolution des turbines (p. ex. Rowe *et al.* 2005). En effet, les turbines pourraient être en conflit avec d'autres structures ou organes pour l'espace dans la cavité nasale. Cette hypothèse a été largement discutée pour les yeux et certaines évidences ont été trouvées chez les Carnivora (Van Valkenburg *et al.* 2014 b, Ruf 2020). Cependant des travaux sur le rat-taupe nu (*Heterocephalus glaber*) pourraient venir contredire cette hypothèse (Martinez *et al.* in prep. a).

Enfin, il a été montré que la taille relative et la complexité des turbines variaient largement avec l'écologie des espèces. C'est notamment le cas avec le régime alimentaire (p. ex. consommation de vers de terre, comportement charognard) ou le mode de vie (p. ex. espèces amphibies, Van Valkenburg *et al.* 2004, 2011, 2014 a, Green *et al.* 2012, Martinez *et al.* 2018, 2020). Par exemple, il pourrait exister une corrélation entre la taille relative des turbines respiratoires et la capacité de conservation de la chaleur et de l'humidité. En effet, le renne (*Rangifer tarandus*) a la plus grande surface relative de maxillo-turbines (= Maxillo RSA, = une turbine respiratoire) de tous les mammifères étudiés (Martinez *et al.* in prep. b, Fig. 7). Cette espèce arctique est connue pour ses importantes capacités de conservation de la chaleur et de l'humidité (Langman 1985). De même, les Pinnipedia (p. ex. éléphants de mer) sont connus pour avoir des maxillo-turbines extrêmement complexes et développées (Van Valkenburg *et al.* 2011, Mason *et al.* 2020, Martinez *et al.* in prep. b, Fig. 7). Or, des études de performances montrent qu'ils ont de bonnes capacités de conservation de l'humidité, ce qui pourrait être une adaptation à un environnement salin (Lester & Costa 2006). Les humains (*Homo sapiens*) expirent un air complètement saturé en humidité et à une température proche de celle du corps (Walker & Wells 1961, Schmidt-Nielsen 1969). De ce fait, ils ont une relative mauvaise capacité de conservation de la température et de l'humidité. Morphologiquement, ils ont des maxillo-turbines de taille

moyenne par rapport aux autres mammifères (Martinez *et al.* in prep. b, Fig. 7). Enfin, le rat taupe nu (*Heterocephalus glaber*) a l'une des plus mauvaises capacités de conservation de l'eau mais aussi de thermorégulation jamais enregistré chez un mammifère (Martin 1903, Collins *et al.* 1971, Buffenstein & Jarvis 1985, Buffenstein & Yahav 1991). Cette espèce présente une perte unique des maxillo-turbines (Martinez *et al.* in prep. a, b, Fig. 4, 7).

2. Objectifs des travaux de thèse

Cette thèse avait pour objectif de caractériser les facteurs évolutifs expliquant la grande diversité anatomique, morphologique mais également de taille et de complexité des turbines. Cela dans un premier temps à l'échelle des rongeurs puis étendue à d'autres mammifères. Pour ce faire, la première étape fut la création d'un jeu de données de scans à haute résolution de la cavité nasale de ces mammifères. Ainsi nous avons scanné plusieurs centaines d'individus dans différents pays et provenant de collections de différentes régions géographiques. Les étapes de traitement des scans et notamment la segmentation (= isolation des structures d'intérêt) ont été les travaux les plus chronophages de cette thèse. En effet, ils ont démarré avant la thèse (stages de master 1 et 2) et se sont poursuivis de manière quotidienne au cours des trois années suivantes. Cela nous a permis d'acquérir le plus gros jeu de données de turbines jamais publié. L'intérêt d'un tel jeu de données est de pouvoir tester de manière statistique et robuste des hypothèses évolutives telles que des événements de convergence (= acquisition indépendante d'un caractère dans des lignées non directement apparentées) ou de compromis évolutifs (p. ex. conflits entre deux structures anatomiques pour l'espace dans la cavité nasale).

Par ces travaux, nous avons pu démontrer statistiquement des adaptations convergentes liées par exemple à la colonisation du milieu aquatique ou à un régime alimentaire hyper-spécialisé (Martinez *et al.* 2018, 2020). Nous avons prouvé qu'il existait un compromis d'espace dans la cavité nasale entre les fonctions de conservation de la température et de l'humidité d'une part, et les fonctions de captations des odeurs d'autre part (Martinez *et al.* 2020). Nous avons proposé une nouvelle méthodologie afin de quantifier la complexité des turbines en 3 dimensions et avons testé sa relation avec la surface relative des turbines (Martinez *et al.* 2018). Nous avons également permis de raffiner la discrimination antero-posterieure des turbines respiratoires et olfactives permettant la réalisation d'études quantitatives plus précises (Martinez *et al.* 2020). Enfin, par la mise en relation de la perte d'une turbine respiratoire avec des études de performances, nous avons apporté de nouvelles évidences quant au rôle fonctionnel des turbines respiratoires (Martinez *et al.* in prep. a).

D'autres travaux ont également été entrepris et sont actuellement en cours. C'est par exemple le cas de l'étude de l'évolution de la maxillo-turbine à l'échelle des mammifères (Martinez *et al.* in prep. b, Fig. 7). En effet, nous essayons de comprendre les facteurs évolutifs qui expliquent les importantes variations observées (p. ex. taille, écologie et relation de parenté

entre espèces). Un second projet vise à caractériser l'anatomie des turbines des rongeurs avec un échantillonnage exhaustif comprenant la plupart des sous-familles (Martinez *et al.* in prep. c, Fig. 4). Ce travail nous permettra de savoir s'il existe réellement des caractères informatifs sur les turbines, permettant potentiellement d'inférer l'évolution des turbines pour des taxons éteints (Fig. 2). En collaboration avec Nelly Pirot du Réseau d'Histologie Expérimentale de Montpellier, nous travaillons actuellement sur la cartographie de la cavité nasale des rongeurs et sur la quantification (= semi-quantification) des récepteurs olfactifs dans l'épithélium olfactif (Martinez *et al.* d). Pour ce faire, nous travaillons avec un marquage d'immuno-histochimie qui révèle par fluorescence les neurones olfactifs et leurs axones (Fig. 8). Enfin, en collaboration avec Marie-Ka Tilak et Rémi Allio, nous travaillons actuellement sur l'expression des gènes des turbines olfactives (= transcriptomique) chez deux espèces de rongeurs non modèles (Martinez *et al.* e). En effet, Martinez *et al.* (2020) ont démontré que le ragondin amphibie (*Myocastor coypus*) possédait des turbines olfactives réduites (= surface relative et nombre de turbines) par rapport à son proche parent terrestre, le rat épineux (*Proechimys guyannensis*). Nous avons donc échantillonné les turbines olfactives de ces deux espèces proches parents et avons réalisé leurs transcriptomes (Fig. 9). Ces données nous permettront de tester une potentielle expression différentielle des gènes codants dans les turbines olfactives. Nous vérifierons si ces résultats correspondent à ceux obtenus sur la surface relative des turbines olfactives. Dans un second temps, nous comparerons ces proxies avec d'autres organes liés à l'olfaction tels que l'organe voméronasal, la plaque cribriforme et le bulbe cérébral olfactif (Fig. 9).

La discussion du manuscrit de thèse présentée ici aborde les limites méthodologiques et conceptuelles de l'étude de l'olfaction. Nous abordons par exemple les aprioris présents dans le domaine (p. ex. sur les performances olfactives), la terminologie non-uniforme des turbines ou encore la sensibilité de certains proxies anatomiques.

Nous discutons également de la difficulté d'étudier les processus liés à l'olfaction. En effet, l'olfaction peut être abordée par différentes approches méthodologiques (p. ex. morphologie, histologie, génomique) et via différents proxies anatomiques (p. ex. turbines, bulbe olfactif, organe voméronasal). De plus, l'olfaction est une fonction complexe qui repose sur des processus multifactoriels avec des pressions sélectives distinctes. Par exemple, une seule molécule odorante peut être détectée par un seul ou par plusieurs récepteurs olfactifs. Cependant, un seul récepteur olfactif peut également détecter plusieurs molécules odorantes. En outre, des molécules odorantes ayant des structures différentes peuvent être perçues comme une seule odeur et différentes molécules odorantes ayant une structure similaire peuvent être perçues comme des odeurs différentes (Niimura 2012, Hayden & Teeling 2014, Yohe & Brand 2018). Ainsi, l'homme peut distinguer au moins mille milliards de stimuli olfactifs différents (Bushdid *et al.* 2014). Par conséquent, sans une compréhension claire de la covariation entre les différents organes olfactifs, il est difficile de discuter en toute confiance des capacités olfactives intrinsèques d'une espèce.

Enfin, nous concluons qu'à l'heure de la démocratisation d'outils technologiques (p. ex. tomographes à rayons X, outils de séquençage par nanopores) et l'explosion des données disponibles (p. ex. génomiques, morphologiques) c'est une période très intéressante pour étudier les processus liés aux fonctions de la cavité nasale.

↑ Back to summary ↑

Abstract

In most tetrapods, the nasal cavity houses a bony or a cartilaginous system (i.e. turbinals or turbinates) supporting epithelium and sensory organs involved in either olfaction or heat and moisture conservation. Among extant tetrapods, mammals have on average, the largest turbinals to skull length ratio. Despite some studies in primates, Carnivora, bats, lagomorphs as well as rodents, our understanding of the selective pressures affecting turbinals remains imprecise.

This PhD aims to unravel the evolutionary processes responsible for the large anatomical and morphological variations of turbinals among mammals. In the course of our work we acquired an extensive dataset of three-dimensional micro-computed tomography scans (micro-CT) in rodents and other small terrestrial mammals. We were then able to statistically test hypotheses linking turbinal morphology to ecology (e.g. diet or ecotype) and evolutionary patterns such as convergence or evolutionary trade-off (e.g. conflict for space in the nasal cavity between different organs).

The present dissertation provides a non-exhaustive review of the olfaction. In the light of our works, we discussed the methodological and conceptual limits of the field. Indeed, olfaction is a complex function relying on multifactorial processes, under various selective pressures. Olfaction may be tackled by resorting to different approaches (e.g. morphology, histology, genomics) and anatomical proxies (e.g. turbinals, olfactory bulb, vomeronasal organ). In this context, our ongoing projects try to refine current functional hypotheses in studying covariation in olfactory-related organs using different anatomical proxies, immunohistochemistry, and transcriptomic.

Résumé

La plupart des tétrapodes actuels, possède dans leur cavité nasale, des rouleaux osseux que l'on appelle les turbines (= turbinaux). Parmi eux, les mammifères ont en moyenne les turbines les plus développées et, qui sont généralement divisées en deux catégories : les turbines respiratoires et olfactives. Les turbines respiratoires participent à la conservation de la chaleur et de l'humidité alors que les turbines olfactives interviennent dans les processus de détection des odeurs. Malgré quelques études chez les primates, Carnivora, chauves-souris, lagomorphes ainsi que chez les rongeurs, notre compréhension globale des pressions de sélection affectant les turbines reste incomplète.

Cette thèse avait pour objectif de caractériser les facteurs évolutifs expliquant la grande diversité anatomique, morphologique mais également de taille et de complexité des turbines. A l'aide d'une technologie d'imagerie non destructive, la tomographie à rayons X (= micro-CT), nous avons généré un jeu de données sans précédent sur les turbines de rongeurs et les petits mammifères terrestres. Ainsi, nous avons pu tester statistiquement des hypothèses évolutives en lien avec l'écologie (p. ex. régime alimentaire ou milieu de vie), la convergence (= acquisition indépendante d'un caractère dans des lignées non directement apparentées) ou les compromis évolutifs (p. ex. conflits entre deux structures anatomiques pour l'espace dans la cavité nasale).

Ce manuscrit de thèse, tente de réaliser une révision non exhaustive sur l'état du domaine de l'étude de l'olfaction et aborde brièvement la question de la conservation et de l'humidité. A la lumière de nos travaux, nous discutons des limites méthodologiques et conceptuelles de ces domaines d'étude ainsi que les difficultés liées à l'étude de l'olfaction. En effet, l'olfaction peut être abordée par différentes approches méthodologiques (p. ex. morphologie, histologie, génomique) et via différents proxies anatomiques (p. ex. turbines, bulbe olfactif, organe voméronasal). Dans ce contexte, nous avons entrepris des travaux intégratifs allant de l'étude de différents organes olfactifs à l'immuno-histochimie et en passant par la transcriptomique.